Syntheses, Characterization and Applications of Bicyclic (Alkyl)(Amino) Carbene (BICAAC) Complexes of Iridium and Some Selected Elements from Group 13-15

Manu Adhikari

A thesis submitted for the partial fulfilment of

the degree of Doctor of Philosophy

Department of Chemical Sciences

Indian Institute of Science Education and Research (IISER) Mohali

Knowledge city, Sector 81, SAS Nagar, Manauli PO, Mohali 140306, Punjab, India.

May 2024

Dedicated to my father

DECLARATION

The work presented in this thesis titled "**Syntheses, Characterization and Applications of Bicyclic (Alkyl)(Amino) Carbene (BICAAC) Complexes of Iridium and Some Selected Elements from Group 13-15**" has been carried out by me under the supervision of Dr. Sanjay Singh in the Department of Chemical Sciences, Indian Institute of Science Education and Research (IISER) Mohali, Mohali. This work has not been submitted in part or full for a degree, diploma or a fellowship to any other university or institute. Whenever contributions of others are involved, every effort is made to indicate this clearly with due acknowledgements of collaborative work and discussions. This thesis is a bonafide record of original work done by me and all sources listed within have been detailed in the bibliography.

Manu Adhikari

Date:

Place:

In my capacity as the supervisor of the candidate's thesis work, I certify that the above statements by the candidate are true to the best of my knowledge.

Dr. Sanjay Singh

Professor

Department of Chemical Sciences

Indian Institute of Science Education and Research Mohali

Date:

Place:

Acknowledgements

journey. As I approach the completion of my doctoral studies, I keenly feel his absence, and I deeply regret that he is not here to witness this significant milestone. I remain forever thankful to him for his enduring influence on my life. I extend my heartfelt thanks to all my family members Mrs. Maya Devi, Mr. Ankit Adhikari, Mrs. Haruli Devi, Mr. Balam S. Adhikari, Mrs. Hema Adhikari, Ms. Shreya Adhikari, Mr. Dan S. Adhikari, Mrs. Lalita Adhikari, Mr. Indra S. Boura, Mrs. Deepa Boura, Mr. Govind S. Negi, Mrs. Heera Devi, Mr. Vikas Adhikari, Mrs. Preeti Adhikari, Mr. Dinesh Negi, Mr. Dan S. Negi and Ms. Prerna Boura for their unwavering love, steadfast support, and unshakeable faith in me. Their contributions have been invaluable, and I am profoundly indebted to each of them for being pillars of strength throughout this progressive journey.

I specially thank Dr. Sandeep K. Thakur, Dr. Chandrakala, Dr. Mamta, Dr. Rajat, Dr. Yogendra, Dr. Shruti, Mr. Arjun, Ms. Nisha, Ms. Anjali, Ms. Manu, Ms. Mamta, Ms. Renu, Mr. Anurag, Ms. Garima, Mr. Sanjay, Mr. Chandan and many more for their steadfast presence during both the ups and downs has been a source of immense strength and encouragement.

I express gratitude to those not mentioned here for their support. Ultimately, I express my gratitude to the Almighty for bestowing upon me the health and vitality that played a pivotal role in the successful culmination of this project.

Manu Adhikari

Table of Contents

ii

Chapter 4

Adducts of ECl3 with bicyclic (alkyl)(amino) carbene (MeBICAAC) and their subsequent three-electron reduction for the preparation of BICAAC stabilized E-E bonded compounds (E = P, Sb)

Chapter 5

Neutral and cationic Ir(I)-complexes supported by BICAAC: Application of Ir(MeBICAAC)Cl(COD) complex as a catalyst for transfer hydrogenation of carbonyls and imines..**177**

Chapter 6

Abbreviations

APCI	Atmospheric pressure chemical ionization
Ar	Aryl
av	Average
C	Celsius
calcd.	Calculated
d	Doublet
dd	Doublet of doublet
decomp.	Decomposition
Dipp	Diisopropylphenyl
EDX	Energy-dispersive X-ray spectroscopy
EI	Electron impact ionization
equiv.	Equivalents
eV	Electron volt
FMO	Frontier Molecular Orbital
g	Grams
HOMO	Highest Occupied Molecular Orbital
h	Hours
Hz	Hertz
^{i}Pr	$i$so-propyl
J	Coupling constant
K	Kelvin
L	Ligand
LUMO	Lowest Unoccupied Molecular orbital
M	Metal
m	Multiplet
m/z	Mass/Charge
M^+	Molecular ion
Me	Methyl
min.	Minutes
MP	Melting Point

MS	Mass Spectrometry, Mass Spectra
BICAAC	Bicyclic (Alkyl)(Amino) Carbene
NHC	N-Heterocyclic Carbene
CAAC	Cyclic (Alkyl)(Amino) Carbene
MIC	Mesoionic Carbenes
NMR	Nuclear Magnetic Resonance
SQUID	Superconducting Quantum Interference Device
EPR	Electron Paramagnetic Resonance
ppm	Parts Per Million
R, R'	Organic Substituents
s	Singlet
SEM	Scanning Electron Microscope
TEM	Transmission Electron Microscope
Sept	Septet
T	Tesla
t	Triplet
THF	Tetrahydrofuran
TMS	Tetramethylsilane
$\tilde{v}$	Wave number
V	Volt
W	Weak
Z	Number of molecules in the unit cell
δ	Chemical shift

Chapter 1

A brief introduction to carbenes

1988 — phosphino-silyl carbene
Bertrand

1991 — N-heterocyclic carbene
(NHC)
Arduengo

2001 — Mesoionic carbene
(MIC)
Bertrand

2005 — Cyclic (alkyl)(amino) carbene
(CAAC)
Bertrand

2017 — Biyclic (alkyl)(amino) carbene
(BICAAC)
Bertrand
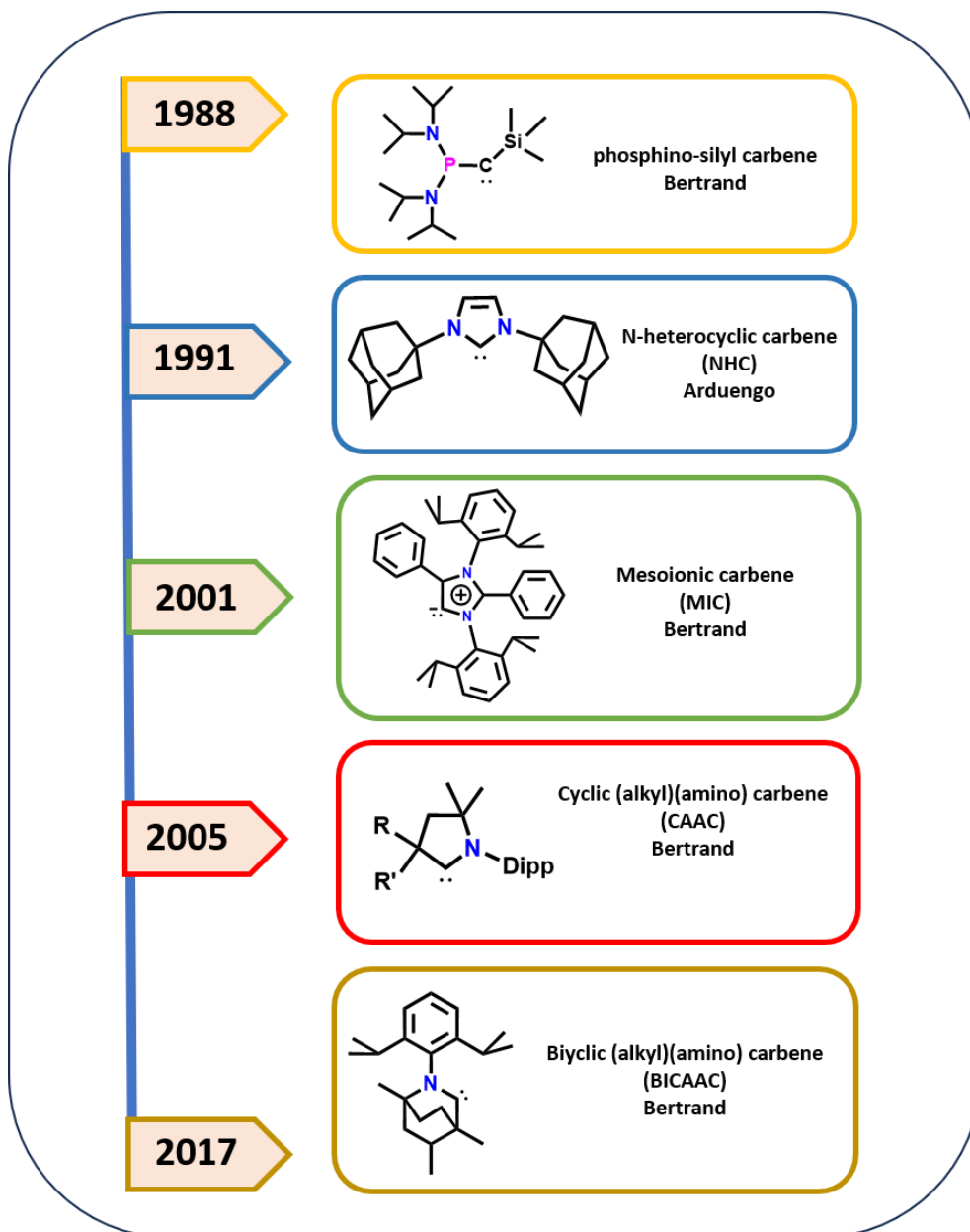
1.1 Brief history and early work on carbenes

Historically, carbenes were perceived as transient intermediates in various organic transformations.[1,2] For nearly a century, carbenes were perceived primarily as theoretical concepts due to the challenges associated with their isolation. They were considered inherently unstable and extremely reactive species in organic reactions like cyclopropanation. Consequently, numerous theoretical and experimental inquiries remained unanswered, including questions regarding the structural arrangement of carbenic carbon and the ambiguity surrounding its electronic configuration, whether it exhibits a singlet or triplet nature.[3] Chemists have made multiple efforts to isolate carbenes dating back to as early as 1835.[4] In 1855, Geuther and Hermann were the first to suggest the existence of a carbene species. They proposed that the alkaline hydrolysis of chloroform leads to the formation of a transient intermediate called dichlorocarbene.[5] A similar type of reaction intermediate was proposed by Nef in 1897 for the widely recognized Reimer-Tiemann reaction and the conversion of pyrrole to α-chloropyridine mediated by chloroform.[6] At the time when these hypotheses were proposed, free radicals were still undiscovered by the scientific community, making these ideas quite innovative. However, just three years later, in 1900, when Gomberg disclosed the first report on free radical, triphenylchloromethylene (as depicted in Scheme 1.1) through elemental analysis, it began to shift people's perspective towards considering the existence of carbenes.[7] Significant advancements in understanding the existence of carbene intermediates were also made by the research groups of Staudinger and Kupfer as they investigated the synthesis of methylene[8] and diazomethane[9] derivatives. By the 1930s, free radical chemistry had been well-established, and people had acknowledged their role as reaction intermediates in organic synthesis.[10] In this context, carbene species were referred to as diradicals.[1a]
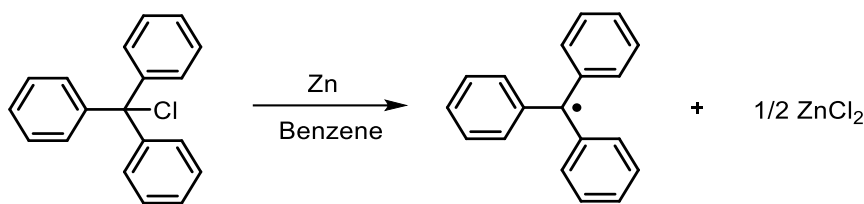
Scheme 1.1 Synthesis of the first stable radical.

In 1953, Doering and Knox introduced carbenes into the organic chemistry, by utilizing a methylene intermediate for the synthesis of a tropolone derivative (Scheme 1.2).[11] A year later in 1954, breakthrough was achieved by Doering and co-workers, when they proved the existence of an intermediate dibromomethylene by reacting an alkene (1-cyclohexene) with bromoform under basic conditions (Scheme 1.3).[12] The methylene derivatives were used extensively by organic chemists to understand the nature of the carbene intermediate.[13] Carbenes were introduced in organometallic chemistry by Fischer in 1964.[14] Since then, carbene metal complexes have a wide applicability in the synthetic chemistry.[15]
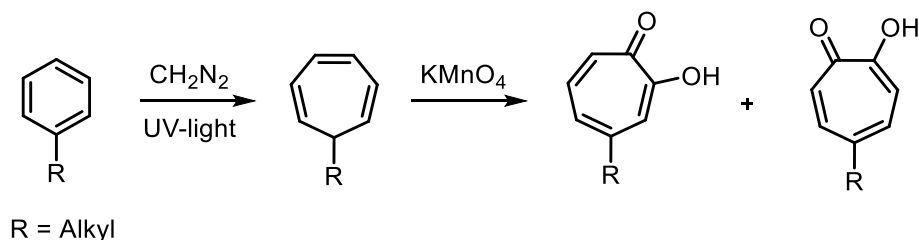
Scheme 1.2 Use of methylene intermediate to synthesize a tropolone derivative.
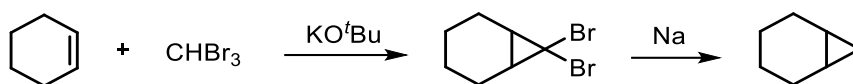
Scheme 1.3 Olefin cyclopropanation by using methylene intermediate.

1.2 Geometry and electronic configurations of carbenes

Carbenes are described as neutral species featuring a divalent carbon atom with six electrons in its valence shell. Depending upon the distribution of two non-bonding electrons and the degree of hybridization, the geometry around carbon atom can either be linear or bent (Figure

1.1). The linear geometry arises as a result of *sp*-hybridized carbene carbon atom (mixing of *s* and p_z orbitals) which leaves two non-bonding degenerate orbitals (p_x and p_y) with half-filled electronic configuration. However, in the bent carbene, the degeneracy of p_x and p_y orbitals get broken and the central carbon atom adopts sp^2 hybridization leaving the p_y orbital unpretentious, which is called as p_π, whereas the pure p_x orbital get stabilized by acquiring the *s* character and called as σ (Figure 1.2). Therefore, frontier orbitals of carbene are generally called as σ and p_π. For a general prototype carbene, four types of electronic configuration can be given as depicted in Figure 1.3.
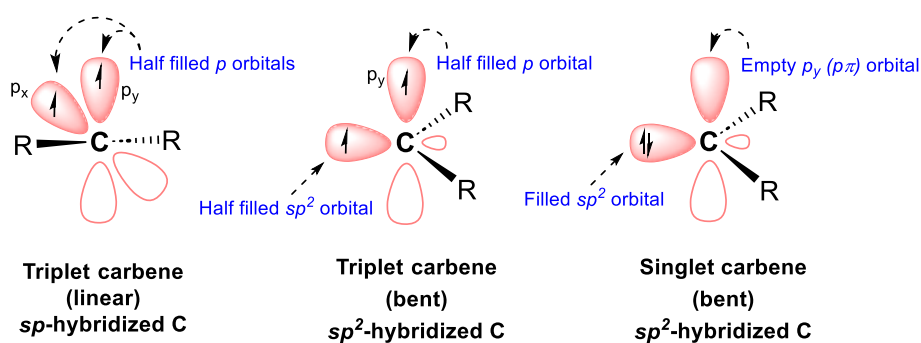
Figure 1.1 Possible electronic states of carbenes.
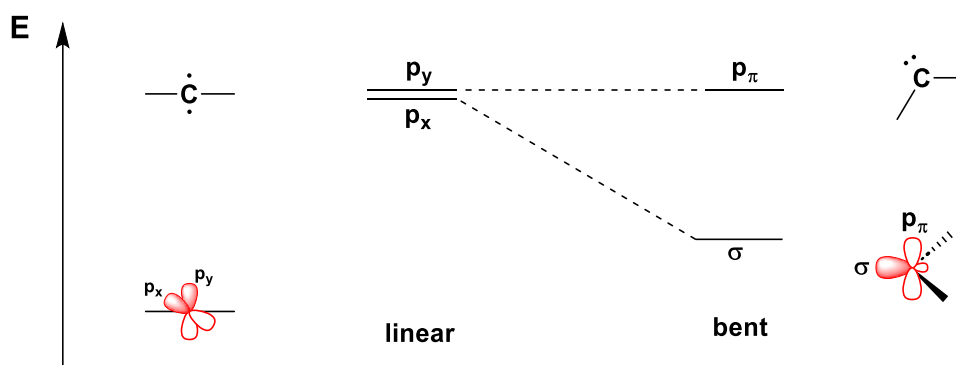
Figure 1.2 Correlation between bond angle and nature of frontier orbitals of carbene (adapted from *Chem. Rev*. **2000**, *100*, 39-91).

The ground state spin multiplicity of carbenes is a direct measure of their reactivity.[16] Singlet carbenes are generally have a filled and an empty orbital, consequently possess ambiphilic character, whereas triplet carbenes have two singly occupied orbitals, and
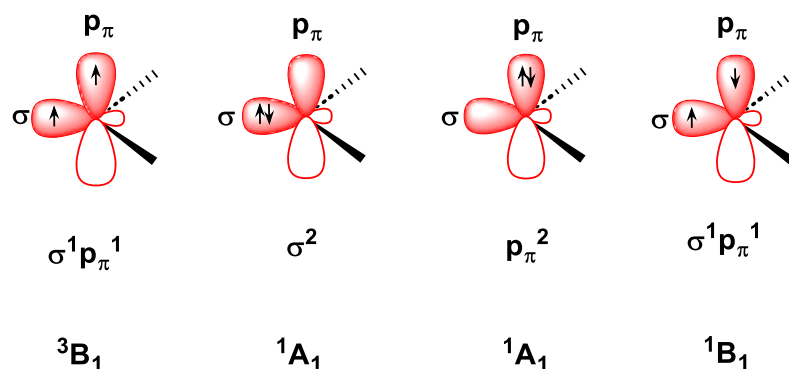
Figure 1.3 Possible electronic configurations of carbenes (adapted from *Chem. Rev.* **2000**, *100*, 39-91).

therefore, called as diradicals. The energy gap of frontier orbitals (σ and p_π orbitals) is somewhat related to the ground state spin multiplicity of carbenes and a large σ-p_π separation favors singlet ground state. Hoffmann and co-workers in 1968 determined the minimum splitting energy which dictate the fate of singlet and triplet ground state, a minimum of 2 eV energy gap is required to get the singlet ground state, while below 1.5 eV it gives rise to a triplet ground state.[17]

1.3 Synthesis, reactivity and stability of carbenes

1.3.1 Triplet carbenes

Triplet carbenes are primarily synthesized at very low temperature (77 K) from diazo compounds using photolysis methods, they typically possess two α-phenyl groups.[18] Due to the presence of diradical nature, triplet carbenes are very reactive and therefore hard to isolate.[19] Tomioka and co-workers synthesized first triplet carbene which is stable up to one week at room temperature in benzene (Scheme 1.4).[20] The room temperature stability is determined by their half-life time in benzene. In term of stability, triplet carbenes can be stabilized by sterically protecting the carbene carbon by incorporation of bulky substituents such as, sterically demanding diaryl groups (polyhalogenated, polymethylated and trifluoromethylated diphenylcarbenes).[21] Large aromatic groups such as anthryl are also

used to stabilize triplet carbenes by means of providing electronic stabilization *via* delocalization of the unpaired electrons.[20]
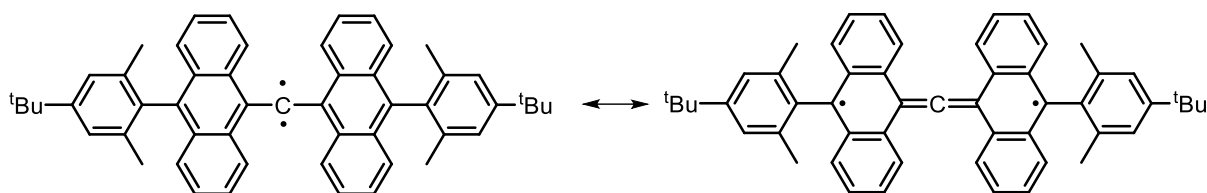
Scheme 1.4 A stable triplet carbene.

Triplet carbenes such as polychlorinated diphenylcarbene dimerizes to *tetrakis*(aryl)ethylene in degassed benzene.[22] They also show rearrangement/decomposition side reactions during olefin dimerization, C-H insertion and cyclopropanation.[23]

1.3.2 Singlet carbenes

Due to the ambiphilic nature, the ground state spin multiplicity of singlet carbene is significantly govern by the electronegativity of the attached α-substituents. The electronic effects caused by the α-substituents can significantly vary the nature of the resulting carbene.[24] The following type of effects are responsible in deciding the fate of resulting carbene:

Inductive effects: σ-electron withdrawing substituents generally favor the singlet state, by increasing the *s*-character of σ nonbonding orbital, as a result the σ-p_π gap is increased and singlet state is favored. On the other hand, σ-electron donating substituents bring a small σ-p_π gap which ultimately favors the triplet state.[24]

Mesomeric effects: The two α-substituents can be electron donating groups (X,X), electron withdrawing groups (Z,Z) or electron donating-withdrawing groups (X,Z), where X = -F, -Cl, -Br, -I, NR_2, PR_2, OR, SR and Z = -COR, -CN, $-CF_3$, BR_2, SiR_3. (X,X) type carbenes are supposed to be bent singlet carbenes e.g., dimethoxycarbenes[25], dihalocarbenes[26] and

diaminocarbenes.[24e-f, 27] The two π-donor α-substituents exhibits push-push mesomeric effect (Figure 1.4). The (Z,Z) type carbenes are predicted to be linear singlet carbenes[24e-f, 27] for example dicarbomethoxycarbenes[28] and diborylcarbenes. The two π-acceptor substituents exhibit pull-pull mesomeric effect (Figure 1.4). Lastly, the quasi-linear (X,Z) type carbenes are a result of both types of electronic interactions, both the interactions are stabilizing which results in a allene-type system e.g., halogenocarboethoxycarbenes[29], phosphinosilyl- and phosphinophosphoniocarbenes. This type of system shows push-pull mesomeric pattern (Figure 1.4).
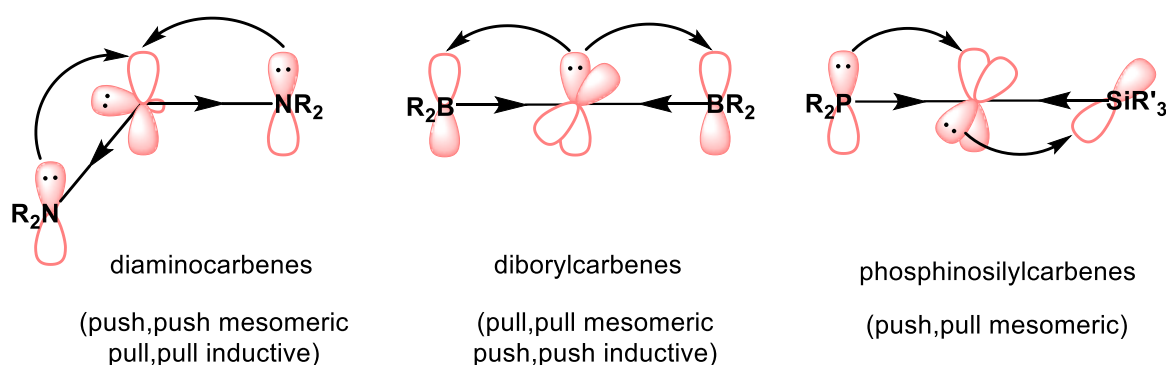
Figure 1.4 Electronic effects induced by the α-substituents in different carbenes. (adapted from *Chem. Rev.* **2000**, *100*, 39-91).

***Steric effects*:** Both type of carbenes are kinetically stabilized by bulky and sterically demanding substituents. However, the steric effects are more prominent in deciding the fate of a triplet carbene.[21b,30]

***Syntheses of singlet carbenes*:** Carbenes were formerly produced from diazirine precursors using thermolysis or photolysis methods[31] (Scheme 1.5) or through oxygen atom transfer (Scheme 1.6).[32] Nowadays, most carbene synthesis relies on deprotonating the precursor salt with alkali metal bases e.g., KHMDS, KO^{t}Bu (Scheme 1.7).[21b] Although the diphosphinocarbenes and diaminocarbene are kinetically stable but their dimerization is thermodynamically favored in the presence of Bronsted acids (Scheme 1.8).[33]
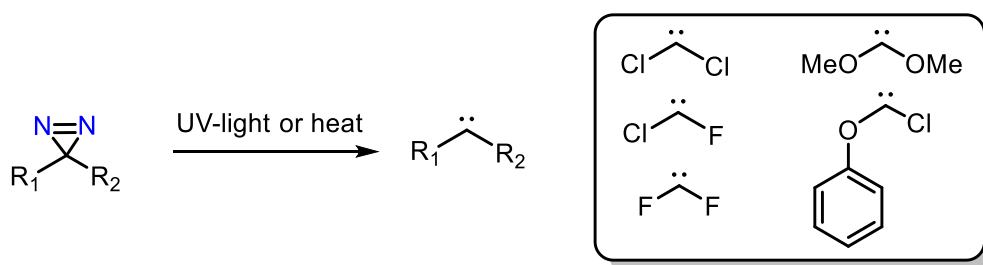
Scheme 1.5 Carbene synthesis from diazirine.
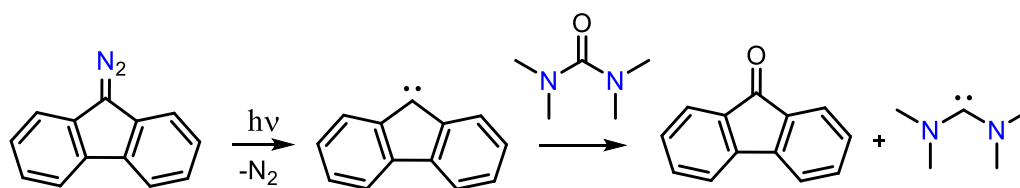
Scheme 1.6 Synthesis of carbene from oxygen atom transfer.

X = OR', SR', NR'$_2$
Y = Cl, OTf, BF$_4$
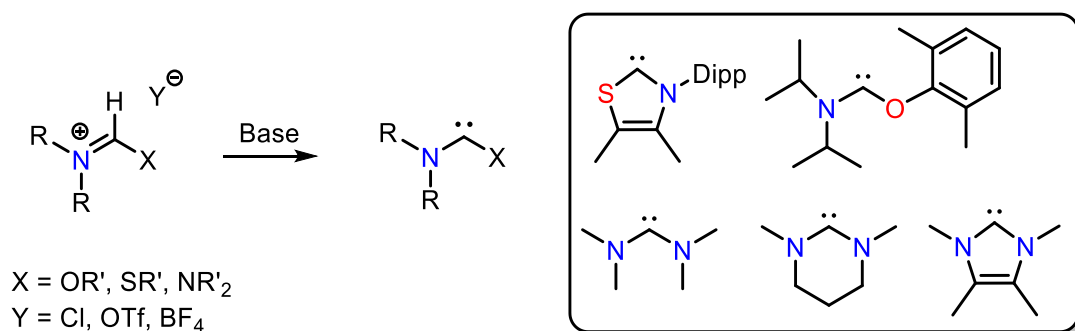
Scheme 1.7 Synthesis of carbene using deprotonation method.
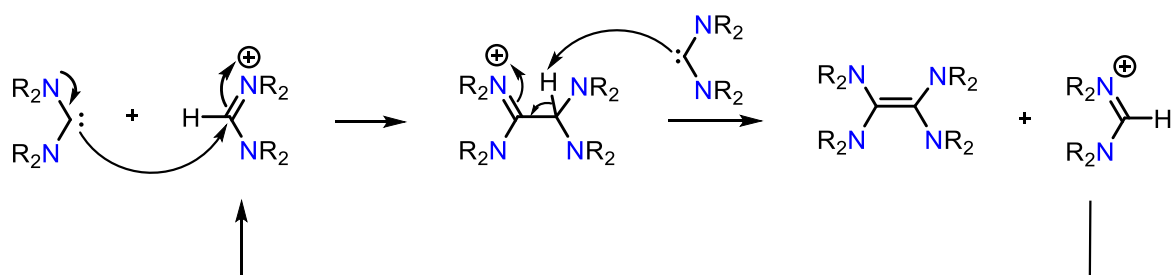
Scheme 1.8 Dimerization of carbene in the presence of Brønsted acid.

1.4 Modern singlet carbenes

Primary work by Wanzlick and co-workers in 1960s laid the foundation of the modern carbenes. In their study, they realized that the presence of amino substituents can enhance the stability of carbenes. Based on that, when they tried to synthesize the 1,3-diphenylimidazolidin-2-ylidene carbene (**B**, Scheme 1.9) by the thermal elimination of CHCl$_3$[34] from the precursor (**A**, Scheme 1.9), they ended up with the dimerized olefin product (**C**, Scheme 1.9) and did not observe any equilibrium between **B** and **C** (Scheme 1.9).[35a-c] Following this study, Denk and co-workers provided some sort of evidence for the existence of such equilibrium.[35d]
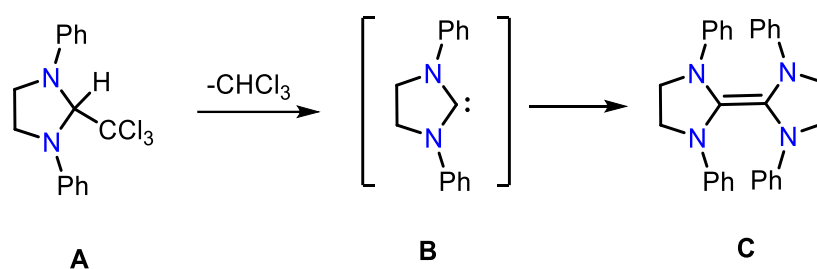
Scheme 1.9 Attempt for the synthesis of 1,3-diphenylimidazolidin-2-ylidene carbene.

Again in 1970, Wanzlick and co-workers used salt deprotonation method, they showed potassium *tert*-butoxide base can be used to deprotonate the precursor imidazolium salts. Unfortunately, they were only able to trap the carbene intermediate but could not isolate it.[36] In 1988, Bertrand and co-workers reported the synthesis of the first isolable acyclic carbene in low yield, stabilized by adjacent phosphorus and silicon substituents (Scheme 1.10).[37]
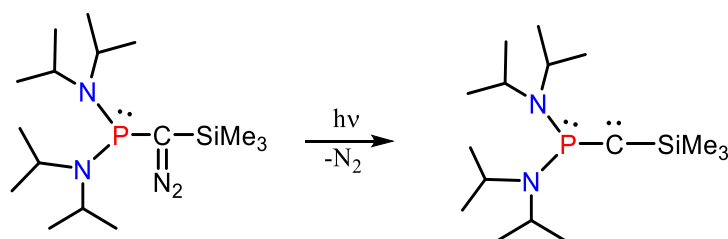
Scheme 1.10 Synthesis of first isolable carbene stabilized by P and Si α-substituents.

The first breakthrough in the domain of carbenes was achieved by the team of Arduengo in 1991, when they reported the preparation of first stable, isolable and bottleable carbene using bulky alpha adamantyl substituents, named as 1,3-di-l-adamantylimidazol-2-ylidene, later popularized as N-heterocyclic carbenes (NHCs) (Scheme 1.11).[38]
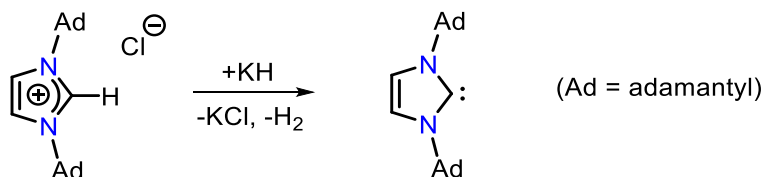
Scheme 1.11 Synthesis of first N-heterocyclic carbene (1,3-di(adamantyl)imidazol-2-ylidene).

In 2001, during the synthesis of an iridium hydride complex, Crabtree and co-workers found the abnormal binding (Scheme 1.12) of carbene through the C-5 position, not at the expected C-2 position.[39] Such abnormal carbenes are an alternative form of NHCs and are termed as abnormal NHCs or aNHCs because the absence of carbene center in between two nitrogen atoms (Figure 1.5). They have also been referred as mesoionic carbenes, because a neutral or non-zwitterionic resonance structure cannot be drawn for it.
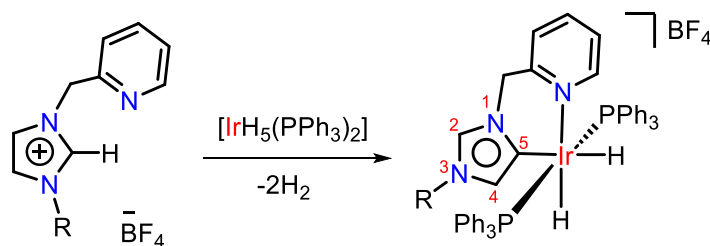
Scheme 1.12 Synthesis of the first metal aNHC complex.

Carbene and metal normal binding

Carbene and metal abnormal binding
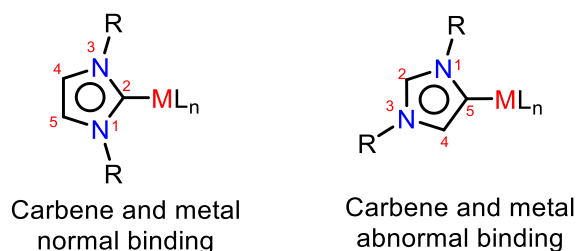
Figure 1.5 General interpretation of a normal and abnormal carbene.

Subsequently, Bertrand and co-workers reported the synthesis of first metal free abnormal NHC which is stable in both solution and solid states at room temperature (Scheme 1.13). Computational studies showed the more basic nature of aNHCs than its normal isomer and exhibit different properties.[40]

X = Cl, Br
Dipp = 2,6-diisopropylphenyl
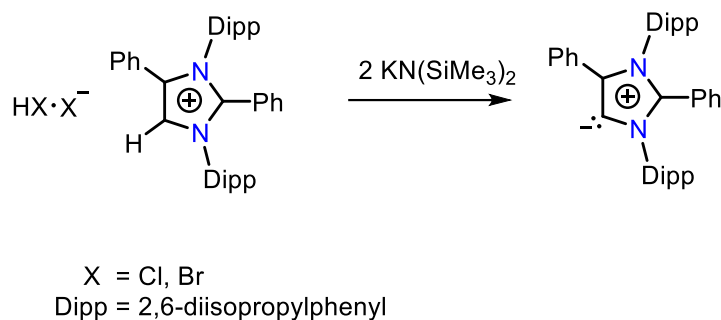
Scheme 1.13 Synthesis of the first mesoionic carbene.

Another modified version of NHC was reported by Bertrand and co-workers in 2005 called as cyclic (alkyl)(amino)carbenes (CAACs), which possess a quaternary carbon atom in place of one of the nitrogens placed α to the carbene center (Scheme 1.14).[41] As a result, CAACs are considered as strong σ-donor and weak π-acceptor ligands and their metal complexes exhibit prominent catalytic activity. Very recently in 2017, the same group has reported another bicyclic version of CAAC carbenes named as bicyclic alkyl amino carbenes (BICAACs) which feature enhanced σ-donating and π-accepting properties.[42]
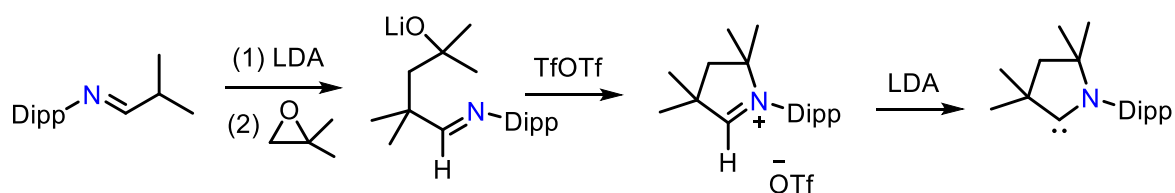
Scheme 1.14 Synthesis of cyclic (alkyl)(amino)carbene (CAAC).

1.4.1 Electronic properties of modern singlet carbenes

Till date, several stable carbenes have been reported which are different from each other in terms of their steric and electronic properties. The structural environment around the carbene

center effects the reactivity of resulting carbene. Various computational studies on carbenes provided the HOMO-LUMO energy data and values for singlet to triplet energy gap. The high HOMO and low LUMO energy levels of CAACs/BICAACs are responsible for better σ-donating and π-accepting properties than NHCs/MICs (Figure 1.6).[43]
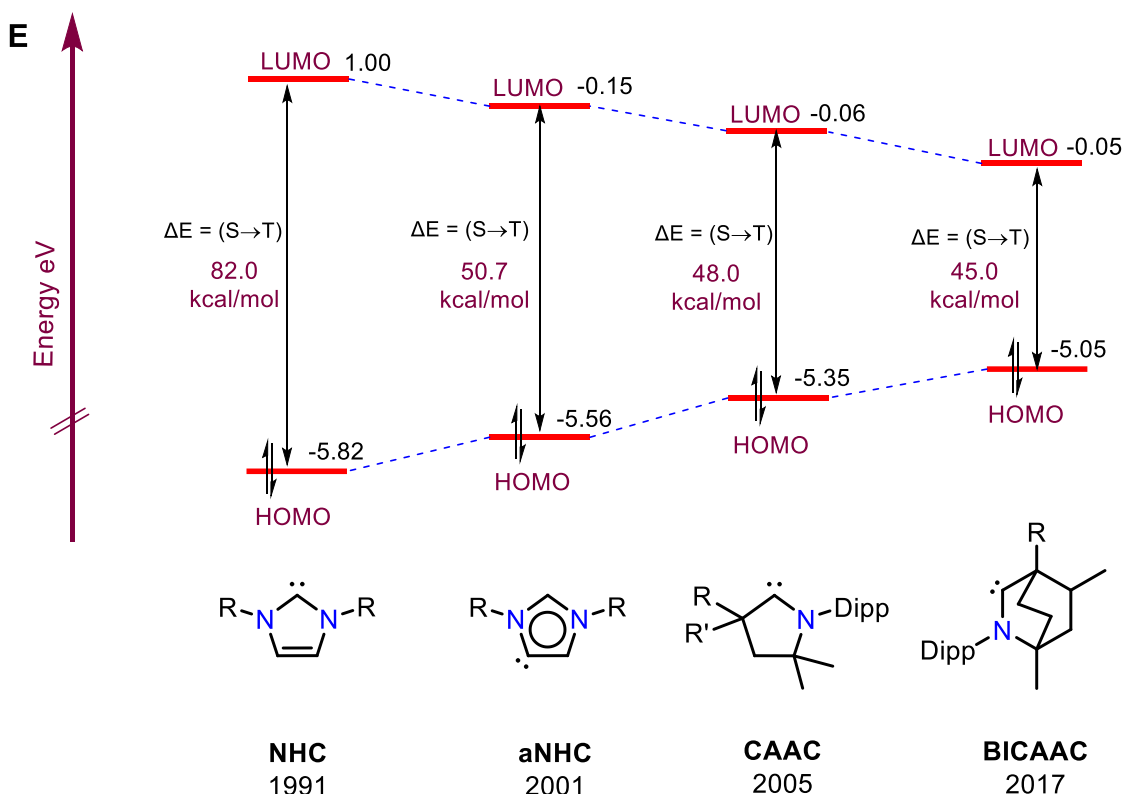
Figure 1.6 Calculated singlet-triplet energy difference (kcalmol^{-1}) and HOMO and LUMO energy values (in eV) for a few model cyclic carbenes (adapted from *Chem. Rev.* **2020**, *120*, 4141-4168).

1.5 Applications of carbenes

1.5.1 Applications of N-heterocyclic carbenes (NHCs)

Due to the strong σ-donating properties, N-heterocyclic carbenes easily form complexes with transition metals and the resulting NHC-metal bond is quite strong in nature. The NHC-metal complexes catalyze various organic transformations. By far, various complexes of NHC with different metals are known. The first NHC-Pd complex **1** (Figure 1.7) was synthesized by

Herrmann and co-workers in 1995 which was used as a catalyst in Mizoroki-Heck reaction.[44] Complexes of palladium and other metals with NHCs have been utilized in various cross-coupling reactions.[45] In 1999, Grubbs and co-workers synthesized the second-generation Grubbs catalyst **2** (Figure 1.7) by substituting one PCy₃ group of the first-generation Grubbs catalyst with an NHC ligand. The second-generation Grubbs catalyst showed air- and water-tolerance and exhibited an increased ring-closing metathesis activity at higher temperature with low catalyst loadings.[46] In 2001, Nolan and group reported the use of cationic Ir^{I}–NHC complex **3** (Figure 1.7) for the transfer hydrogenation of carbonyl compounds.[47] Thereafter, several Ir- and Ru-NHC complexes were reported by different groups which are capable of catalyzing important organic transformations.[48] The first Ag(I)-NHC complex **4** (Figure 1.7) was reported by Youngs and co-workers in 2004 which possess antimicrobial activity against *E. coli*, *P. aeruginosa* and *Staph. aureus*.[49] Other applications
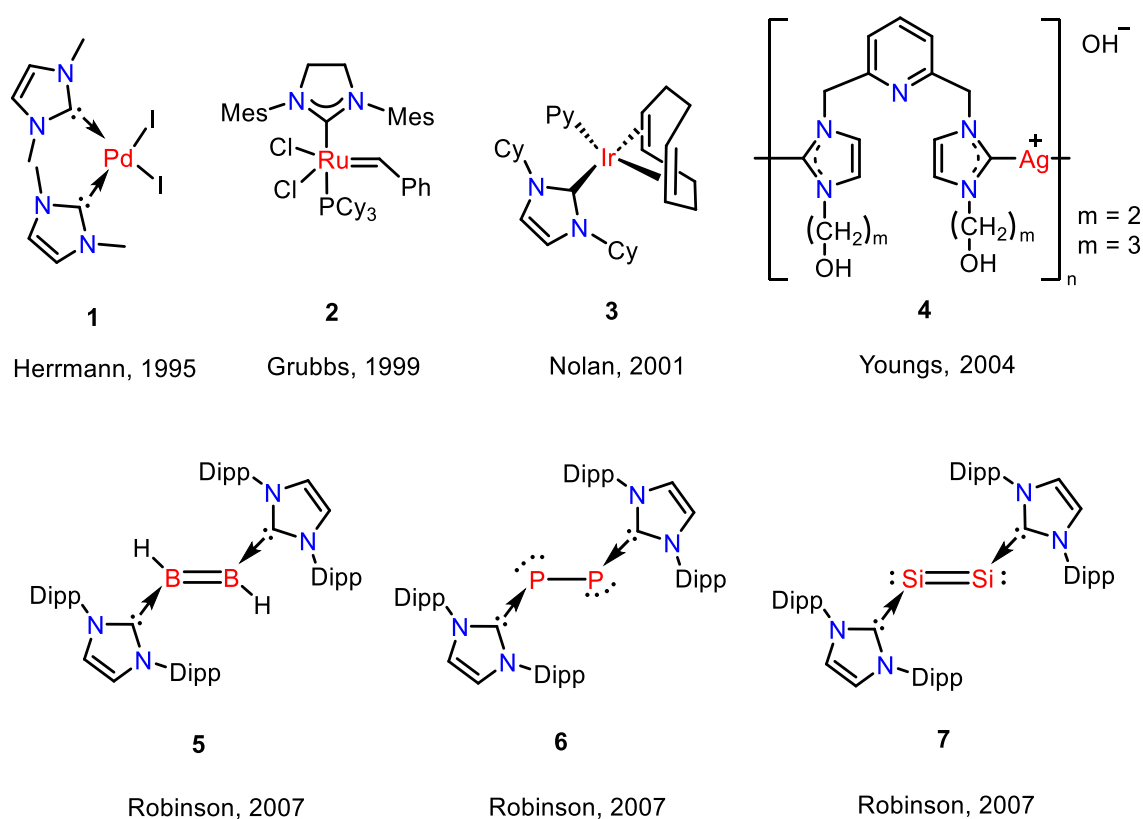
Figure 1.7 Selected examples of NHC stabilized transition metal and main-group complexes.

of NHC-metal complexes include the Au-catalyzed π-bond activation[50] and Pt-catalyzed hydrosilylation reactions.[51]

N-heterocyclic carbenes have also proven to be an essential tool to stabilize the main-group elements in their unusual oxidation states. Robinson and co-workers in 2007, showed the importance of NHC ligands to synthesize multiply bonded main-group compounds e.g., carbene stabilized diborane and diborene **5** (Figure 1.7), diphosphorus **6** (Figure 1.7) and silylene **7** (Figure 1.7) complexes.[52] The ability of NHC ligands to coordinate with carbon-based electrophiles give rise to another class of applications e.g., NHCs as organocatalysts.[53] This involves the nucleophilic attack of the carbene to the carbonyl center present in the substrate which ultimately forms enamine type "Breslow intermediate".[54] The field of NHC supported organocatalysis has gained significant attention in the past two decades.[55]

1.5.2 Applications of mesoionic carbenes (MICs)

As discussed previously, on blocking the C-2 position of an imidazolium salt, the removal of proton by a base occurred at the C-5 position, which afforded the abnormal NHC (aNHC). Over the last 15 years, the aNHC has been utilized to synthesize a wide range of transition metal and main-group based catalysts, which are proven to catalyze many organic transformations with improved selectivity and reactivity.[56] Apart from that, aNHCs are also capable of carrying out some metal-free catalysis. In 2001, Crabtree and co-workers reported the first cationic iridium complex **8** (Figure 1.8a) featuring aNHC as supporting ligand[39] and again in 2004 his group reported a new aNHC supported iridium complex featuring COD as assisting ligand **9** (Figure 1.8a).[57] Nolan and co-workers in 2004 reported an aNHC Pd complex **10** (Figure 1.8a) which catalyze the Suzuki-Miyaura and Mizoroki-Heck cross-coupling reactions.[58] Cavell and co-workers reported the synthesis of an aNHC-Pt complex **11** (Figure 1.8a).[59] Furthermore, Bertrand and co-workers reported an aNHC-Au complex **12**
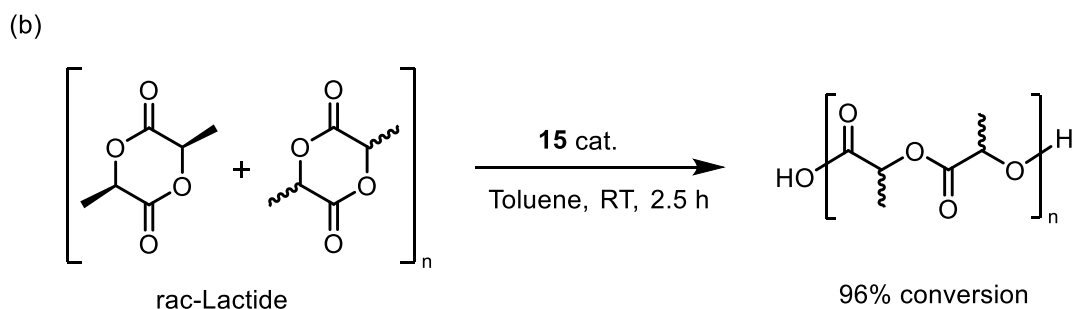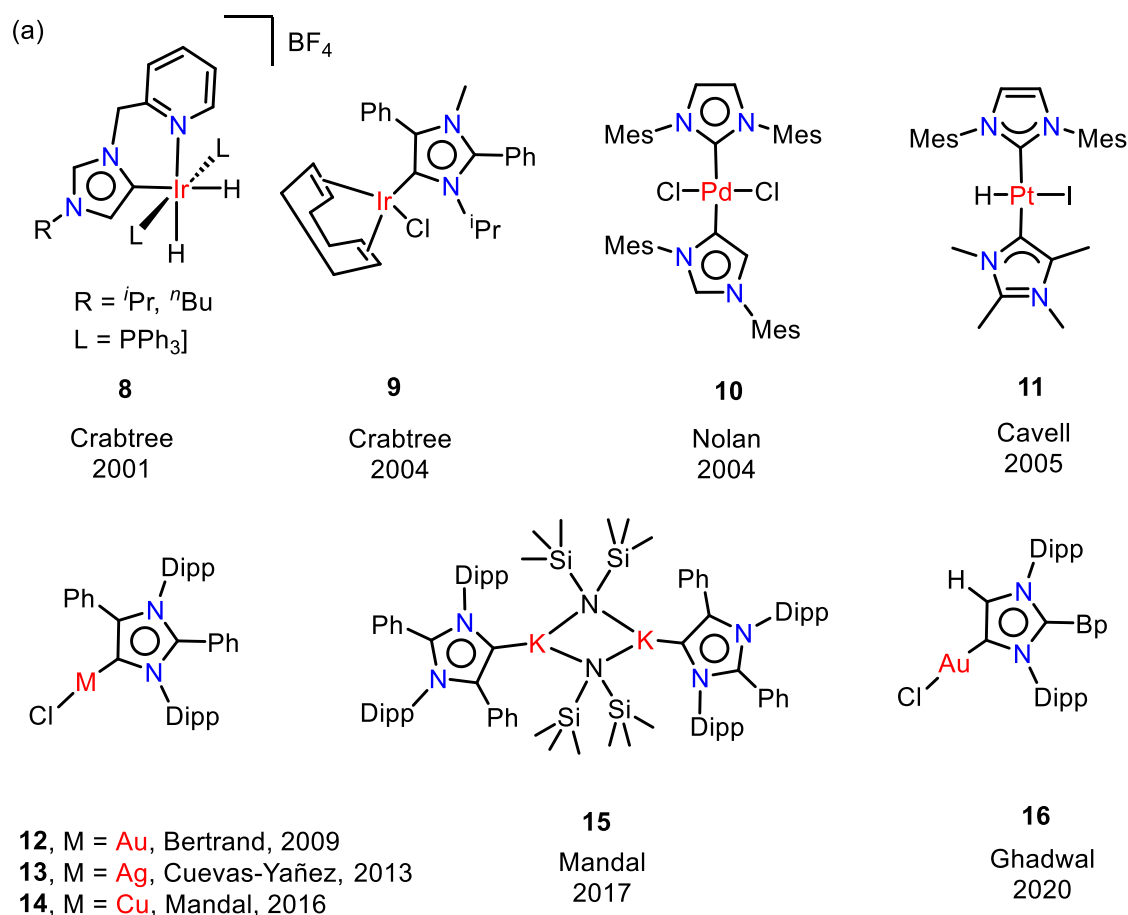
Figure 1.8 (a) Selected examples of aNHC supported metal and main-group complexes; (b) ring opening polymerization of *rac*-LA catalyzed by **15**.

(Figure 1.8a).[40] Later, it was realized that aNHC-Au complexes can take part in migratory insertion of carbenes into Au-C bonds at lower temperatures.[60] In 2013, Aldeco-Perez, Cuevas-Yanez and co-workers showed that aNHC-Ag complex **13** (Figure 1.8a) can catalyze [3+2] cycloaddition reaction of azides with alkynes even in the absence of copper additives.[61] In the same year, Mandal and co-workers synthesize aNHC supported Cu

complex **14** (Figure 1.8a), which is catalytically active for the Huisgen 1,3-dipolar cycloaddition reactions (click reactions). Mandal and co-workers also demonstrated the catalytic potential of Ni(I) and Fe(0) complexes of aNHC for the hydrosilylation of different unsaturated functional groups[62] and also showed the role of aNHC supported potassium complex **15** (Figure 1.8a) for the ring opening polymerization reactions (Figure 1.8b).[63] Lastly, the more basic nature of aNHCs than their NHC isomers, enable them to exhibits properties like small molecule activation[64] and metal free ring opening polymerization[65] reactions. Very recently, Ghadwal and co-workers isolated a C-5 protonated aNHC in which the C-2 position is blocked by a bulky biphenyl group, and showed reactivity with $Ni(CO)_4$, $(Me_2S)AuCl$ **16** (Figure 1.8a), white phosphorus and CO_2.[66]

1.5.3 Applications of cyclic (alkyl)(amino)carbenes (CAACs)

The replacement of one of the nitrogen atoms by a quaternary carbon in the heterocyclic backbone of a carbene results in the decrease in the HOMO-LUMO energy gap. Consequently, CAACs are proven to be more ambiphilic in nature (better σ-donor and better π-acceptor) than the NHCs.[41] In last 15 years or so, we have witnessed a range of CAAC supported transition metal complexes which have been utilized as a catalyst for various organic transformations, e.g., alkylation, cycloaddition, hydroamination, hydroarylation, hydrogenation, hydrosilylation, homocoupling, cross-coupling reactions and olefin metathesis.[67] These transition metal complexes can be reduced with potassium graphite (KC_8), Na, K and Na-naphthalenide etc. to give zero-valent species (Figure 1.9a).[68] The more ambiphilic nature of CAACs have also helped chemists to synthesize challenging complexes form the domain of main-group elements including the unusual multiple bonded compounds and radical species.[69-70] In 2013-14, Bertrand and co-workers reported CAAC derived bottleable amino carboxy radical **17** (Figure 1.9b) and neutral antimony-based radical **18** (Figure 1.9b) characterized in solution.[71] Furthermore, the groups of Braunschweig and
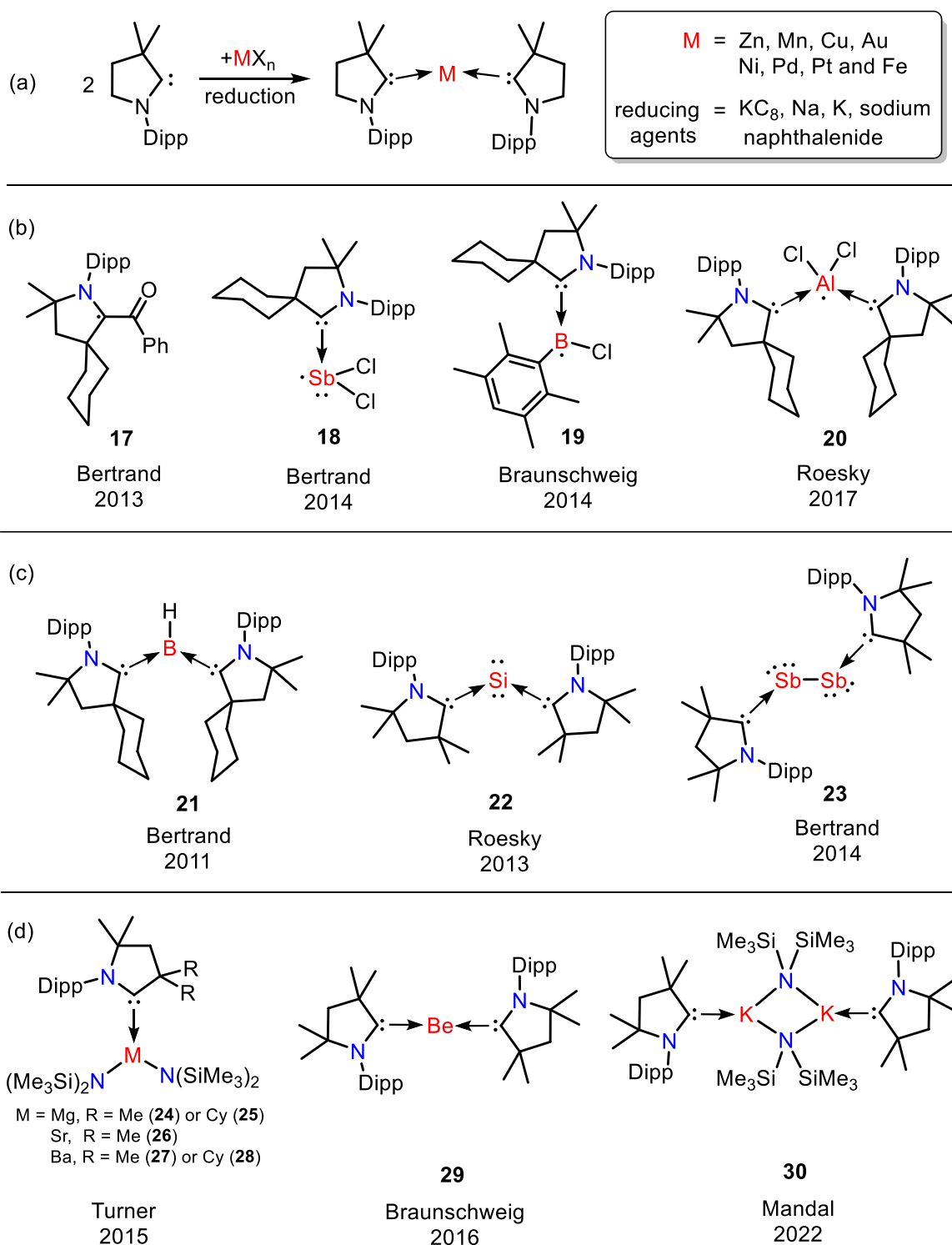
Figure 1.9 (a) General representation for the synthesis of [(CAAC)₂M(0)] complexes; (b) selected examples of CAAC derived main-group radicals; (c) selected examples of CAAC derived low-valent complexes with *p*-block elements; (d) selected examples of CAAC derived low-valent complexes with *s*-block metals.

Roesky independently synthesized CAAC supported boron and aluminum radicals **19** and **20** (Figure 1.9b), respectively.[72] A significant number of CAAC-based complexes featuring the *p*-block elements in low-valent state have been documented in the recent years.[69] Bertrand and co-workers reported a neutral tricoordinate CAAC-organoboron complex **21** (Figure 1.9c), isoelectronic with amines.[73] Roesky and co-workers reported a singlet biradicaloid siladicarbene (L:)$_2$Si (L = CAAC), called as silylone **22** (Figure 1.9c) in which the silicon atom is present in formal zero oxidation state.[74] Bertrand and his team found that CAAC can stabilize antimony in the formal oxidation state of zero by synthesizing a Sb-Sb bonded complex **23** (Figure 1.9c).[71b] Talking about the less explored carbene *s*-block complexes, Turner and co-workers reported the syntheses of CAAC supported Mg, Sr and Ba complexes **24-28** (Figure 1.9d).[75] Thereafter in 2016, utilizing CAAC as ancillary ligand, Braunschweig and co-workers synthesized the very first Be(0) complex **29** (Figure 1.9d).[76] Next, Mandal and co-workers synthesized a CAAC-based potassium complex **30** (Figure 1.9d), which is catalytically active for the ring-opening polymerization of *ε*-caprolactone.[63] The other major
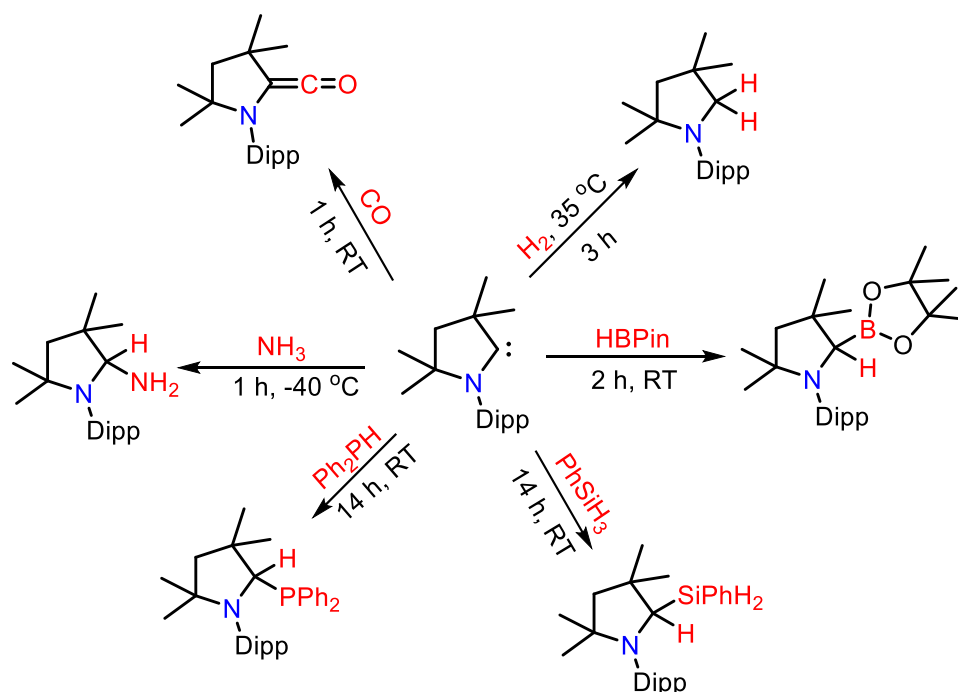
Scheme 1.15 Small molecule activation shown by CAAC.

application of CAACs includes the activation of a variety of small molecules having enthalpically strong bonds such as CO, HBPin, H_2, $PhSiH_3$, Ph_2PH and NH_3 under mild conditions (Scheme 1.15).[69b, 77]

1.5.4 Metalla-N-heterocyclic carbenes (MNHCs) and their applications

So far, we have discussed how modifying the heterocyclic structure of NHCs can introduce new categories of carbenes. By altering the position of the carbene carbon, we have seen the emergence of mesoionic carbenes (MICs). Additionally, by substituting ring nitrogen atoms with various heteroatoms like oxygen (O), sulfur (S), phosphorus (P), and carbon (C), chemists paved the way for the development of novel carbenes.[78] In 2014, Ruiz and co-workers introduced a new type of carbene known as metalla-N-heterocyclic carbenes (MNHCs).[79] This innovation involved replacing the C4 carbon in Arduengo's carbene **A** (Scheme 1.16) with a transition metal fragment, ultimately resulting in the creation of a new carbene **B** (Scheme 1.16) within the NHC framework. Subsequently, the species **B** undergoes
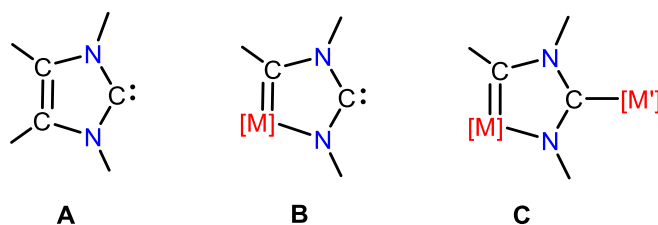
Scheme 1.16 Arduengo carbene (**A**), and a new carbene complex within an NHC framework (**B**), and heterometallic dicarbene derivatives (**C**). [M], [M'] = transition-metal fragments.

coordination with a new metallic center, giving rise to an unprecedented heterometallic dicarbene species, denoted as **C** (Scheme 1.16). The reaction involving a dichloromethane solution of the cationic diaminocarbene complex *fac*-[Mn{C(NHPh)(NHMe)}(CO)$_3$(bipy)]$^+$ (**31**) and [AuCl-(PPh$_3$)] in a 1:1 ratio, conducted in the presence of an excess of KOH, resulted in the formation of the heterometallic neutral complex **33a** with Mn^I and Au^I units (Scheme 1.17). Detailed IR studies indicated the presence of the formamidinyl complex **32** as
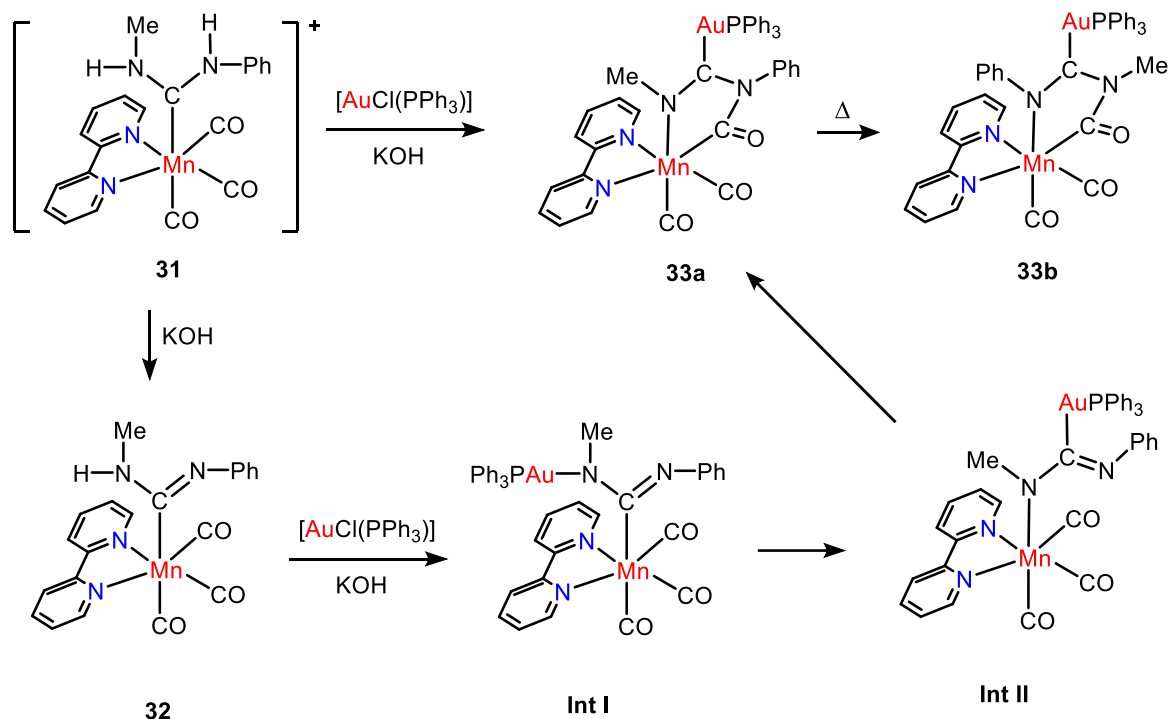
Scheme 1.17 Synthesis of Mn^I/Au^I based heterometallic neutral complexes.

intermediate in the reaction. Subsequently, **33a** was completely transformed into isomer **33b** by heating the THF solution at reflux for 20 minutes. Isomer **33a** closely resembles **33b**, with the only difference being the translocation of the NMe and NPh groups, swapping their positions. Additionally, this translocation process involved the migration of Mn^I and Au^I ions (intermediates **I** and **II**, Scheme 1.17), resulting in the nitrogen atom being bonded to Mn and the carbene carbon atom being bonded to Au center.

Furthermore, they also found that complexes **33a** and **33b** can undergo alkylation at the carbamoyl oxygen atom, following a similar transformation process by which acyl complexes are converted into Fischer carbenes.[80] This conversion is accomplished through treatment with methyl triflate, resulting in the formation of cationic complexes **34a** and **34b**, respectively (Scheme 1.18).
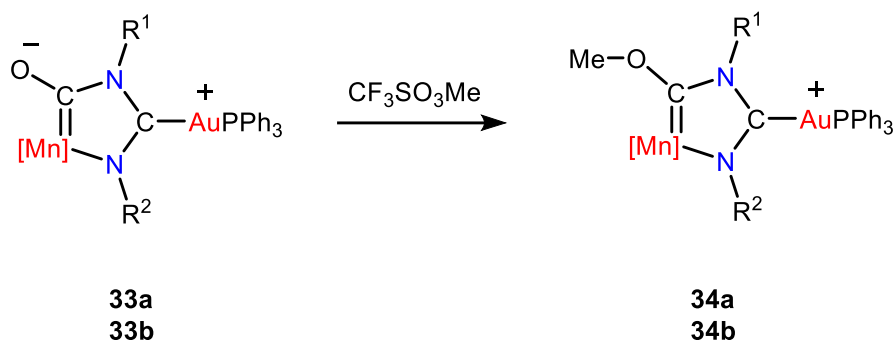
Scheme 1.18 Syntheses of the mixed Fischer/Arduengo carbene complexes **34a** and **34b**. [**33a**, **34a**: R^1 = Ph, R^2 = Me; **33b**, **34b**: R^1 = Me, R^2 = Ph. [Mn] = [Mn(CO)$_2$(bipy)]].

In 2014, the same group also documented a novel procedure for syntheses of iron-based MNHCs, which were subsequently validated for their robust electron-donating characteristics through a comparison of the ν(CO) and ν(CN) stretching frequencies. The synthetic procedure includes the transformation of precursor complex [Fe(Cp)(CO)(CNxylyl)$_2$]$^+$ (**35**) into a ruthena-N-heterocyclic carbene (**40**) through a multi-step reaction pathway (Scheme 1.19).[81]
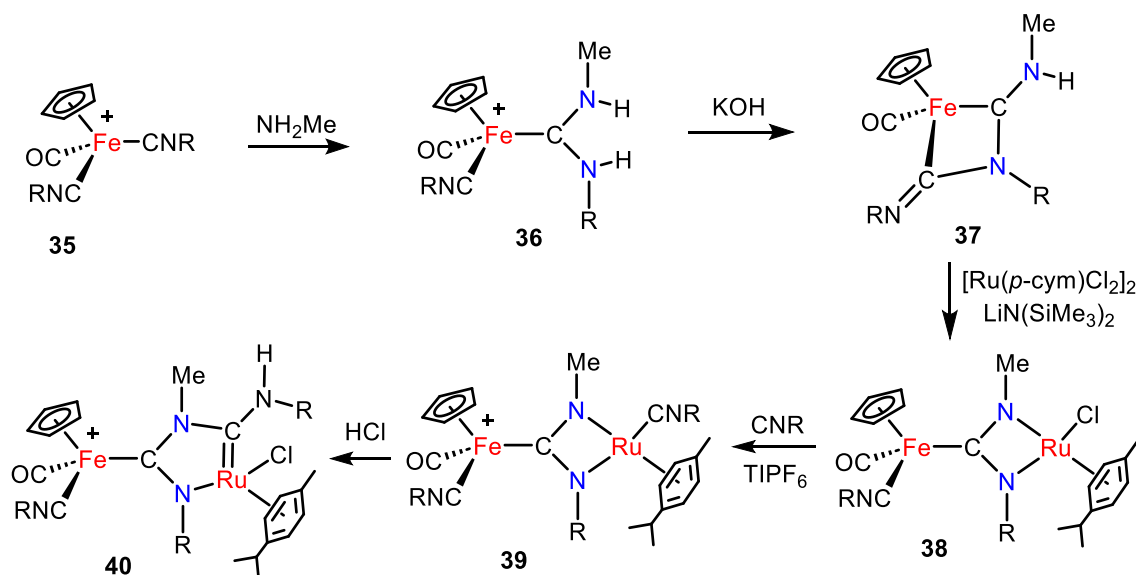
Scheme 1.19 Synthesis of Fe-based metalla-N-heterocyclic carbene (**40**) from a coordinated isocyanide ligand in (**35**) (R = xylyl).

The IR spectrum of complex **40** showed stretching bands for ν(CO) at 1975 cm^{-1} and ν(CN) at 2114 cm^{-1} which is relatively lower than the acyclic diamino carbene (ADC)

precursor **36** (1976 and 2130 cm^{-1}, respectively) indicating the stronger donor nature of the MNHC than the ADC.[81]

Moreover, in order to compare the structural and electronic attributes of this recently developed metalla-N-heterocyclic carbene in relation to its classical NHC counterpart when coordinated to the same metal fragment, the precursor complex **35** was further transformed into the cationic complex **41** through a [3+2] coupling reaction between **35** and propargylamine (Scheme 1.20). Complex **41** exhibits the most elevated ν(CN) and ν(CO) values, measured at 2132 and 1983 cm^{-1} respectively, signifying that its imidazol-2-ylidene ligand can be considered the least potent electron donor within this series.[81] Further, complex **41** can be alkylated at the nitrogen center to give **42**.
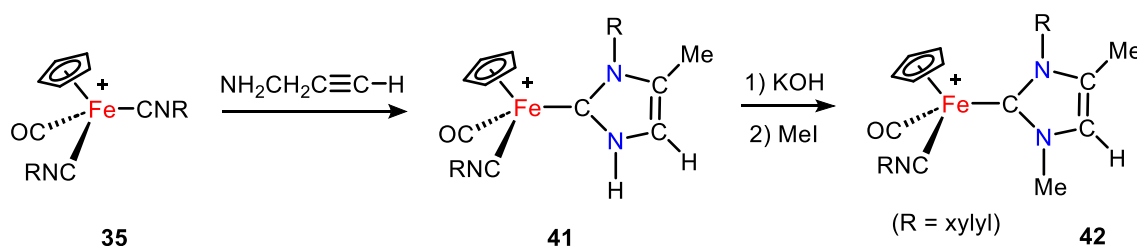
Scheme 1.20 Synthesis of cationic complex **41** by a [3+2] coupling reaction of propargylamine and isocyanide precursor **35**, and its further derivatization to give **42**.

Furthermore, the density functional theory (DFT) calculations carried out by Phukan and co-workers on a set of newly designed metalla-N-heterocyclic carbenes (MNHCs) to achieve singlet state stability. They found all MNHCs exhibited a stable singlet ground state. The incorporation of π-donor groups like OMe and NMe$_2$ into the carbene framework notably increased ΔE_{S-T} values for the five-membered MNHCs.[82] Additionally, some MNHCs displayed substantial ΔE_{S-T} values (ranging from 30 to 50 kcal mol^{-1}), akin to experimentally known carbenes. Interestingly, the MNHCs demonstrated superior σ-donation capabilities compared to their parent carbenes. Calculated parameters such as proton affinities (PA), *p*Ka, and gallium pyramidalization were consistent with the MNHCs' σ-donation capabilities. In

another report, they also showed via DFT calculations how MNHCs react with various small molecules (H_2, NH_3, PH_3, SiH_3Ph, and CH_4) for activation process. These MNHCs were found to possess a stable singlet ground state and suitable electronic properties for activating small molecules.[83] The computed energy barriers for E–H (E = H, C, N, Si, P) activation by MNHCs closely matched those observed in experiments with cyclic (alkyl)(amino) carbenes (CAACs) and diamidocarbenes (DACs). This suggests that incorporating an additional metal center within a cyclic NHC enhances their ability to activate bonds, introducing a novel and underexplored strategy for challenging bond activations with carbenes.

1.5.5 Synthesis and applications of bicyclic (alkyl)(amino) carbenes (BICAACs)

After the successful isolation of CAACs in 2005, Bertrand and co-workers in 2017 reported another version of stable and storable carbenes called as bicyclic alkyl amino carbenes (BICAACs).[42] While CAACs were synthesized from an intramolecular 5-*exo* cyclization of an imine under acidic conditions, the BICAAC synthesis involved the replacement of 2-methyl-2-propenyl group by a methyl or isopropyl group (Scheme 1.21). As a result, the
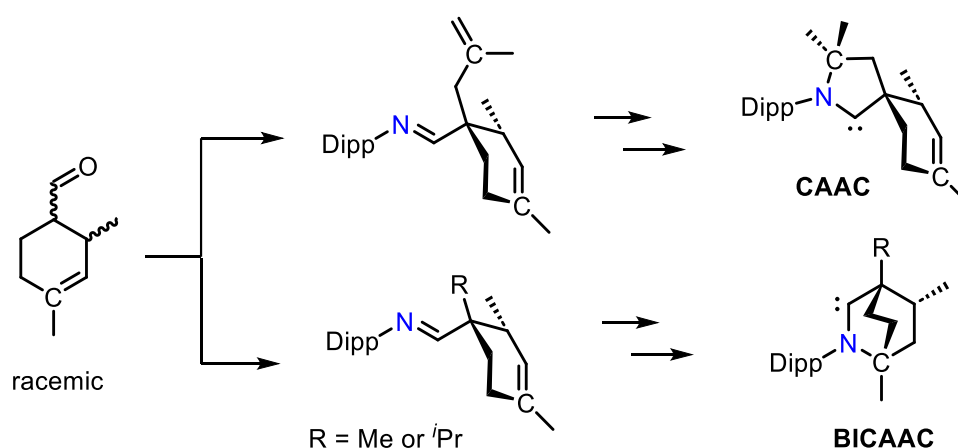
Scheme 1.21 Methodology for the synthesis of BICAACs (adapted from *J. Am. Chem. Soc*. **2017**, *139*, 7753-7756).

cyclization and rearrangement would occur at the endocyclic double bond of cyclohexane ring through 6-*endo* cyclization leading to the bicyclic iminium salt.

By doing so, the steric environment around the carbene center in BICAACs becomes similar to those of traditional NHCs. Consequently, the BICAACs become more σ-donating and π-accepting in nature than the monocyclic CAACs which is also proven from the computational and experimental evidences. The synthesis of BICAAC starts off with condensation of 2,6-diisopropylaniline and 2,4-dimethylcyclohex-3-ene-1-carbaldehyde (trivertal) under acidic conditions to afford the aldimine. Deprotonation of aldimine with *n*-butyl lithium and subsequent alkylation with methyliodide or 2-bromopropane diastereoselectively forms the alkylated product, which undergo a 6-*endo* cyclization in the presence of excess HCl followed by the anion exchange (from Cl$^-$ to BF$_4^-$) leading to the formation of the final iminium salt. The iminium salt upon deprotonation with KHMDS generates free BICAAC (Scheme 1.22).[42]
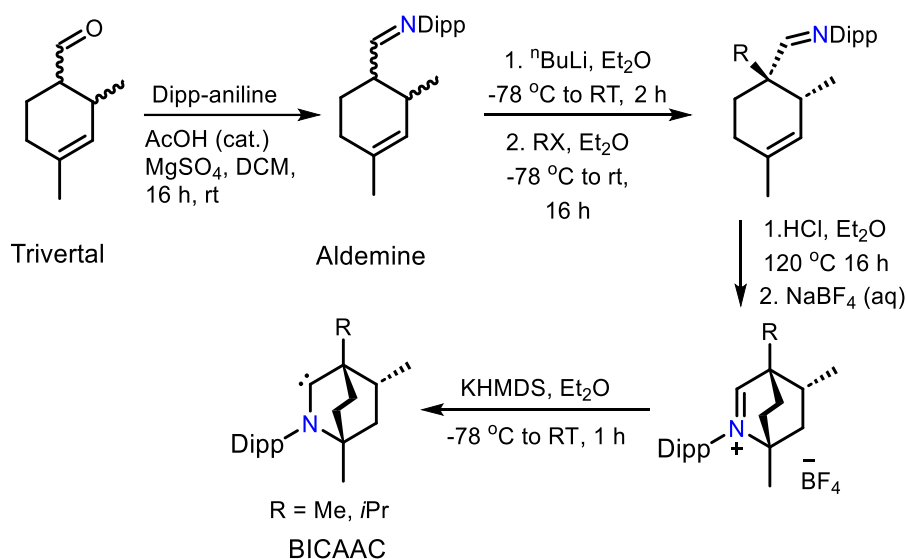
Scheme 1.22 Synthetic route for the preparation of BICAACs (adapted from *J. Am. Chem. Soc.* **2017**, *139*, 7753-7756).

After isolating of BICAAC they synthesized few BICAAC complexes and adducts **43-45** (Scheme 1.23) to study the electron donation property of BICAAC ligand via the perturbation in spectroscopic measurements (IR and NMR), owing to the change in the electronic properties of resulting molecule. By examining the CO bond stretching frequency,

^{31}P and ^{77}Se NMR, and ligand exchange reactions, they concluded that the BICAAC is slightly better σ-donor and π-acceptor as compared to CAAC. Computational studies showed the singlet-triplet energy gap in BICAAC to be 45.7 kcal/mol (49.2 kcal/mol in CAAC), which further supports the experimental results.[42]
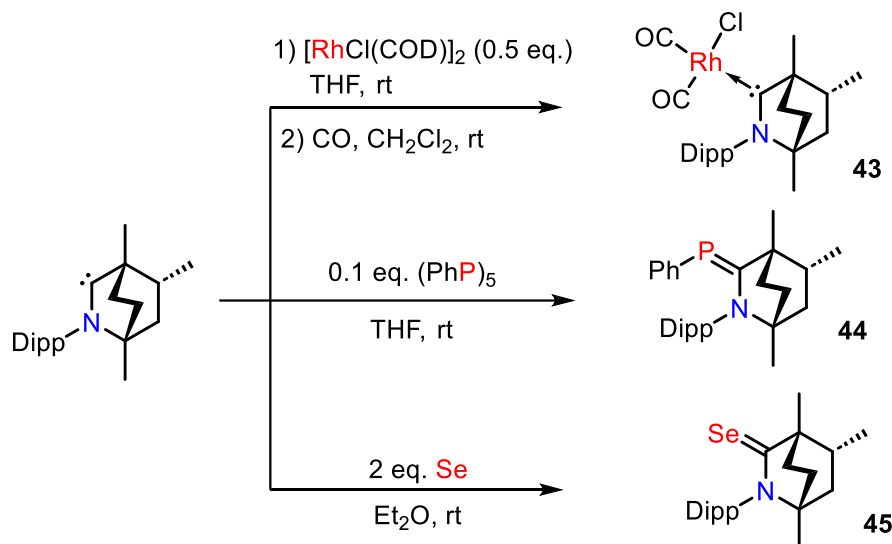
Scheme 1.23 Synthesis of BICAAC-Rh complex, and BICAAC derived phosphinidene and selenium adducts (adapted from *J. Am. Chem. Soc*. **2017**, *139*, 7753-7756).

BICAAC's ambiphilic properties could be used to create novel and unconventional compounds. Recognizing the significance of BICAAC, in 2019 Singh and co-workers demonstrated how reactive BICAAC is to a variety of hydro- and haloboranes (Scheme 1.24). We found that the reaction of BICAAC generates Lewis adducts with borontrihalides e.g.,
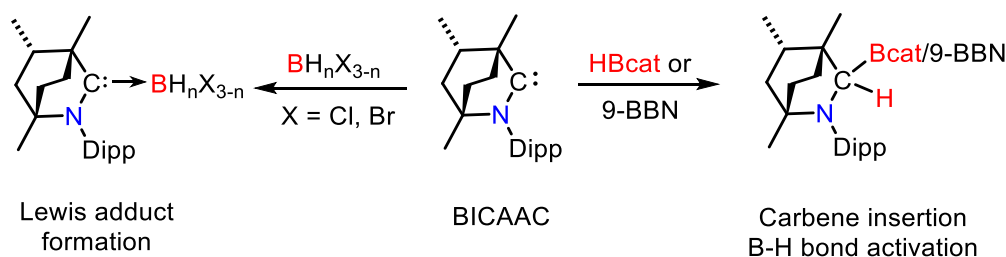
Scheme 1.24 Reactivity of BICAAC towards different boranes.

BICAAC−BF_3, BICAAC−BCl_3, BICAAC−BBr_3, BICAAC−$B(C_6F_5)_3$, and similar adducts with less hydridic boranes BICAAC−BH_3, BICAAC−BH_2Cl, BICAAC−$BHCl_2$, whereas

with more hydridic boranes [9-borabicyclo[3.3.1]nonane (9-BBN) and catecholborane (HBcat)] the insertion of the carbene carbon into the B–H bond was observed (Scheme 1.24).[84]

Next, Singh and co-workers have shown the execution of BICAAC ligand to generate two-coordinated neutral Cu complex **46** (Figure 1.10). In the presence of an extra equivalent of BICAAC, **46** reacts with KPF$_6$ to produce homoleptic cationic complex **47** (Figure 1.10).[85]
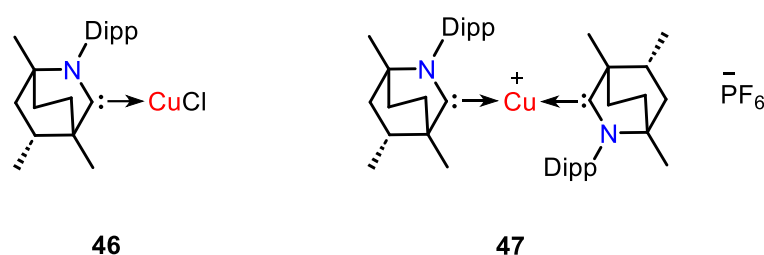
Figure 1.10 Neutral and cationic BICAAC-Cu complexes.

Moreover, Bertrand and co-workers have shown the catalytic activity of Au-complexes supported by a variety of ligands (R$_3$P, NHC, CAAC-5, CAAC-6, and BICAAC) in the hydroamination and hydrohydrazination of alkynes (Scheme 1.25). According to kinetic measurements, the BICAAC-Au complex is the most active catalyst for these conversions, which was further validated by mechanistic and DFT investigation. The metal is
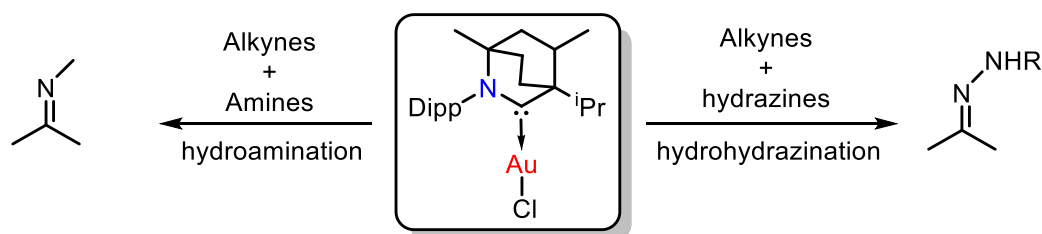
Scheme 1.25 Catalytic application of BICAAC-Au complex.

protected from decomposition by the BICAAC ligand's particular steric and electronic environment, which also stabilizes the π-alkyne key intermediate complex and promotes a

low proton transfer barrier.[86] In 2021, Singh and co-workers reported BICAAC derived palladium complex (BICAAC)$_2$PdCl$_2$ (**48**) (Scheme 1.26) which was found to be catalytically active for Heck-Mizoroki and Suzuki-Miyaura cross-coupling reactions under low catalyst loading and open-air conditions.[87]
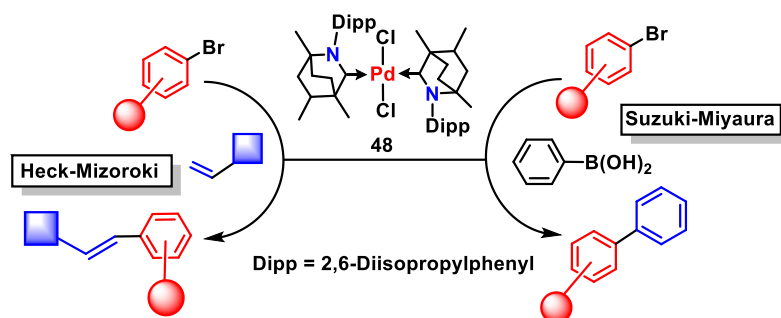
Scheme 1.26 Implementation of (BICAAC)$_2$PdCl$_2$ complex as a catalyst for Heck-Mizoroki and Suzuki-Miyaura cross-coupling reactions.

In the same year, Mandal and co-workers synthesized BICAAC stabilized dicoordinated zinc(0) complex [(BICAAC)$_2$Zn] (**49**) (Scheme 1.27). DFT studies showed that the BICAAC plays a key role in stabilizing this complex. Complex **49** produces the Gomberg's free radical **50** (Scheme 1.27) by activating the C(sp3)-Cl bond of trityl chloride.[88]
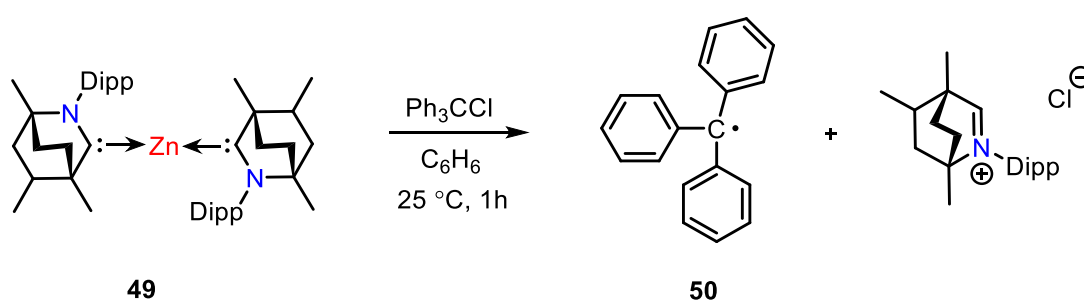
Scheme 1.27 BICAAC derived Zn(0) complex **49** and generation of Gomberg's free radical **50** by activating the C(sp^3)-Cl bond of trityl chloride.

Next, a variety of structurally and electronically diverse novel BICAAC-Ru complexes **51-53** were reported (Figure 1.11) by Tuba and co-workers in 2022, which were

found to be efficient catalyst for the temperature-activated olefin metathesis. These catalysts demonstrated activity for the conversion of long-chain olefins to propylene. When compared with second generation Hoveyda-Grubbs or CAAC-Ru catalysts, these thermally stable catalysts exhibit much greater selectivity to propylene at a reaction temperature of 75 °C.[89]

51 **52** **53**
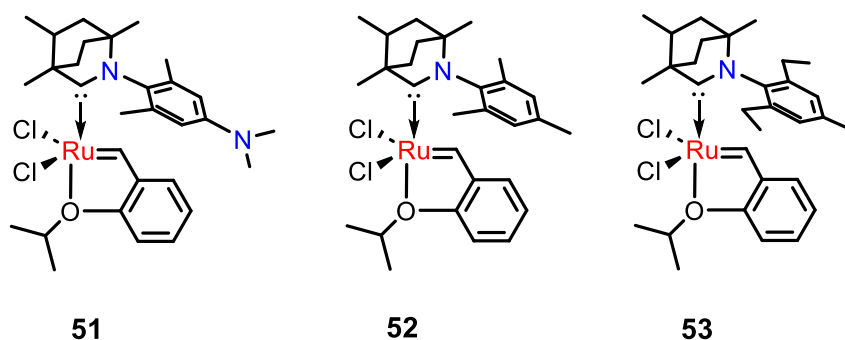
Figure 1.11 Selected examples of BICAAC-Ru complexes.

In 2022, Singh and co-workers have synthesized a number of BICAAC stabilized Ni(II) complexes [(BICAAC)$_2$NiX$_2$] (X = Cl, Br, and I) (**54-56**) (Figure 1.12), and when these complexes were reduced with KC$_8$, two coordinated low valent Ni(0) complex [(BICAAC)$_2$Ni(0)] (**57**) (Figure 1.12) was produced. In the presence of 3 mol% catalyst loading, these complexes were catalytically effective for the Negishi cross-coupling reaction of different aryl halides using 2,6-difluorophenylzinc bromide or phenylzinc bromide as the coupling partner. The UV-vis and HRMS measurements of controlled experiments supported

X = Cl, XX (**54**)
X = Br, XX (**55**)
X = I, XX (**56**)

57
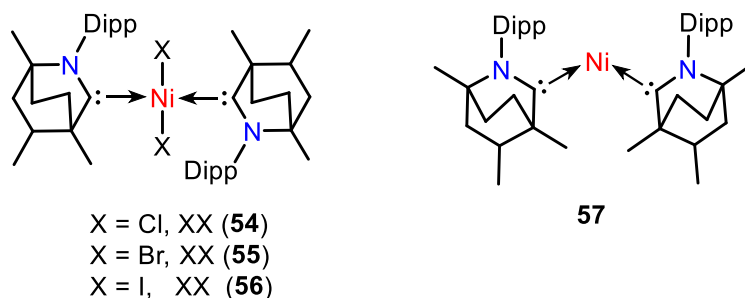
Figure 1.12 A variety of BICAAC supported Ni complexes **54-57**.

the involvement of Ni(I)/NI(III) species in catalytic cycle with a penta-coordinated Ni(III)-aryl species as the key intermediate for catalyst [(BICAAC)$_2$NiCl$_2$].[90] Very recently in 2022,

Mandal and co-workers employed BICAAC as a metal-free catalyst for the reduction of different nitriles with pinacolborane to give the corresponding amine hydrochloride salts after workup (Scheme 1.28). DFT calculations and other control experiments suggested the addition of B–H bond to the carbene center to generate the active catalyst **58** (Scheme 1.28), which further serves as a carrier for the hydride source.[91]
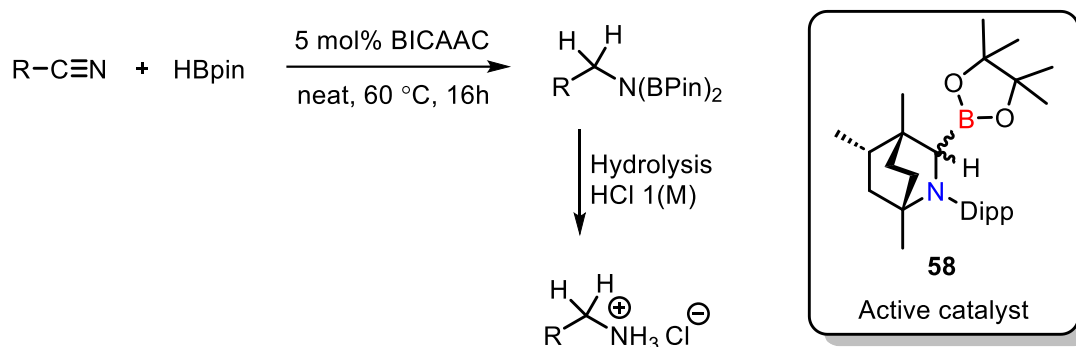
Scheme 1.28 BICAAC as a metal free catalyst for the reduction of nitriles to amine salts using pinacolborane.

1.6 Aims and objectives

Drawing upon the remarkable ambiphilic properties of BICAAC, as elucidated by us and others earlier, we aimed to extend our exploration further into the realm of main group chemistry. Recently synthesized BICAAC-borane adducts offer ample opportunities to broaden the application of BICAAC in the domains of cationic boron compounds and low-valent boron chemistry containing multiply bonded B atoms. Therefore, our current goal is to utilize the BICAAC-haloborane adducts for creating low-valent boron-boron multiply bonded complexes and explore their reactivity towards coinage metal salts. Moreover, the recently prepared BICAAC−BH₃ adduct serves as a promising precursor for synthesizing BICAAC-stabilized borenium cations or their equivalents. The resulting boron cations exhibit enhanced polarizing power, compared to their covalent precursors, making them valuable catalysts for various organic transformations. Concurrently, we are exploring the interactions of BICAAC

with group 15 and 16 compounds, with a specific focus on synthesizing novel low-valent complexes in this category. In addition to our primary focus on main-group chemistry, we aim to investigate the potential of BICAAC in the synthesis of Ir(I) complexes. While there is a substantial body of research on Ir(III) complexes supported by various ligand frameworks, and their applications in a wide range of organic transformations are well-documented, Ir(I) complexes remain relatively underexplored. Given the unique properties of BICAAC as a superior ambiphilic ligand, we are particularly interested in delving deeper into the mechanistic aspects of these Ir(I) complexes. By leveraging BICAAC's distinctive capabilities, we hope to uncover novel insights and expand the current understanding of their reactivity and potential applications. The ensuing discussion across different chapters provide detailed insights into the current work and outcome of our efforts.

1.7 References

1. (a) Kirmse, W. *Carbene Chemistry*; Academic Press: New York, **1964** and **1971**; (b) Jones, M.; Moss, R. A. *Carbenes*; Wiley: New York, **1973** and **1975**; Vols. 1 and 2.

2. (a) Regitz, M. *Carbene (carbenoide) In Methoden der Organischen Chemie (Houben-Weyl)*, Georg Thieme: Stuttgart, **1989**; Vols. 1 and 2; (b) Brinker, U. H. *Advances in Carbene Chemistry*; Jai Press: Greenwich and Stamford, **1994** and **1998**; Vols. 1 and 2.

3. Frémont, P. D.; Marion, N.; Nolan, S. P. *Coord. Chem. Rev.* **2009**, *253*, 862-892.

4. Dumas, J. B.; Peligot, E. M. *Ann. Chim. Phys.* **1835**, *58*, 5-74.

5. Geuther, A.; Hermann, M. *Liebigs Ann. Chem.* **1855**, *95*, 211-225.

6. Nef, J. U. *Liebigs Ann. Chem.* **1897**, *298*, 202-374.

7. Gomberg, M. *J. Am. Chem. Soc.* **1900**, *22*, 757-771.

8. Staudinger, H.; Kupfer O. *Berichte der deutschen chemischen Gesellschaft* **1911**, *44*, 2194-2197.

9. Staudinger, H.; Kupfer O. *Berichte der deutschen chemischen Gesellschaft* **1912**, *45*, 501-509.

10. Davis Jr, W. H.; Pryor, W. A. *Organic Free Radicals*, American Chemical Society, Washington, D.C., **1977**.

11. Doering, W. v. E.; Knox, L. H. *J. Am. Chem. Soc.* **1953**, *75* 297-303.

12. Doering, W. v. E.; Hoffmann A. K. *J. Am. Chem. Soc.* **1954**, *76*, 6162-6165.

13. (a) Parham, W. E.; Reiff, H. E. *J. Am. Chem. Soc.* **1955**, *77*, 1177-1178; (b) Parham, W. E.; Twelves, R. R. *J. Org. Chem.* **1957**, *22*, 730-734; (c) Skell, P. S.; Sandler, S. R. *J. Am. Chem. Soc.* **1958**, *80*, 2024-2025.

14. Fischer, E. O.; Maasbol, A. *Angew. Chem. Int. Ed. Engl.* **1964**, *3*, 580-581.

15. (a) Chinoporos, E. *Chem. Rev.* **1963**, *63*, 235-255; (b) Schubert, U. *Coord. Chem. Rev.* **1984**, *55*, 261-286; (c) Lappert, M. F.; Rowe, R. S. *Coord. Chem. Rev.* **1990**, *100*, 267-292; (d) Bertrand, G.; Reed, R. *Coord. Chem. Rev.* **1994**, *137*, 323-355.

16. Schuster, G. B. *Adv. Phys. Org. Chem.* **1986**, *22*, 311-361.

17. Gleiter, R.; Hoffmann, R. *J. Am. Chem. Soc.* **1968**, *90*, 1475-1485.

18. (a) Bally, T.; Matzinger, S.; Truttmann, L.; Platz, M. S.; Morgan, S. *Angew. Chem. Int. Ed. Engl.* **1994**, *33*, 1964-1966; (b) Ford, F.; Yuzawa, T.; Platz, M. S.; Matzinger, S.; Fulscher, M. *J. Am. Chem. Soc.* **1998**, *120*, 4430-4438.

19. (a) Regitz M. *Angew. Chem. Int. Ed. Engl.* **1991**, *30*, 674-676; (b) Heinemann, C.; Müller, T.; Apeloig, Y.; Schwartz, H. *J. Am. Chem. Soc.* **1996**, *118*, 2023-2038; (c) Tomioka H. *Acc. Chem. Res.* **1997**, *30*, 315-321; (d) Nemirowski, A.; Schreiner, P. R. *J. Org. Chem.* **2007**, *72*, 9533-9540.

20. Iwamoto, E.; Hirai, K.; Tomioka, H. *J. Am. Chem. Soc.* **2003**, *125*, 14664-14665.

21. (a) Tomioka, H.; Taketsuji, K. J. *Chem. Soc., Chem. Commun.* **1997**, 1745; (b) Bourissou, D.; Guerret, O.; Gabbaï, F. P.; Bertrand, G. *Chem. Rev.* **2000**, *100*, 39-91.

22. (a) Zimmermann, H. E.; Paskovich, D. H. *J. Am. Chem. Soc.* **1964**, *86*, 2149-2160; (b) Tomioka, H.; Hirai, K.; Fujii, C. *Acta Chem. Scand.* **1992**, *46*, 680-682.

23. (a) Tomioka, H.; Okada, H.; Watanabe, T.; Hirai, K. *Angew. Chem. Int. Ed. Engl.* **1994**, *33*, 973-975; (b) Sander, W.; Kirschfeld, A.; Kappert, W.; Muthusamy, S.; Kiselewsky, M. *J. Am. Chem. Soc.* **1996**, *118*, 6508-6509; (c) Hirai, K.; Komatsu, K.; Tomioka, H. *Chem. Lett.* **1994**, *23*, 503-506; (d) Hideo, T.; Kumiko, O.; Yasuji, I.; Moss, R. A.; Ramesh, M. C. *Tetrahedron Lett.* **1984**, *25*, 5415-5418.

24. (a) Harrison, J. F. *J. Am. Chem. Soc.* **1971**, *93*, 4112-4119; (b) Bauschlicher, C. W., Jr.; Schaefer, H. F., III; Bagus, P. S. *J. Am. Chem. Soc.* **1977**, *99*, 7106-7110; (c) Harrison, J. F.; Liedtke, C. R.; Liebman, J. F. *J. Am. Chem. Soc.* **1979**, *101*, 7162-

7168; (d) Feller, D.; Borden, W. T.; Davidson, E. R. *Chem. Phys. Lett.* **1980**, *71*, 22-26; (e) Schoeller, W. W. *J. Chem. Soc., Chem. Commun.* **1980**, 124-125; (f) Pauling, L. *J. Chem. Soc., Chem. Commun.* **1980**, 688-689.

25. (a) Moss, R. A.; Wlostowski, M.; Shen, S.; Krogh-Jespersen, K.; Matro, A. *J. Am. Chem. Soc.* **1988**, *110*, 4443-4444; (b) Du, X. M.; Fan, H.; Goodman, J. L.; Kesselmayer, M. A.; Krogh-Jespersen, K.; La Villa, J. A.; Moss, R. A.; Shen, S.; Sheridan, R. S. *J. Am. Chem. Soc.* **1990**, *112*, 1920-1926.

26. (a) Mitsch, R. A. *J. Am. Chem. Soc.* **1965**, *87*, 758-761; (b) Moss, R. A.; Mallon, C. B. *J. Am. Chem. Soc.* **1975**, *97*, 344-347; (c) Koda, S. *Chem. Phys. Lett.* **1978**, *55*, 353-357.

27. Irikura, K. I.; Goddard, W. A., III; Beauchamp, J. L. *J. Am. Chem. Soc.* **1992**, *114*, 48-51.

28. (a) Wang, J. L.; Toscano, J. P.; Platz, M. S.; Nikolaev, V.; Popik, V. *J. Am. Chem. Soc.* **1995**, *117*, 5477-5483; (b) Visser, P.; Zuhse, R.; Wong, M. W.; Wentrup, C. *J. Am. Chem. Soc.* **1996**, *118*, 12598-12602.

29. Moss, R. A.; Mallon, C. B.; Ho, C. T. *J. Am. Chem. Soc.* **1977**, *99*, 4105-4110.

30. Gilbert, B. C.; Griller, D.; Nazran, A. S. *J. Org. Chem.* **1985**, *50*, 4738-4742.

31. (a) Moss, R. A.; Gersti, R. *J. Org. Chem.* **1967**, *32*, 2268-2272; (b) Moss, R. A.; Mallon B. M. *J. Am. Chem. Soc.* **1975**, *97*, 344-347; (c) Fedorynski, M. *Chem. Rev.* **2003**, *103*, 1099-1132; (d) Moss, R. A.; Tian, J.; Sauers, R. R.; Ess, D. H.; Houk, K. N.; Krogh-Jespersen, K. *J. Am. Chem. Soc.* **2007**, *129*, 5167-5174. (e) Moss, R. A.; Huselton, J. K. *J. Chem. Soc., Chem. Commun.* **1976** 950-951; (f) Moss, R. A.; Wlostowski, M.; Terpinski, J.; Kmiecik-Lawrynowicz, G.; KroghJespersen, K. *J. Am. Chem. Soc.* **1987**, *109*, 3811-3812; (g) Liu, X.; Chu, G.; Moss, R. A.; Sauers, R. R.; Warmuth, R. *Angew. Chem. Int. Ed.* **2005**, *44*, 1994-1997.

32. Kovacs, D.; Lee, M. S.; Olson, D.; Jacskon, J. E *J. Am. Chem. Soc.* **1996**, *118*, 8144-8145.

33. Alder, R.W.; Chaker L.; Paolini, F. P. V. *Chem. Commun.* **2004**, 2172-2173.

34. (a) Wanzlick, H. W.; Kleiner, H. J. *Angew. Chem.* **1961**, *73*, 493; (b) Wanzlick, H. W. *Angew. Chem. Int. Ed. Engl.* **1962**, *1*, 75-80; (c) Wanzlick, H. W.; Esser, F.; Kleiner, H. J. *Chem. Ber.* **1963**, *96*, 1208-1212.

35. (a) Lemal, D. M.; Lovald, R. A.; Kawano, K. I. *J. Am. Chem. Soc.* **1964**, *86*, 2518-2519; (b) Winberg, H. E.; Carnahan, J. E.; Coffman, D. D.; Brown, M. *J. Am. Chem. Soc.* **1965**, *87*, 2055-2056; (c) Wiberg, N. *Angew. Chem. Int. Ed. Engl.* **1968**, *7*, 766-779; (d) Denk, M. K.; Hatano, K.; Ma, M. *Tetrahedron Lett.* **1999**, *40*, 2057-2060.

36. (a) Wanzlick, H. W.; Schonherr, H. J. *Liebigs Ann. Chem.* **1970**, *731*, 176-179; (b) Schonherr, H. J.; Wanzlick, H. W. *Chem. Ber.* **1970**, *103*, 1037-1046.

37. Igau, A.; Grutzmacher, H.; Baceiredo, A.; Bertrand, G. *J. Am. Chem. Soc.* **1988**, *110*, 6463-6466.

38. Arduengo, A. J., III; Harlow, R. L.; Kline, M. *J. Am. Chem. Soc.* **1991**, *113*, 361-363.

39. Gründemann, S.; Kovacevic, A.; Albrecht, M.; Faller, J. W.; Crabtree, R. H. *Chem. Commun.* **2001**, *21*, 2274-2275.

40. Aldeco-Perez, E.; Rosenthal, A. J.; Donnadieu, B.; Parameswaran, P.; Frenking, G. Bertrand, G. *Science*, **2009**, *326*, 18124-18137.

41. Lavallo, V.; Canac, Y.; Präsang, C.; Donnadieu, B.; Bertrand, G. *Angew. Chem. Int. Ed.* **2005**, *44*, 5705-5709.

42. (a) Mendivil, E. T.; Hansmann, M. M.; Weinstein, C. M.; Jazzar, R.; Melaimi, M.; Bertrand, G. *J. Am. Chem. Soc.* **2017**, *139*, 7753-7756; (b) Please refer to section 1.5.5.

43. Jazzar, R.; Soleilhavoup, M.; Bertrand, G. *Chem. Rev.* **2020**, *120*, 4141-4168.

44. Herrmann, W. A.; Elison, M.; Fischer, J.; Kocher, C.; Artus, G. R. J. *Angew. Chem. Int. Ed. Engl.* **1995**, *34*, 2371-2374.

45. (a) Kantchev, E. A. B.; O'Brien, C. J.; Organ, M. G. *Angew. Chem. Int. Ed.* **2007***, 46,* 2768-2813; (b) Fortman, G. C.; Nolan, S. P. *Chem. Soc. Rev.* **2011**, *40*, 5151-5169; (c) Wurtz, S.; Glorius, F. *Acc. Chem. Res.* **2008**, *41*, 1523-1533; (d) Valente, C.; Çalimsiz, S.; Hoi, K. H.; Mallik, D.; Sayah, M.; Organ, M. G. *Angew. Chem. Int. Ed.* **2012**, *51*, 3314-3332.

46. (a) Scholl, M.; Ding, S.; Lee, C. W.; Grubbs, R. H. *Org. Lett.* **1999**, *1*, 953-956; (b) Vougioukalakis, G. C.; Grubbs, R. H. *Chem. Rev.* **2010**, *110*, 1746-1787; (c) Samojlowicz, C.; Bieniek, M.; Grela, K. *Chem. Rev.* **2009**, *109*, 3708-3742.

47. Hillier, A. C.; Lee, H. M.; Stevens, E. D.; Nolan, S. P. *Organometallics* **2001**, *20*, 4246-4252.

48. Normand, A. T.; Cavell, K. J. *Eur. J. Inorg. Chem.* **2008**, 2781-2800.

49. Melaiye, A.; Simons, R. S.; Milsted, A.; Pingitore, F.; Wesdemiotis, C.; Tessier, C. A.; Youngs, W. J. *J. Med. Chem.* **2004**, *47*, 973-977.

50. Marion, N.; Nolan, S. P. *Chem. Soc. Rev.* **2008**, *37*, 1776-1782.

51. Marciniec, B. *Hydrosilylation. Advances in Silicon Science*; Springer, **2009**.

52. (a) Wang, Y.; Quillian, B.; Wei, P.; Wannere, C. S.; Xie, Y.; King, R. B.; Schaefer, H. F.; Schleyer, P. v. R.; Robinson, G. H. *J. Am. Chem. Soc.* **2007**, *129*, 12412-12413. (b) Wang, Y.; Quillian, B.; Wei, P.; Xie, Y.; Wannere, C. S.; King, R. B.; Schaefer, H. F.; Schleyer, P. v. R.; Robinson, G. H. *J. Am. Chem. Soc.* **2008**, *130*, 3298-3299; (c) Wang, Y.; Xie, Y.; Wei, P.; King, R. B.; Schaefer, H. F., III; Schleyer, P. v. R.; Robinson, G. H. *J. Am. Chem. Soc.* **2008**, *130*, 45, 14970-14971; (d) Wang, Y.; Xie, Y.; Wei, P.; King, R. B.; Schaefer, H. F., III; Schleyer, P. v. R.; Robinson, G. H. *Science* **2008**, *321*, 1069-1071.

53. Enders, D.; Niemeier, O.; Henseler, A. *Chem. Rev.* **2007**, *107*, 5606-5655.

54. Berkessel, A.; Elfert, S.; Yatham, V. R.; Neudörfl, J.-M.; Schlörer, N. E.; Teles, J. H. *Angew. Chem. Int. Ed.* **2012**, *51*, 12370-12374.

55. (a) Biju, A. T.; Kuhl, N.; Glorius, F. *Acc. Chem. Res.,* **2011**, *44*, 1182-1195; (b) Ryan, S. J.; Candish, L.; Lupton, D. W. *Chem. Soc. Rev.* **2013**, *42*, 4906-4917; (c) Flanigan, D. M.; Romanov-Michailidis, F.; White, N. A.; Rovis, T. *Chem. Rev.* **2015**, *115*, 9307-9387; (d) Hopkinson, M. N.; Richter, C.; Schedler, M.; Glorius, F. *Nature*, **2014**, *510*, 485-496.

56. Sau, S. C.; Hota, P. K.; Mandal, S. K.; Soleilhavoup, M.; Bertrand, G. *Chem. Soc. Rev.* **2020**, *49*, 1233-1252.

57. Chianese, A. R.; Kovacevic, A.; Zeglis, B. M.; Faller, J. W.; Crabtree, R. H. *Organometallics* **2004**, *23*, 2461-2468.

58. Lebel, H.; Janes, M. K.; Charette, A. B.; Nolan, S. P. *J. Am. Chem. Soc.* **2004**, *126*, 5046-5047.

59. Bacciu, D.; Cavell, K. J.; Fallis, I. A.; Ooi, L.-l. *Angew. Chem. Int. Ed.* **2005**, *44*, 5282-5284.

60. Zhukhovitskiy, A. V.; Kobylianskii, I. J.; Wu, C.-Y.; Toste, F. D. *J. Am. Chem. Soc.* **2018**, *140*, 466-474.

61. Ortega-Arizmendi, A. I.; Aldeco-Perez, E.; Cuevas-Yanez, E. *Sci. World J.* **2013**, *2013*, 186537.

62. (a) Vijaykumar, G.; Mandal, S. K. *Dalton Trans.* **2016**, *45*, 7421-7426; (b) Bhunia, M.; Hota, P. K.; Vijaykumar, G.; Adhikari, D.; Mandal, S. K. *Organometallics* **2016**, *35*, 2930-2937.

63. Bhunia, M.; Vijaykumar, G.; Adhikari, D; Mandal, S. K. *Inorg. Chem.* **2017**, *56*, 14459-14466.

64. Thakur, A.; Vardhanapu, P. K.; Vijaykumar, G.; Hota, P. K.; Mandal, S. K. *Eur. J. Inorg. Chem.* **2016**, 913-920.

65. Sen, T. K.; Sau, S. C.; Mukherjee, A.; Modak, A.; Mandal, S. K.; Koley, D. *Chem. Commun.* **2011**, *47*, 11972-11974.

66. Rottschäfer, D.; Glodde, T.; Neumann, B.; Stammler, H. G.; Ghadwal, R. S. *Chem. Commun.* **2020**, *56*, 2027-2030.

67. (a) Jazzar, R.; Soleilhavoup, M.; Bertrand, G. *Chem. Rev.* **2020**, *120*, 9, 4141-4168; (b) Singh, R. K.; Khan, T. K.; Misra, S.; Singh, A. K. *J. Organomet. Chem.* **2021**, *956*, 122133.

68. Roy, S.; Mondal, K. C.; Roesky, H. W. *Acc. Chem. Res.* **2016**, *49*, 357-369.

69. (a) Soleilhavoup, M.; Bertrand, G. *Acc. Chem. Res.* **2015**, *48*, 256-266; (b) Melaimi, M.; Jazzar, R.; Soleilhavoup, M.; Bertrand G. *Angew. Chem. Int. Ed.* **2017**, *56*, 10046-10068.

70. Kundu, S.; Sinhababu, S.; Chandrasekhar, V.; Roesky, H. W. *Chem. Sci.* **2019**, *10*, 4727-4741.

71. (a) Mahoney, J. K.; Martin, D.; Moore, C. E.; Rheingold, A. L.; Bertrand, G. *J. Am. Chem. Soc.* **2013**, *135*, 50, 18766-18769; (b) Kretschmer, R., Ruiz, D. A.; Moore, C. E.; Rheingold, A. L.; Bertrand, G. *Angew. Chem. Int. Ed.* **2014**, *53*, 8176-8179.

72. a) Bissinger, P.; Braunschweig, H.; Damme, A.; Krummenacher, I.; Phukan, A. K.; Radacki, K.; Sugawara, S. *Angew. Chem. Int. Ed.* **2014**, *53*, 7360-7363; (b) Li, B.; Kundu, S.; Stgckl, C.; Zhu, H.; Keil, H.; HerbstIrmer, R.; Stalke, D.; Schwederski, B.; Kaim, W.; Andrada, D. M.; Frenking, G.; Roesky, H. W. *Angew. Chem. Int. Ed.* **2017**, *56*, 397-400.

73. Kinjo, R.; Donnadieu, B.; Celik, M. A.; Frenking, G.; Bertrand, G. *Science* **2011**, *333*, 610-613.

74. Mondal, K. C.; Roesky, H. W.; Schwarzer, M. C.; Frenking, G.; Niepötter, B.; Wolf, H.; Herbst-Irmer, R.; Stalke, D. *Angew. Chem. Int. Ed.* **2013**, *52*, 2963-2967.

75. Turner, Z. R.; Buffet, J. C. *Dalton Trans.* **2015**, *44*, 12985-12989.

76. Arrowsmith, M.; Braunschweig, H.; Celik, M. A.; Dellermann, T.; Dewhurst, R. D.; Ewing, W. C.; Hammond, K.; Kramer, T.; Krummenacher, I.; Mile, J.; Radacki, K.; Schuster, J. K. *Nat. Chem.* **2016**, *8*, 890-894.

77. Kushvaha, S. K.; Mishra, A.; Roesky, H. W.; Mondal. K. C. *Chem Asian J.* **2022**, *17*, e202101301.

78. (a) Ruiz, J.; Perandones, B. F. *Chem. Commun.* **2009**, 2741-2743; (b) Tamm, M.; Ekkehardt Hahn, F. E. *Coord. Chem. Rev.* **1999**, *182*, 175-209; (c) Vougioukalakis, G. C.; Grubbs, R. H. *J. Am. Chem. Soc.* **2008**, *130*, 2234-2245; (d) Raubenheimer, H. G.; Stander, Y.; Marais, E. K.; Thompson, C.; Kruger, G. J.; Cronje, S.; Deetlefs, M. *J. Organomet. Chem.* **1999**, *590*, 158; (e) Martin, D.; Baceiredo, A.; Gornitzka, H.; Schoeller, W. W.; Bertrand, G. *Angew. Chem. Int. Ed.* **2005**, *44*, 1700-1703; (f) Masuda, J. D.; Martin, D.; Lyon-Saunier, C.; Baceiredo, A.; Gornitzka, H.; Donnadieu, B; Bertrand, G. *Chem. Asian J.* **2007**, *2*, 178-187.

79. Ruiz, J.; García, L.; Perandones, B. F.; Vivanco, M. *Angew. Chem. Int. Ed.* **2011**, *50*, 3010-3012.

80. Dötz, K. H.; Stendel, J. *Chem. Rev.* **2009**, *109*, 3227-3274

81. Ruiz, J.; García, L.; Mejuto, C.; Vivanco, M.; Díaz, M. R.; García-Granda, S. *Chem. Commun.* **2014**, 2129-2132.

82. Rohman, S. S.; Ghosh, B.; Phukan, A. K. *Dalton Trans.* **2019**, *48*, 11772-11780.

83. Ghosh, B.; Phukan, A. K. *Dalton Trans.* **2020**, *49*, 9505-9515.

84. Manar, K. K.; Porwal, V. K.; Kamte, R. S.; Adhikari, M.; Thakur, S. K.; Bawari, D.; Choudhury, A. R.; Singh, S. *Dalton Trans.* **2019**, *48*, 17472-17478.

85. Manar, K. K.; Chakrabortty, S.; Porwal, V. K.; Prakash, D.; Thakur, S. K.; Choudhury, A. R.; Singh, S. *ChemistrySelect* **2020**, *5*, 9900-9907.

86. Yazdani, S.; Junor, G. P.; Peltier, J. L.; Gembicky, M.; Jazzar, R.; Grotjahn, D. B.; Bertrand, G. *ACS Catal.* **2020**, *10*, 5190-5201.

87. Chakrabortty, S.; Kaur, M.; Adhikari, M.; Manar, K. K.; Singh, S. *Inorg. Chem.* **2021**, *60*, 6209-6217.

88. Rajendran, N. M.; Gautam, N.; Sarkar. P.; Ahmed, J.; Das, A.; Das, S.; Pati, S. K; Mandal, S. K. *Chem. Commun*. **2021**, *57*, 5282-5285.

89. Nagyházi, M.; Lukács, Á.; Turczel, G.; Hancsók, J.; J Valyon, J.; Bényei, A.; Kéki, S.; Tuba. R. *Angew. Chem. Int. Ed*. **2022**, *61*, e202204413.

90. Thakur, S. K.; Kaur, M.; Manar, K. K.; Adhikari, M.; Choudhury, A. R.; Singh S. *Chem. Eur. J.* **2022**, *28*, e202202237.

91. Gautam, N.; Logdi, R.; Sreejyothi, P.; Rajendran, N. M.; Tiwari, A. K.; Mandal, S. K. *Chem. Commun*. **2022**, *58*, 3047-3050.

BICAAC stabilized diborane and diborene complexes and reactivity of diborene towards coinage metal salts (CuCl, AgBr and CuI)
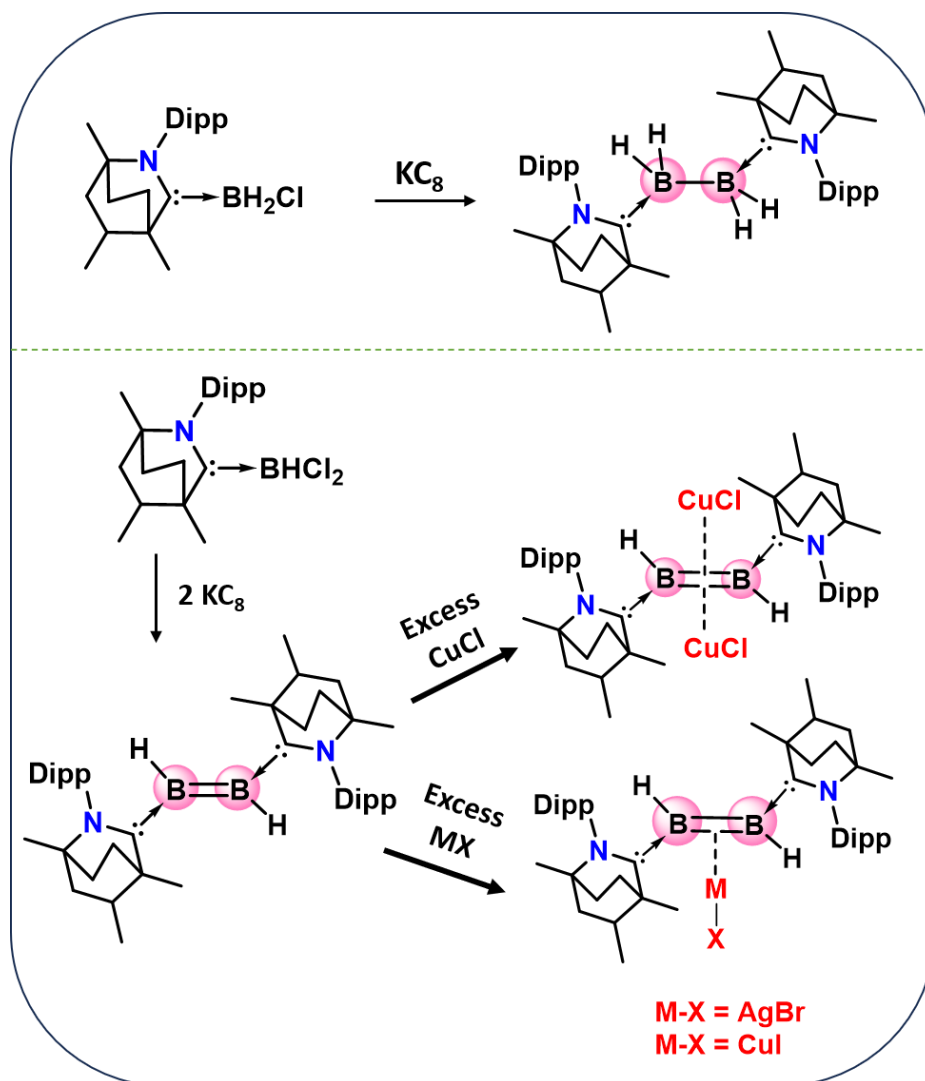
Adhikari, M.; De, S.; Manar, K. K.; Thakur, S. K.; Kamte, R. S.; Koley, D.; Singh S. Diborane, Diborene and M(I)-η^2-Diborene Complexes Stabilized by Bicyclic (Alkyl)(Amino)Carbene (M = Cu and Ag), *Eur. J. Inorg. Chem.* **2024**, e202400129.

Abstract: Bicyclic (alkyl)(amino) carbene (BICAAC) as an ambiphilic carbene was proven to have a smaller HOMO-LUMO energy gap compared to its predecessor NHCs and cAAC carbenes. Taking the advantage of its electronic properties, in this chapter, we describe the successful syntheses and characterization of BICAAC-BF$_3$ (**1**) and BICAAC-B(C$_6$F$_5$)$_3$ (**2**) adducts. Further, in order to create stable, neutral tetrahydrodiborane [BICAAC $\rightarrow$ (H$_2$)B-B(H$_2$) $\leftarrow$ BICAAC] (**3**) and dihydrodiborene [BICAAC $\rightarrow$ (H)B=B(H) $\leftarrow$ BICAAC] (**4**) compounds, BICAAC haloborane adducts have been utilized as precursors. Since the Lewis base stabilized dihydrodiborene is isoelectronic and isolobal to ordinary olefins, it is feasible to investigate the synthesis of its complexes with different metals. The dihydrodiborene **4** reacts with coinage metal salts (CuCl, AgBr and CuI), by means of η^2 side-on coordination, to produce η^2-diborene metal complexes (**5**), (**6**) and (**7**), respectively. Compounds **3**-**7** have been studied using spectroscopic methods, and X-ray crystallography has also verified their solid-state structures. These are the earliest coinage metal complexes of dihydrodiborene. It is interesting to note that in **5** two CuCl units have coordinated to the diborene for the first time, and this has been accompanied by a significant lengthening of the >B=B< and B-C$^{\text{BICAAC}}$ bonds, demonstrating the crucial role played by BICAAC along with the minimal steric requirements of hydride substituents in stabilizing these complexes. Furthermore, to elucidate the bonding scenarios within these complexes, a computational study was also undertaken. Additionally, the absorption behavior of complexes **3**-**6** have been studies in toluene and subsequently interpreted by TDDFT calculations. Energy Decomposition Analysis (EDA) simulations showed that the interaction between the diborene and Cu(I)/Ag(I) is primarily electrostatic in nature.

2A.1 Introduction

The homoatomic multiple bonding in carbon, nitrogen and oxygen is very common and ubiquitous. However, the multiple bonding between their heavier congeners were not seen in the literature till 1950s and the absence of these molecules has led the origin of so-called *double bond rule*,[1] which states "It should be impossible for elements with principal quantum numbers greater than 2 to establish $(p\text{-}p)\pi$ bonds with either other elements or with themselves".[2a] However, this rule started to lose its validity within two decades as examples of so called "*non-existent*" multiply bonded heavier main group compounds started to appear in the literature by 1970s.[2b] The preliminary ground-breaking work by the groups of Lappert,[3] West,[4] Berndt,[5] Power,[6a] Yoshifuji[6b] and Sekiguchi[6c] laid the foundation of multiple bonding between heavier main group elements. It might be argued that the isolation of the first distannene by Lappert and Thomas (**A**, Figure 2A.1) in 1976 marked the beginning of advancement in the field of multiple bonding in heavier main-group elements.[3] This work was followed by other chemists and we have witnessed the syntheses of different group 14 enes [(R)(R)E=E(R)(R)] (E = Si, Ge and Pb).[4,7] Similarly, synthesis of the first group 13 radical anion, a diboranyl radical anion, (**B**, Figure 2A.1) was reported by Berndt and co-workers in 1981,[5] other examples of Al, Ga and B based radical anions were latter reported by different groups.[8] In 1992, Power and co-workers reported the isolation of first diboranyl dianion, (**C**, Figure 2A.1) which possess a B=B bond order of 2.[6a,9]

The above-mentioned compounds are associated with the *Tricoordinate era* (1976-1998), as outlined by Braunschweig in his recent review. They exhibit a tricoordinated geometry around the E centers and characterized by a formal E-E bond order of 1.5 or 2.[10] The R ligand systems in these complexes mostly are anionic in nature and bulky enough to stabilize the E atoms. The subsequent period, known as the *Dicoordinate era* (1997-2006), marked the

Previous work:

A
Lappert, 1976

B
Berndt, 1981

C
Power, 1992

D
Robinson, 2007

E = (L = NHC, R = Br)
F = (L = PEt₃, R = Mes)
G = (L = cAAC, R = H)

Braunschweig
2012, 2014, 2018

H
(M = Ag, Cu)

Braunschweig
2012, 2015

I

Braunschweig
2013

J

Braunschweig
2017

(Dur = duryl = 2,3,5,6-tetramethylphenyl)
(NHC = N-heterocyclic carbene)
(cAAC = cyclic (Alkyl)(Amino) carbene)
(Mes = mesityl group)

This work:

M-X = AgBr
M-X = CuI

L = Bicyclic (alkyl)(amino) carbene (BICAAC)
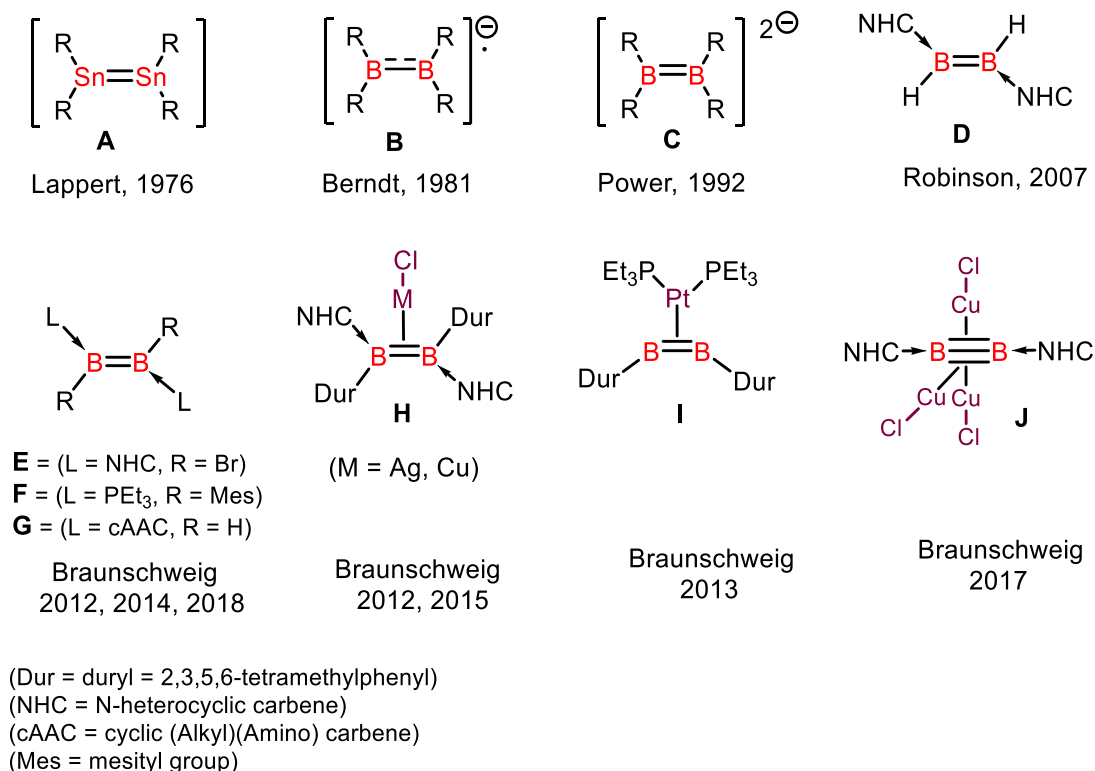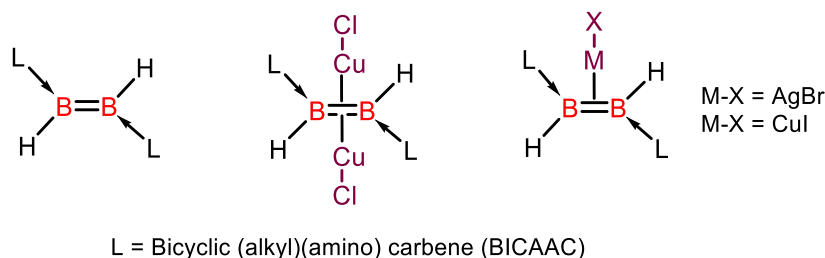
Figure 2A.1 Known examples of multiply bonded compounds (top) and BICAAC stabilized dihydrodiborene and Cu(I) and Ag(I) complexes of the diborene reported in this work (bottom).

accomplishment of synthesizing the first dicoordinate compound, the digallyne dianion [RGa≡GaR]²⁻, by Robinson and co-workers in 1997[11a] although the extent of triple bond character in this species is debatable, and similar dialumyne dianion was later reported by Power and co-workers.[11b] In the same *Dicoordinate* timeline, groups of Power and Sekiguchi independently reported group 14 "ynes", which are trans-bent in nature [RE≡ER],

(E = Pb, Ge, Sn and Si)[6c,12] and neutral group 13 "enes" [RE=ER] (E = Ga, In, Tl).[13] These

pioneering research not only challenged the established double bond rule but also enabled the

isolation of a diverse array of multiply bonded compounds. As a result, it significantly

advanced our understanding of fundamental bonding principles and the characteristics of

supporting ligands.

In various scenarios, boron exhibits the ability to form strong and stable multiple bonds,

akin to its neighboring elements carbon, nitrogen, and oxygen. Boron can establish multiple

bonds with elements possessing a π-electron pair, such as the sp^2 hybridized nitrogen atom

(seen in aminoboranes, $R_2B=NR'_2$, and iminoboranes, $RB\equiv NR'$)[14], as well as with oxygen

(observed in alkoxyboranes, R_2BOR').[15] It has been observed that boron can form

alkylideneboranes ($RB=CR'_2$) and alkylideneboryl ($MB=CR_2$) type complexes with carbon,

despite carbon not being able to provide an electron pair.[16] Despite the potential for

participating in heteroatomic multiple bonding, boron exhibits reluctance to form multiple

bonds with itself. A fundamental example is diborenes ($RB=BR$), which, in the early days,

were exclusively generated in matrix environments.[17a-b] Although these compounds were

employed as ligands for transition metals, they had never been isolated in their free form.[17c]

As mentioned previously, until 2007, only a handful of multiply bonded boron compounds

were reported. These examples suggest that the formation of multiple bonds in heavier main-

group elements is easier compared to boron, contradicting the double bond rule.[10]

Discussing boron-boron multiple bonding, a new era was uncovered by Robinson and co-

workers in 2007, referred to as the Lewis base era (2007-onwards).[10] They found by

replacing the anionic R ligand system with a neutral and strong σ-donating ligand like NHC

(NHC = N-heterocyclic carbene) can easily produce the doubly base stabilized neutral

diborane [IDip→B(H)$_2$−B(H)$_2$←IDip], IDip = 1,3-bis(2,6-diisopropylphenyl)imidazole-2-

ylidene, and diborene [IDip→B(H)=B(H)←IDip][18] (**D,** Figure 2A.1) complexes *via* a

radical mediated pathway and subsequent hydrogen abstraction from the solvent molecules. To mitigate such side reactions, Braunschweig and co-workers in 2012 came up with a new strategy which involved the reaction of B_2Br_4 (containing a pre-existing B-B bond) with free NHC to synthesize the diborane [IDip→B(Br)$_2$−B(Br)$_2$←IDip] and subsequent reduction with sodium naphthalenide produced the diborene [IDip→B(Br)=B(Br)←IDip] (**E,** Figure 2A.1) and diboryne [IDip→B≡B←IDip] complexes.[19] Robinson's discovery marked a significant milestone, providing chemists with insights into the role of strong donor ligands and paving the way for further exploration into the electronically precise realm of multiply bonded chemistry.[20] Subsequently, stabilization of other diborenes (**F-G,** Figure 2A.1) were also achieved using neutral bulky donors.[21]

The omnipresence of olefins and acetylenes made their transition metal complexes easily accessible, as a result these are well documented in the literature and such complexes are considered as key intermediates in many synthetic transformations and polymerization reactions.[22] Iwamoto and co-workers demonstrated the reactivity of a dialkyldisilyne with [M(PCy$_3$)$_2$], (M = Pd, Pt) to generate M-η^2-disilyne complexes which possess a trans bent geometry and showed significant metallacycle character.[23] Moreover, an NHC-stabilized disilicon-copper(I) chloride complex [(NHC→Si=Si←NHC)(CuCl)], was synthesized by Robinson and co-workers, which showed equilibrium in the solid and solution states, probably *via* a π-complex intermediate.[24] In contrast, the reactivity of diborenes and diborynes (boron analogs of olefins and alkynes) are not well explored and less number of reports have appeared to date. In the context of diborenes and diborynes, Braunschweig and co-workers have synthesized highly fluorescent π-diborene complexes of MCl (M = Cu, Ag)[25] (**H,** Figure 2A.1) and [Pt(PEt$_3$)$_2$][17c] complex of non-base-stabilized diborane (**I,** Figure 2A.1). Later the same group reported syntheses of copper π-diboryne complexes which are strongly phosphorescent (quantum yields up to 58%)[26a] (**J,** Figure 2A.1) and

Zn(II)/Cd(II) diborene complexes.[26b] From these reports it is clear that in contrast to the conventional metal π-olefin complexes which are non-luminescent, the boron analogues are strongly luminescent due to the high energetic HOMO levels of the diborenes are significantly stabilized by coordination to the metal.[25] The metal diborene bond is mainly dominated by electrostatic interactions which produces S_1 and T_1 states of pure IL(π- π^*) nature that results in the significant hypsochromic shift in the absorption.[25] Lately, Kinjo and co-workers have shown the coordination of asymmetric diborenes towards cationic coinage metals (Au, Ag, Cu).[27] Very recently, Braunschweig and co-workers reported the syntheses of different types of metal π diborene complexes (stabilized by NHC and various donor ligands) and their photophysical properties.[28]

Recognizing the significance of BICAAC[29a], in 2019 our team demonstrated how reactive the BICAAC is to a variety of hydro- and haloboranes (Scheme 2A.1). We found the
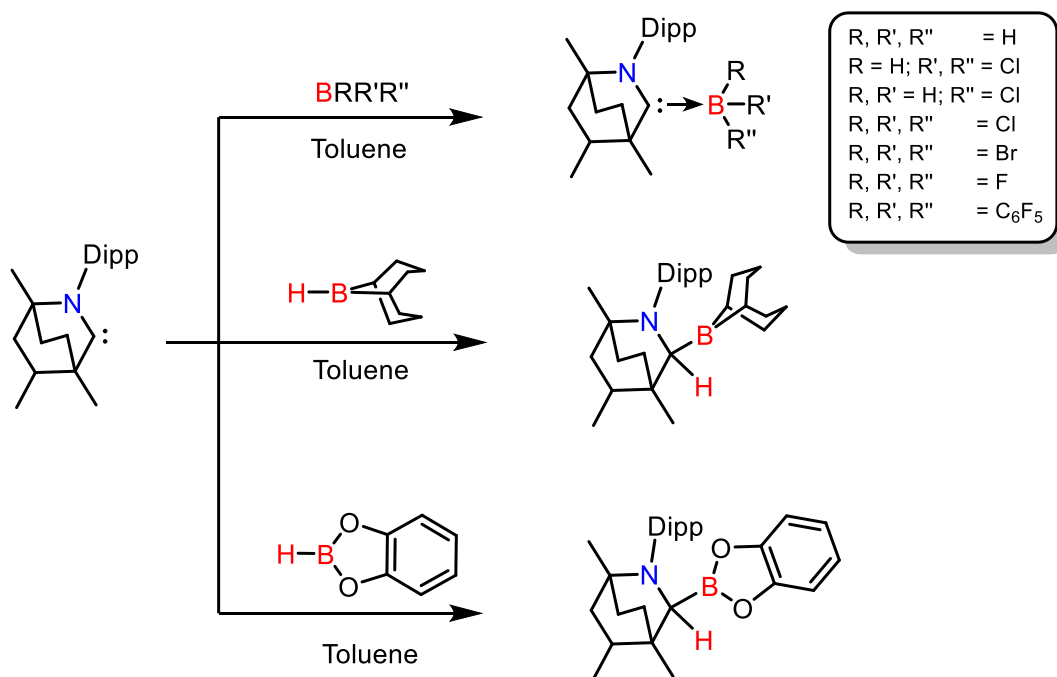
Scheme 2A.1 Synthesis of BICAAC borane-adducts (top); and the B–H bond activation of 9−BBN and HBcat leading to the formation of [BICAAC(H)−(9-BBN)] (middle) and [BICAAC(H)−Bcat] (bottom).

reaction of BICAAC with less hydridic boranes generates Lewis adducts e. g., BICAAC−BH$_3$, BICAAC−BF$_3$, BICAAC−BH$_2$Cl, BICAAC−BHCl$_2$, BICAAC−BCl$_3$, BICAAC−BBr$_3$, BICAAC−B(C$_6$F$_5$)$_3$, while with more hydridic boranes (9-borabicyclo[3.3.1]nonane (9−BBN) and catecholborane (HBcat)) insertion of the carbene carbon into the B–H bond was observed.[29b]

The upcoming section deals with the syntheses and characterization of BICAAC−BF$_3$ and BICAAC−B(C$_6$F$_5$)$_3$ adducts and further describes the applications of BICAAC haloborane adducts to produce new diborane and diborene compounds. We further demonstrated the reactivity of diborene towards coinage metal salts. Consequently, herein we describe successful synthesis and characterization of complexes BICAAC−BF$_3$ (**1**), BICAAC−B(C$_6$F$_5$)$_3$ (**2**), [BICAAC→(H$_2$)B−B(H$_2$)←BICAAC] (**3**), [BICAAC→(H)B=B(H)←BICAAC] (**4**), [BICAAC(BH)]$_2$(CuCl)$_2$ (**5**), [BICAAC(BH)]$_2$(AgBr) (**6**) and [BICAAC(BH)]$_2$(CuI) (**7**).

2A.2 Results and discussion

2A.2.1 Syntheses and characterization of complexes BICAAC−BF$_3$ (1) and BICAAC−B(C$_6$F$_5$)$_3$ (2)

The reaction of BICAAC with one equivalent of BF$_3$·OEt$_2$ in toluene yielded the BICAAC−BF$_3$ adduct (**1**) in 82% yield (Scheme 2A.2). Similarly, the reaction of BICAAC with one equivalent of B(C$_6$F$_5$)$_3$ in toluene produced the BICAAC−B(C$_6$F$_5$)$_3$ adduct (**2**) in a 78% isolated yield (Scheme 2A.2). The ^{19}F{^{1}H} NMR spectrum of **1** showed equal intensity quartet centered at δ = -139.7 ppm ($^1J_{\text{F-B}}$ = 41 Hz), while ^{11}B NMR spectrum exhibits a quartet at δ = -0.72 ppm ($^1J_{\text{B-F}}$ = 41 Hz) indicates the exclusive formation of **1**. The ^{1}H NMR spectrum of the same showed two septets (corresponds to the Dipp group) resonating at δ =
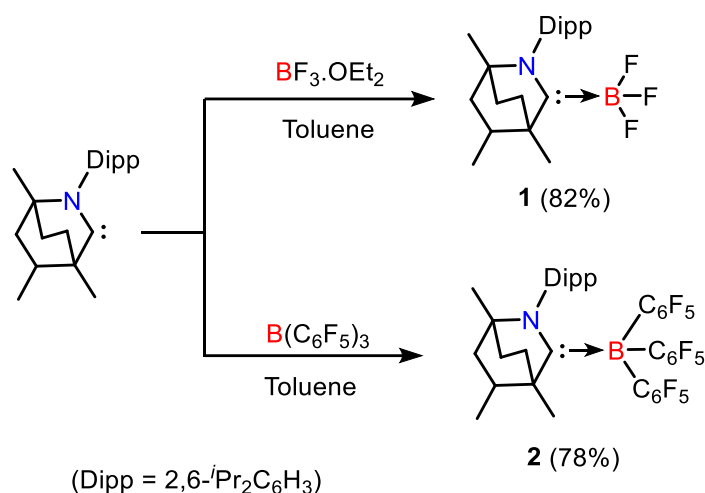
Scheme 2A.2 Syntheses of BICAAC−BF$_3$ (**1**) and BICAAC−B(C$_6$F$_5$)$_3$ (**2**) complexes.

2.77 and 2.48 ppm. The ^{13}C{^{1}H} NMR spectrum of **1** did not show any peak for boron bound carbon most probably due to the quaternary nature of this carbon and the quadrupolar effect of ^{11}B nucleus. Further, the HRMS spectrum of **1** showed signal at m/z = 360.2661(calcd. 360.2678), as [M-F]$^+$. Complex **2** showed 15 different peaks in ^{19}F{^{1}H} NMR spectrum ranging from δ = -105.91 to -167.0 ppm suggesting the restricted rotation across the BICAAC−B bond due to the present of bulky C$_6$F$_5$ groups on boron and thus formation of BICAAC−B(C$_6$F$_5$)$_3$ adduct. The ^{11}B NMR spectrum of **2** showed signal at δ = -12.6 ppm. Additionally, the mass spectrum of the crude sample of **2** revealed a signal at m/z = 822.2360 (calcd. 822.2395), as [M-H]$^-$ which supports the formation of complex **2**. Complexes **1** and **2** crystallized in the orthorhombic and monoclinic crystal systems and possess $Pca2_1$ and $I2/a$ space groups, respectively. In both the complexes boron atom adopts distorted tetrahedral geometry. Complex **1** showed N1−C1, C1−B1 and B1−F1 bond distances as 1.298(5), 1.660(5) and 1.378(5) Å respectively (Figure 2A.2), while the N1−C1−B1 and C1−B1−F1 bond angles were found to be 124.8(3) and 112.3(3)°, respectively. Complex **2** showed N1−C1, C1−B1 and B1−C29 bond distances as 1.327(4), 1.733(4) and 1.672(4) Å respectively, whereas the N1−C1−B1 and C1−B1−C29 bond angles were found to be 128.5(3) and 102.8(2)°, respectively (Figure 2A.2).
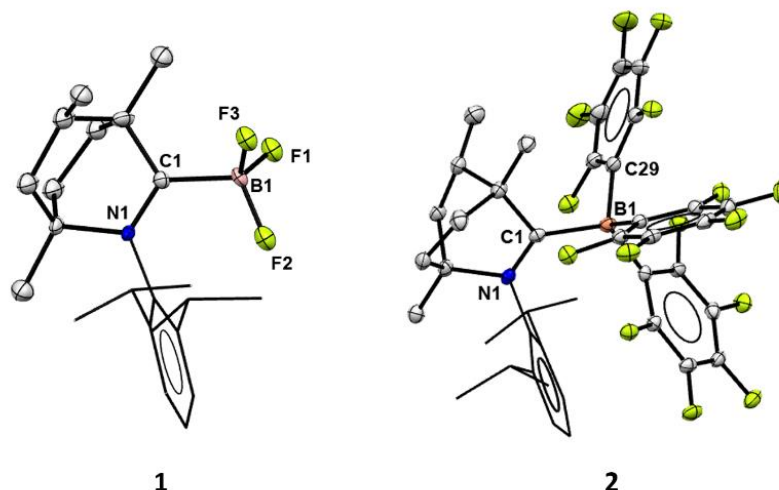
Figure 2A.2 Single crystal X-ray structure of adducts [BICAAC−BF$_3$] (**1**) and [BICAAC−B(C$_6$F$_5$)$_3$] (**2**). Ellipsoids are shown at the 50% probability level (hydrogen atoms have been omitted for clarity). Selected bond lengths (Å) and bond angles (°) for **1**: N1−C1 1.298(5), C1−B1 1.660(5), B1−F1 1.378(5); N1−C1−B1 124.8(3), C1−B1−F1 112.3(3) and for **2**: N1−C1 1.327(4), C1−B1 1.733(4), B1−C29 1.672(4); N1−C1−B1 128.5(3), C1−B1−C29 102.8(2).

2A.2.2 Syntheses and characterization of complexes BICAAC→(H)$_2$B−B(H)$_2$←BICAAC (3) and BICAAC→(H)B=B(H)←BICAAC (4)

After the successful syntheses of different BICAAC borane adducts[29b] we extended the scope of BICAAC−BH$_2$Cl and BICAAC−BHCl$_2$ adducts for the synthesis of BICAAC derived B−B and B=B compounds, respectively. The synthesis of diborane complex BICAAC→(H)$_2$B−B(H)$_2$←BICAAC (**3**) was first attempted by the reduction of the BICAAC−BH$_2$Cl adduct with K metal and afforded compound **3** in low yield (55 %).[29c] The low yield and the synthetic approach hampered the isolation of the product in pure form and its spectroscopic characterization was incomplete. In a modified procedure complex **3** was prepared by the KC$_8$ reduction of BICAAC−BH$_2$Cl adduct that gave **3** in 76 % yield in the pure form.

Diborane BICAAC→(H)$_2$B−B(H)$_2$←BICAAC (**3**) was synthesized as a yellow solid by the reduction of BICAAC−BH$_2$Cl adduct with one equivalent of KC$_8$, respectively in toluene (76 % yield) or THF (68 % yield) under inert conditions (Scheme 2A.3). Similar

(Dipp = 2,6-^{i}Pr$_2$C$_6$H$_3$)
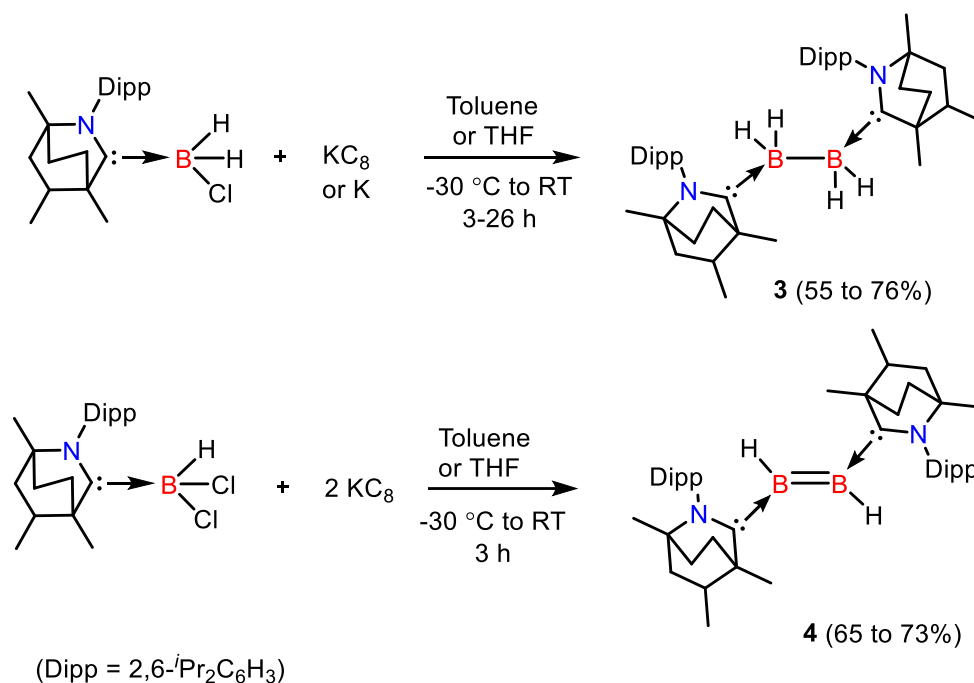
Scheme 2A.3 Syntheses of BICAAC supported tetrahydrodiborane **3** and dihydrodiborene **4**. reduction can also be achieved by using K metal in THF (24-26 hours) to get **3** in 55% yield. The diborene BICAAC→(H)B=B(H)←BICAAC (**4**) can either be synthesized in toluene or THF with 73% and 65% respective yields as crystalline green solid upon the reaction of BICAAC−BHCl$_2$ adduct with 2.2 equivalents of KC$_8$ (Scheme 2A.3). Due to their extreme sensitivity to air and moisture, complexes **3** and **4** rapidly decolorize when exposed to open atmosphere. we anticipate complex **3** produced a mixture of two diastereomers as indicated by the ^{1}H and ^{13}C{^{1}H} NMR spectra, unfortunately, the diastereomeric mixture could not be separated. Complex **3** exhibits a broad signal at δ = -16.4 ppm in its ^{11}B NMR spectrum, whereas the ^{11}B-^{1}H HSQC 2D NMR spectrum showed a peak resonating at δ = 1.46 ppm which corresponds to the hydrogens of BH_2 moiety (Figure 2A.3). The formation of **3** was also supported by the HRMS spectrum which showed peak at *m/z* = 647.5635 (calcd.

647.5661) as [M-H]⁺. The IR spectrum of **3** showed signal at 2387 cm⁻¹ which correspond to the B-*H* stretching bands. Similarly, complex **4** showed a broad peak at δ = 5.0 ppm in ¹H NMR spectrum for boron bonded hydrogens, and a peak at δ = 298 ppm in its ¹³C{¹H} NMR spectrum for boron bound carbons. The ¹¹B NMR spectrum of **4** detected a peak at δ = 42.6
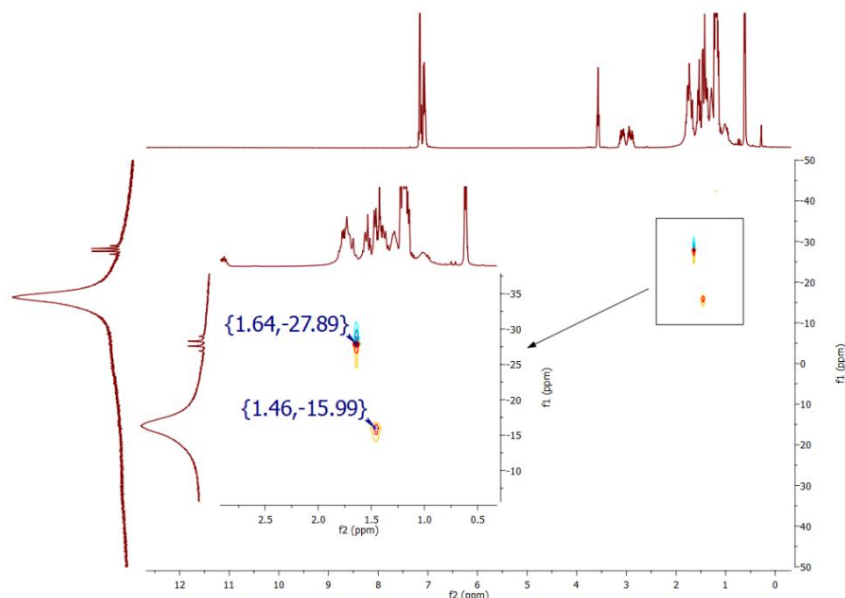
Figure 2A.3 ¹H-¹¹B 2D (HSQC) NMR spectrum of **3**.

ppm, which is consistent with the coordination number and nature of bonding between Boron centers.[19] The IR spectrum of **4** exhibited signal at 2463 cm⁻¹ which correspond to the B-*H* stretching bands. Other signals in ¹H NMR spectra of **3** and **4** were found to be as expected for the BICAAC backbone. HRMS spectra of **4** showed peak at *m/z* = 646.5435 (calcd. 646.5583) as [M]⁺.

The solid-state structure determination divulged that **3** crystallized in the triclinic system and bear $P\bar{1}$ space group. Each boron adopts nearly tetrahedral geometry as shown in Figure 2A.4. The B−B bond distance in **3** was found to be 1.851(4) Å which is slightly longer than those previously reported [{NHC:(H)₂B−B(H)₂:NHC}, (1.828(4))[18a] and {OC(H)₂B−B(H)₂CO}, (1.819 Å)[18c]], however, the C1-B1 distance in **3** is marginally shorter, 1.563(4) Å than Robinson's diborane [1.577(2) Å].[18a] The C1−B1−B2−C23 unit in

51

Figure 2A.4 Single crystal X-ray structures of **3** and **4**. Thermal ellipsoids are shown at 50% probability level. All the hydrogen atoms on carbon and disordered parts of BICAAC backbone in **4** were omitted for clarity. Selected bond lengths (Å) and angles (°): **3**: N1-C1 1.335(3), C1-B1 1.563(4), B1-B2 1.851(4), B1-H1A 1.14(3), B1-H1B 1.13(3), B2-C23 1.566(4); N1-C1-B1 125.3(2), C1-B1-B2 108.98(19), C1-B1-H1A 102.4(14). **4**: N2-C23 1.336(4), C23-B2 1.546(6), B2-B2′ 1.578(10), B2-H2 0.95; N2-C23-B2 119.2(4), C23-B2-B2' 127.2(6).

3 is nearly coplanar with the torsion angle of 172.1(2)° and the Dipp groups of carbene backbone are oriented on the same side of the B-B plane. The C1−B1−B2 bond angle was found to be 108.98(19)° which is slightly wider than Robinson's diborane (107.45(16)°).[18a] The diborene **4** crystallized in the triclinic crystal system with $P\bar{1}$ space group carrying a centre of inversion along the B−B axis. Among of three proposed structures for a diborene, **4**showed a planar geometry rather than twisted or trans-bent.[18b] The $B_2H_2C_2$ core of **4** was found to be coplanar (torsion angle between C23−B2−B2′−C23′ is 180.0(5)°) while the nitrogen atoms of the backbone are twisted with the torsion angle between B2′−B2−C23−N2 was 154.8(5)° and two carbene moieties attached with B_2H_2 core are oriented opposite to each other (Figure 2A.4). The bond angle between C23−B2−B2′ was found to be 127.2(6)°. Additionally, the B═B bond distance in **4** was found to be 1.578(10) Å which is significantly shorter than **3** and comparable with the reported values.[18a-b,19] Moreover, the C23−B2 bond distance in **4** was found to be 1.546(6) Å, which is also comparable with the reported diborenes.[18a-b,19]

2A.2.3 Syntheses and characterization of complexes [BICAAC(BH)]₂(CuCl)₂ (5), [BICAAC(BH)]₂(AgBr) (6) and [BICAAC(BH)]₂(CuI) (7)

We were curious to find out how complex **4** would react to coinage metal salts like CuCl, AgBr, and AuCl because it has been estimated that the BICAAC has a smaller HOMO-LUMO energy gap than NHCs and CAACs.[29a] The reaction of diborene **4** with slight excess of CuCl produced **5** (Scheme 2A.4) as an orange solid which is stable under inert conditions

Dipp = 2,6-^{i}Pr₂C₆H₃
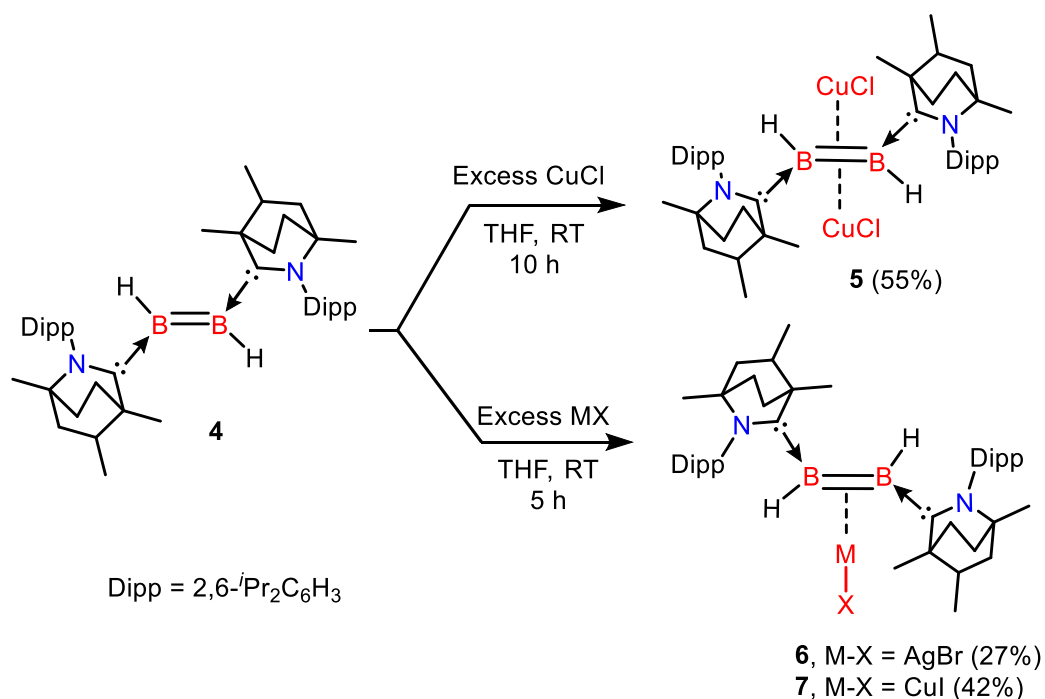
Scheme 2A.4 Reaction of diborene **4** with excess of CuCl, AgBr and CuI to form η2-diborene coinage metal π-complexes **5, 6** and **7**.

for at least six months. ¹H NMR spectrum of **5** revealed a broad signal for B*H* hydrogens at δ = 4.34 ppm which is about 0.7 ppm upfield shifted compare to the precursor **4**. The formation of **5** was also suggested by the ¹¹B NMR spectra which gave a broad signal at δ = 17.9 ppm (42.6 ppm for precursor **4**). The ¹³C{¹H} NMR spectrum of **5** clearly indicates the formation of an unequal mixture of diastereomers. Previously, Bertrand's group has also reported the

formation of diastereomeric mixture while synthesizing $[(^{Me}BICAAC)_2Cu][CuBr_2]$ complex[29a] which showed double peaks in $^{13}C\{^1H\}$ NMR spectrum for every single peak. Very recently, our research has also unveiled the formation of the complex BICAAC=P−P=BICAAC, occurring as a diastereomeric mixture (kindly refer to the chapter 4 of the thesis).[29d] We would also like to mention that BICAAC itself is a racemic mixture of a single diastereomer and it is an equimolar mixture of two enantiomers. For the compounds having two BICAAC moieties, two different combinations are possible: (i) a combination of the same enantiomers or (ii) a combination of opposite enantiomers. These two possibilities give rise to two diastereomers. Based on these observations, we predict the formation of similar type of diastereomeric mixture for compound **3** and **5**. Sadly, despite numerous attempts, only one of the two diastereomers crystallized for complexes **3** and **5**, and attempts to crystallize the other isomers were unsuccessful. Furthermore, under dark conditions the addition of excess AgBr to a THF solution of **4** resulted in the formation of a red compound **6** (Scheme 2A.4) which exhibits a broad signal in the ^{11}B spectrum at $\delta = 18.4$ ppm. Complex **6** is stable only under inert and low temperature conditions at -15 to -20 °C and decomposes upon the exposure to light and higher temperature. During the crystallization process, elemental black silver was also observed, suggesting decomposition, although the specific decomposed products could not be identified. Moreover, **6** can be converted back to **5** when reacted with an excess CuCl with the removal of AgBr (Scheme 2A.4). Moreover, we found that complex **4** reacts with excess CuI in a fashion similar to its reaction with AgBr. Upon addition of excess CuI in THF solution of **4**, the dark green colour of **4** immediately turned sangria red to give **7** (Scheme 2A.4). HRMS spectrum of **7** showed peak at $m/z =$ 709.4897 (calcd. 709.4880) as $[M-I]^+$. Additionally, when **4** was combined with AuCl, the formation of elemental Au was observed and decomposed products could not be identified.

Single crystal X-ray diffraction studies revealed that compound **5** crystallized in the monoclinic system and possess $P21/n$ space group. Complex **5** has the B−B bond distance of 1.689(7) Å which is intermediate between the B−B bond lengths of **3** and **4** (Figure 2A.5). Unlike the coinage metal diborene complexes described by Braunschweig, which only demonstrated coordination with one M−Cl (M = Cu, Ag)[25] unit, **5** exhibits coordination with two CuCl units in the η2-coordination mode (Figure 2A.5). X-ray analysis also showed both the CuCl units are perpendicular to the B−B axis in the direction mutually opposite to each other. The mutual trans orientation of BICAAC units and hydrogens, which was present in **4**, also preserved in **5**. The coordination of two CuCl units to diborene **4** does not bring any change in the $B_2C_2H_2$ core as it remains planar in **5** (Figure 2A.5). It was observed that the C1−B1 bond length in **5** had increased to 1.598(4) Å from 1.546(6) Å in precursor **4**. The B1−Cu1 and Cu1−Cl1 distances, which were found to be 2.105(4) and 2.125(1) Å, respectively, are equivalent to the data from the literature.[25b]

The diborene metal complexes **6** and **7** crystallized in the triclinic and monoclinic crystal systems with $P\bar{1}$ and $C2/c$ space groups, respectively. In both these complexes, only one MX unit showed coordination with the B=B axis in η2-coordination mode (Figure 2A.5). Complexes **6** and **7** possesses a B−B bond lengths of 1.654(8) and 1.630(6) Å which are marginally shorter than **5** (1.689(7) Å), and slightly elongated if compared with the B−B bond distance in **4** (1.578(10) Å). Similarly, the C1−B1 bond distances in **6** and **7** was found 1.577(7) and 1.563(4) Å respectively, which is also shorter than **5** (1.598(4) Å) and among all the reported metal π-diborene complexes (1.594(6) Å and 1.593(4) Å).[25] The planar arrangement of $C_2B_2H_2$ core in **4** (torsional angle 180°) became trans-bent in **6** (torsional angle 164.4(5)°) and **7** (torsional angle 163.1(3)°). Based on the above results, we believe that the strong donor properties of BICAAC and the tiny hydride ligands on B centers of **4**

55

will be crucial in the formation of the dinuclear η^2-coordination complex with smaller CuCl and mononuclear $\eta 2$- coordination complex with substantially larger AgBr and CuI units.
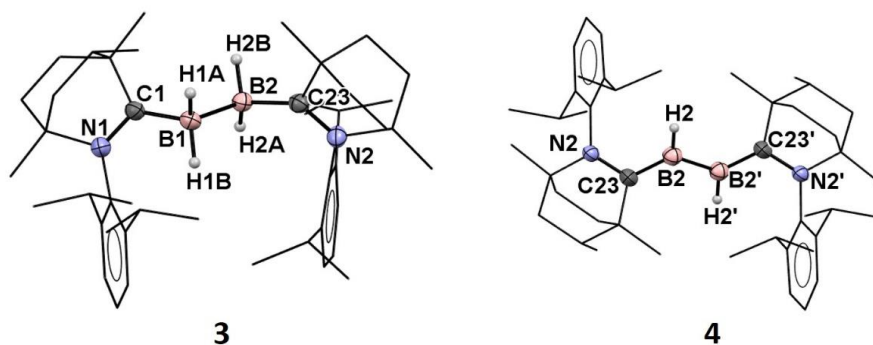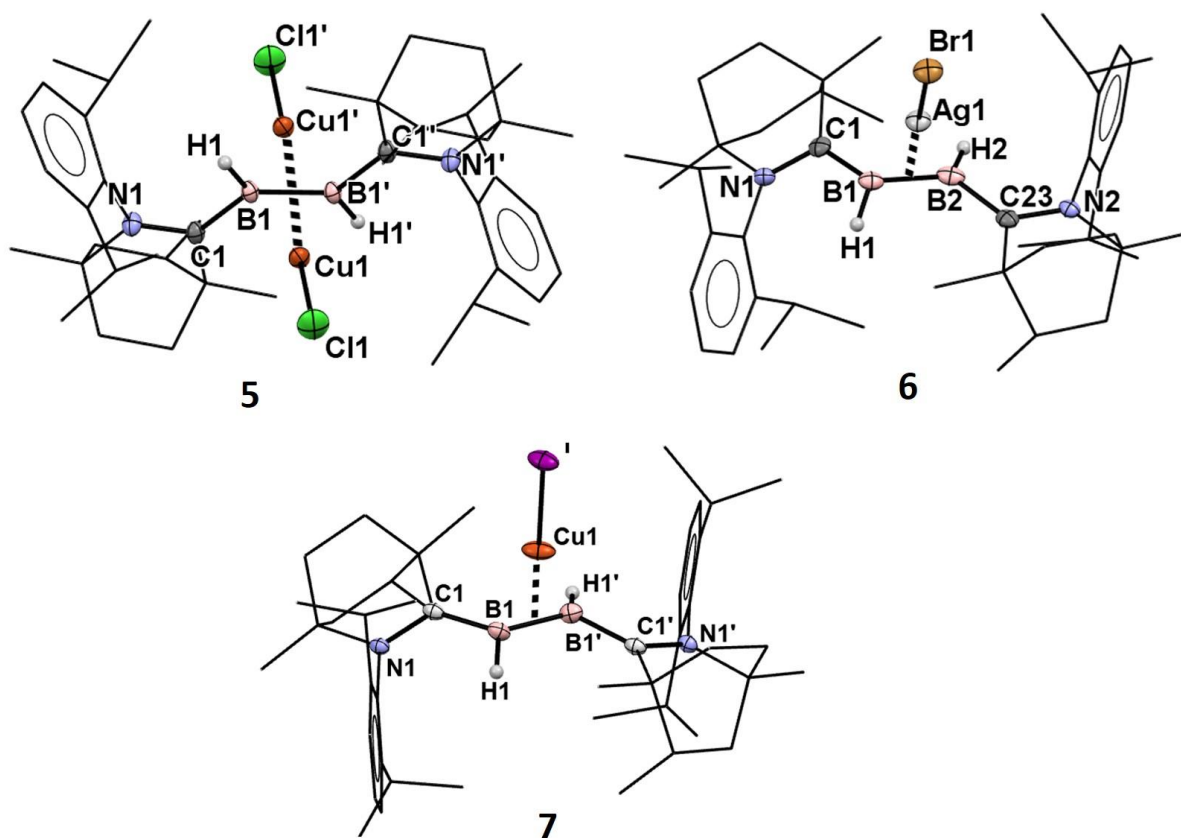

Figure 2A.5 Single crystal X-ray structures of **5, 6** and **7**. Thermal ellipsoids are shown at 50% probability level. All the hydrogen atoms on carbon were omitted for clarity. Selected bond lengths (Å) and angles (°) for **5**: C1−B1 1.598(4), B1−H1 1.03(3), B1−B1′ 1.689(7), B1−Cu1 2.105(4), B1′−Cu1 2.101(4), Cu1−Cl1 2.125(1); N1−C1−B1 119.8(3), C1−B1−B1′ 128.8(4), C1−B1−Cu1 108.5(2), B1−Cu1−Cl1 158.3(1); for **6**: C1−B1 1.577(7), B1−H1 0.98, B1−B2 1.654(8), B2−C23 1.579(7), B1−Ag1 2.315(5), B2−Ag1 2.340(5), Ag1−Br1 2.5005(6); C1−B1−B2 122.7(4), Ag1−B1−B2 70.0(3), B1−Ag1−Br1 156.86(13), B1−Ag1−B2 41.61(19), B1−B2−C23 129.3(4); for **7**: N1−C1 1.350(3), C1−B1 1.563(4), B1−B1′ 1.630(6), B1−H1 1.00; N1−C1−B1 120.4(2), C1−B1−B1′ 126.4(3), B1−B1′−Cu1 67.57(9).

2A.2.4 Computational results

Geometry optimizations of compounds **3**-**6** were performed (In collaboration with Prof. D. Koley) at the M06-2X/def2-SVP level of theory to show the bonding scenario and the electronic structures. When compared to the experimentally reported crystal structures, the geometrical parameters of compounds **3**-**6** showed good agreement, which can be seen from the alignments and superposition of the conformers. Natural bond orbital analysis (NBO) of complex **3** disclosed that the B1−B1′ manifests a σ-occupancy of 1.641e (Figure 2A.6) with equal contributions with the bonding partners (B ~ 50%). This is also evident from the HOMO of complex **3**. The two boron atoms (B1/B1′) in **3** are connected to (C1/C1′) of the BICAAC through the single-bond occupancies of 1.951e, where due to the greater electronegativity of carbene carbons the electron occupancies of B1−C1/B1′−C1′ bonds are mostly localized on the carbon centers (~66%).[30] The QTAIM (Quantum Theory of Atoms

HOMO (3)   HOMO (4)   HOMO-1 (4)

HOMO (5)   HOMO-1 (5)

HOMO (6)   HOMO-3 (6)
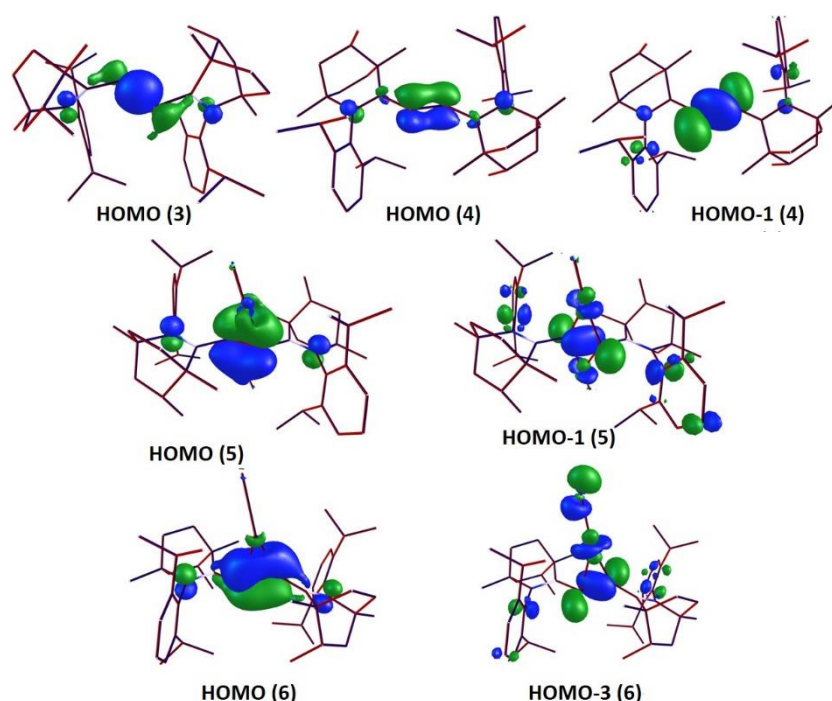
Figure 2A.6 Selected KS-MOs of diborane **3**, diborene **4**, and complexes of diborene **4** with CuCl and AgBr **5** and **6**, respectively (isosurface = 0.060 a.u.) at M062X/def2-TZVPP/SMD//M062X/def2-SVP level of theory. Hydrogen atoms are omitted for clarity.

57

in Molecules) calculations also supports the electronic structures derived from NBO analysis. At the (3,-1) bond critical point (BCP), electron density $[\rho(r) = 0.098]$ of the B1−B1′ bond along with the respective Laplacian $[\nabla^2\rho(r) = -0.143]$ suggests a covalent interaction whereas the electron density $[\rho(r)]$ at the BCP of B1−C1/B1′−C1′ [0.158] bonds along with Laplacian value $[\nabla^2\rho(r) = +0.222]$ indicate significant donor-acceptor type interaction.[31] The calculated Wiberg bond indices (WBI) of the B1−B1′ (0.689) bond also support the B−B single bond character in the diborane complex **3**. For diborene **4**, the HOMO showed B−B π-bonding orbital character while HOMO-1 showed a mixed B−B and B−H σ-bonding character (Figure 2A.7). The formation of π-bond is primarily caused by the overlap of boron's $2p$ orbitals. The B2−C23/B2′−C23′ bonds exhibit donor-acceptor type interaction $[\nabla^2\rho(r) = +0.176]$ while the $\nabla^2\rho(r)$ of -0.400 for B2−B2′ bond clearly indicates its covalent nature. Additionally, WBI of B−B bond (1.341) of **4** undoubtably indicates a double bond character, while the Wiberg bond indices of B−C^{carbene} bonds [B2−C23/B2′−C23′] are found to be 1.07 which indicates the partial double bond character and describes the presence of slight B−C^{carbene} π-backdonation.

We have also studied the bonding possibilities in NHC-diborene (**4^{NHC}**) and cAAC-diborene (**4^{cAAC}**) in addition to diborene **4^{BICAAC}**. The B−B bond lengths were found to be similar in each case (**4**/**4^{NHC}**/**4^{cAAC}** = 1.617/1.616/1.607 Å). As shown in the frontier MO diagram, the HOMO-LUMO gap is largest for the NHC adduct **4^{NHC}** and least for **4^{BICAAC}**. This is in line with the previous literature reports, which shows the increase in the HOMO−LUMO energy gap from BICAAC to NHC matches well with the singlet-triplet gap.[29a,32] Further examination of the frontier orbitals revealed that from **4^{BICAAC}** → **4^{NHC}**, there is a higher relative destabilization of both the σ-orbital (HOMO) and the pπ-orbital (LUMO) of NHC fragments.[29a, 32a, 33] The WBI(BB) values for the B−B bonds in **4^{NHC}** and **4^{cAAC}** are computed to be 1.554 and 1.379, respectively.

Furthermore, the bonding scenario of the Cu and Ag complexes **5** and **6** were also computationally studied. The B−B bond distances in **5** and **6** are higher than the diborene **4** (|ΔL| = 0.038/0.018 Å for **5**/**6**). This is primarily owing to the involvements of the Cu and Ag metals into bonding in complexes **5** and **6**, respectively.[25b] Similar to **4**, HOMO of both **5** and **6** displayed π-bonding character whereas HOMO-1 of **5** and HOMO-3 of **6** showed mixed B−B and B−H σ-bonding interactions (Figure 2A.7). Moreover, similar to **4**, the AIM
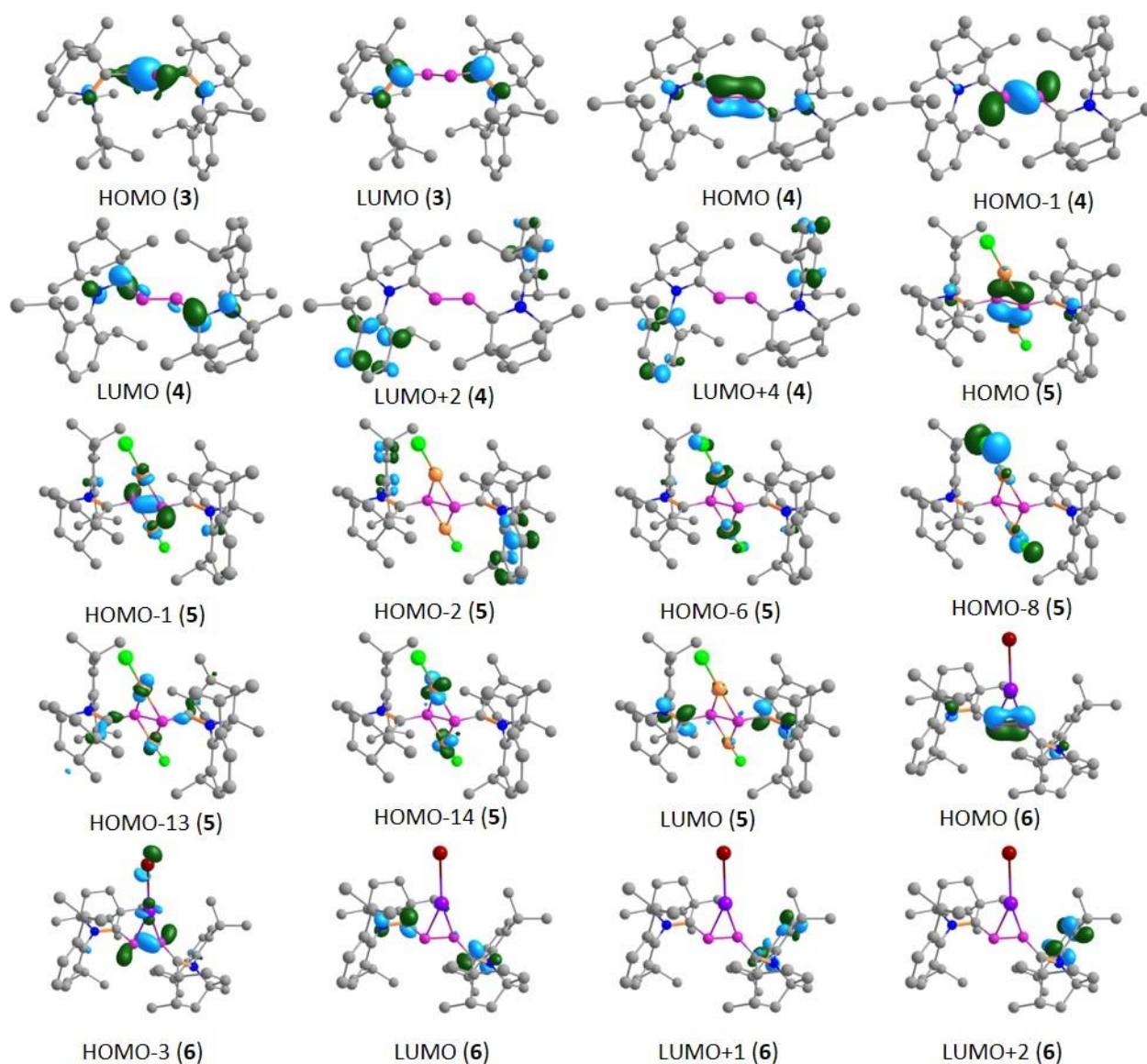
Figure 2A.7 KS-MOs of complexes **3**-**6** (isosurface = 0.075 a.u.) at M06-2X/def2-TZVPP(SMD=Toluene) //M06-2X/def2-SVP level. All hydrogen atoms are omitted for clarity.

calculations of **5** and **6** showed covalent nature of the B–B bond with respective Laplacians of -0.293 and -0.357. The Wiberg bond indices (WBI) of B−B bonds in both the diborene metal complex **5** and **6** are calculated to be 1.452 and 1.402, indicating double bond character in both the complexes.[18a] The energy decomposition analysis (EDA) revealed that in **5** and **6**, the coordination between the >B=B< and Cu/Ag are mainly electrostatic in nature (E_{el} = -219.6/-105.0 kcal/mol for **5**/**6**), whereas the covalent interactions are smaller for both the cases (E_{orb} = -136.9/-51.5 kcal/mol for **5**/**6**). These findings are in line with the observations reported by Braunschweig and co-workers in their coinage metal π-diborene complexes.[25b]

2A.2.5 UV-vis spectroscopic studies

The formation of complex **3** having two CuCl units engaged across the B=B axis motivated us to study the absorption behavior of this complex as the previously reported molecules feature only one MCl (M = Cu, Ag) unit.[25] Therefore, the absorption behavior of compounds **3-6** were recorded in toluene and the absorption profiles were corroborated by using TDDFT calculations (Figure 2A.8 and Table 2A.1). The yellow diborane **3** showed an absorption maximum located at λ_{max} = 397 nm (molar extinction coefficient: 3886 Lmol^{-1}cm^{-1}) while the green diborene **4** displayed intense lower energy band at λ_{max} = 635 nm (molar extinction coefficient: 9840 Lmol^{-1}cm^{-1}) and two higher energy broad bands at λ_{abs} = 392 nm (molar extinction coefficient: 1142 Lmol^{-1}cm^{-1}) and λ_{abs} = 305 nm (molar extinction coefficient: 1499 Lmol^{-1}cm^{-1}) (Figure 2A.8).

The UV-vis absorption maximum of orange diborene-Cu(I) complex **5** was found at λ_{max} = 401 nm (molar extinction coefficient: 12047 Lmol^{-1}cm^{-1}) with a higher energy absorption band detected at λ_{abs} = 341 nm (molar extinction coefficient: 5741 Lmol^{-1}cm^{-1}) (Figure 2A.8). The absorption spectrum of the red diborene-Ag(I) complex **6** showed lower energy absorption band at λ_{max} = 505 nm (molar extinction coefficient: 291 Lmol^{-1}cm^{-1}) and
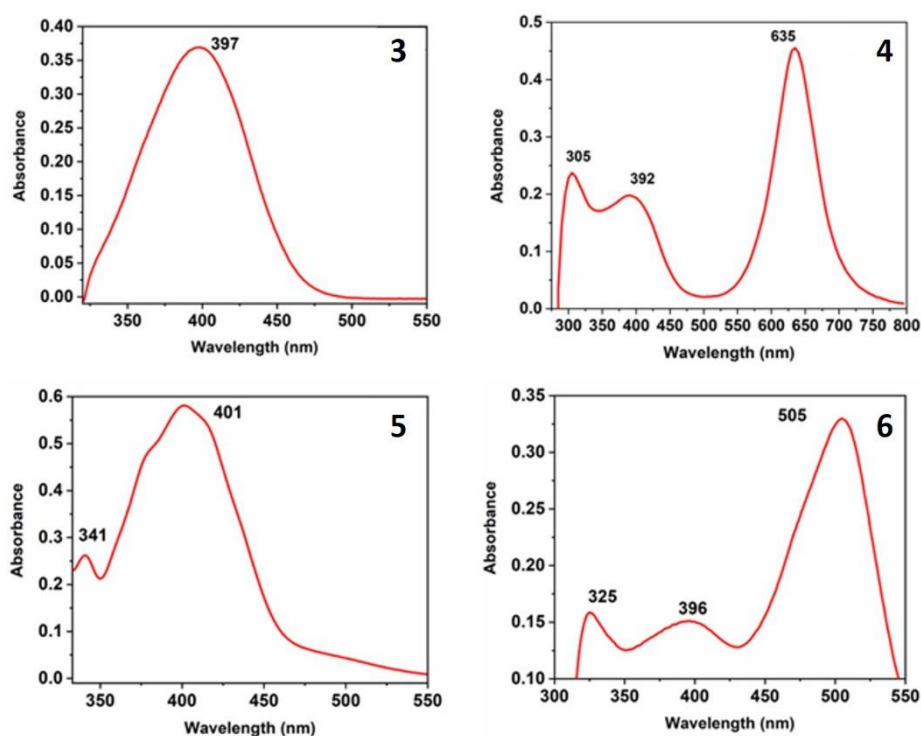
Figure 2A.8 Experimental absorption spectra of compounds **3-6** recorded at room temperature in toluene at 0.0000606, 0.0001435, 0.0000497 and 0.0009387 molar concentrations, respectively.

higher energy absorption bands at λ_{abs} = 396 nm (molar extinction coefficient: 152 Lmol^{-1}cm^{-1}) and 325 nm (molar extinction coefficient: 202 Lmol^{-1}cm^{-1}) (Figure 2A.8).

In order to interpret the UV/Vis spectra, we have performed the TDDFT calculations at the B3LYP/def2-TZVPP/SMD//M06-2X/def2-SVP level of theory under SMD model (solvent = toluene). Theoretical UV spectrum of diborane **3** showed the characteristic band at λ = 352.3 nm (Table 2A.1) with an oscillator strength of 0.58, classifying the transition between B-B σ bond to the vacant *p*-orbital of the carbene carbon, which is in line with the experimentally observed band at λ = 397 nm. Diborene **4** exhibits three absorption bands at 607.7, 420.9 and 284.5 nm which are in close agreement with the experimental signatures (see below). The higher-lying signal was designated as HOMO → LUMO excitation, whereas the lower-lying absorptions were characterized with HOMO → LUMO+4 and HOMO-4 → LUMO excitations. Complex **5** showed two signals at 436.2, 345.2 nm and the

two main contributions to the observed spectra are due to transitions between HOMO-2 → LUMO and HOMO-14 → LUMO.

Table 2A.1 Experimental (at room temperature in toluene) and calculated UV/vis data (at B3LYP/def2-TZVPP/SMD//M06-2X/def2-SVP level of theory) for compounds **3**-**6**.

Compound	λ(exp.) [nm]	λ(calcd.) [nm]	ε [Lmol^{-1}cm^{-1}]	Transitions
3	397	352	3886	HOMO→LUMO (98%)
4	635	607	9840	HOMO→LUMO (102%)
	392	420	1142	HOMO→LUMO+4 (88%)
				HOMO→LUMO+2 (12%)
	305	284	1499	HOMO-4→LUMO (97%)
5	401	436	12047	HOMO-2→LUMO (58%)
				HOMO→LUMO (32%)
				HOMO-6→LUMO (5%)
	341	345	5741	HOMO-14→LUMO (48%)
				HOMO-13→LUMO (17%)
				HOMO-8→LUMO (19%)
6	505	483	291	HOMO→LUMO (99%)
	396	372	152	HOMO-3→LUMO (22%)
				HOMO-2→LUMO (76%)
	325	323	202	HOMO→LUMO+1 (91%)
				HOMO→LUMO+2 (6%)

Similar to **4**, complex **6** also showed three signals at 483.5, 372.1 and 323.3 nm and the transitions are from HOMO → LUMO, HOMO-2 → LUMO and HOMO → LUMO+1 (Table 2A.1). In complexes **4**-**6**, HOMO represents the B-B bonding orbital of π-symmetry, while the LUMO is composed of orbitals with p character located at the BICAAC ligand. The molecular orbitals involved in the major excitations are collected in Figure 2A.7.

2A.3 Conclusion

In summary, we have described the synthesis of stable diborane and diborene compounds supported by bicyclic (alkyl)(amino) carbene (BICAAC). The dihydrodiborene complex is isolobal and isoelectronic to conventional olefins and provides the opportunity to investigate the formation of π-complexes with transition metals. The findings show that diborene exhibits substantial carbene-boron interaction and the presence of small hydride ligands on boron centers in diborene allow the formation of mononuclear and the unprecedented dinuclear η^2-diborene metal complex with AgBr/CuI and CuCl, respectively. Structural and computational study revealed lengthening of the >B=B< and B−C^{BICAAC} bonds upon metalation of diborene. As revealed by EDA (energy decomposition analysis) calculations, the interaction between >B=B< and Cu/Ag metal is primarily electrostatic in nature. The TDDFT calculations were also performed and showed good agreement with the experimentally reported absorption profile of these complexes.

2A.4 Experimental section

2A.4.1 General methods

All the manipulations were performed under an inert atmosphere of dry nitrogen or argon using a glove box or standard Schlenk techniques. All the glassware were dried at 150 °C in an oven for at least 12 h and assembled hot and cooled in vacuo prior to use. Solvents were purified by MBRAUN solvent purification system MB SPS-800 and were used directly from the SPS system. Chemicals were purchased from Sigma-Aldrich, HIMEDIA, and Avra and were used without further purification. Bicyclic (alkyl)(amino) carbene (BICAAC) and BICAAC−BH$_2$Cl and BICAAC−BHCl$_2$ adducts were prepared using reported procedures.[29a-b]

2A.4.2 Physical measurements

The ^{1}H, ^{13}C{^{1}H} and ^{11}B NMR spectra were recorded using Bruker 400 MHz spectrometer with tetramethylsilane (TMS) (for ^{1}H and ^{13}C{^{1}H}) and BF$_3$·OEt$_2$ (for ^{11}B) as external reference; chemical shift values are reported in ppm. FT-IR spectra of complexes **3**, **4** and **6** were recorded (in the range 4000-400 cm^{-1}) with a Perkin-Elmer Lambda 35-spectrophotometer using Nujol mull and IR spectrum of **5** was recorded as neat solid on a Bruker Alpha ZnSe ATR spectrometer. High resolution mass spectrometry (HRMS) was performed with Waters SYNAPT G2-S. Solution state UV-Vis. spectra of complexes **3**-**6** were recorded on LABINDIA UV-Vis. spectrophotometer 3000+. Melting point of compounds **3**-**6** were recorded in sealed capillary using Büchi B-540 melting point apparatus. The single-crystal X-ray diffraction data of compounds **1**, **2**, **3**, **5, 6** and **7** was collected using a Rigaku XtaLAB mini diffractometer equipped with Mercury375M CCD detector. The data were collected with MoKα radiation (λ = 0.71073 Å) using omega scans. During the data collection, the detector distance was 49.9 mm (constant) and the detector was placed at 2θ = 29.85° (fixed) for all the data sets. The data collection and data reduction of compounds **1**, **2**, **3**, **5** and **6** were done using Crystal Clear suite.[34a] Single crystal X-ray diffraction data of complex **4** was collected on a Bruker *AXS KAPPA APEX-II* CCD diffractometer with MoKα radiation using omega scans. Unit cell determination, refinement and data collection were done using the Bruker APPEX-II suite,[34b] data reduction and integration were performed using SAINT v8.34A (Bruker, 2013)[34c] and absorption corrections and scaling were done using SADABS-2014/5 (Bruker,2014/5).[34d] All non-hydrogen atoms were refined anisotropically. Using Olex2[35], the structures of complexes **1**, **5, 6** and **7** were solved with the SHELXT[36a] structure solution program using Intrinsic Phasing and refined with the SHELXL[36b] refinement package using Least Squares minimization. The structure of complex **2**, **4** was solved using Olex2[35], with the SHELXT[36a] structure solution program

using intrinsic phasing and refined with the SHELXH-1997[36c] refinement package using Least Squares minimization. Using Olex2[35], the structure of complex **3** was solved with the olex2.solve[36d] structure solution program using Charge Flipping and refined with the SHELXH-1997[36c] refinement package using Least Squares minimization.

2A.4.3 Syntheses and characterization of complexes 1-6

Synthesis and characterization of [BICAAC−BF₃] (1): In a Schlenk flask, BICAAC (0.31 g, 1.00 mmol) was dissolved in toluene (10 mL) and was cooled to -40 °C. BF₃·OEt₂ (0.12 mL, 1.00 mmol) was added to it and the mixture was allowed to warm to room temperature and stirred for 2 h followed by the evaporation of all volatiles under vacuum. The residue obtained was washed with hexane (15 mL) and dried under vacuum. The resulting white solid was crystallized from a mixture of dichloromethane (DCM) and pentane at -30 °C that afforded colorless crystals of adduct **1**. Yield: 0.30 g, 79.3 %. **Mp**: 203-205 °C. **IR** (nujol mull, cm⁻¹) ν: 2953, 2923, 2853, 1619, 1588, 1560, 1475, 1466, 1455, 1446, 1435, 1377, 1366, 1345, 1317, 1258, 1230, 1217, 1182, 1090, 1048, 942, 876, 751, 741, 626, 564, 574. **¹H NMR** (400 MHz, CDCl₃): δ = 7.39-7.36 (m, 1H, pAr-H), 7.23- 7.21 (m, 2H), 2.77 (sept, 1H, CH(CH₃)₂, $^3J_{H-H}$ = 8 Hz), 2.48 (sept, 1H, CH(CH₃)₂, $^3J_{H-H}$ = 8 Hz), 2.21-2.15 (m, 1H), 2.06-1.97 (m, 1H), 1.85-1.78 (m, 3H), 1.72 (s, 3H), 1.60-1.55 (m, 1H), 1.31 (d, 3H, $^3J_{H-H}$ = 4 Hz), 1.26-1.22 (m, 10H), 1.09 (d, 3H), 0.97 (s, 3H) ppm. **¹³C{¹H} NMR** (100 MHz, CDCl₃): δ = 143.2, 142.9, 137.9, 129.4, 124.5, 124.3, 65.6, 46.7, 43.6, 38.2, 32.8, 29.4, 28.7, 24.7, 24.5, 24.4, 23.6, 23.5, 21.4, 21.4, 20.2 ppm. **¹¹B NMR** (128 MHz, CDCl₃): δ = -0.72 (q, $^1J_{B-F}$ = 41 Hz) ppm. **¹⁹F{¹H} NMR** (376 MHz, CDCl₃): δ = -139.7 (q, $^1J_{F-B}$ = 41) ppm. **HRMS** (AP⁺): m/z calculated for C₂₂H₃₃NBF₂: 360.2678; found: 360.2661 [M-F]⁺.

Synthesis and characterization of [BICAAC−B(C₆F₅)₃] (2): In a Schlenk flask, BICAAC (0.31 g, 1.00 mmol) was dissolved in toluene (10 mL) and was cooled to -30 °C. Thereafter,

B(C_6F_5)$_3$ (0.51 g, 1.00 mmol) was added to it and the mixture was allowed to warm to room temperature and stirred for 2 h followed by the evaporation of all volatiles under vacuum. The residue obtained was washed with pentane (15 mL) and dried under vacuum. The resulting solid was crystallized from a mixture of dichloromethane (DCM) and pentane at room temperature that afforded colorless crystals of adduct **2**. Yield: 0.58 g, 71 %. **Mp**: 138-139 °C. **^{11}B NMR** (128 MHz, CDCl$_3$): δ = -12.6 (s) ppm. **^{19}F{^{1}H} NMR** (376 MHz, CDCl$_3$): δ = -105.91 (d, J = 26.32 Hz), -120.80 (d, J = 22.56 Hz), -126.89 (d, J = 22.56 Hz), -127.50 (d, J = 18.8 Hz), -128.0 (d, J = 18.8 Hz), -132.0 (t, J = 11.28 Hz), -157.2 (t, J = 18.8 Hz), -159.3 (t, J = 18.8 Hz), -159.6 (t, J = 18.8 Hz), -163.8 (t, J = 18.8 Hz), -164.0 (t, J = 22.56 Hz), -164.9 (t, J = 22.56 Hz), -165.6 (t, J = 22.56 Hz), -166.3 (t, J = 22.56 Hz), -167.0 (t, J = 18.8 Hz) ppm. **HRMS** (ES$^-$): *m/z* calculated for C$_{40}$H$_{32}$NBF$_{15}$: 822.2395; found: 822.2360 [M-H]$^-$.

Synthesis and characterization of [BICAAC→(H)$_2$B−B(H)$_2$←BICAAC] (3): via KC$_8$ route: In a 50 mL Schlenk flask, BICAAC−BH$_2$Cl (0.20 g, 0.56 mmol) was dissolved in 10 mL of toluene or THF inside argon-filled glove box thereafter, KC$_8$ (0.08 g 0.56 mmol,) was added in it at -30 °C. It gave light yellow colored reaction mixture in both toluene and THF. The reaction mixture was stirred for 3 hours. Excess graphite was removed by filtration to give a light-yellow filtrate. The filtrate was reduced to approximately 3 mL and kept at -30 °C. Yellow colored crystals were grown after 72 hours (Yield: 0.14 g, 76% in toluene; 0.12 g, 68% in THF) (approximately 50:50 mixture of diastereomers). **Via K metal route:** In a 50 mL Schlenk flask, BICAAC-BH$_2$Cl (0.20 g 0.56 mmol,) was dissolved in 10 mL of THF inside argon-filled glove box thereafter, an excess of K metal (0.06 g, 1.5 mmol) was added in it at -30 °C. It took 24-26 hours to complete the reaction and gave an orange-colored reaction mixture. Excess K was removed by filtration to give an orange filtrate. The filtrate was reduced to approximately 3 mL and kept at -30 °C. Orange crystals were grown after 72

hours (Yield: 0.10 g, 55%) (approximately 50:50 mixture of diastereomers). **Mp**: 185 °C (melts with decomposition). **FT-IR** (nujol mull, cm^{-1}) ν: 2954, 2387, 1458, 1377, 1326, 1222, 936, 807, 754, 694. **^{1}H NMR** (400 MHz, C$_6$D$_6$): δ = 7.19-7.13 (m, 2H, pAr-H), 7.09-7.04 (m, 4H, mAr-H), 3.06 (sept, 2H, CH(CH$_3$)$_2$, $^3J_{\text{H-H}}$ = 8.0 Hz), 2.95 (sept, 2H, CH(CH$_3$)$_2$, $^3J_{\text{H-H}}$ = 8.0 Hz), 1.81-1.67 (m, 12H), 1.58-1.46 (m, 10H), 1.39-1.29 (m, 8H), 1.23-1.15 (m, 20H), 1.01 (broad s, 4H), 0.62-0.61 (m, 6H) ppm. **^{13}C{^{1}H} NMR** (100 MHz, C$_6$D$_6$): δ = 145.91, 145.81, 145.77, 140.67, 140.65, 127.62, 127.58, 124.57, 124.53, 124.46, 60.43, 60.30, 46.68, 44.84, 44.46, 37.78, 37.76, 34.62, 34.43, 33.91, 33.50, 28.76, 28.62, 28.44, 28.35, 26.13, 25.94, 25.76, 25.67, 25.54, 25.39, 25.23, 24.77, 24.72, 24.68, 20.36, 20.15 ppm (diastereomeric mixture). ^{13}C{^{1}H} NMR chemical shift value for the carbene carbon could not be detected, presumably due to quadrupolar nature of boron nucleus. As indicated by ^{1}H and ^{13}C{^{1}H} NMR spectra, compound **3** has formed an equal diastereomeric mixture, due to which there are double peaks present in the ^{13}C{^{1}H} NMR spectrum which corresponds to two diastereomers (we anticipate that this is not due to the impurities). **^{11}B NMR** (128 MHz, C$_6$D$_6$): δ = -16.4 ppm (broad). **HRMS** (AP$^+$): calculated for [C$_{44}$H$_{69}$B$_2$N$_2$]: m/z = 647.5661, found: m/z = 647.5635 [M-H]$^+$.

Synthesis and characterization of [BICAAC→(H)B=B(H)←BICAAC] (4): In a 50 mL Schlenk flask, BICAAC−BHCl$_2$ (0.20 g, 0.51 mmol) was dissolved in 10 mL of toluene or THF solution then KC$_8$ (0.15 g 1.12 mmol) was added to this at -30 °C in a glove box. In THF the color of the reaction mixture immediately becomes green after KC$_8$ addition while in toluene it took 20 minutes to appear the green color. The reaction mixture was stirred for 3 hours in both the solutions. After that graphite was removed by filtration to give an intense green colored filtrate. The volume of the filtrate was reduced to 3-4 mL and was kept at -5 °C. After 3 days plate-shaped green crystals of **4** were grown from it. (Yield: 0.12 g, 73% in toluene; 0.11 g, 65% in THF). **Mp** = 164-166 °C. **FT-IR** (nujol mull, cm^{-1}) ν: 3052, 2955,

2924, 2855, 2499, 1985, 1532, 1455, 1377, 1261, 906, 800, 769. **¹H NMR** (400 MHz, C$_6$D$_6$):

δ = 7.22-7.18 (m, 2H, pAr-H), 7.12-7.09 (m, 4H mAr-H), 5.00 (broad s, 2H, B-H), 3.11 (sept,

2H, CH(CH$_3$)$_2$, $^3J_{\text{H-H}}$ = 8.0 Hz), 2.91 (sept, 2H, CH(CH$_3$)$_2$, $^3J_{\text{H-H}}$ = 8.0 Hz), 1.81-1.79 (m,

4H), 1.69 (broad s, 6H), 1.62-1.60 (m, 6H), 1.50-1.40 (m, 16H), 1.25-1.20 (m, 12H), 1.12-

1.11 (m, 6H), 0.65 (s, 6H) ppm. **¹³C{¹H} NMR** (100 MHz, C$_6$D$_6$): δ = 297.9, 145.7, 141.0,

127.6, 124.2, 124.0, 58.9, 46.5, 45.1, 37.8, 36.8, 34.4, 29.0, 28.5, 27.9, 26.3, 26.1, 25.2, 24.8,

24.1, 20.4 ppm. **¹¹B NMR** (128 MHz, C$_6$D$_6$): δ = 42.6 ppm (broad). **HRMS** (AP$^+$): calculated

for [C$_{44}$H$_{68}$B$_2$N$_2$]: m/z = 646.5583, found: m/z = 646.5435 [M]$^+$.

Synthesis and characterization of [BICAAC(BH)]$_2$(CuCl)$_2$ (5): In a 50 mL Schlenk flask,

excess CuCl (0.05 g, 0.5 mmol, 2.5 equiv.) was added to a solution of **4** (0.13 g, 0.2 mmol) in

10 mL of THF at room temperature in a glove box. The intense green color of **4** faded to light

yellow upon addition of CuCl. The reaction mixture was stirred for further 10 hours to give

orange colored reaction mixture. Excess CuCl was removed by filtration to give clear

orange/dark yellow solution which was reduced to 3-4 mL and kept at -30 °C. Orange

colored crystals were grown after 2 days. (Yield: 0.09 g, 55%). X-ray quality crystals were

grown from a concentrated solution of **5** in toluene at -10 °C. **Mp** = 198 °C with

decomposition. **IR** (ATR, cm^{-1}) ν: 2954, 2922, 2854, 2361, 1463, 1377, 1366, 1263, 1226,

1180, 1028, 928, 812, 723, 631. **¹H NMR** (400 MHz, CDCl$_3$): δ = 7.34-7.30 (m, 2H, pAr-H),

7.24-7.19 (m, 4H, mAr-H), 4.34 (broad s, 2H, B-H), 2.85 (sept, 2H, CH(CH$_3$)$_2$, $^3J_{\text{H-H}}$ = 8.0

Hz), 2.66 (sept, 2H, CH(CH$_3$)$_2$, $^3J_{\text{H-H}}$ = 8.0 Hz), 2.07-1.98 (m, 4H), 1.76-1.69 (m, 4H), 1.61

(s, 6H), 1.52-1.46 (m, 2H), 1.44-1.33 (m, 14H), 1.28-1.26 (m, 14H), 1.23-1.21 (m, 6H), 0.79

(s, 6H) ppm. **¹³C{¹H} NMR** (100 MHz, CDCl$_3$): δ = 144.02, 143.49, 143.44, 142.92, 138.73,

138.49, 129.16, 128.64, 128.56, 128.35, 125.12, 124.97, 65.74, 65.56, 50.03, 49.94, 43.58,

42.59, 38.79, 37.89, 35.86, 35.35, 33.28, 32.13, 29.84, 29.50, 28.95, 28.88, 28.82, 28.71,

28.49, 28.27, 28.08, 24.80, 24.68, 24.55, 24.50, 24.27 ppm. (diastereomeric mixture).

$^{13}\text{C}\{^1\text{H}\}$ NMR chemical shift value for the carbene carbon could not be detected, presumably due to quadrupolar nature of boron nucleus. As indicated by $^{13}\text{C}\{^1\text{H}\}$ NMR spectrum, compound **5** has formed as diastereomeric mixture, due to which there are double peaks for each carbon nucleus present in the $^{13}\text{C}\{^1\text{H}\}$ NMR spectrum which corresponds to two diastereomers. **^{11}B NMR** (128 MHz, CDCl$_3$): δ = 17.9 ppm (broad). **HRMS** (AP$^+$): calculated for [C$_{44}$H$_{68}$B$_2$N$_2$Cu$_2$Cl$_2$]: m/z = 844.3535, found: m/z = 844.3577 [M]$^+$.

Synthesis and characterization of [BICAAC(BH)]$_2$(AgBr) (6): In a 50 mL Schlenk flask, compound **4** (0.13 g 0.2 mmol,) was dissolved in 10 mL of THF inside a glove box. AgBr (0.11 g, 0.6 mmol, 3 equiv.) was added in it at room temperature under dark conditions. The color of the reaction mixture became light orange. After 2 hours of stirring reaction mixture became red. The reaction mixture was stirred for 5 hours under dark then an unreacted AgBr was removed by filtration to give an intense red filtrate. This filtrate was reduced to 3-4 mL and kept at -15 °C. Red colored crystals were grown after 3 days. Some black colored metal deposition was also observed along with crystals. (Yield: 0.05 g, 27%). **Mp** = 205 °C with decomposition. **FT-IR** (nujol mull, cm^{-1}) ν: 2961, 2924, 2854, 2455, 1587, 1521, 1463, 1377, 1317, 1262, 1093, 1053, 929, 802, 723. **^{1}H NMR** (400 MHz, CDCl$_3$): δ = 7.38-7.33 (m, 2H, pAr-H), 7.23-7.20 (m, 4H mAr-H), 2.68 (sept, 2H, CH(CH$_3$)$_2$, $^3J_{\text{H-H}}$ = 8.0 Hz), 2.50 (sept, 2H, CH(CH$_3$)$_2$, $^3J_{\text{H-H}}$ = 8.0 Hz), 2.16-2.03 (m, 4H), 2.0 (s, 4H), 1.88-1.81 (m, 8H), 1.54-1.49 (m, 4H), 1.30-1.23 (m, 24H), 1.16-1.15 (m, 4H), 1.10-1.08 (m, 4H), 0.97-0.95 (m, 6H) ppm. **^{11}B NMR** (128 MHz, CDCl$_3$): δ = 18.4 ppm (broad). **HRMS** (AP$^+$): calculated for [C$_{44}$H$_{68}$B$_2$N$_2$AgBrNa]: m/z = 857.3707, found: m/z = 857.3752 [M+Na]$^+$. Due to rapid decomposition $^{13}\text{C}\{^1\text{H}\}$ NMR spectrum of the product could not be obtained.

Synthesis of [BICAAC(BH)]$_2$(CuCl)$_2$ (5) from [BICAAC(BH)]$_2$(AgBr) (6): In a 50 mL Schlenk flask, compound **4** (0.13 g, 0.2 mmol) was dissolved in 10 mL of THF inside a glove box. AgBr (0.11 g, 0.6 mmol, 3 equiv.) was added in it at room temperature under dark

conditions. The reaction mixture was stirred for 5 hours under dark then an unreacted AgBr was removed by filtration to give an intense red filtrate. Thereafter, excess CuCl (0.03 g, 0.3 mmol) was added in this red filtrate in the exclusion of light and stirred for 5-6 hours. After 4 hours deposition of yellow precipitate was observed, which showed the removal of AgBr from complex **6**. Also, the color of reaction mixture changed from red (in **6**) to orange after 5-6 hours, which indicates the formation of complex **5** (Yield: 0.02 g, 20%). The formation of complex **5** from complex **6** was monitored by ^{1}H and ^{11}B NMR measurements and further confirmed by single crystal X-ray technique.

Synthesis and characterization of [BICAAC(BH)]₂(CuI) (7): In a 50 mL Schlenk flask, compound **4** (0.13 g, 0.2 mmol) was dissolved in 10 mL of THF inside a glove box and CuI (0.11 g, 0.6 mmol, 3 equiv.) was added in it at room temperature. The intense green color of **4** immediately turned sangria red and the reaction mixture was stirred for 5 hours. The excess CuI was filtered off to give intense sangria red filtrate. This filtrate was reduced to half of its initial volume and kept at -10 °C. After 3-4 days, red colored crystals were grown from it. (Yield: 0.04 g, 42%). **HRMS** (ES$^+$): calculated for [C$_{44}$H$_{68}$B$_2$N$_2$Cu]: *m/z* = 709.4880, found: *m/z* = 709.4897 as [M-I]$^+$.

2A.5 Crystallographic data

Table 2A.2 Crystallographic details of complexes **1-4.**

Compound	1	2	3	4
Chemical formula	$C_{22}H_{33}BF_3N$	$C_{41}H_{35}BCl_2F_{15}N$	$C_{48}H_{78}B_2N_2O$	$C_{44}H_{68}B_2N_2$
Molar mass	379.30	908.41	720.74	646.62
Crystal system	orthorhombic	monoclinic	triclinic	triclinic
Space group	$Pca2_1$	$I2/a$	P-1	P-1
T [K]	100.02(10)	100.00(10)	150.0(10)	100.0(1)
a [Å]	17.8370(5)	20.0309(9)	10.1122(4)	9.678(3)
b [Å]	23.3635(7)	19.8785(10)	10.1771(4)	13.499(4)
c [Å]	15.3109(6)	19.4208(8)	22.0534(10)	16.382(5)
α [º]	90.00	90.00	78.556(4)	78.367(9)
β [º]	90.00	91.440(4)	88.953(3)	85.124(9)
γ [º]	90.00	90.00	87.112(3)	70.503(9)
V [Å^3]	6380.6(4)	7730.6(6)	2221.55(16)	1975.5(10)
Z	4	8	2	2
D(calcd.) [g·cm^{-3}]	1.185	1.561	1.077	1.087
μ(No-K$_\alpha$) [mm^{-1}]	0.085	0.274	0.062	0.061
Reflections collected	31150	27899	31422	13059
Independent reflections	11255	6851	7825	7027
Data/restraints/ parameters	11255/0/751	6851/36/576	7825/0/505	7027/360/744
R1, wR2[I>2σ(I)]$^{[a]}$	0.0668, 0.1782	0.0546, 0.1340	0.0847, 0.2246	0.0816, 0.1968
R1, wR2 (all data)$^{[a]}$	0.0898, 0.2029	0.0855, 0.1667	0.1024, 0.2434	0.1258, 0.2235
GOF	1.036	1.072	1.031	1.037
CCDC	**1954942**	**2329703**	**2030914**	**2030915**

[a] $R1 = \Sigma||Fo| - |Fc||/\Sigma|Fo|$. $wR2 = [\Sigma w(|Fo^2| - |Fc^2|)^2/\Sigma w|Fo^2|^2]^{1/2}$

Table 2A.3 Crystallographic details of complexes **5**-**7.**

Compound	5	6	7
Chemical formula	$C_{44}H_{68}B_2N_2Cu_2Cl_2$	$C_{44}H_{68}B_2N_2AgBr$	$C_{44}H_{68}B_2CuIN_2$
Molar mass	844.60	834.40	837.06
Crystal system	monoclinic	triclinic	monoclinic
Space group	$P2_1/n$	P-1	$C2/c$
T [K]	99.99(10)	100.0(10)	150.01(10)
a [Å]	10.1978(7)	10.8916(6)	19.6695(14)
b [Å]	15.0149(10)	11.4059(5)	11.9878(4)
c [Å]	15.6700(11)	17.7418(8)	17.9700(7)
α [º]	90	74.154(4)	90.00
β [º]	101.783(7)	84.263(4)	91.527(5)
γ [º]	90	85.458(4)	90.00
V [Å^3]	2348.8(3)	2106.56(18)	4235.7(4)
Z	2	2	4
D(calcd.) [g·cm^{-3}]	1.194	1.315	1.313
μ(No-K$_\alpha$) [mm^{-1}]	1.049	1.458	1.276
Reflections collected	20594	29835	23843
Independent reflections	4126	7433	7305
Data/restraints/parameters	4126/144/331	7433/0/465	7305/0/237
R1,wR2[I>2σ(I)][a]	0.0454, 0.0993	0.0522, 0.1187	0.0541, 0.1073
R1, wR2 (all data)[a]	0.0662, 0.1088	0.0712, 0.1312	0.1404, 0.1443
GOF	1.041	1.064	0.984
CCDC	**2030916**	**2030917**	**2329670**

[a] R1 = Σ||Fo| − |Fc||/Σ|Fo|. wR2 = [Σw(|Fo^2| − |Fc^2|)^2/Σw|Fo^2|^2]$^{1/2}$

2A.6 References

1. (a) Pitzer, K. S. *J. Am. Chem. Soc.* **1948**, *70*, 2140-2145; (b) Mulliken, R. S. *J. Am. Chem. Soc.* **1950**, *72*, 4493-4503; (c) Mulliken, R. S. *J. Am. Chem. Soc.* **1955**, *77*, 884-887.

2. (a) Jutzi, P. New Element-Carbon (p-p)π Bonds. *Angew. Chem. Int. Ed. Engl.* **1975**, *14*, 232-245; (b) Jutzi, P. *Chem. Unserer Zeit* **1981**, *15*, 149-154.

3. Goldberg, D. E.; Harris, D. H.; Lappert, M. F.; Thomas, K. M. *J. Chem. Soc. Chem. Commun.* **1976**, 261-262.

4. West, R.; Fink, M. J.; Michl, J. *Science* **1981**, *214*, 1343-1344.

5. Klusik, H.; Berndt, A. *Angew. Chem. Int. Ed. Engl.* **1981**, *20*, 870-871.

6. (a) Moezzi, A.; Bartlett, R. A.; Power, P. P. *Angew. Chem. Int. Ed. Engl.* **1992**, *31*, 1082-1083; (b) Yoshifuji, M.; Shima, I.; Inamoto, N.; Hirotsu, K.; Higuchi, T. *J. Am. Chem. Soc.* **1981**, *103*, 4587−4589; (c) Sekiguchi, A.; Kinjo, R.; Ichinohe, M. *Science* **2004**, *305*, 1755-1757.

7. (a) Snow, J. T.; Murakami, S.; Masamune, S.; Williams, D. J. *Tetrahedron Lett.* **1984**, *25*, 4191-4194; (b) Hitchcock, P. B.; Lappert, M. F.; Miles, S. J.; Thorne, A. J. *J. Chem. Soc. Chem. Commun.* **1984**, 480-482; (c) Klinkhammer, K. W.; Fassler, T. F.; Grützmacher, H. *Angew. Chem. Int. Ed.* **1998**, *37*, 124-126.

8. (a) Pluta, C.; Pörschke, K. R.; Krüger, C.; Hildenbrand, K. *Angew. Chem. Int. Ed. Engl.* **1993**, *32*, 388-390; (b) He, X.; Bartlett, R. A.; Olmstead, M. M.; Ruhlandt-Senge, K.; Sturgeon, B. E.; Power, P. P. *Angew. Chem. Int. Ed. Engl.* **1993**, *32*, 717-719; (c) Grigsby, W. J.; Power, P. P. *Chem. Commun.* **1996**, 2235-2236.

9. (a) Moezzi, A.; Olmstead, M. M.; Power, P. P. *J. Am. Chem. Soc.* **1992**, *114*, 2715-2717; (b) Power, P. P. *Inorg. Chim. Acta* **1992**, 198-200, 443-447.

10. Braunschweig, H.; Dewhurst, R. D. *Organometallics* **2014**, *33*, 6271-6277.

11. (a) Su, J.; Li, X.-W.; Crittendon, C.; Robinson, G. H. *J. Am. Chem. Soc.* **1997**, *119*, 5471-5472; (b) Wright, R. J.; Brynda, M.; Power, P. P. *Angew. Chem. Int. Ed.* **2006**, *45*, 5953-5956.

12. (a) Pu, L.; Twamley, B.; Power, P. P. *J. Am. Chem. Soc.* **2000**, *122*, 3524-3525; (b) Stender, M.; Phillips, A. D.; Wright, R. J.; Power, P. P. *Angew. Chem. Int. Ed.* **2002**, *41*, 1785-1787; (c) Phillips, A. D.; Wright, R. J.; Olmstead, M. M.; Power, P. P. *J. Am. Chem. Soc.* **2002**, *124*, 5930-5931; (d) Fischer, R. C.; Power, P. P. *Chem. Rev.* **2010**, *110*, 3877-3923.

13. (a) Hardman, N. J.; Wright, R. J.; Phillips, A. D.; Power, P. P. *Angew. Chem. Int. Ed.* **2002**, *41*, 2842-2844; (b) Hardman, N. J.; Wright, R. J.; Phillips, A. D.; Power, P. P. *J. Am. Chem. Soc.* **2003**, *125*, 2667-2679; (c) Wright, R. J.; Phillips, A. D.; Hardman, N. J.; Power, P. P. *J. Am. Chem. Soc.* **2002**, *124*, 8538-8539; (d) Wright, R. J.; Phillips, A. D.; Hino, S.; Power, P. P. *J. Am. Chem. Soc.* **2005**, *127*, 4794-4799.

14. (a) Paetzold, P.; Richter, A.; Thijssen, T.; Würtenberg, S. *Chem. Ber.* **1979**, *112*, 3811-3827; (b) Paetzold, P.; von Plotho, C. *Chem. Ber.* **1982**, *115*, 2819-2825.

15. Braunschweig, H.; Radacki, K.; Schneider, A. *Science* **2010**, *328*, 345-347.

16. (a) Glaser, B.; Nöth, H. *Angew. Chem. Int. Ed.* **1985**, *24*, 416-417; (b) Berndt, A. *Angew. Chem. Int. Ed.* **1993**, *32*, 985-1009; (c) Eisch, J. J. *Adv. Organomet. Chem.* **1995**, *39*, 355-392; (d) Brand, J.; Braunschweig, H.; Hupp, F.; Phukan, A. K.; Radacki, K.; Sen, S. S. *Angew. Chem. Int. Ed.* **2014**, *53*, 2240-2244.

17. (a) Dill, J. D.; Schleyer, P. v. R.; Pople, J. A. *J. Am. Chem. Soc.* **1975**, *97*, 3402-3409; (b) Knight, L. B.; Kerr, K.; Miller, P. K.; Arrington, C. A. *J. Phys. Chem.* **1995**, *99*, 16842-16848; (c) Braunschweig, H.; Damme, A.; Dewhurst, R. D.; Vargas, A. *Nat. Chem.* **2013**, *5*, 115-121.

18. (a) Wang, Y.; Quillian, B.; Wei, P.; Wannere, C. S.; Xie, Y.; King, R. B.; Schaefer, H. F.; Schleyer, P. v. R.; Robinson, G. H. *J. Am. Chem. Soc.* **2007**, *129*, 12412-12413; (b) Wang, Y.; Quillian, B.; Wei, P.; Xie, Y.; Wannere, C. S.; King, R. B.; Schaefer, H. F.; Schleyer, P. v. R.; Robinson, G. H. *J. Am. Chem. Soc.* **2008**, *130*, 3298-3299; (c) Wang, Z.-X.; Chen, Z.; Jiao, H. J.; Schleyer, P. v. R. *J. Theoret. Comput. Chem.* **2005**, *4*, 669-688.

19. Braunschweig, H.; Dewhurst, R. D.; Hammond, K.; Mies, J.; Radacki, K.; Vargas, A. *Science* **2012**, *336*, 1420-1422.

20. Arrowsmith, M.; Braunschweig, H.; Stennett T. E. *Angew. Chem. Int. Ed.* **2017**, *56*, 96-115.

21. (a) Bissinger, P.; Braunschweig, H.; Damme, A.; Kupfer, T.; Krummenacher, I.; Vargas, A. *Angew. Chem. Int. Ed.* **2014**, *53*, 5689-5693; (b) Lu, W.; Li, Y.; Ganguly, R.; Kinjo, R. *Angew. Chem. Int. Ed.* **2017**, *56*, 9829-9832; (c) Arrowsmith, M.; Mattock, J. D.; Bohnke, J.; Krummenacher, I.; Vargas, A.; Braunschweig, H. *Chem. Commun.* **2018**, *54*, 4669-4672.

22. Hartwig, J. F. *Organotransition Metal Chemistry: From Bonding to Catalysis*, University Science Books, Sausalito, **2010**.

23. Ishida, S.; Sugawara, R.; Misawa, Y.; Iwamoto, T. *Angew. Chem. Int. Ed.* **2013**, *52*, 12869-12873.

24. Chen, M.; Wang, T.; Xie, Y.; Wei, P.; Gilliard, R. J.; Schwartz, N. A.; Schaefer, H. F.; Schleyer, P. v. R.; Robinson, G. H. *Chem. Eur. J.* **2014**, *20*, 9208-9211.

25. (a) Bissinger, P.; Braunschweig, H.; Damme, A.; Kupfer, T.; Vargas, A. *Angew. Chem. Int. Ed.* **2012**, *51*, 9931-9934; (b) Bissinger, P.; Steffen, A.; Vargas, A.; Dewhurst, R. D.; Damme, A.; Braunschweig, H. *Angew. Chem. Int. Ed.* **2015**, *54*, 4362-4366.

26. (a) Braunschweig, H.; Dellermann, T.; Dewhurst, R. D.; Hupp, B.; Krame, T.; Mattock, J. D.; Mies, J.; Phukan, A. K.; Steffen, A.; Vargas, A. *J. Am. Chem. Soc.* **2017**, *139*, 4887-4893; (b) Wang, S. R.; Arrowsmith, M.; Braunschweig, H.; Dewhurst, R. D.; Dömling, M.; Mattock, J. D.; Pranckevicius, C.; Vargas, A. *J. Am. Chem. Soc.* **2017**, *139*, 10661-10664.

27. Lu, W.; Kinjo, R. *Chem. Eur. J.* **2018**, *24*, 15656-15662.

28. Dömling, M.; Stennett, T. E.; Belyaev, A.; Hupp, B.; Claes, C.; Ullrich, S.; Endres, S.; Freytag, E.; Kramer, T.; Kupfer, T.; Schorr, F.; Thiess, T.; Arrowsmith, M.; Steffen, A.; Braunschweig, H. *Inorg. Chem.* **2022**, *61*, 14058-14066.

29. (a) Mendivil, E. T.; Hansmann, M. M.; Weinstein, C. M.; Jazzar, R.; Melaimi, M.; Bertrand, G. *J. Am. Chem. Soc.* **2017**, *139*, 7753-7756; (b) Manar, K. K.; Porwal, V. K.; Kamte, R.; Adhikari, M.; Thakur, S. K.; Bawari, D.; Choudhury, A. R.; Singh, S. *Dalton Trans.* **2019**, *48*, 17472-17478; (c) Kamte, R. S. MS thesis dissertation, *Bicyclic (alkyl)(amino) carbene (BICAAC) complexes with boranes and their reactivity*, IISER Mohali, **2019**; (d) Adhikari, M.; Thakur, S. K.; Singh, S. *Eur. J. Inorg. Chem.* **2023**, e202300379.

30. Dutta, S.; De, S.; Bose, S.; Mahal, E.; Koley, D. *Eur. J. Inorg. Chem.* **2020**, 638-655.

31. (a) Mondal, T.; Dutta, S.; De, S.; Thirumalai, D.; Koley, D. *J. Phys. Chem. A* **2019**, *123*, 565-581. (b) Dutta, S.; Mondal, T.; De, S.; Rudra, K.; Koley, D. *Inorg. Chim. Acta* **2019**, *485*, 162-172. (c) Kundu, S.; Sinhababu, S.; Luebben, A. V.; Mondal, T.; Koley, D.; Dittrich, B.; Roesky, H. W. *J. Am. Chem. Soc.* **2018**, *140*, 151-154. (d) Mondal, K. C.; Roy, S.; Maity, B.; Koley, D.; Roesky, H. W. *Inorg. Chem.* **2016**, *55*, 163-169. (e) Kundu, S.; Sinhababu, S.; Dutta, S.; Mondal, T.; Koley, D.; Dittrich, B.; Schwederski, B.; Kaim, W.; Stückl, A. C.; Roesky, H. W. *Chem. Commun.* **2017**, *53*,

10516-10519. (f) Dutta, S.; Maity, B.; Thirumalai, D.; Koley, D. *Inorg. Chem.* **2018**, *57*, 3993-4008.

32. (a) Weinstein, C. M.; Junor, G. P.; Tolentino, D. R.; Jazzar, R.; Melaimi, M.; Bertrand, G. *J. Am. Chem. Soc.* **2018**, *140*, 9255-9260; (b) Martin, D.; Melaimi, M.; Soleilhavoup, M.; Bertrand, G. *Organometallics* **2011**, *30*, 5304-5313; (c) Roy, S.; Mondal, K. C.; Roesky, H. W. *Acc. Chem. Res.* **2016**, *49*, 357-369.

33. (a) Welz, E.; Böhnke, J.; Dewhurst, R. D.; Braunschweig, H.; Engels, B. *J. Am. Chem. Soc.* **2018**, *140*, 12580-12591; (b) Soleilhavoup, M.; Bertrand, G. *Acc. Chem. Res.* **2015**, *48*, 256-266.

34. (a) CrystalClear 2.0; Rigaku Corporation: Tokyo, Japan, **2013**; (b) Bruker (**2012**). Apex-II. Bruker AXS Inc., Madison, Wisconsin, USA; (c) Bruker (**2013**). SAINT v8.34A. Bruker AXS Inc., Madison, Wisconsin, USA; (d) Bruker (**2014**/5). Sadabs, 2014/5. Bruker AXS Inc., Madison, Wisconsin, USA.

35. Dolomanov, O. V.; Bourhis, L. J.; Gildea, R. J.; Howard, J. A. K.; Puschmann, H. *J. Appl. Crystallogr.* **2009**, *42*, 339-341.

36. (a) Sheldrick, G. M.; *Acta Cryst. A* **2015**, *71*, 3-8; (b) Sheldrick, G. M.; *Acta Cryst. C* **2015**, *71*, 3-8; (c) Sheldrick, G. M.; *Acta Cryst. A* **2008**, *64*, 112-122; (d) Bourhis, L. J., Dolomanov, O. V., Gildea, R. J., Howard, J. A. K., Puschmann, H. *Acta Cryst. A* **2015**, *71*, 59-75.

BICAAC stabilized borenium cation equivalents: Syntheses, characterization, and application in hydrosilylation of carbonyls
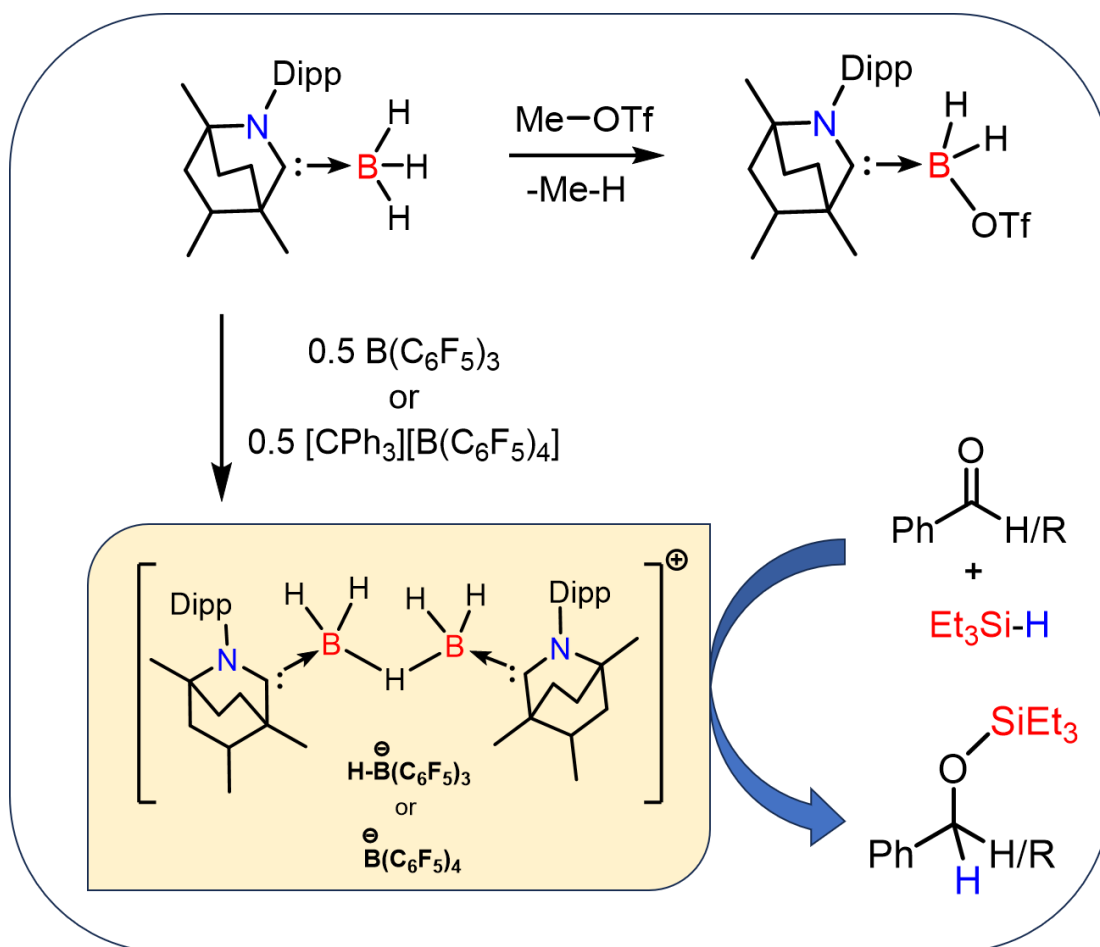
Adhikari, M.; Thakur, S. K.; Singh S. BICAAC stabilized borenium cation equivalents: Syntheses, characterization and application in hydrosilylation of carbonyls. *(unpublished results).*

Abstract: The current chapter deals with the syntheses and characterization BICAAC supported borenium ion equivalent complexes, [L→BH$_2$−H−BH$_2$←L][H−B(C$_6$F$_5$)$_3$] (**1**), [L→BH$_2$−H−BH$_2$←L][B(C$_6$F$_5$)$_4$] (**2**), [L→BH$_2$−OTf] (**3**), [L→BH$_2$−Nu][OTf] (Nu = pyridine, (**4**); Nu = DMAP, (**5**)) (L = BICAAC), followed by the Lewis acidic assessment using Gutmann-Beckett method for **1** and **2**. The resulting acceptance number (AN) values of synthesized cations advocate the Lewis acidic nature of these complexes. Moreover, complexes **1** and **2** have displayed excellent catalytic efficacy in the hydrosilylation of a diverse range of carbonyl compounds. Specifically, utilizing 1 mol% catalyst loading and a reaction time of 5 minutes, complex **1** emerged as a highly efficient catalyst for a variety of aldehydes and ketones. It achieved the highest turnover frequency (TOF) of up to 1200 h^{-1}, particularly notable in the case of benzaldehyde. Additionally, complex **1** demonstrated catalytic activity in the hydrosilylation of *para*-quinone methides (*p*-QMs) as well. In a similar fashion, complex **2** also displayed catalytic activity in the hydrosilylation of carbonyl compounds, employing 1 mol% catalyst loading, however, a longer reaction time was required for optimal performance. A comprehensive mechanistic investigation is currently underway to further elucidate the underlying reaction processes.

2B.1 Introduction

Boron, the first and lightest group 13 element, substantially impacts modern organic chemistry, both in stoichiometric as well as in catalytic processes.[1] The main feature that makes boron unique is its exceptional Lewis acidity, resulting from its native electron deficiency. Consequently, the resulting bonding outcomes largely depend on it. Boron compounds demonstrates the following crucial reactivity characteristics, e.g., functioning as a Lewis acid towards weak unsaturated nucleophiles, serving as a reducing agent based on hydride, and facilitating the easy redistribution of ligands in its coordination sphere, particularly in transmetallation reactions. Over the past 50 years, it has become indispensable for crucial transformations such as borohydride reductions, olefin hydroboration, Suzuki-Miyaura cross-coupling and frustrated Lewis pair chemistry, and therefore essential in contemporary synthetic chemistry.[2] The characteristics exhibited by boron complexes hold significant potential for their application in catalytic processes as well. Subsequently, in recent years, boron-based catalysts have emerged as viable alternatives replacing the need for precious-transition-metal-based catalysts like Pd, Pt, Rh, Ir for diverse hydroelementation and C-C bond formation reactions.[3] Seminal work by Piers and co-workers in late 90s and others showed the utility of tris(pentafluorophenyl)borane ($B(C_6F_5)_3$) for various catalytical applications such as hydrosilylation of carbonyls, esters, and olefins.[4] Neutral boron-group compounds display notable electrophilic traits, however, their cationic counterparts exhibit even higher reactivity due to increased electronic deficiency and occasional coordinative unsaturation. Nöth and Kölle have systematically categorized such boron cations into three distinct groups, as depicted in Figure 2B.1.[5] Borinium cations are two-coordinated species (**I**, Figure 2B.1), having two perpendicular vacant *p*-orbitals, exhibit heightened reactivity. The successive coordination of neutral 2e-donor ligand (L) to one or both of the unoccupied p-orbitals of **I** results respectively in the creation of a planar, three-coordinated borenium ion
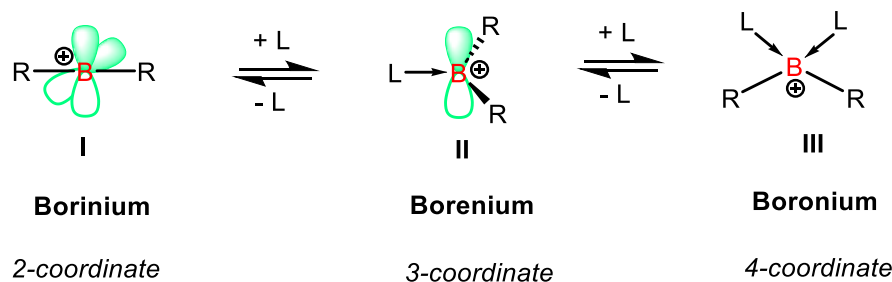
Figure 2B.1 Type and structure of borocations.

II and a four-coordinate tetrahedral boronium cation **III**. Among these cations, the 3-coordinated borenium cations garner particular interest due to their heightened reactivity compared to the 4-coordinated boronium ions and their superior stability in comparison to the 2-coordinated borinium ions.[6]

Syntheses of borenium cations:

Borenium cations can be synthesized by a variety of methods.[6-7] Gabbai and co-workers reported the synthesis of cation **A** (Scheme 2B.1; a) by reaction of NHC with FB(Mes)$_2$, succeeded by fluoride abstraction utilizing an *in-situ* generated Lewis acidic silylium cation. The stabilization offered by the NHC ligand, coupled with the steric shielding from Mes groups and the formation of a robust Si-F bond, serves as the driving force for this reaction.[8] Hydride abstraction by Brønsted acid (TfOH) from a B-H bond also led to the generation of borenium cation **B** (Scheme 2B.1; b).[9]

Moreover, the most popular method includes the abstraction of hydride moieties using strong Lewis acids e.g. tris(pentafluorophenyl)borane B(C$_6$F$_5$)$_3$ or a trityl salt, [CPh$_3$][B(C$_6$F$_5$)$_4$] (*vide infra*).[6-7] The cationic complex **C** was synthesized by using [DABCO−B(C$_6$F$_5$)$_3$] precursor (Scheme 2B.1; c).[10] Another method comprises the halide abstraction by means of metathesis to afford a borenium cation such as **D** (Scheme 2B.1; d).[11a] The complex **D** showed good catalytic activity for the hydrosilylation of acetophenone with Et$_3$SiH as hydride source and afforded 60% conversion with 20% *ee*.

(a) Lewis acid induced halide abstraction:
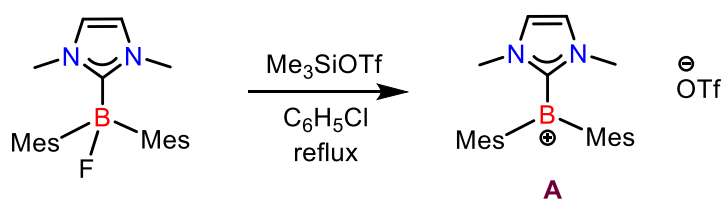
(b) Brønsted acid induced hydride abstraction:
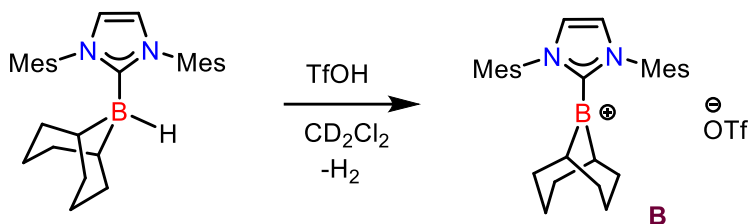
(c) Lewis acid induced hydride abstraction:
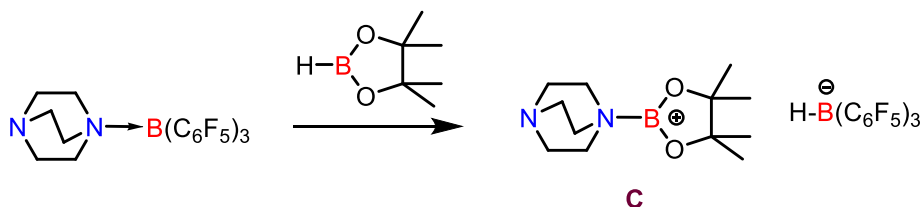
(d) Halide abstraction by metathesis:

endo:exo 2.5:1
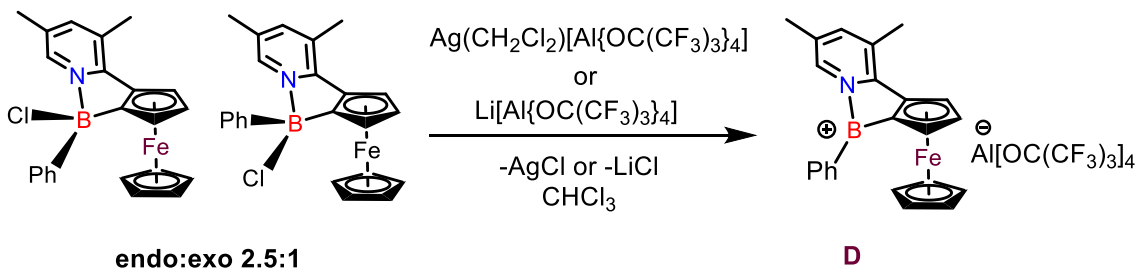
Scheme 2B.1 Syntheses of borenium cations via (**a**) Lewis acid induced halide abstraction; (**b**) Brønsted acid induced hydride abstraction; (**c**) Lewis acid induced hydride abstraction; (**d**) halide abstraction using metathesis route.

Other methodologies were also reported for the synthesis of borenium cations.[11b] In 2008, Piers and co-workers isolated a BODIPY dye based borenium hydride complex **E** (Scheme 2B.2) via sequential fluoride abstraction using [Et₃Si]⁺ and F/H exchange with DIBAL−H.[12]

(a)= [Et$_3$Si][B(C$_6$F$_5$)$_4$]
(b) = DIBAL-H
(X) = B(C$_6$F$_5$)$_4$]

E
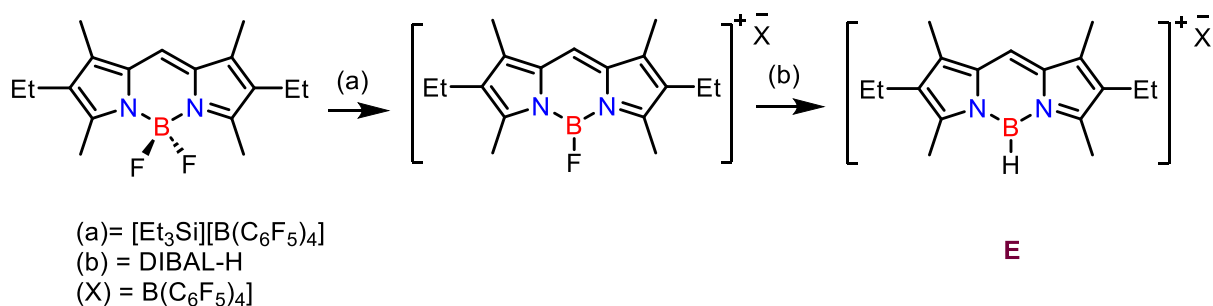
Scheme 2B.2 Synthesis of borenium cation **E** via halide abstraction by triethylsilylium perfluoroborate salt and halide to hydride metathesis using DIBAL−H.

In 2007, Vedejs and co-workers presented an important report providing NMR data (Figure 2B.2) demonstrating that borenium cations, synthesized from L:→BH$_3$ precursors (where L = NMe$_3$, NEt$_3$, PBu$_3$, and pyridine derivatives) using trityl salt [CPh$_3$][B(C$_6$F$_5$)$_4$] as a hydridophile, do not typically accumulate in the form of [L:→BH$_2$]$^+$. Instead, a subsequent reaction with precursor L:→BH$_3$ occurs, resulting in the formation of a *3c-2e* hydride-bridged

	δ ^{1}H^{bridging} (ppm)	δ ^{11}B (ppm)
1: R = Et	-2.6	-3
2: R = Me	-1.9	0
3: R = H	0.5	-2
4: R = NMe$_2$	0.1	-1
5	-3.7	-27
6	-2.2	-27

NMR data recorded in CD$_2$Cl$_2$ for all complexes at -20 °C, X$^-$ = [B(C$_6$F$_5$)$_4$] for all

Figure 2B.2 ^{1}H and ^{11}B NMR data reported for a library of hydrogen bridged cationic dimers.

cation (L:→BH$_2$-H-BH$_2$←:L).[13] These monocationic dimers exhibit sufficient stabilization

and they resist further hydride abstraction by trityl salt. However, in the presence of

nucleophiles, these bridged dimers break down, giving rise to mononuclear borenium ion

equivalents (L:→BH$_2$−Nu) and release (L:→BH$_3$). These authors found the ^{1}H NMR

chemical shift value for the bridged hydrogen resonates around δ = +0.1 to -3.7 ppm. Figure

2B.2 provides a summary of compounds along with their ^{1}H and ^{11}B NMR chemical shifts, as

reported by Vedejs and co-workers.

Applications of borenium cations:

In 2009, Vedejs and co-workers showed when amine borane Ar(CH$_2$)NMe$_2$·BH$_3$ was reacted

with [CPh$_3$][B(C$_6$F$_5$)$_4$] (TrPFPB) the formation of a hydrogen bridged cationic dimer was

observed (Scheme 2B.3) which subsequently led to the internal borylation to give the cyclic

amine-borane derivative **F** which upon quenching with Bu$_4$BH$_4$ gave product **G**.[14] Similarly,

they found similar results for the hindered pyrrolidine-based borane complexes which

undergo intramolecular aliphatic C-H borylation through the borenium cation **H** (Figure

2B.3).[15] In a subsequent report, they discovered that treatment of alkenes (e.g., 3- hexene or

3-octene) with NHC based borane and catalytic HNTf$_2$ brings the hydroboration of olefins
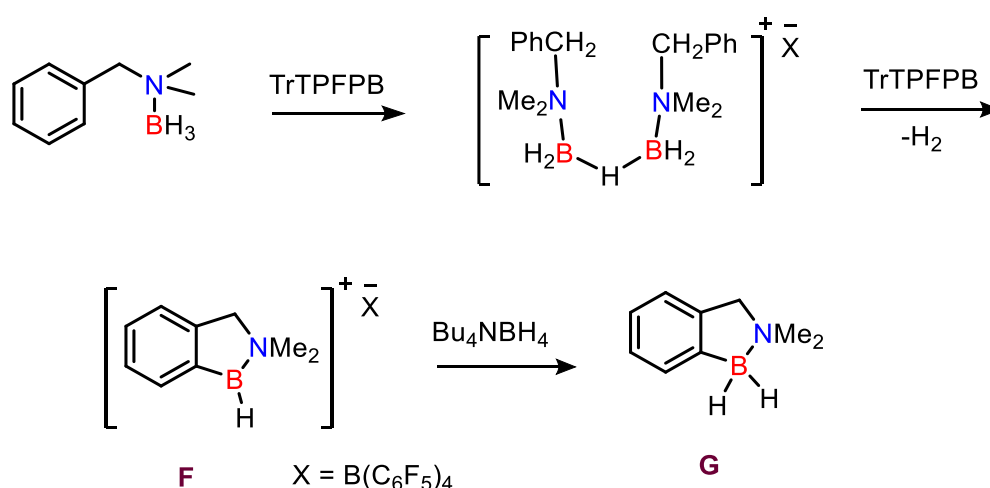
Scheme 2B.3 Synthesis of a hydride bridged cationic dimer and its subsequent internal

borylation.
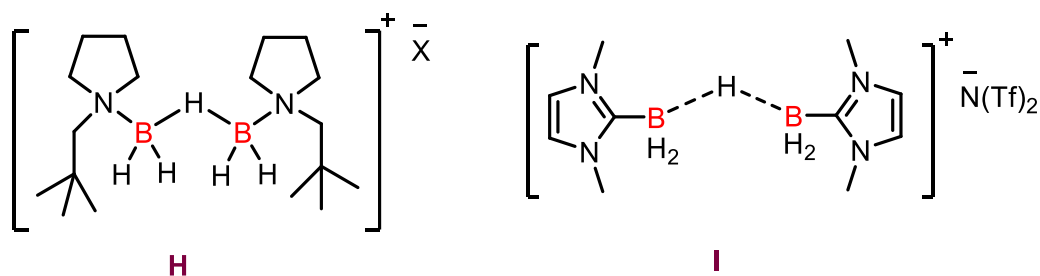
Figure 2B.3 Borenium cation equivalents based on cyclic amine and NHC scaffolds.

catalyzed by *in-situ* generated dimeric NHC-borenium cation or NHC-borenium equivalents **I** (Figure 2B.3).[16]

In 2011, Alcarazo and co-workers successfully isolated a dihydridoborenium cation **J** (Scheme 2B.4) stabilized by strong σ and π-donor ligand called as carbodiphosphorane.[17] The reaction of $(PPh_3)_2C:\rightarrow BH_3$ with $B(C_6F_5)_3$ afforded **J**, while the NHC:→BH₃ adduct gives the dimeric bridged cation **K** (Scheme 2B.4) when reacted with 1 equivalent of $B(C_6F_5)_3$. The strong σ and π-donation of electrons from the carbodiphosphane ligand provide necessary stabilization to the boron center. The borenium cation **C** (Scheme 2B.1; c) reported by Crudden and co-workers showed competent catalytic activity in the reduction of
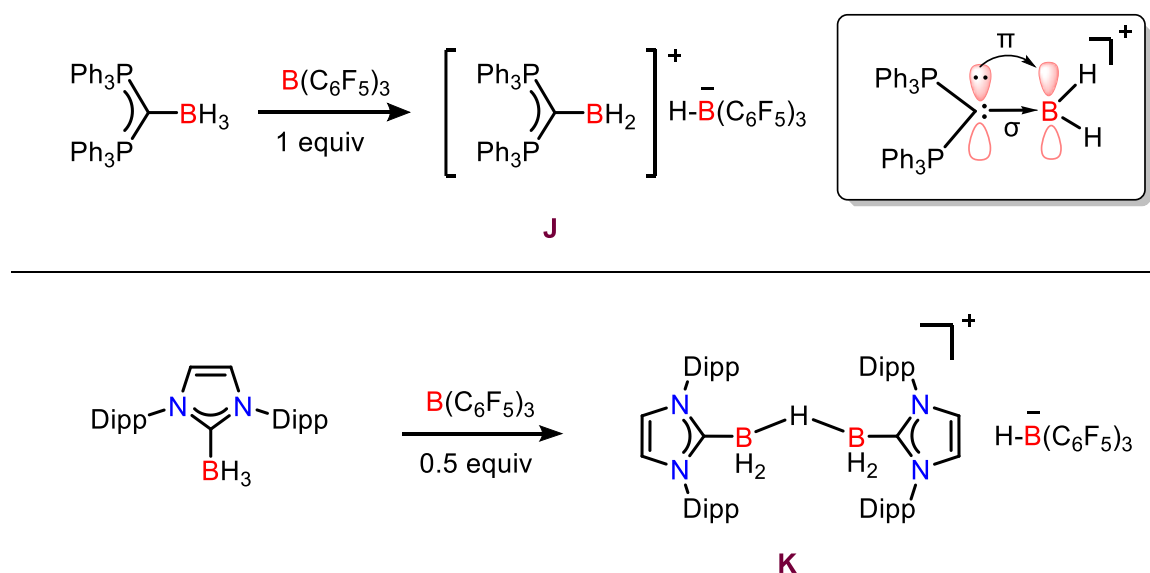
Scheme 2B.4 Synthesis of carbodiphosphorane derived borenium cation (top); and NHC stabilized hydride bridged dimeric borenium cation (bottom).

a variety of imines. The mechanism involves the activation of the imine substrate by borenium ion and the subsequent hydride delivery from the HBPin (in combination with DABCO) instead from the $[H-B(C_6F_5)_3]^-$ anion.[10]

Curran and co-workers, in 2012 synthesized the dihydroxyborenium triflate complex $[NHC-B(OH)_2]^+[TfO^-]$ (**L**, Figure 2B.4) by reaction of NHC:→BH$_3$ with excess triflic acid [NHC = 1,3-bis(2,6-diisopropylphenyl)imidazol-2-ylidene].[18] In 2013, Denmark and co-workers reported a 2,6-lutidine stabilized borenium cation **M** (Figure 2B.4) which catalyzed hydrosilylation of a variety of ketones using Et$_3$SiH as hydride source at room temperature.[19] Vedejs and co-workers in 2013 reported the evidence for the existence of a dicationic dimeric boron complex **N** (Figure 2B.4), by reacting the monocationic hydride bridged salt with hydride abstractor $[CPh_3][Al_2Br_7]$, which is the first of its class in main-group chemistry.[20] Other reports on dicationic boron complexes were published by the groups of Ong and Ghadwal (2014-15) dealing with the isolation of a series of dicationic hydrido boron complexes supported by carbodicarbene and NHC ligands, respectively (**O-P**, Figure 2B.4).[21] Subsequently in 2015, Crudden and co-workers isolated an mesoionic carbene based borenium ion and used it as a catalyst in hydrogenation reaction of imines under ambient temperature and pressure conditions (**Q**, Figure 2B.4).[22] Afterwards, in 2016, Singh and co-workers disclosed syntheses of a series of stable borenium hydride complexes (**R**, Figure 2B.4) derived from sterically demanding bis(phosphinimino)amide ligands by Lewis acid-mediated hydride abstraction.[23a] Later, they also showed their application in hydrosilylation of a variety of the carbonyls.[23b] Furthermore, in 2016, Ingleson and co-workers found that the NHC based borenium cation (**S**, Figure 2B.4) produces selective trans-hydroboration of alkynes.[24] Moreover, in 2020 Wang and co-workers published the synthesis of an extremely electrophilic *o*-carboranyl-substituted hydroborenium cation **T** (Figure 2B.4) and its η^2-σ-(H−Si)-complex, this hydroborenium cation can catalyze the direct
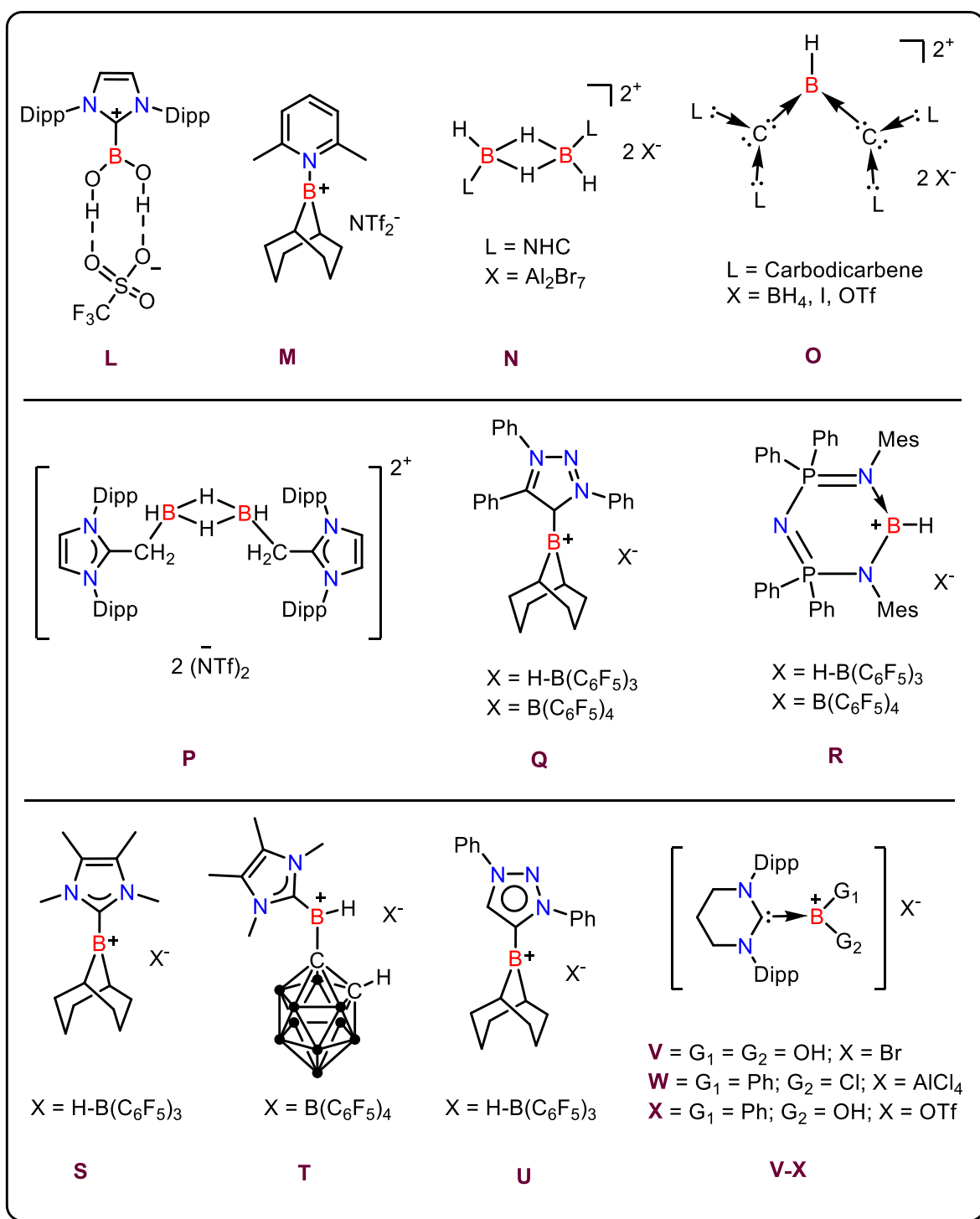
Figure 2B.4 Selected examples of previously isolated borenium cation.

hydroboration of cyclopropane C−C bonds via a σ-bond metathesis route.[25] Lately, in 2021,

Crudden and co-workers reported the mesoionic carbene supported borenium ion **U** (Figure

2B.4) catalyzed hydrosilylation of imines to amines using PhSiH₃ as a hydride source.[26]

Very recently in 2022, Sen and co-workers reported the syntheses and characterization of a

series of borenium cations **V-X** (Figure 2B.4) based on a 6-membered NHC ligand.[27] In 2022, Mandal and co-workers introduced a novel benzimidazolylidene-stabilized borane adduct and corresponding borenium ion as a metal-free catalyst for hydrogenating quinoline N-heterocycles under ambient conditions. The method was utilized to synthesize drug molecules galipinine and angustureine.[28]

Extensive evidences indicate the remarkable versatility of borenium cations in diverse applications, encompassing hydrogenation, hydrosilylation, hydroboration, C−H borylation, and C−C bond hydrogenolysis.[6,7] Comprehensive reviews on these subjects are available in relevant references.[6-7, 29] Motivated by the insights gained from these multifaceted applications, the current research endeavors to leverage the recently synthesized BICAAC-BH$_3$ adduct.[30] This adduct serves as a valuable precursor for the synthesis of cationic borenium counterparts, with B(C$_6$F$_5$)$_3$ and [CPh$_3$][B(C$_6$F$_5$)$_4$] selected as hydridophiles. The primary objective is to systematically explore and expand the scope of borenium cation chemistry, with a particular emphasis on identifying catalytic applications for organic transformations.

2B.2 Results and discussion

2B.2.1 Syntheses and characterization of complexes [BICAAC→BH$_2$−H−BH$_2$←BICAAC][H−B(C$_6$F$_5$)$_3$] (1) and [BICAAC→BH$_2$−H−BH$_2$←BICAAC][B(C$_6$F$_5$)$_4$] (2)

To begin with, we performed an NMR tube reaction of the adduct BICAAC−BH$_3$ with an stoichiometric amount of tris(pentafluorophenyl)borane (B(C$_6$F$_5$)$_3$). The ^{1}H and ^{11}B NMR spectra showed consumption of only half equivalents of B(C$_6$F$_5$)$_3$ and complete consumption of BICAAC−BH$_3$ to form a single product. This observation clearly suggested the formation

of a symmetrical monocationic dimeric species. Consequently, the scaled-up 2:1 molar reaction of BICAAC−BH$_3$ and B(C$_6$F$_5$)$_3$ was performed in toluene which as expected afforded the borenium ion equivalent complex, [BICAAC→BH$_2$−H−BH$_2$←BICAAC][H−B(C$_6$F$_5$)$_3$] (**1**) in 89% yield as a white fluffy compound (Scheme 2B.5). The ^{1}H NMR spectrum of **1** (in C$_6$D$_5$Br + C$_6$D$_6$ mixture) showed a
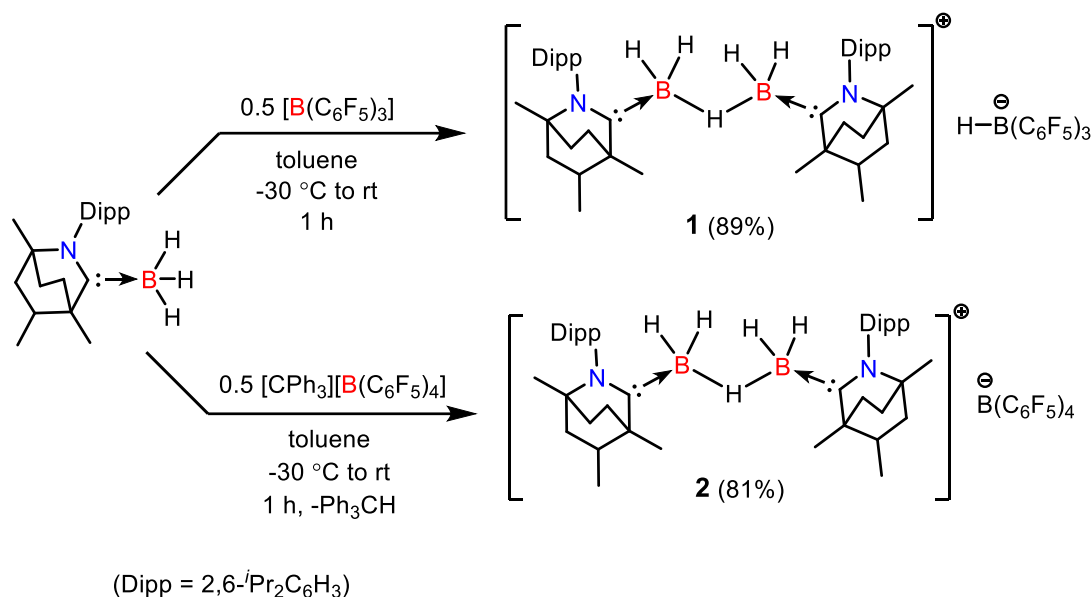
Scheme 2B.5 Syntheses of borenium cation equivalent complexes **1** and **2**.

peak in the shielded region at δ = -2.07 ppm,[13] which was assigned for bridged hydride while a broad peak emerged around δ = 4.66-3.83 ppm which corresponds to the B-*H* of the anion H−B(C$_6$F$_5$)$_3$ (Figure 2B.5). Additionally, in ^{1}H NMR spectrum of **1** two merged septets have also been found to resonate around δ = 2.28-2.17 and 1.97-1.86 ppm which were attributed to the Dipp group of the carbene moiety (*note the two septets that correspond to the BICAAC−BH$_3$ precursor in C$_6$D$_5$Br resonate at δ = 2.83 and 2.53 ppm, and the significant shift in the position of these hydrogens indicates the complete consumption of BICAAC−BH$_3$ adduct*). The ^{11}B NMR spectrum of **1** showed a doublet (at -24.6 ppm) and a quartet (at -28.7 ppm) respectively, for the [H−B(C$_6$F$_5$)$_3$]$^-$ anion and the [BICAAC→BH$_2$−H−BH$_2$←BICAAC]$^+$ cationic unit. The ^{1}H-^{11}B 2D(HSQC) NMR spectrum
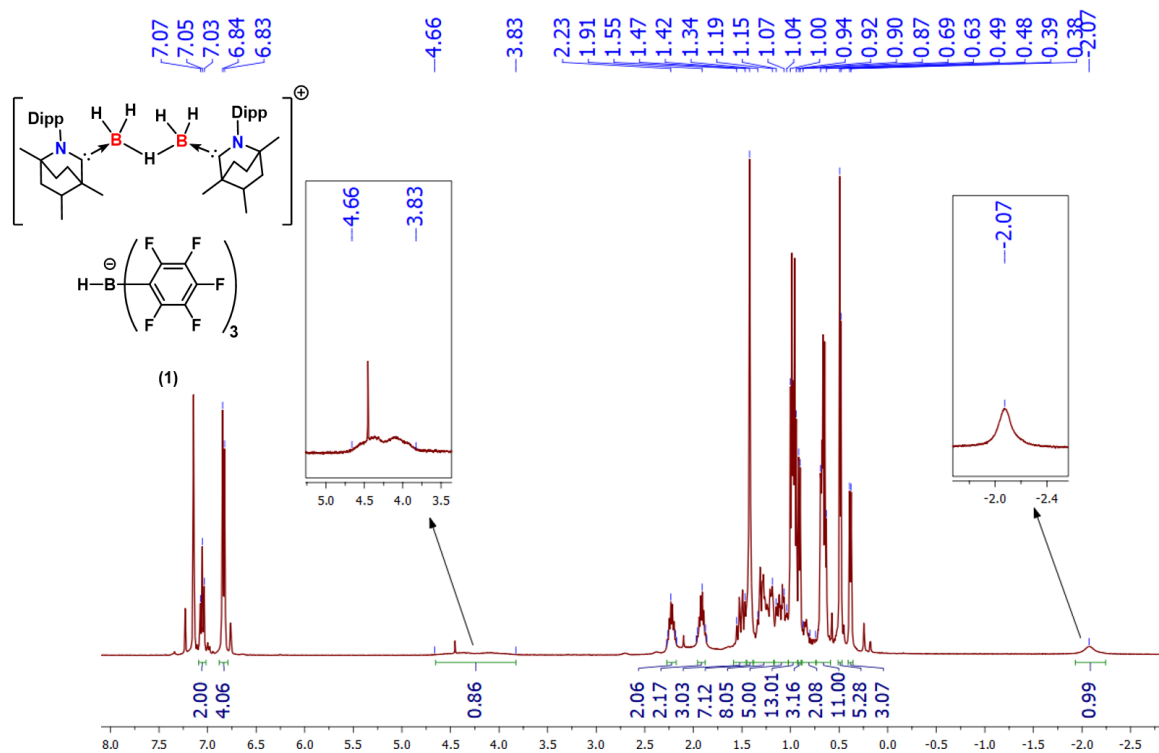
Figure 2B.5 ^{1}H NMR (400 MHz, C$_6$D$_5$Br + C$_6$D$_6$) spectrum of complex **1**.
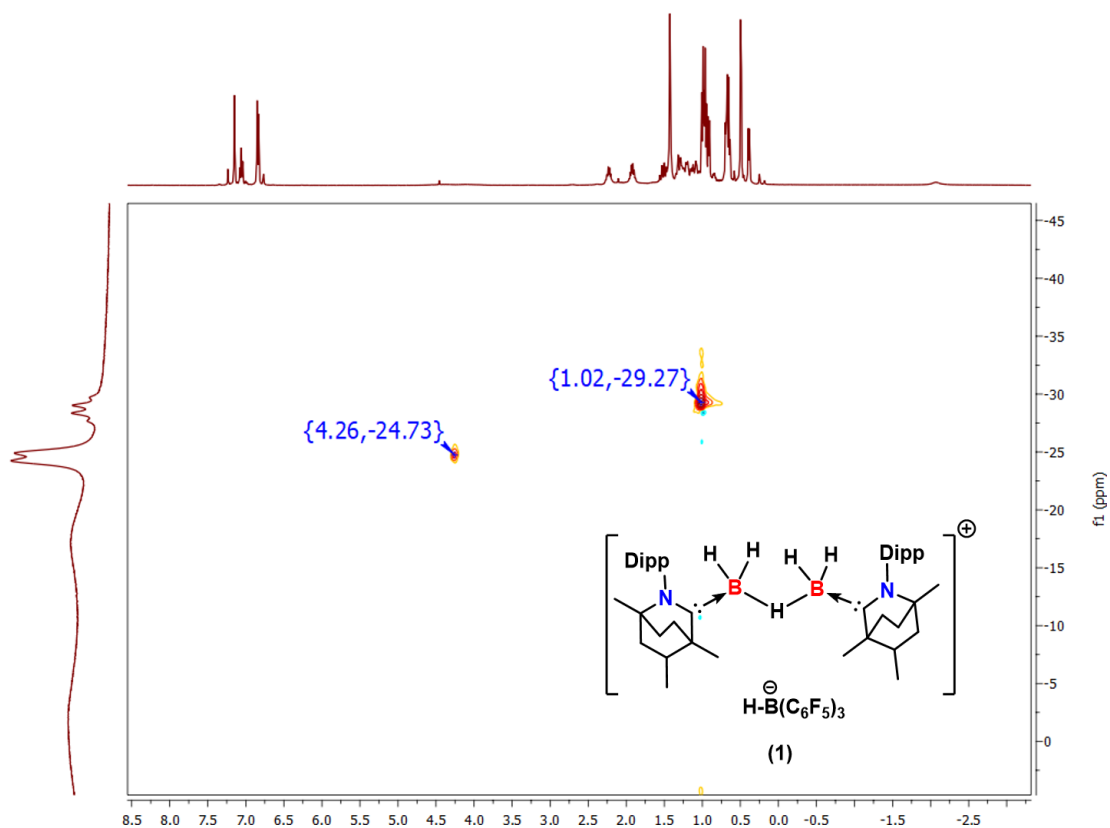
Figure 2B.6 ^{1}H-^{11}B 2D(HSQC) NMR (C$_6$D$_5$Br + C$_6$D$_6$) spectrum of complex **1**.

of **1** showed two contour signals (Figure 2B.6), the first contour at δ = {4.26, -24.73} ppm corresponds to the $[H-B(C_6F_5)_3]^-$ anion, while the later one at δ = {1.02, -29.27} ppm belongs to the two BH_2 units of $[BICAAC{\rightarrow}BH_2-H-BH_2{\leftarrow}BICAAC]^+$ cationic moiety (note the precursor $BICAAC\text{-}BH_3$ gives signals in $^1H\text{-}^{11}B$ 2D(HSQC) NMR spectrum at δ = {1.53, -28.17} ppm, and the absence of which after the reaction supports the complete consumption of the precursor and the generation of complex **1**). The $^{19}F\{^1H\}$ NMR spectrum of **1** showed three sets of signals, a doublet (at -132.0 ppm), a triplet (at -163.3 ppm) and a multiplet (at -165.9 to -166.0 ppm), which correspond to the fluorine atoms of $[H-B(C_6F_5)_3]^-$ unit. The $^{13}C\{^1H\}$ NMR spectrum showed double peaks for each carbon nuclei in the aliphatic region which might suggest the presence of the diastereomeric mixture (Figure 2B.7) which originates from the BICAAC unit because BICAAC itself is a racemic mixture of a single diastereomer or the two $BICAAC-BH_2$ units of complex **1** give separate signals. The IR spectrum of **1** showed B-H stretching bands at 2454, 2373 and 2351 cm^{-1} for the cationic and anionic moieties. Furthermore, the formation of **1** was further supported by its HRMS
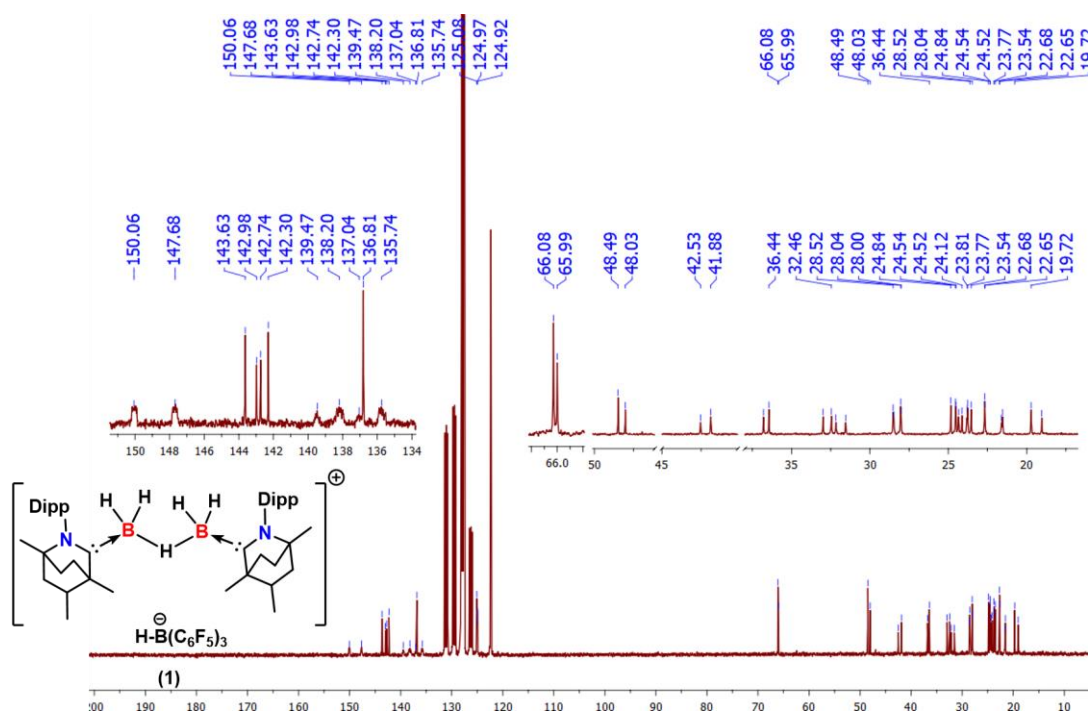
Figure 2B.7 $^{13}C\{^1H\}$ NMR (100 MHz, $C_6D_5Br + C_6D_6$) spectrum of complex **1**.

spectrum which gives peak for the cationic counterpart $C_{44}H_{69}N_2B_2$ at m/z = 647.5684 (calcd. 647.5661) as $[M-2H]^+$, while for the anionic counterpart $C_{18}H_1B_1F_{15}$ at m/z = 512.9934 (calcd. 512.9935) as $[M]^-$. Multiple efforts made to grow single crystals of complex **1** from different solvents unfortunately remained unsuccessful till now.

Similarly, 2:1 molar reaction of BICAAC−BH₃ with trityl salt, $[CPh_3][B(C_6F_5)_4]$ under the elimination of Ph₃C-H afforded another borenium ion equivalent complex, [BICAAC→BH₂−H−BH₂←BICAAC][B(C₆F₅)₄] (**2**) as a white solid in 81% yield (Scheme 2B.5). Due to identical cationic moieties in **1** and **2**, the ¹H NMR spectrum of **2** was found to be identical as that of **1** (Figure 2B.8), though the signal for anion H-BR₃ was absent (as expected), instead signals for triphenylmethane (Ph₃C−H) was observed. The septets for the Dipp group were found to resonate at δ = 2.29-2.21 and 1.99-1.91 ppm and the signal for the -C*H* of triphenylmethane was found at δ = 5.44 ppm. Similar to the complex **1**, the signal for the bridging hydride in **2** was found at -2.05 ppm (Figure 2B.8). The ¹¹B NMR spectrum of **2**
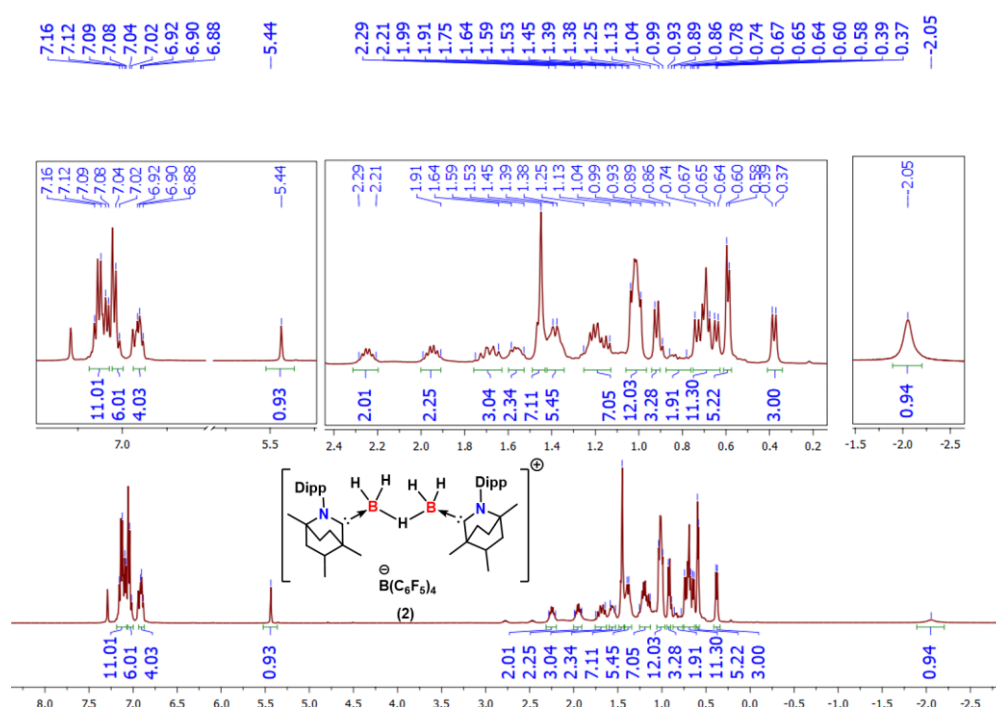
Figure 2B.8 ¹H NMR (400 MHz, C₆D₅Br) spectrum of complex **2** (insets showing the expanded view of the selected spectral region).
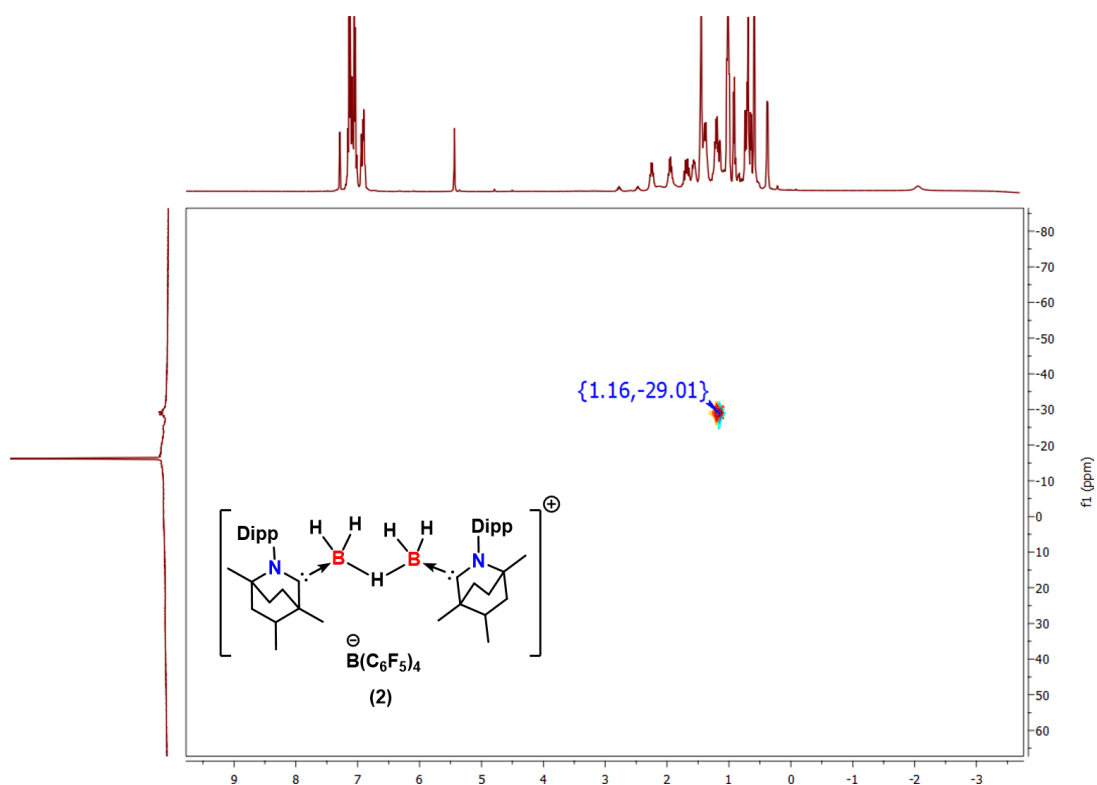
Figure 2B.9 ^{1}H-^{11}B 2D(HSQC) NMR (C$_6$D$_5$Br) spectrum of complex **2**.
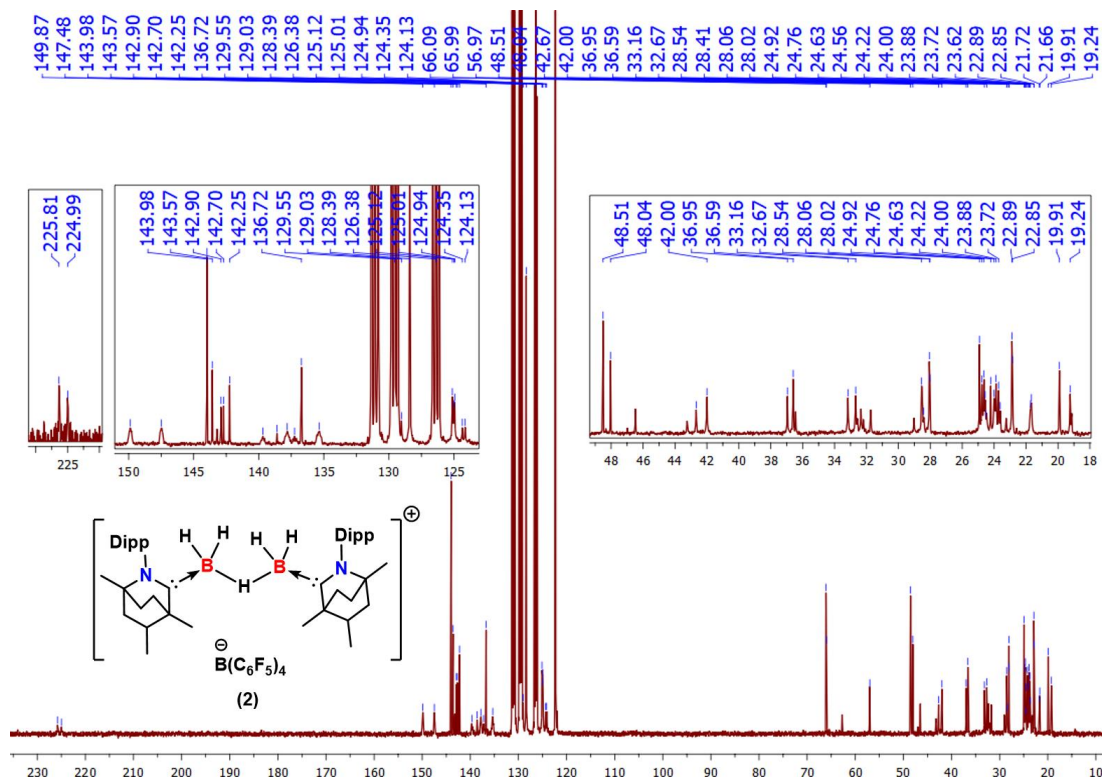
Figure 2B.10 ^{13}C{^{1}H} NMR (100 MHz, C$_6$D$_5$Br) spectrum of complex **2**.

showed a sharp signal at -16.2 ppm for the $[B(C_6F_5)_4]^-$ anion and a quartet at δ = -28.9 ppm for the cationic boron centers. The ^1H-^{11}B 2D(HSQC) NMR spectrum of complex **2** exhibited one contour signal at δ = {1.16, -29.27} ppm (Figure 2B.9), which corresponds to two BH_2 units of the cationic unit [BICAAC→BH_2−H−BH_2←BICAAC]$^+$. The $^{19}F\{^1H\}$ NMR spectrum of complex **2** exhibits three set of signals, a broad doublet at -131.7 ppm, a triplet at -162.3 ppm and a multiplet at -166.1 to -166.0 ppm which correspond to the anion $[B(C_6F_5)_4]^-$. Akin to complex **1**, $^{13}C\{^1H\}$ NMR spectrum of **2** also suggested the formation of diastereomers (Figure 2B.10) as we found two closely spaced signals for each carbon nucleus. Moreover, the peak for the carbenic carbon were found to resonate at δ = 225.8 and 225.0 ppm as broad multiplets. The IR spectrum of **2** showed B−H stretching bands at 2383, 2344 and 2280 cm^{-1}. Additionally, HRMS spectrum also supported the formation of complex **2**, which showed a signal for the cationic part $C_{44}H_{71}B_2N_2$ at m/z = 649.5850 (calcd. 649.5818) as [M]$^+$, and for the anionic part $C_{24}BF_{20}$ at m/z = 678.9764 (calcd. 678.9778) as [M]$^-$.

Further, the structure of complex **2** was confirmed by single crystal X-ray technique as [BICAAC→BH_2−H−BH_2←BICAAC][$B(C_6F_5)_4$] (Figure 2B.11). Complex **2** crystallized in the triclinic crystal system and possesses $P\bar{1}$ space group. The solid-state structure showed that one hydrogen atom is flanked in the bridging position between two [BICAAC−BH_2] units and the $[B(C_6F_5)_4]^-$ anion remained present without any interaction with the cationic counterpart. The two BICAAC units attached with the B−H−B core were found to orient on the same side of the central B−H−B core. The N1−C1 and C1−B1 bond distances in **2** were found to be 1.310(5) and 1.585(7) Å respectively, while the B1−H1A, B1−H1B and B1−H1C bond separations were measured to be 1.27(4), 1.03(4) and 1.24(5) Å, respectively. The N1−C1−B1 and C1−B1−H1A bond angles were measured to be 122.0(4) and 106.1(19)° respectively.
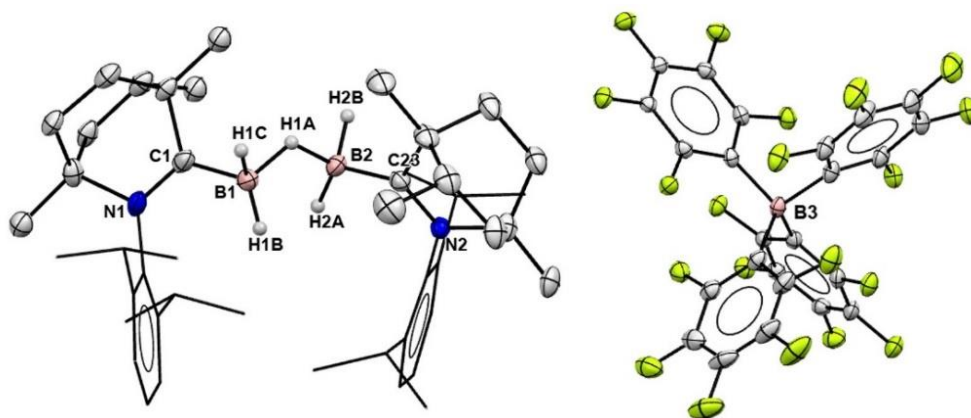
2

Figure 2B.11 Single-crystal X-ray structure of **2**. Ellipsoids are shown at 30% probability level (hydrogen atoms have been omitted for clarity except for those attached with B1 and B2). Selected bond lengths (Å) and bond angles (°) for **2**: N1−C1 1.310(5), C1−B1 1.585(7), B1−H1A 1.27(4), B1−H1B 1.03(4), B1−H1C 1.24(5), B2−H1A 1.33(4), B2−C23 1.602(6); N1−C1−B1 122.0(4), C1−B1−H1A 106.1(19).

2B.2.2 Synthesis and characterization of complex BICAAC−BH₂-(OTf) (3)

The 1:1 molar reaction of BICAAC−BH₃ adduct with methyl trifluoromethanesulfonate (Me−OTf) afforded the white compound, BICAAC−BH₂(OTf) (**3**) in 92 % yield (Scheme 2B.6). The formation of **3** was observed from different spectroscopic techniques. ^{1}H NMR spectrum of **3** in CDCl₃ showed that the two septets for the Dipp group located at 2.76 and 2.45 ppm (compared to 2.83 and 2.52 ppm for the precursor in CDCl₃). Other signals were as expected for the BICAAC backbone. The two hydrogens attached to boron center gave a
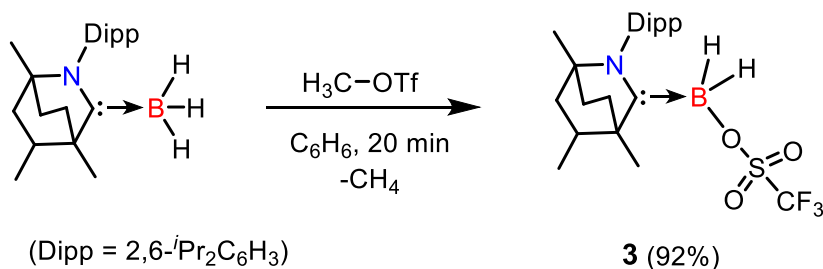
Scheme 2B.6 Synthesis of complex **3.**

broad signal ranging from 3.49 to 2.52 ppm, however the exact position of the broad signal was identified at δ = 2.92 ppm through ^{11}B-^{1}H 2D-HSQC NMR (Figure 2B.12). The ^{19}F{^{1}H} and ^{11}B NMR spectra displayed single peaks respectively, at δ = -76.2 ppm (for the -CF_3 group) and δ = -6.3 ppm for the boron center. The ^{13}C{^{1}H} NMR spectrum displayed a quartet for the carbon atom of -CF_3 group centered at δ = 118.8 ppm, while the signal for the
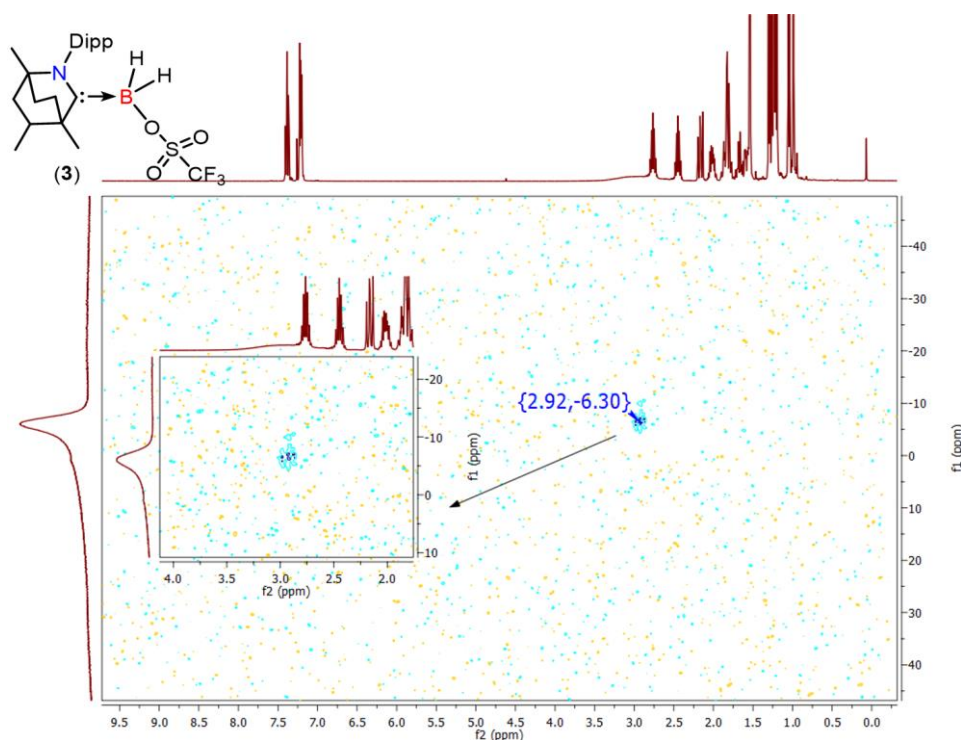
Figure 2B.12 ^{11}B-^{1}H 2D-HSQC NMR spectrum of **3**.

carbenic carbon was located at 227.3 ppm. The IR spectrum of **3** showed B−H stretching bands at 2470, 2379 and 2350 cm^{-1}. Furthermore, the formation of **3** was also supported by its HRMS spectrum which gave peak for the cationic part $C_{22}H_{33}BN$ at m/z = 322.2713 (calcd. 322.2710) as [M-2H]$^{+}$, and for the anionic part CF_3O_3S at m/z = 148.9535 (calcd. 148.9520) as [M]$^{-}$. Finally, the isolation of **3** was confirmed by single crystal X-ray technique (Figure 2B.13). Complex **3** crystallized in the orthorhombic system and possesses *Pbca* space group. The boron atom in **3** adopts distorted tetrahedral geometry. The N1−C1 and C1−B1 bond distances were found to be 1.314(3) and 1.613(4) Å respectively. The C1−B1 bond distance
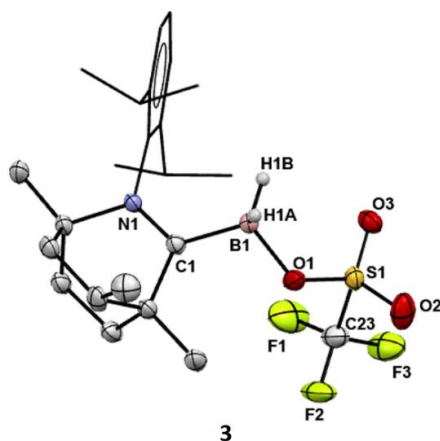
Figure 2B.13 Single-crystal X-ray structure of [BICAAC−BH$_2$(OTf)] (**3**). Ellipsoids are shown at the 50% probability level (hydrogen atoms have been omitted for clarity except for those attached with B1). Selected bond lengths (Å) and bond angles (°) for **3**: N1−C1 1.314(3), C1−B1 1.613(4), B1−O1 1.561(4); N1−C1−B1 120.3(2), C1−B1−O1 110.4(3), C1−B1−H1A 103.9(16), C1−B1−H1B 115.8(16).

of 1.613(4) Å in **3** is found to be slightly longer than its precursor BICAAC−BH$_3$ [1.585(3) Å], while the B1−O1 and O1−S1 bond distances in **3** were found to be 1.561(4) and 1.496(4) Å, respectively. Moreover, the N1−C1−B1 and C1−B1−O1 bond angles were found to be 120.3(2) and 110.4(3)°, respectively.

2B.2.3 Syntheses and characterization of complexes [BICAAC→BH$_2$−py][OTf] (4) and [BICAAC→BH$_2$−DMAP][OTf] (5)

Complex **3** upon treatment with equivalent amount of Lewis bases (pyridine or 4-dimethylaminopyridine (DMAP)) under heating conditions afforded the white foamy adducts **4** and **5** respectively, in 96 and 94 % isolated yields (Scheme 2B.7). The ^{1}H NMR spectrum of **4** showed two merged septets spanning from 2.65 to 2.51 ppm that corresponds to the Dipp group of the carbene backbone. The ^{1}H NMR spectrum also revealed that two hydrogens attached with the boron center resonate at around 3.19-2.50 ppm as a broad signal, however, the exact chemical shift value for the broad signal was detected using the ^{11}B-^{1}H 2D-HSQC NMR technique which showed the signal centered at δ = 2.87 ppm (Figure 2B.14). The ^{11}B
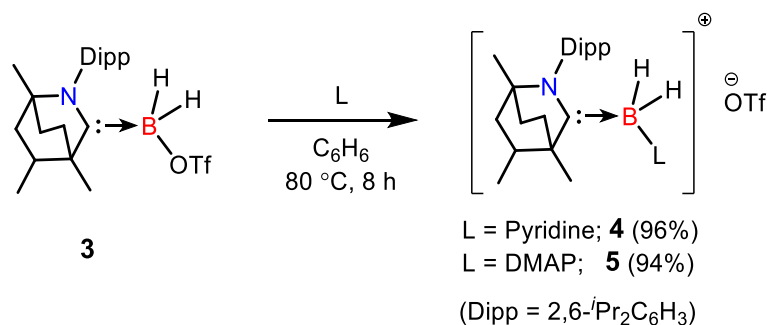
Scheme 2B.7 Syntheses of complexes **3** and **4**.

NMR spectrum of **4** exhibited a broad signal at -7.23 ppm (compared to -6.3 for the precursor **3**), also the ^{19}F{^{1}H} NMR spectrum showed a single peak at -78.09 ppm (-76.2 ppm for the precursor **3**). The ^{13}C{^{1}H} NMR spectrum of **4** displayed a quartet for the carbon atom of -CF$_3$ group centered at δ = 120.9 ppm, while the peak for the carbenic carbon was located at 225.6 ppm. The IR spectrum of **4** showed B-H stretching bands at 2443 and 2374 cm^{-1}. Moreover, the HRMS data supports the formation of complex **4** as it gives peak at *m/z* = 403.3296 (calcd. 403.3289) for the cationic moiety C$_{27}$H$_{40}$BN$_2$ as [M]$^+$.
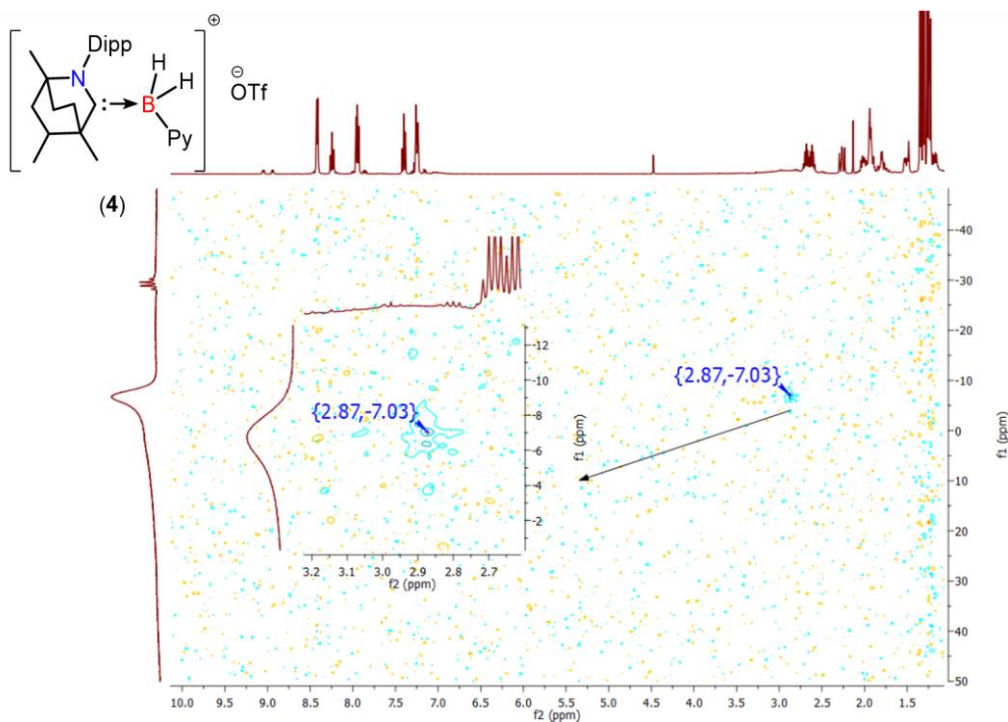
Figure 2B.14 ^{11}B-^{1}H 2D-HSQC NMR spectrum of **4**.

98

Similarly, complex **5** has also been characterized by different spectroscopic techniques. In the ^{1}H NMR spectrum of **5** we found two septets resonating at 2.64 and 2.48 ppm for the Dipp group of the carbene backbone, while the -BH_2 hydrogens were found to resonate between 2.87 to 2.31 ppm (merged with the septets) as a broad peak. For better assessment, ^{1}H NMR spectral comparison of complexes BICAAC−BH$_3$, **3**, **4** and **5** in CDCl$_3$ has been given below (Figure 2B.15). The exact chemical shift value for the broad -BH_2 signal was detected using the ^{11}B-^{1}H 2D-HSQC NMR technique which showed the signal centered at 2.63 ppm (Figure 2B.16). The ^{11}B NMR spectrum of **5** revealed the peak for the boron atom at -8.42 ppm (vs -6.3 ppm for precursor **3**). The ^{19}F{^{1}H} NMR spectrum of **5** displayed a single peak at -78.04 ppm (vs.-76.2 ppm for the precursor **3**). Also, the ^{13}C{^{1}H} NMR spectrum of **5** displayed a quartet for the carbon atom of -CF$_3$ group centered at δ = 120.9 ppm, while the peak for the carbenic carbon was located at 228.6 ppm. The IR spectrum of **5** showed B−H stretching bands at 2422 and 2350 cm^{-1}. Moreover, the HRMS
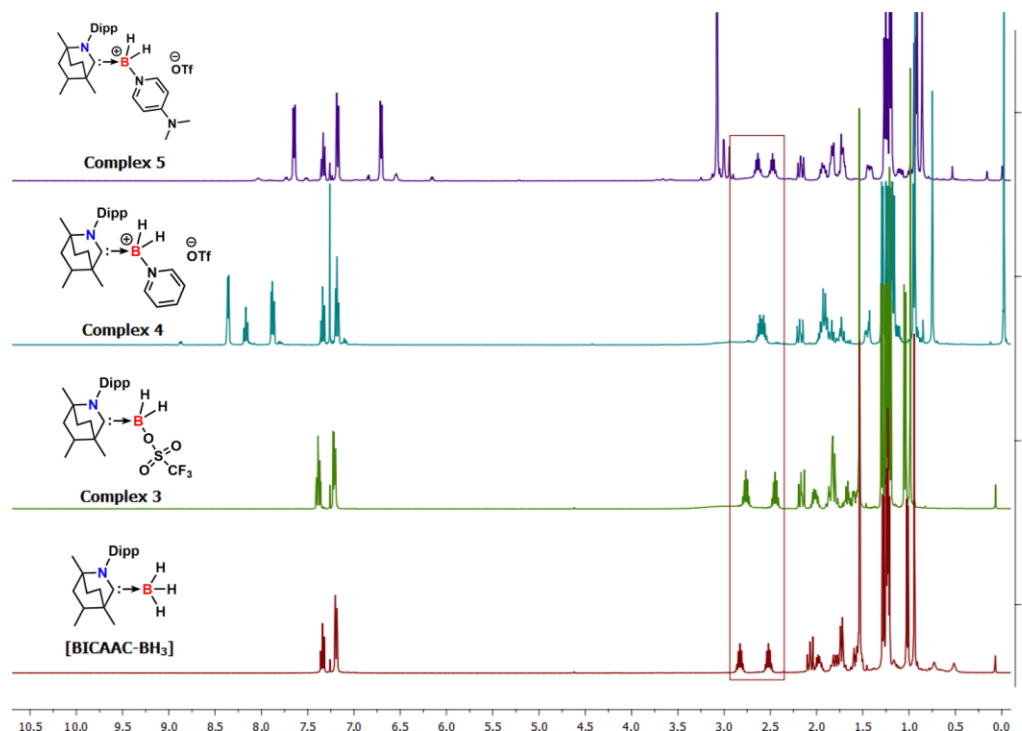
Figure 2B.15 ^{1}H NMR spectral comparison of **BICAAC−BH$_3$**, **3**, **4** and **5** complexes showing the change in the pattern of septets.
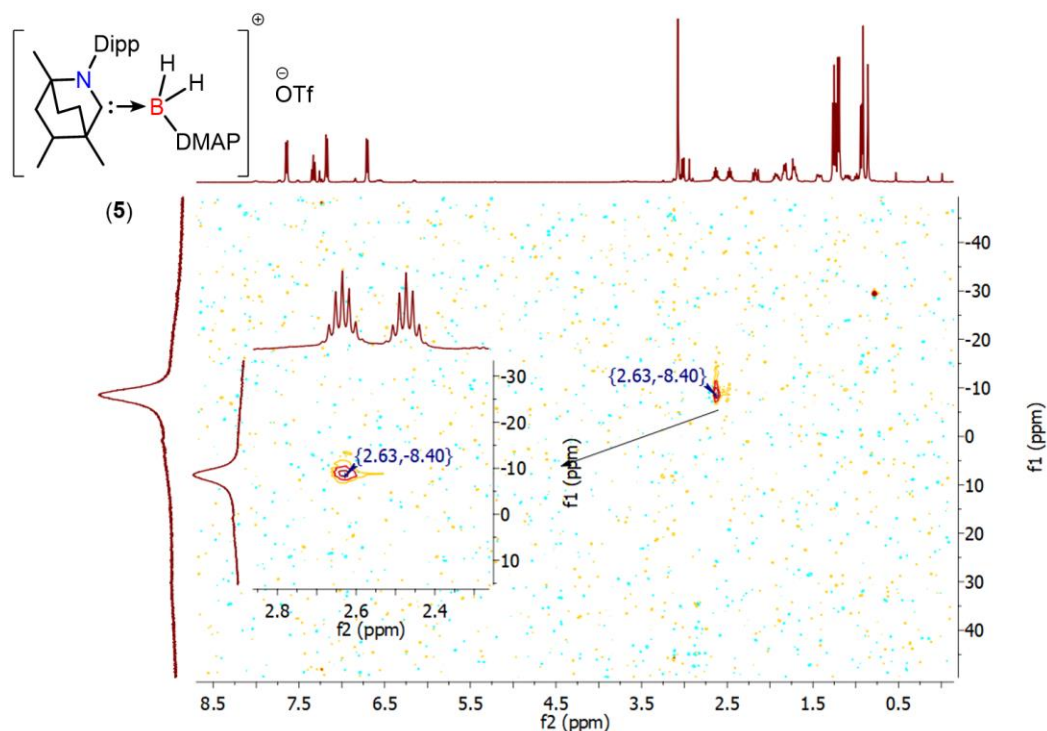
Figure 2B.16 ^{11}B-^{1}H 2D-HSQC NMR spectrum of **5**.

data also supported the formation of complex **5** as it gave signal at (ES$^+$): m/z = 446.3739 (calcd. 446.3712) for the cationic moiety $C_{29}H_{45}BN_3$ as [M]$^+$. Efforts to crystallize complexes **4** and **5** from different solvents such as DCM, CHCl$_3$, toluene, and benzene have so far been unsuccessful.

Gutmann-Beckett assessment of Lewis acidity of complexes 1-2

The conventional approach for quantitative evaluation of relative Lewis acidity involves employing the Gutmann-Beckett method.[31] In this technique, the Lewis acid under examination is allowed to create an adduct with triethylphosphine oxide (Et$_3$PO), causing a perturbation in its ^{31}P NMR signal. The value of ^{31}P NMR chemical shift is thus used to calculate the acceptance number (AN) using the formula AN = 2.21 × (δ_{sample}− 41.0) which provides an estimate of the relative Lewis acidity. In the ^{31}P{^{1}H} NMR of the Et$_3$PO adducts of complexes **1** and **2**, namely [L→BH$_2$(Et$_3$PO)][HB(C$_6$F$_5$)$_3$] and [L→BH$_2$(Et$_3$PO)][B(C$_6$F$_5$)$_4$] [L = BICAAC], signals were observed at 83.31 and 83.51 ppm.

The corresponding acceptance numbers were calculated, AN = 93.50 and 93.94 and affirm the Lewis acidic nature of both **1** and **2** and found to be more Lewis acidic than the popular Lewis acid $B(C_6F_5)_3$ (AN = 77.0-77.7).[32]

2B.2.4 Catalytic activity of complexes 1-2 for hydrosilylation of carbonyls

Over the preceding decades, the hydrosilylation of carbonyl and imine functional groups has evolved as a practical alternative to conventional reduction techniques like hydrogenation with molecular hydrogen, the utilization of hydride donor agents, and transfer hydrogenation.[33] In the direct synthesis of silyl ethers (or protected alcohols), the hydrosilylation of carbonyls mediated by precious-transition-metal catalysts such as Pd, Pt, Rh, Ir, etc., has proven to be a convenient avenue.[34] There is a growing enthusiasm for exploring the catalytic potential of cost-effective, environmentally friendly, and less toxic metal complexes like Fe, Co, Mn, Cu, and Ni for the activation of Si–H bonds.[35] Nevertheless, achieving a level of activity comparable to precious-metal complexes with catalysts based on late transition metals has met with limited success. Notably, hydroelementation catalysts derived from main-group elements have recently emerged, offering alternatives to both precious-metal and late-3d-metal complexes.[4] Within the prevailing landscape of scientific advancements and evolving methodologies, it is foreseeable that these hydroelementation catalysts originating from main-group elements will experience a substantial and accelerated surge in their utilization across various chemical processes and catalytic applications. To date, a limited number of published reports address hydrosilylation catalyzed by borenium cations.[7] Following the successful isolation of complexes **1**-**5**, we further proceed to utilize complexes **1**-**2** as catalysts in the hydrosilylation of carbonyls, e.g., aldehydes and ketones.

Hydrosilylation of carbonyls catalyzed by [BICAAC-BH₂-H-BH₂-BICAAC][H-B(C₆F₅)₃] *(1)*:

We initiated our investigation using benzaldehyde as a test substrate and triethylsilane (Et₃SiH) as hydride source. The first reaction was carried out in the absence of any catalyst in CHCl₃, however no product was formed after 1 h, which emphasize the mandatory presence of catalyst (Table 2B.1, entry 1). The precursor (to **1** and **2**) complex BICAAC-BH₃ also failed to catalyze the model reaction with 2 mol% of catalyst loading in CHCl₃ at 70 °C (Table 2B.1, entry 2). Similar model reaction when performed using 5 mol% of catalyst **1** in CHCl₃, provided the product **6a** in 99% yield after 1 h (Table 2B.1, entry 3). Upon decreasing the catalyst loading to 1 mol%, temperature to 40 °C and time to 5 minutes, no destructive effect on the yield of the product **6a** was noticed (Table 2B.1, entries 4-5). Keeping other parameters same and decreasing the catalyst loading to 0.5 mol% caused a decrease in the product yield to 66% (Table 2B.1, entry 6). Next, we screened a variety of solvents, out of which toluene, benzene and hexane turn out to be competent and DCM and THF on the other hand turn out to be poor reaction medium (Table 2B.1, entries 7-11). Additionally, catalytic activity of the BICAAC→BH₂−OTf complex (**3**) was also investigated for the model reaction which gave only 3 % conversion in CHCl₃ after 1 h at 70°C (Table 2B.1, entry 12).

After having the optimized reaction protocol in hand (Table 2B.1, entry 5) we proceeded for the substrate scope. A library of aldehydes, ketones and *para*-quinone methides (*p*-QMs) substrates were investigated for hydrosilylation reaction using Et₃SiH as hydride source and afforded their reduced product in good to excellent yields (Table 2B.2). The maximum turnover frequency (TOF) of 1200 h^{-1} was calculated for the benzaldehyde substrate (TOF was calculated after 5 minutes). We found aldehydes having different halogens at different positions of the aromatic ring show different reactivity for the hydrosilylation. When the second position of the benzaldehyde is occupied with halogens, the

Table 2B.1 Optimization of reaction conditions for hydrosilylation of benzaldehyde with complex **1**[a]

6a
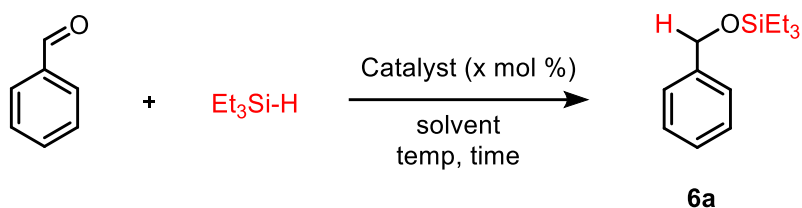
Entry	Catalyst (mol %)	Solvent	Temperature (°C)	Time	Yield (%)[b]
1	-	CHCl$_3$	70	1 h	0
2	BICAAC−BH$_3$ (2)	CHCl$_3$	70	1 h	0
3	**1** (5)	CHCl$_3$	70	1 h	99
4	**1** (2)	CHCl$_3$	40	1 h	99
5	*1 (1)*	*CHCl$_3$*	*40*	*5 min*	*99*
6	**1** (0.5)	CHCl$_3$	40	5 min	66
7	**1** (1)	toluene	40	5 min	91
8	**1** (1)	C$_6$H$_6$	40	5 min	85
9	**1** (1)	hexane	40	5 min	89
10	**1** (1)	CH$_2$Cl$_2$	40	5 min	30
11	**1** (1)	THF	40	5 min	38
12	**3** (2)	CHCl$_3$	70	1 h	3

[a]Reaction conditions: benzaldehyde (1 mmol), Et$_3$SiH (1.2 mmol), catalyst, temperature and time as specified in the table; [b]yield of isolated products

reactivity decreases as the size of halogen atom increases (from 2-F to 2-Br) (Table 2B.2, **6b-6d**), the 2-bromo benzaldehyde took 6h to give 95% yield at 70 °C. Interestingly, the reverse trend was observed when fourth position of the benzaldehyde is taken by the halogens, the reactivity for hydrosilylation increases from 4-fluorobenzaldehyde to 4-iodobenzaldehyde. The 4-fluoro- and 4-chlorobenzaldehyde took 2.5-2 h and required harsh heating conditions

Table 2B.2 Screening of aldehyde substrates for hydrosilylation catalyzed by complex **1**[a]

6a
99%, 40 °C, 5 min

6b
8%, 40 °C, 5 min
97%, 70 °C, 3 h

6c
1%, 40 °C, 5 min
98%, 70 °C, 5 h

6d
NC, 40 °C, 5 min
95%, 70 °C, 6 h

6e
4%, 40 °C, 5 min
97%, 70 °C, 2.5 h

6f
4%, 40 °C, 5 min
99%, 70 °C, 2 h

6g
99%, 40 °C, 10 min

6h
99%, 40 °C, 5 min

6i
99%, 40 °C, 5 min

6j
2%, 40 °C, 5 min
96%, 70 °C, 2 h

6k
2%, 40 °C, 5 min
90%, 70 °C, 4 h

6l
3%, 40 °C, 5 min
95%, 40 °C, 2 h

6m
14%, 40 °C, 5 min
98%, 40 °C, 2 h

6n
1%, 40 °C, 5 min
94%, 70 °C, 4 h

6o
7%, 40 °C, 5 min
96%, 40 °C, 3 h

6p
99%, 40 °C, 10 min

6q
NC, 70 °C, 8 h

6r
12%, 40 °C, 5 min
97%, 40 °C, 3h

6s
8%, 40 °C, 5 min
71%, 70 °C, 3 h

6t
99%, 40 °C, 5 min

6u
2%, 40 °C, 5 min
96%, 70 °C, 3 h

6v
6%, 40 °C, 5 min
67%, 40 °C, 3 h

6w[c]
99%, 40 °C, 5 min

6x[c]
68%, 40 °C, 5 min
98%, 40 °C, 15 min

6y
94%, 40 °C, 10 min

6z1
95%, 40 °C, 10 min

6z2
65%, 40 °C, 5 min
96%, 40 °C, 30 min

6z3
NC, 40 °C, 5 min
97%, 70 °C, 1 h

6z4
92%, 40 °C, 3 h
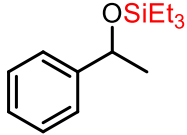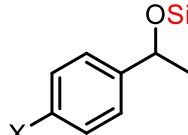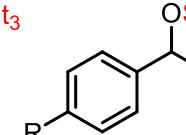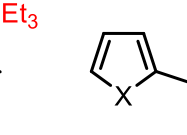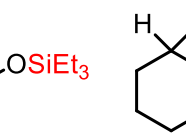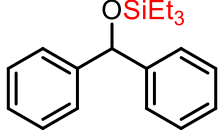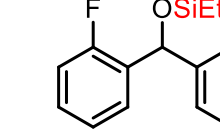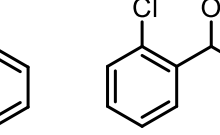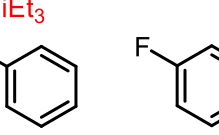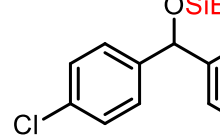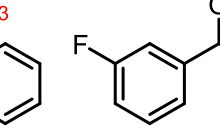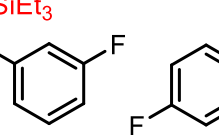
[a]Reaction conditions: aldehyde (0.5 mmol), Et$_3$SiH (0.6 mmol), catalyst **1** (1 mol% = 5.8 mg); [b]yield of isolated products; [c]Et$_3$SiH (1.2 mmol); NC = no conversion

for the reduction (Table 2B.2, **6e-6f**) while 2,4-dichlorobenzaldehyde, 4-bromo- and 4-iodobenzaldehyde smoothly gave up to 99% yield in 5-10 minutes under gentle heating

conditions (Table 2B.2, **6g-6i**). The benzaldehyde derivatives having electron donating groups (-Me, -Et, -OMe, -OEt and -^{i}Pr,) were converted to their reduced products in 90-98% yields in 2-3 h provided 40-70 °C temperature (Table 2B.2, **6j-6o**), however, the 2,3-dimethoxybenzalehyde gave 99 % yield in 10 minutes at 40 °C (Table 2B.2, **6p**). Benzaldehyde substrates with electron withdrawing groups (-NO$_2$ and -CN) were also screened and we found 2-nitrobenzaldehyde did not give any product (Table 2B.2, **6q**), however the 4-nitro- and 4-cyanobenzaldehyde afforded the reduced product in 97 and 71 % isolated yields respectively, in 3 h at 70 °C (Table 2B.2, **6r-6s**). The bulky aldehydes were also well tolerated during the hydrosilylation reaction. The 4-phenylbenzaldehyde gave 99 % of yield in 5 minutes (Table 2B.2, **6t**), while the bulky 1-naphthaldehyde and 9-anthracenecarboxaldehyde gave 96 and 67 % yields respectively in 3h at 70 °C (Table 2B.2, **6u-6v**). Next, the aldehydes having two -CHO groups e.g., terephthalaldehyde and isophthalaldehyde smoothly furnished the corresponding hydrosilylated products in excellent yields, 99 and 98 % respectively in 5-15 minutes (Table2B.2, **6w-6x**). Additionally, the scope was extended to the heteroaromatic aldehydes e.g., furfural, 5-bromo-2-furaldehyde and 2-thiophenecarboxaldehyde which were pleasantly reduced in 94-96 % yield (Table 2B.2, **6y-6z2**). Further, the aliphatic aldehydes cyclohexanecarboxaldehyde and 2-methylvaleraldehyde also afforded their hydrosilylated products in good yields in 1-3 hours (Table 2B.2, **6z3-6z4**).

Having effectively converted various aldehydes into silylated products, our efforts were then directed towards the more challenging task of working with ketone moieties. We found the optimized reaction protocol (Table 2B.1, entry 5) is also well suited for the ketone moieties. The acetophenone and its derivatives (4-F-, 4-Cl-, 4-OMe-, 4-SMe-) were nicely converted to the reduced products in just 5 minutes at 40 °C (Table 2B.3, **7a-7e**). The heteroaromatic substrates 2-acetylfuran and 2-acetylthiophene were also found to be good

Table 2B.3 Screening of ketone substrates for hydrosilylation catalyzed by complex **1**[a]

$$R_1 \overset{O}{\underset{}{\|}} R_2 \quad + \quad Et_3Si\text{-}H \quad \xrightarrow[\substack{CHCl_3 \\ temp, \ time}]{Cat. \ 1 \ (1 \ mol \ \%)} \quad R_1 \overset{OSiEt_3}{\underset{H}{|}} R_2$$

(7a-p)[b]

7a 99%, 40 °C, 5 min	

7b, X = F, 99% 40 °C, 5 min
7c, X = Cl, 96% 40 °C, 5 min

7d, R = OMe, 91% 40 °C, 5 min
7e, R = SMe, 92% 40 °C, 5 min

7f, X = O, 92% 70 °C, 4 h
7g, X = S, 89% 70 °C, 4 h

7h 96%, 40 °C, 5 min

7i 99%, 40 °C, 5 min

7j NR, 40 °C, 5 min 99%, 70 °C, 6 h

7k NR, 40 °C, 5 min 96%, 70 °C, 3 h

7l 98%, 40 °C, 5 min

7m 97%, 40 °C, 5 min

7n 98%, 40 °C, 5 min

7o 98%, 40 °C, 5 min

7p 99%, 40 °C, 5 min

[a]Reaction conditions: ketones (0.5 mmol), Et$_3$SiH (0.6 mmol), catalyst **1** (1 mol% = 5.8 mg); [b]yield of isolated products

candidates for the hydrosilylation reaction and afforded the reduced products in good yields (89-92%) in 4 hours (Table 2B.3, **7f-7g**). The aliphatic ketone cyclohexanone was also acceptable for hydrosilylation and gave the product **7h** in 96 % yield in 5 minutes (Table 2B.3, **7h**). Moreover, the sterically demanding benzophenone and its mono and di halogen derivatives smoothly converted to their reduced products in excellent yields (Table 2B.3, **7i-7p**). The 2-fluoro- and 2-chlorobenzophenone derivatives took longer time (3-6 h) to give

quantitative yields (Table 2B.3, **7j-7k**), while other derivatives (3-fluorobenzophenone, 4-fluorobenzophenone, 4-chlorobenzophenone, 3,3′-difluorobenzophenone, 4,4′-difluorobenzophenone) smoothly afforded the reduced products in excellent yields in 5 minutes (Table 2B.3, **7l-7p**).

We further extended the scope of hydrosilylation for a few *para*-quinone methides (*p*-QMs) (Table 2B.4). *para*-quinone methides (*p*-QMs) crucial synthon in organic synthesis for the construction of various organic structural moieties, such as diaryl/triarylmethanes, carbocycles, heterocycles, and spiro-cycles, etc. owing to their high reactivity. *p*-QMs are not only valuable for synthetic applications, but are also commonly found in nature, where they function as intermediates in various biological and biosynthesis pathways.[36] Taking these

Table 2B.4 Screening of *para*-quinone methides (*p*-QMs) for hydrosilylation catalyzed by complex **1**[a]

8a, 69%   8b, 74%   8c, 76%   8d, 82%
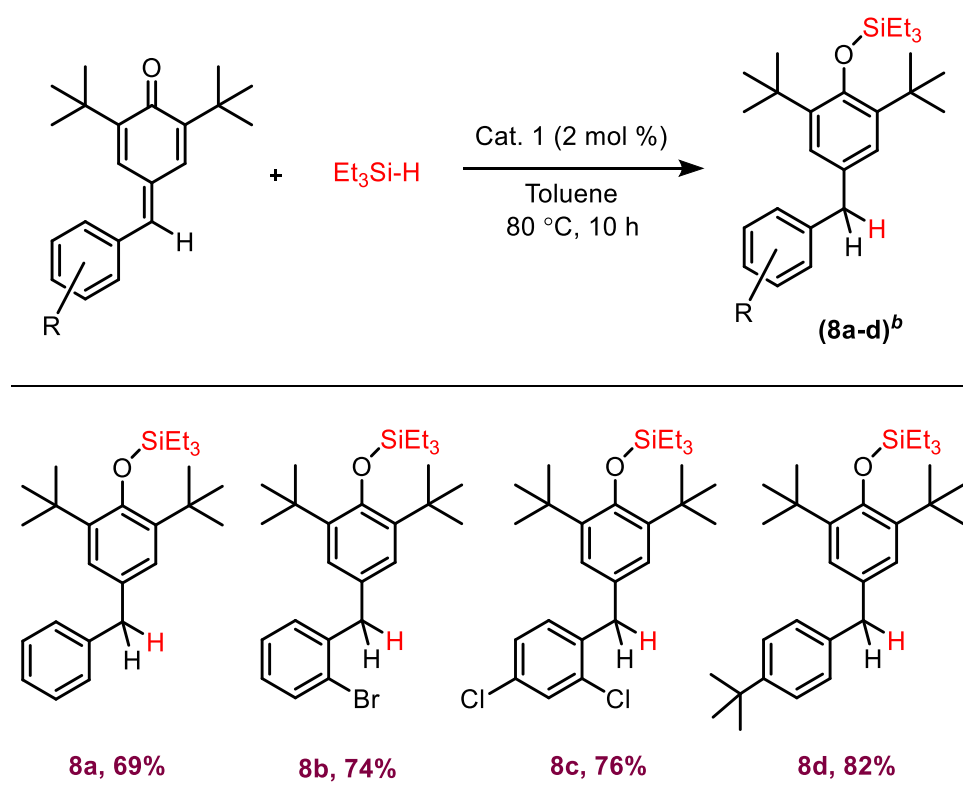
[a]Reaction conditions: para-quinone methides (0.25 mmol), Et₃SiH (0.3 mmol), catalyst **1** (2 mol% = 5.8 mg); [b]yield of isolated products

advantages into consideration we utilized hydrosilylation strategy utilizing *p*-QM as a 1,6-conjugate acceptor and triethylsilane as hydride source with 2 mol% load of **1** in toluene and heating it for 10 hours gave moderate to good yields (69-82 %) of the unsymmetrical diarylmethane silane derivatives (Table 2B.4, **8a-8d**).

*Hydrosilylation of carbonyls catalyzed by [BICAAC-BH$_2$-H-BH$_2$-BICAAC][B(C$_6$F$_5$)$_4$] (2)***:**

After realizing excellent catalytic activity of complex **1** for the hydrosilylation of various carbonyls, we further aimed to investigate the catalytic potential of complex **2** for the same purpose. This was intriguing due to identical boron cation equivalents present in **1** and **2**. A model reaction was performed using benzaldehyde as a test substrate and triethylsilane as a hydride source in the presence of 2 mol% BICAAC−BH$_3$ adduct in toluene, no product formation was noticed even after 12 h of heating at 100 °C (Table 2B.5, entry 1). When similar model reaction was performed in the presence of 5 mol% of catalyst **2** in toluene at 90 °C, it led to the isolation of product **6a** in 99% yield after 8 h (Table 2B.5, entry 2). Keeping other parameters constant and decreasing the catalyst loading to 2 and 1 mol% did not affect the product yield (Table 2B.5, entries 3-4). Further, decreasing the catalyst load to 0.5 mol% or lowering the temperature to 70 °C caused the lowering in the yield of the product (Table 2B.5, entries 5-6). Next, we explored a set of solvents for the model reaction, out of which CHCl$_3$ brought the conversion in 94% yield in 8 h at 70 °C (Table 2B.5, entry 7) and other solvents e.g., THF and DCM gave a low yield of 54 and 75% respectively (Table 2B.5, entries 8-9).

Consequently, for benzaldehyde as the model substrate together with Et$_3$SiH and 1 mol% of catalyst **2** in toluene under heating conditions for 8 hours at 90 °C was found to be an efficient protocol (Table 2B.5, entry 4). Since a broad array of substrates were already screened with catalyst **1**, therefore we examined a subset of them using catalyst **2**. A variety

Table 2B.5 Optimization of hydrosilylation reaction conditions for benzaldehyde with complex **2**[a]

6a
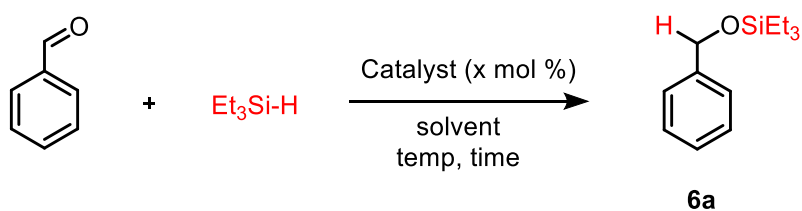
Entry	Catalyst (mol %)	Solvent	Temperature (°C)	Time (h)	Yield (%)[b]
1	BICAAC−BH$_3$ (2)	Toluene	100	12	0
2	**2** (5)	Toluene	90	8	99
3	**2** (2)	Toluene	90	8	99
4	**2 (1)**	**Toluene**	**90**	**8**	**99**
5	**2** (0.5)	Toluene	90	8	82
6	**2** (1)	Toluene	70	8	67
7	**2** (1)	CHCl$_3$	70	8	94
8	**2** (1)	THF	70	8	54
9	**2** (1)	DCM	40	8	75

[a]Reaction conditions: benzaldehyde (1 mmol), Et$_3$SiH (1.2 mmol), catalyst, temperature and time as specified in the table; [b]yield of isolated products

of aldehyde, acetophenone and benzophenone substrates holding different substituents afforded their reduced products in good to excellent yields (Table 2B.6), however, for the ketone substrates (acetophenone and benzophenone) the reaction was required to be performed at 100 °C for 10 hours to obtain good yields.

Table 2B.6 Screening of aldehyde and ketone substrates for hydrosilylation reaction catalyzed by complex **2**[a,b,d]

6a, 99% 6g, 98% 6h, R = Br, 99% 6o, 93% 6p, 71% 6q, 10%
6j, R = Me, 95%
6l, R = OMe, 90%

6r, X = NO$_2$, 97% 6u, 98% 6v, 38% 6x, 98%[c] 6z1, (X = O; R = Br), 98%
6s, X = CN, 96% 6z2, (X = S; R = H), 97%
6t, X = Ph, 99%

6z3, 93% 6z4, 95% 7a, X = H, 98% 7d, R = OMe, 96% 7f, X = O, 96% 7h, 93%
7c, X = Cl, 97% 7e, R = SMe, 98% 7g, X = S, 97%

7i, 98% 7k, 98% 7l, 98% 7p, 98%
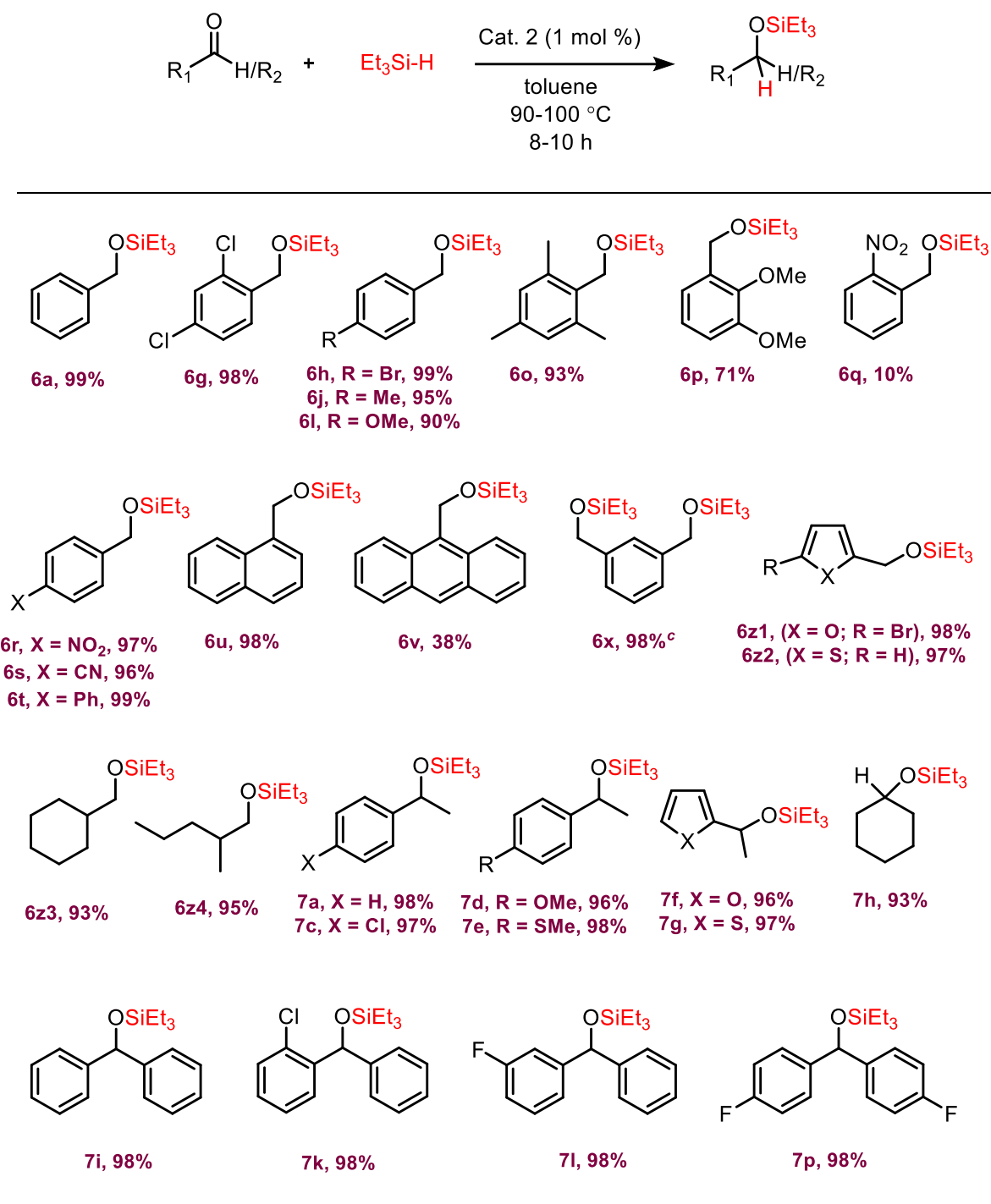
[a]Reaction conditions: aldehyde (0.5 mmol), Et$_3$SiH (0.6 mmol), catalyst **2** (1 mol% = 5.8 mg); [b]yield of isolated products; [c]Et$_3$SiH (1.2 mmol); Temp and time: 90 °C and 8 h (for aldehydes), 100 °C and 10 h (for ketones)

2B.2.5 Mechanistic investigation

Initial findings indicate that the hydrosilylation of carbonyls catalyzed by complex **1** encompasses through the involvement of both the cationic and anionic moieties. To investigate the mechanism, a stoichiometric NMR tube reaction was performed using benzaldehyde and catalyst **1** in C_6D_5Br, the reaction mixture was analyzed using heteronuclear NMR spectroscopy and HRMS. In the ^{11}B NMR spectrum we observed a peak at δ = 2.05 ppm, which was attributed to boron center of $Ph-CH_2-O-B(C_6F_5)_3$ of **Int. 1** (Figure 2B.17),[23b] however, in the ^1H NMR spectrum the peak for the bridged hydrogen of cationic part remained intact and was observed at δ = -1.9 ppm, while the peak for the anionic part $[H-B(C_6F_5)_3]^-$ disappeared and a new sharp singlet was observed at δ = 4.89 ppm, which
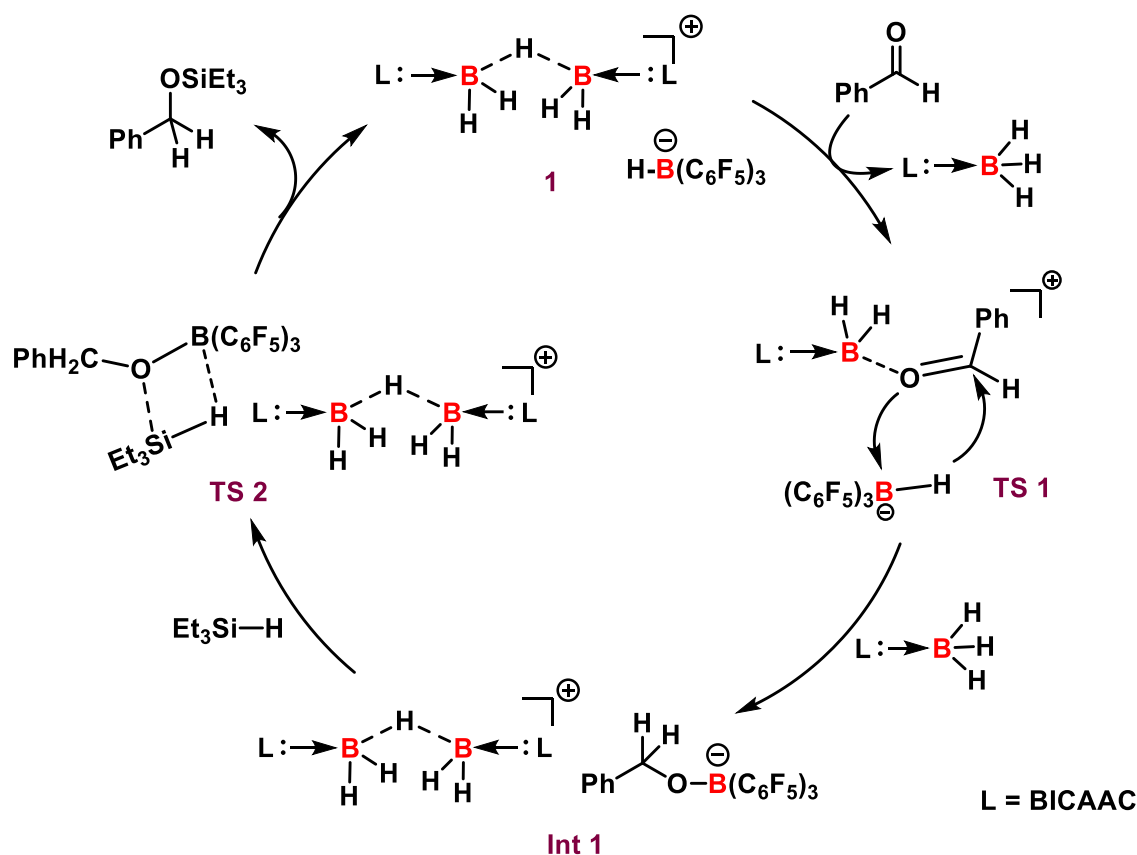
Figure 2B.17 Proposed mechanistic cycle for hydrosilylation of benzaldehyde catalyzed by complex **1**.

corresponds to the methylene protons of Ph−CH_2−O−B(C$_6$F$_5$)$_3$ of **Int. 1**. HRMS analysis of the reaction mixture also supported the formation of **Int. 1** as we found a peak for the Ph−CH$_2$−O−B(C$_6$F$_5$)$_3$ moiety at *m/z* = 619.0358 (calcd. 619.0355). A comprehensive mechanistic investigation is currently in progress.

2B.3 Conclusion

In conclusion we have successfully synthesized and thoroughly characterized BICAAC supported borenium ion equivalent complexes, [L→BH$_2$−H−BH$_2$←L][H-B(C$_6$F$_5$)$_3$] (**1**), [L→BH$_2$−H−BH$_2$←L][B(C$_6$F$_5$)$_4$] (**2**), [L→BH$_2$(OTf)] (**3**), and [L→BH$_2$(Nu)][OTf] (Nu = pyridine, (**4**); Nu = DMAP, (**5**)) (L = BICAAC). The quantitative Lewis acid estimation of complexes **1**-**2** have been conducted, revealing acceptance numbers (AN) within the range of 93.5-93.9, which supports the Lewis acidic nature. Additionally, complexes **1** and **2** have demonstrated notable catalytic activity in the hydrosilylation of a diverse array of carbonyls. Specifically, under 1 mol% catalyst loading and 5 minutes of reaction time, complex **1** emerged as an efficient catalyst for a majority of aldehydes and ketones, achieving the highest turnover frequency (TOF) of up to 1200 h^{-1} with benzaldehyde. Furthermore, complex **1** exhibited catalytic activity in the hydrosilylation of para-quinone methides. Similarly, complex **2** displayed good activity in the hydrosilylation of carbonyls.

2B.4 Experimental section

2B.4.1 General methods

All manipulations were performed under an inert atmosphere of dry nitrogen or argon using a glove box or standard Schlenk techniques. All glassware were dried at 150 °C in a hot air oven for at least 12 h and assembled hot and cooled in vacuo prior to use. Solvents were

purified by MBRAUN solvent purification system MB SPS-800 and were used directly from the SPS system. Chemicals were purchased from Sigma-Aldrich, HIMEDIA, and Avra and were used without further purification. Bicyclic (alkyl)(amino) carbene (BICAAC) was synthesized using reported procedure.[37]

2B.4.2 Physical measurements

The ^{1}H, ^{13}C{^{1}H} and ^{11}B NMR spectra were recorded using Bruker 400 MHz spectrometer with tetramethylsilane (TMS) (for ^{1}H and ^{13}C{^{1}H}) and BF$_3$·OEt$_2$ (for ^{11}B) as external reference; chemical shift values are reported in ppm. FT-IR spectra of complexes **1-5** were recorded (in the range 4000-400 cm^{-1}) with a Perkin-Elmer Lambda 35-spectrophotometer using Nujol mull. High resolution mass spectrometry (HRMS) was performed with Waters SYNAPT G2-S. Melting point of compounds were recorded in sealed capillary using Büchi B-540 melting point apparatus. The single-crystal X-ray diffraction data of compounds **2** and **3** were collected using a Rigaku XtaLAB mini diffractometer equipped with Mercury375M CCD detector. The data were collected with MoKα radiation (λ = 0.71073 Å) using omega scans. During the data collection, the detector distance was 49.9 mm (constant) and the detector was placed at 2θ = 29.85° (fixed) for all the data sets. The data were reduced using CrysAlisPro 1.171.38.46, and the space group determination was done using Olex2[38] with the SHELXT[39] structure solution program using Intrinsic Phasing and refined with the SHELXH-1997[40] refinement package using Least Squares minimization. All non-hydrogen atoms were refined anisotropically. Crystallographic data are summarized in Table 2B.7.

2B.4.3 Syntheses and characterization of complexes 1-5

Synthesis and characterization of [BICAAC→BH$_2$−H−BH$_2$←BICAAC][H−B(C$_6$F$_5$)$_3$] (1): In a 100 mL Schlenk flask, BICAAC−BH$_3$ adduct (0.16 g, 0.5 mmol) was dissolved in 15 mL of toluene and allowed to cool for 1 h at -30 °C. This was followed by the addition of

B(C$_6$F$_5$)$_3$ (0.13 g, 0.25 mmol) and the reaction mixture was warmed to room temperature and further stirred for 1 h. After 1 h of stirring a clathrate was observed at the bottom of the flask. Subsequently, all the volatiles were removed under reduced pressure afforded the oily compound which was further triturated with pentane to give compound **1** as a fluffy solid. (**Yield:** 0.26 g, 89.0 %). **IR** (nujol mull, cm^{-1}) ν: 2922, 2851, 2454, 2373, 2351, 1979, 1639, 1510, 1456, 1377, 1274, 1098, 971, 909, 802. **^{1}H NMR** (400 MHz, C$_6$D$_6$ + C$_6$D$_5$Br): δ = 7.07-7.03 (m, 2H, Ar), 6.84-6.83 (m, 4H, Ar), 4.66-3.83 (broad signal, 1H, *H*-BR$_3$), 2.28-2.17 (sept, 2H, C*H*(CH$_3$)$_2$), 1.97-1.86 (sept, 2H, C*H*(CH$_3$)$_2$), 1.55-1.47 (m, 3H), 1.42 (s, 7H), 1.34-1.19 (m, 8H), 1.15-1.04 (m, 5H), 1.0-0.94 (m, 13H), 0.91 (d, *J* = 6.8 Hz, 3H), 0.87-0.74 (m, 2H), 0.72-0.60 (m, 11H), 0.49-0.48 (m, 5H), 0.38 (d, *J* = 6.4 Hz, 3H), -2.07 (broad singlet, 1H, for bridged hydrogen) ppm. **^{19}F{^{1}H} NMR** (376 MHz, C$_6$D$_6$ + C$_6$D$_5$Br): δ = -132.0 (d, *J* = 18.8 Hz, 6F), -163.3 (t, *J* = 18.8 Hz, 3F), -(165.9-166.0) (m, 6F) ppm. **^{11}B NMR** (128 MHz, C$_6$D$_6$ + C$_6$D$_5$Br): δ = -24.6 (d, *J* = 83.2 Hz, for borate anion, H-*B*R$_3$), -28.7 (q, *J* = 88.3 Hz, for cationic boron) ppm. **^{1}H-^{11}B 2D(HSQC)** (C$_6$D$_5$Br) δ = {4.26, -24.73} ppm for H-BR$_3$ and {1.02, -29.27} ppm for boron bound protons of the cation. **^{13}C{^{1}H} NMR** (100 MHz, C$_6$D$_6$ + C$_6$D$_5$Br): δ = 225.8-225.0 (dm, for carbenic carbon), 150.1-147.7 (dm), 143.6, 143.0, 142.7, 142.3, 139.5-137.0 (dm), 138.2-135.7 (dm), 136.8, 125.1, 125.0, 124.9, 66.1, 66.0, 48.5, 48.0, 42.5, 41.9, 36.8, 36.4, 33.0, 32.5, 32.2, 31.5, 28.52, 28.47, 28.04, 28.0, 24.8, 24.54, 24.52, 24.3, 24.1, 23.81, 23.77, 23.5, 22.68, 22.65, 21.6, 21.5, 19.7, 19.0 ppm. **HRMS** (ES$^+$): *m/z* calculated for C$_{44}$H$_{69}$N$_2$B$_2$: (647.5661) [M-2H]$^+$; found: (647.5684). HRMS (ES$^-$): *m/z* calculated for C$_{18}$HBF$_{15}$: (512.9935) [M]$^-$; found: (512.9934).

Synthesis and characterization of [BICAAC-BH$_2$-H-BH$_2$-BICAAC][B(C$_6$F$_5$)$_4$] (2): In a 100 mL Schlenk flask BICAAC−BH$_3$ adduct (0.16 g, 0.5 mmol) was dissolved in 15 mL of toluene and allowed to cool for 1 h at -30 °C. This was followed by the addition of [CPh$_3$][B(C$_6$F$_5$)$_4$] (0.23 g, 0.25 mmol) and the reaction mixture was warmed to room

temperature and further stirred for 1 h. After 1 h of stirring, a clathrate formation was observed at the bottom of the flask. Thereafter all volatiles were removed under reduced pressure afforded a sticky compound, which was further washed thrice with *n*-hexane to remove the byproduct triphenylmethane (Ph$_3$CH) followed by drying under vacuum for about 12 h to give a white residue of compound **2**. Crystals of complex **2**, suitable for XRD analysis, were grown from a mixture of *n*-hexane and toluene at -30 °C over a span of 4-5 days. (**Yield:** 0.33 g, 81 %). **IR** (nujol mull, cm^{-1}) ν: 2914, 2854, 2560, 2383, 2344, 2280, 2001, 1983, 1642, 1514, 1461, 1376, 1273. *(Note- All the NMR data for complex 2 given below were obtained before the hexane washing)* **^{1}H NMR** (400 MHz, C$_6$D$_5$Br): δ = 7.16-7.08 (m, 11H, Ar), 7.05-7.02 (m, 6H, Ar), 6.92-6.88 (m, 4H, Ar), 5.44 (s, 1H, C*H*Ph$_3$), 2.29-2.21 (sept, 2H, C*H*(CH$_3$)$_2$), 1.99-1.91 (sept, 2H, C*H*(CH$_3$)$_2$), 1.75-1.64 (m, 3H), 1.59-1.53 (m, 2H), 1.45 (s, 7H), 1.42-1.35 (m, 5H), 1.25-1.13 (m, 7H), 1.04-0.99 (m, 12H), 0.93-0.89 (m, 3H), 0.86-0.78 (m, 2H), 0.74-0.64 (m, 11H), 0.60-0.58 (m, 5H), 0.38 (d, *J* = 6.4 Hz, 3H), -2.05 (1H, broad singlet, for bridged hydrogen) ppm. **^{19}F{^{1}H} NMR** (376 MHz, C$_6$D$_5$Br): δ = -131.7 (broad d, *J* = 11.28 Hz, 8F), -162.3 (t, *J* = 18.8 Hz, 4F), -(166.1-166.0) (m, 8F) ppm. **^{11}B NMR** (128 MHz, C$_6$D$_5$Br): δ = -16.2 (s, for borate anion, BR$_4$), -28.9 (q, *J* = 85.8 Hz, for cationic boron) ppm. **^{1}H-^{11}B 2D(HSQC)** (C$_6$D$_5$Br) δ = {1.16, -29.01} ppm. **^{13}C{^{1}H} NMR** (100 MHz, C$_6$D$_5$Br): δ = 225.8-225.0 (dm, carbenic carbon), 149.9-147.5 (dm), 144.0, 143.6, 124.9, 142.7, 142.2, 139.7-137.8 (dm), 138.6, 137.8-135.3 (dm), 136.7, 129.5, 129.0, 128.4, 126.4, 125.1, 125.0, 124.9, 124.4, 124.1, 66.1, 66.0, 57.0 (Ph$_3$*C*H), 48.5, 48.0, 42.7, 42.0, 37.0, 36.6, 33.2, 32.7, 28.5, 28.4, 28.1, 28.0, 24.9, 24.8, 24.63, 24.56, 24.5, 24.2, 24.0, 23.9, 23.7, 23.6, 22.89, 22.85, 21.72, 21.66, 19.9, 19.2 ppm. **HRMS** (ES$^+$): *m/z* calculated for C$_{44}$H$_{71}$B$_2$N$_2$: (649.5818) [M]$^+$; found: (649.5850). HRMS (ES$^-$): *m/z* calculated for C$_{24}$BF$_{20}$: (678.9778) [M]$^-$; found: (678.9764).

Synthesis and characterization of [BICAAC→BH$_2$−OTf] (3): In a 100 mL Schlenk flask, BICAAC−BH$_3$ adduct (0.32 g, 1.0 mmol) was dissolved in 10 mL of precooled (-30 °C) toluene inside an argon filled glove box, subsequently methyl trifluoromethanesulfonate (Me-OTf) (110 µL, 1.0 mmol) was added into it in dropwise manner. Immediately methane gas evolution was observed inside the flask and the reaction mixture was further allowed to stirred at room temperature for 20 minutes. The volatiles were removed under reduced pressure and the material obtained was triturated with pentane and the residue was further dried for 15 hours to give analytically pure **3** as a white powder in 92 % isolated yield. The X-ray quality crystals were grown from a concentrated chloroform solution of **3** within four days at -30 °C. (**Yield:** 0.44 g, 92 %), **Mp**: 168-169 °C. **FT-IR** (nujol mull, cm^{-1}) ν: 2925, 2852, 2470, 2379, 2350, 1590, 1535, 1460, 1361, 1246, 1190, 1125, 962. **^{1}H NMR** (400 MHz, CDCl$_3$) δ = 7.41-7.37 (m, 1H, Ar), 7.22-7.19 (m, 2H, Ar), 3.49-2.52 (broad signal, 2H, BH_2 merged with the septet), 2.76 (sept, J = 6.8 Hz, 1H, CH(CH$_3$)$_2$), 2.45 (sept, J = 6.8 Hz, 1H, CH(CH$_3$)$_2$), 2.19-2.13 (m, 1H), 2.04-1.97 (m, 1H), 1.88-1.77 (m, 3H), 1.72-1.63 (m, 1H), 1.61-1.56 (m, 1H), 1.54 (s, 3H), 1.29 (d, J = 6.8 Hz, 3H), 1.26-1.20 (m, 9H), 1.04 (d, J = 7.2 Hz, 3H), 0.99 (s, 3H) ppm. **^{19}F{^{1}H} NMR** (376 MHz, CDCl$_3$) δ = -76.17 ppm. **^{11}B NMR** (128 MHz, CDCl$_3$) δ = -6.29 ppm. **^{11}B-^{1}H 2D(HSQC)** (CDCl$_3$) δ = 2.92 ppm (for ^{1}H) and -6.3 ppm (for ^{11}B). **^{13}C{^{1}H} NMR** (100 MHz, CDCl$_3$) δ = 227.3 (broad signal, for carbonic carbon), 143.5, 143.0, 137.2, 129.8, 124.8, 124.7, 118.8 (q, $^1J_{C-F}$ = 320 Hz, -CF$_3$), 64.9, 47.3, 43.3, 37.3, 33.1, 32.6, 29.3, 28.6, 24.6, 24.3, 24.2, 23.8, 23.3, 21.1, 19.6 ppm. **HRMS** (ES$^+$): m/z calculated for C$_{22}$H$_{33}$BN: (322.2710) [M-2H]$^+$; found: (322.2713); HRMS (ES$^-$): m/z calculated for CF$_3$O$_3$S: (148.9520) [M]$^-$; found (148.9535).

Synthesis and characterization of [BICAAC→BH$_2$−py][OTf] (4): In a 100 mL Schlenk flask, complex **3** (0.24 g, 0.5 mmol) was dissolved in 10 mL of benzene at room temperature inside an argon filled glove box, subsequently pyridine (40 µL, 0.5 mmol) was added into it.

The reaction mixture was then taken out from the glove box and stirred for 8 hours under gentle heating conditions at 60-70 °C. The volatiles were removed under reduced pressure followed by trituration with pentane and the residue obtained was dried for 15 hours to give analytically pure **4** as a white fluffy powder in 96 % isolated yield. (**Yield:** 0.26 g, 96 %). **FT-IR** (nujol mull, cm^{-1}) ν: 2957, 2865, 2443, 2374, 1622, 1457, 1374, 1269, 1147, 1028, 801, 754. **^{1}H NMR** (400 MHz, CDCl$_3$): 8.36 (d, J = 5.2 Hz, 2H, Ar), 8.17 (t, J = 8.0 Hz, 1H, Ar), 7.90-7.86 (m, 2H, Ar), 7.34 (t, J = 8.0 Hz, 1H, Ar), 7.18 (t, J = 6.8 Hz, 2H, Ar), 3.19-2.51 (broad signal, 2H, BH_2), 2.65-2.52 (merged septet, 2H), 2.21-2.15 (m, 1H), 1.98-1.88 (m, 3H), 1.86-1.78 (m, 1H), 1.75-1.70 (m, 1H), 1.47-1.43 (m, 1H), 1.29 (d, J = 6.8 Hz, 3H), 1.24 (d, J = 6.8 Hz, 3H), 1.20-1.16 (m, 6H), 0.96-0.94 (m, 6H), 0.75 (s, 3H) ppm. **^{19}F{^{1}H} NMR** (376 MHz, CDCl$_3$): -78.09 ppm. **^{11}B NMR** (128 MHz, CDCl$_3$): -7.23 ppm. **^{11}B-^{1}H 2D(HSQC)** (CDCl$_3$) δ = 2.87 ppm (for ^{1}H) and -7.03 ppm (for ^{11}B). **^{13}C{^{1}H} NMR** (100 MHz, CDCl$_3$): 225.6, 147.6, 142.9, 142.7, 142.4, 137.1, 129.9, 127.7, 125.2, 125.0, 120.9 (q, $^1J_{C-F}$ = 320 Hz, CF$_3$), 66.4, 48.5, 42.6, 38.6, 32.7, 32.1, 28.9, 28.7, 25.0, 24.6, 24.2, 24.0, 23.4, 21.3, 19.4 ppm. **HRMS** (ES$^+$): m/z calculated for C$_{27}$H$_{40}$BN$_2$: (403.3289) [M]$^+$; found: (403.3296).

Synthesis and characterization of [BICAAC→BH$_2$−DMAP][OTf] (5): Similar procedure was followed as given for the synthesis of complex **4**. Reagent used: complex **3** (0.24 g, 0.5 mmol), 4-dimethylaminopyridine (DMAP) (0.06 g, 0.5 mmol). (**Yield:** 0.28 g, 94 %). **FT-IR** (nujol mull, cm^{-1}) ν: 2925, 2857, 2422, 2350, 1640, 1556, 1454, 1378, 1265, 1148, 1029. **^{1}H NMR** (400 MHz, CDCl$_3$): 7.65 (d, J = 7.2 Hz, 2H, Ar), 7.33 (t, J = 7.6 Hz, 1H, Ar), 7.18 (d, J = 7.6 Hz, 2H, Ar), 6.71 (d, J = 7.2 Hz, 2H, Ar), 3.08 (s, 6H, N(CH_3)$_2$), 2.87-2.31 (broad signal merged with the two septets, 2H, BH_2), 2.64 (sept, J = 6.8 Hz, 1H, CH(CH$_3$)$_2$), 2.48 (sept, J = 6.8 Hz, 1H, CH(CH$_3$)$_2$), 2.20-2.14 (m, 1H), 1.98-1.90 (m, 1H), 1.86-1.82 (m, 2H), 1.76-1.69 (m, 2H), 1.45-1.40 (m, 1H), 1.25 (t, J = 7.6 Hz, 6H), 1.20 (d, J = 6.8 Hz, 6H), 0.95-

0.91 (m, 6H), 0.86 (s, 3H) ppm. ^{19}**F{^{1}H} NMR** (376 MHz, CDCl$_3$): -78.04 ppm. ^{11}**B NMR** (128 MHz, CDCl$_3$): -8.42 ppm. ^{11}**B-^{1}H 2D(HSQC)** (CDCl$_3$) δ = 2.63 ppm (for ^{1}H) and -8.4 ppm (for ^{11}B). ^{13}**C{^{1}H} NMR** (100 MHz, CDCl$_3$): 228.6, 155.4, 146.2, 142.7, 142.4, 137.2, 129.6, 125.0, 124.8, 120.9 (q, $^1J_{C-F}$ = 320 Hz, CF$_3$), 107.7, 65.7, 48.2, 42.7, 39.7, 38.1, 32.9, 32.1, 28.9, 28.6, 25.0, 24.6, 24.3, 24.0, 23.4, 21.6, 19.6, ppm. **HRMS** (ES$^+$): *m/z* calculated for C$_{29}$H$_{45}$BN$_3$: (446.3712) [M]$^+$; found: (446.3739).

2B.5 Crystallographic data

Table 2B.7 Crystallographic details of complexes **2** and **3**

Compound[a]	2	3
Chemical formula	$C_{143}H_{150}B_6F_{40}N_4$	$C_{23}H_{35}BF_3NO_3S$
Molar mass	2749.53	473.39
Crystal system	triclinic	orthorhombic
Space group	*P*-1	*Pbca*
T [K]	150.00(10)	150.01(10)
a [Å]	10.8639(5)	17.3407(6)
b [Å]	15.9267(8)	15.5302(5)
c [Å]	20.2463(12)	18.2080(8)
α [°]	77.760(5)	90.00
β [°]	76.234(5)	90.00
γ [°]	89.704(4)	90.00
V [Å^3]	3321.4(3)	4903.5(3)
Z	1	8
ρ(calcd.) [g·cm^{-3}]	1.375	1.282
μ [mm^{-1}]	0.118	0.179
F(000)	1426.0	2016.0
Radiation [Å]	Mo Kα (λ = 0.71073)	Mo Kα (λ = 0.71073)
Reflections collected	46677	30112
Independent reflections	11705	4336
Data/restraints/parameters	11705/120/988	4336/72/383
$R1$, wR_2 [$I>2\sigma(I)$][a]	0.0670, 0.1419	0.0669, 0.1877
R1, wR$_2$ (all data)[a]	0.1224, 0.1811	0.0822, 0.2056
GOF	1.044	1.043

[a] $R1 = \Sigma||Fo| - |Fc||/\Sigma|Fo|$. $wR_2 = [\Sigma w(|Fo^2| - |Fc^2|)^2/\Sigma w|Fo^2|^2]^{1/2}$

2B.6 References

1. Fernández, E.; Whiting, A. *Synthesis and Application of Organoboron Compounds*, Springer, **2015**.

2. (a) Brown, H. C. *Hydroboration*, Benjamin, New York, **1962**; (b) Männig, D.; Nöth, H. *Angew. Chem. Int. Ed. Engl.*, **1985**, *24* , 878-879; (c) Hayashi, T.; Matsumoto, Y.; Ito, Y. *J. Am. Chem. Soc.* **1989**, *111* , 3426-3428; (d) Schlesinger, H. I.; Brown, H. C.; Abraham, B.; Bond, A. C.; Davidson N.; Finholt, A. E.; Gilbreath, J. R.; Hoekstra, H.; Horvitz, L.; Hyde, E. K.; Katz, J. J.; Knight, J.; Lad, R. A.; Mayfield, D. L.; Rapp, L.; Ritter, D. M.; Schwartz, A. M.; Sheft, I.; Tuck, L. D.; Walker, A. O. *J. Am. Chem. Soc.* **1953**, *75* , 186-190; (e) Chaikin, S. W.; Brown W. G. *J. Am. Chem. Soc.* **1949**, *71* , 122-125; (f) Suzuki, A. *Angew. Chem. Int. Ed.*, **2011**, *50*, 6722-6737; (g) Miyaura, N.; Suzuki, A. *Chem. Rev.* **1995**, *95*, 2457-2483; (h) Suzuki, A. *J. Organomet. Chem.* **1999**, *576*, 147-168; (i) Johansson Seechurn, C. C. C.; Kitching, M. O.; Colacot, T. J.; Snieckus, V. *Angew. Chem. Int. Ed.*, **2012**, *51*, 5062-5085; (j) Stephan, D. W.; Erker, G. *Angew. Chem. Int. Ed.* **2015**, *54*, 6400-6441.

3. (a) Rao, B.; Kinjo, R. *Chem. Asian J.* **2018**, *13*, 1279-1292; (b) Nori, V.; Pesciaioli, F.; Sinibaldi, A.; Giorgianni, G.; Carlone, A. *Catalysts* **2022**, *12*, 5.

4. (a) Parks, D. J.; Piers, W. E. *J. Am. Chem. Soc.* **1996**, *118*, 9440-9441; (b) Parks, D. J.; Blackwell, J. M.; Piers, W. E. *J. Org. Chem.* **2000**, *65*, 3090-3098; (c) Chase, P. A.; Jurca, T.; Stephan, D. W. *Chem. Commun.* **2008**, 1701-1703; (d) Lawson, J. R.; Melen, R. L. *Inorg. Chem.* **2017**, *56*, 8627-8643; (e) Hackel, T.; McGrath, N. A. *Molecules* **2019**, *24*, 432; (f) Kumar, G.; Roy, S.; Chatterjee, I. *Org. Biomol. Chem.* **2021**, *19*, 1230-1267; (f) Sakata, K.; Fujimoto, H. *J. Org. Chem.* **2013**, *78*, 12505-12512; (g) Hog, D. T.; Oestreich, M. *Eur. J. Org. Chem.* **2009**, 5047-5056.

5. Kölle, P.; Nöth, H. *Chem. Rev.* **1985**, *85*, 399-418.

6. Piers, W. E.; Bourke, S. C.; Conroy, K. D. *Angew. Chem. Int. Ed*. **2005**, *44*, 5016-5036.

7. (a) Eisenberger, P.; Crudden, C. M. *Dalton Trans*. **2017**, *46*, 4874-4887; (b) Tan, X.; Wang, H. *Chem. Soc. Rev*. **2022**, *51*, 2583-2600.

8. (a) Matsumoto, T.; Gabbaï, F. P. *Organometallics* **2009**, *28*, 4252-4253; (b) Matsumoto, T.; Gabbaï, F. P. *Organometallics* **2009**, *28*, 4898; (c) Chiu, C.-W.; Gabbaï, F. P. *Organometallics* **2008**, *27*, 1657-1659.

9. McArthur, D.; Butts, C. P.; Lindsay, D. M. *Chem. Commun*. **2011**, *47*, 6650-6652.

10. Eisenberger, P.; Bailey, A. M.; Crudden, C. M. *J. Am. Chem. Soc*. **2012**, *134*, 17384-17387.

11. (a) Krossing, I. *Chem. Eur. J*. **2001**, *7*, 490-502; (b) Mercea, D. M.; Howlett, M. G.; Piascik, A. D.; Scott, D. J.; Steven, A.; Ashley, A. E.; Fuchter, M. J. *Chem. Commun*. **2019**, *55*, 7077-7080.

12. Bonnier, C.; Piers, W. E.; Parvez, M.; Sorensen, T. S. *Chem. Commun*. **2008**, 4593-4595.

13. De Vries, T. S.; Vedejs, E. *Organometallics* **2007**, *26*, 3079-3081.

14. De Vries, T. S.; Prokofjevs, A.; Harvey, J. N.; Vedejs, E. *J. Am. Chem. Soc*. **2009**, *131*, 14679-14687.

15. Prokofjevs, A.; Vedejs, E. *J. Am. Chem. Soc*. **2011**, *133*, 20056-20059.

16. Prokofjevs, A.; Boussonnière, A.; Li, L.; Bonin, H.; Lacôte, E.; Curran, D. P.; Vedejs, E. *J. Am. Chem. Soc*. **2012**, *134*, 12281-12288.

17. Inés, B.; Patil, M.; Carreras, J.; Goddard, R.; Thiel, W.; Alcarazo, M. *Angew. Chem. Int. Ed.* **2011**, *50*, 8400-8403.

18. Solovyev, A.; Geib, S. J.; Lacôte, E.; Curran, D. P. *Organometallics* **2012**, *31*, 54-56.

19. Denmark, S. E.; Ueki, Y. *Organometallics* **2013**, *32*, 6631-6634.

20. Prokofjevs, A.; Kampf, J. W.; Solovyev, A.; Curran, D. P.; Vedejs, E. *J. Am. Chem. Soc*. **2013**, *135*, 15686-15689.

21. (a) Chen, W.-C.; Lee, C.-Y.; Lin, B.-C.; Hsu, Y.-C.; Shen, J.-S.; Hsu, C.-P.; Yap, G. P. A.; Ong, T.-G. *J. Am. Chem. Soc.* **2014**, *136*, 914-917; (b) Ghadwal, R. S.; Schurmann, C. J.; Andrada, D. M.; Frenking, G. *Dalton Trans*. **2015**, *44*, 14359-14367.

22. Eisenberger, P.; Bestvater, B. P.; Keske, E. C.; Crudden, C. M. *Angew. Chem. Int. Ed.* **2015**, *54*, 2467-2471.

23. (a) Jaiswal, K.; Prashanth, B.; Singh, S. *Chem. Eur. J*. **2016**, *22*, 11035-11041; (b) Rawat, S.; Bhandari, M.; Porwal, V. K.; Singh, S. *Inorg. Chem*. **2020**, *59*, 7195-7203.

24. McGough, J. S.; Butler, S. M.; Cade, I. A.; Ingleson, M. J. *Chem. Sci*. **2016**, *7*, 3384-3389.

25. (a) Liu, Y.; Su, B.; Dong, W.; Li, Z. H.; Wang, H. *J. Am. Chem. Soc*. **2019**, *141*, 8358-8363; (b) Su, B.; Li, Y.; Li, Z. H.; Hou, J.-L.; Wang, H. *Organometallics* **2020**, *39*, 4159-4163.

26. Clarke, J. J.; Devaraj, K.; Bestvater, B. P.; Kojima, R.; Eisenberger, P.; DeJesus, J. F.; Crudden, C. M. *Org. Biomol. Chem*. **2021**, *19*, 6786-6791.

27. (a) Kundu, G.; Balayan, K.; Tothadi, S.; Sen, S. S. *Inorg. Chem*. **2022**, *61*, 12991-12997; (b) Kundu, G.; Dixit, R.; Tothadi, S.; Vanka, K.; Sen, S. S. *Dalton Trans*. **2022**, *51*, 14452-14457.

28. Maji, S.; Sarkar, P.; Das, A.; Pati, S. K.; Mandal, S. K. *Inorg. Chem*. **2022**, *61*, 14282-14287.

29. (a) De Vries, T. S.; Prokofjevs, A.; Vedejs, E. *Chem. Rev*. **2012**, *112*, 4246-4282; (b) Radcliffe, J. E.; Dunsford, J. J.; Cid, J.; Fasano, V.; Ingleson, M. J. *Organometallics* **2017**, *36*, 4952-4960; (c) Franz, D.; Inoue, S. *Chem. Eur. J*. **2019**, *25*, 2898-2926.

30. Manar, K. K.; Porwal, V. K.; Kamte, R. S.; Adhikari, M.; Thakur, S. K.; Bawari, D.; Choudhury, A. R.; Singh, S. *Dalton Trans*. **2019**, *48*, 17472-17478.

31. (a) Gutmann, V. *Coord. Chem. Rev*. **1976**, *18*, 225-255; (b) Singh, S.; Bhandari, M.; Rawat, S.; Nembenna, S. "Cationic Compounds of Group 13 Elements: Entry Point to the p-block for Modern Lewis Acid Reagents." *Polar Organometallic Reagents: Synthesis, Structure, Properties and Applications* (Eds.: A. E. H. Wheatley, M. Uchiyama), Wiley, **2022**, 201-269.

32. Sivaev, I. B.; Bregadze, V. I. *Coord. Chem. Rev*. **2014**, *270-271*, 75-88.

33. (a) Ojima, I. *The Hydrosilylation Reaction. Organic Silicon Compounds*; Wiley: Chichester, U.K., **1989**; (b) Marciniec, B. *Coord. Chem. Rev*. **2005**, *249*, 2374-2390; (c) Nakajima, Y.; Shimada, S. *RSC Adv*. **2015**, *5*, 20603-20616.

34. (a) Tafazolian, H.; Yoxtheimer, R.; Thakuri, R. S.; Schmidt, J. A. *Dalton Trans*. **2017**, *46*, 5431-5440; (b) Kong, Y. K.; Kim, J.; Choi, S.; Choi, S. B. *Tetrahedron Lett*. **2007**, *48*, 2033-2036; (c) Park, S.; Brookhart, M. *Organometallics* **2010**, *29*, 6057-6064.

35. (a) Bleith, T.; Gade, L. H. *J. Am. Chem. Soc*. **2016**, *138*, 4972-4983; (b) Raya-Barón, A.; Oña-Burgos, P.; Fernández, I. *ACS Catal*. **2019**, *9*, 5400-5417; (c) Tamang, S. R.; Findlater, M. *Molecules* **2019**, *24*, 3194-4018; (d) Chakraborty, S.; Krause, J. A.; Guan, H. *Organometallics* **2009**, *28*, 582-586.

36. (a) Parra, A.; Tortosa, M. *ChemCatChem* **2015**, *7*, 1524; (b) Caruana, L.; Fochi, M.; Bernardi, L. *Molecules* **2015**, *20*, 11733; (c) Li, W.; Xu, X.; Zhang, P.; Li, P. *Chem. Asian J.* **2018**, *13*, 2350; (d) Wang, J. Y.; Hao, W. J.; Tu, S. J.; Jiang, B. *Org. Chem. Front.* **2020**, *7*, 1743; (e) Lima, C. G. S.; Pauli, F. P.; Costa, D. C. S.; de Souza, A. S.; Forezi, L. S. M.; Ferreira, V. F.; de Carvalho da Silva, F. *European J. Org. Chem.* **2020**, *2020*, 2650.

37. Mendivil, E. T.; Hansmann, M. M.; Weinstein, C. M.; Jazzar, R.; Melaimi, M.; Bertrand, G. *J. Am. Chem. Soc.* **2017**, *139*, 7753-7756

38. Dolomanov, O. V., Bourhis, L. J., Gildea, R. J., Howard, J. A. K. and Puschmann, H. *J. Appl. Cryst.* **2009**, *42*, 339-341.

39. Sheldrick, G. M. *Acta Cryst., Sect. A* **2015**, *71*, 3-8.

40. Sheldrick, G. M. *Acta Cryst., Sect. A* **2008**, *64*, 112-122.

Syntheses, structure and reactivity of BICAAC stabilized Ge(II)/Sn(II) dihalide complexes
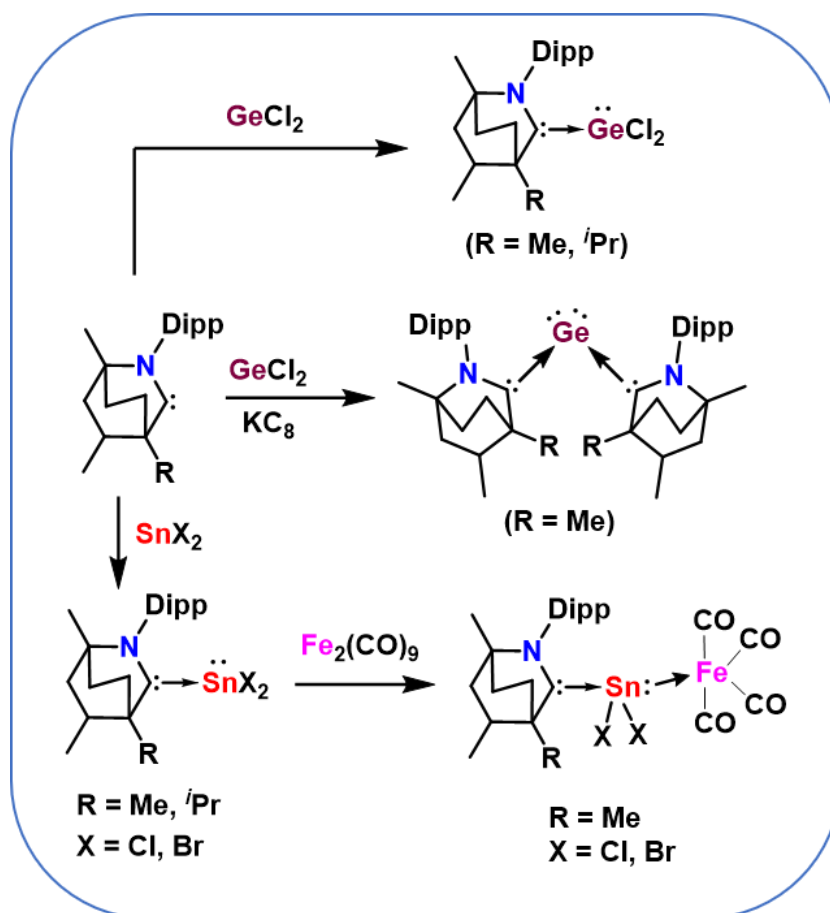
Adhikari, M.; Thakur, S. K.; Singh S. Syntheses, structures and reactivity of BICAAC stabilized Ge/Sn(II) dihalide complexes *(unpublished results).*

Abstract: The current chapter deals with the syntheses and characterization of a series of $^{Me/iPr}$BICAAC supported Ge(II) and Sn(II) complexes, [^{Me}BICAAC−GeCl$_2$ (**1**), [^{iPr}BICAAC−GeCl$_2$ (**2**), ^{Me}BICAAC−SnX$_2$ (X = Cl (**4**); X = Br (**5**), ^{iPr}BICAAC−SnX$_2$ (X = Cl (**6**); X = Br (**7**))]. Furthermore, the *in-situ* reaction of ^{Me}BICAAC, GeCl$_2$·dioxane and KC$_8$ afforded the germylone (^{Me}BICAAC)$_2$Ge (**3**). Additionally, complexes **3** and **4** upon reaction with a metal carbonyl, Fe$_2$(CO)$_9$ led to the syntheses of the adducts ^{Me}BICAAC→SnX$_2$→Fe(CO)$_4$ (X = Cl (**8**); X = Br (**9**)). In our endeavors, attempts were made to convert the Sn-halide adducts **3** and **4** into the corresponding hydrides, ^{Me}BICAAC−SnH$_2$, through treatment with excess LiBH$_4$. Unfortunately, this process resulted in uncontrolled hydrogenation, with the major identified products being hydrogenated ^{Me}BICAACH$_2$ (**10**) and Sn metal.

3.1 Introduction

Over the past three decades, carbenes have found extensive utility in the chemistry of group-14 elements, playing a significant role in shaping the overall progress in this field.[1] The focus of this chemistry primarily involves carbene adducts with Si(IV) and Ge/Sn(II) compounds. However, realizing the potential of carbene ligands, considerable attention has also been devoted to isolate corresponding low-coordinate, low-valent, and open-shell species.[2] Additionally, the utilization of carbenes in organic synthesis (as organocatalysts) has attracted considerable interest in both experimental and theoretical research.[3] In context of low-valent group-14 complexes, the first carbon(0) complex (**A**, Figure 3.1) was isolated in 1961 by Ramirez and co-workers, in which the carbon center contains two lone pair of electron and is stabilized by two PPh$_3$ ligands, these species were called as carbodiphosphoranes (CDPs).[4] The feasibility of the corresponding carbene analogue called as carbodicarbenes was computationally described by Frenking and co-workers which suggested the donor-acceptor type of bonding in such bent-allenes.[5] Soon after, Bertrand and co-workers isolated the first carbodicarbene complex (**B**, Figure 3.1), providing evidence of the synthetic accessibility of this species.[6] In contrast to carbon, various Si(IV) adducts (**C1-C5**, Figure 3.1), low-valent Si(III) radicals (**D1-D4**, Figure 3.1), Si(II) dihalides (**E1-E2**, Figure 3.1) and silylene (**F**, Figure 3.1) stabilized by carbenes have also been successfully isolated and thoroughly characterized.[1e,2,7] Additionally, the isolation of zero-valent Si complexes, poses a challenging task, yet leveraging the strong ambiphilic properties of carbenes has enabled the syntheses of various elusive silicon compounds for examples the carbene stabilized diatomic Si(0) complexes (**G1-G2**, Figure 3.1) and silylone species (**H1-H3**, Figure 3.1).[7e,8] The heavier congeners of group-14 elements (Ge, Sn, and Pb) typically exhibit a preference for the +2 oxidation state over +4 due to the participation of the inert pair effect. Consequently, low-valent germanium precursors (such as GeCl$_2$·dioxane) are readily
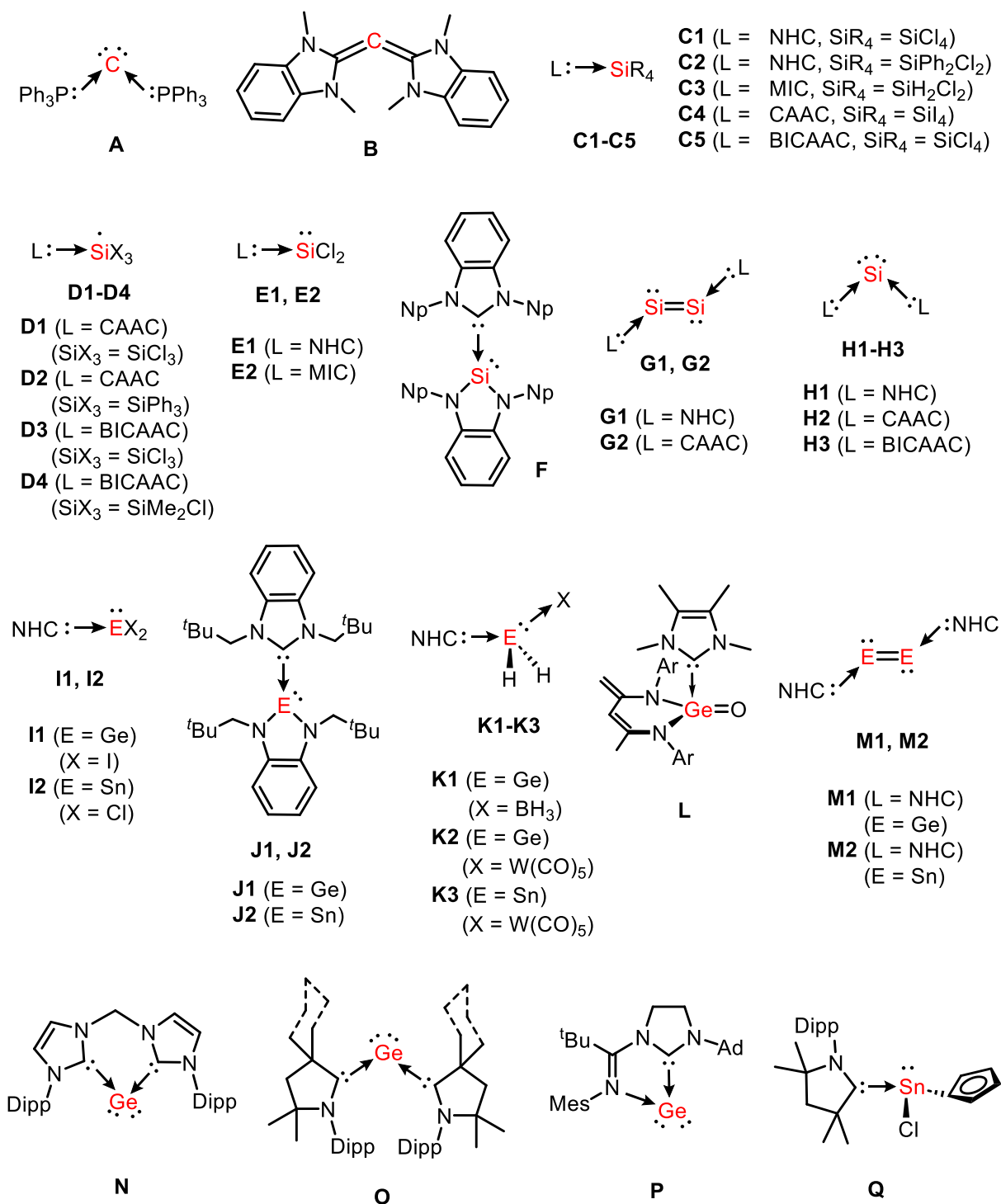
Figure 3.1 Example of a phosphine stabilized carbone and selected examples of carbene stabilized group 14 complexes.

available when compared to the Si precursors, therefore the syntheses of carbene stabilized Ge(II) complexes is quite relaxed.[9] Germylenes exhibit isovalency with singlet carbenes, meaning their frontier orbitals involve an electron lone pair and an empty *p*-orbital at the

germanium center, consequently, they display ambiphilic reactivity.[2] The first germylene was isolated by Arduengo and co-workers in 1993 by reacting NHC with GeI$_2$ (**I1,** Figure 3.1).[10] In 2000, Lappert and co-workers successfully synthesized germylene complex (**J1,** Figure 3.1), which was stabilized by an NHC ligand.[11] Subsequently, in the following years, a range of germylene complexes stabilized by various ligand scaffolds were documented.[2] Due to the presence of a lone pair of electrons, germylenes can function as Lewis bases, forming various germylene-Lewis acid adducts, such as with BH$_3$ or W(CO)$_5$ (**K1** and **K2,** Figure 3.1).[12] The first Ge(IV) chalcogen complex, a germanone (heavier ketone analogue) was reported by Driess and co-workers in 2009, by the oxidation of the precursor NHC-germylenes with N$_2$O at room temperature (**L,** Figure 3.1).[13] Furthermore, the dimeric Ge(0) complex (**M1,** Figure 3.1) stabilized by NHC ligands was isolated by Jones and co-workers in 2009.[14] Additionally, the carbene-stabilized Ge(0) complexes, called as germylones, (the heavier analogues of carbones and silylones) were successfully synthesized. Only three reports have been published so far that deal with the isolation of germylones. The first cyclic germylone (**N,** Figure 3.1) was isolated and characterized by Driess and co-workers, while the first acyclic germylone was synthesized by Roeskey and co-workers in 2013, in which the Ge center is stabilized by two CAAC units (**O,** Figure 3.1).[15] In 2014, Kinjo and co-workers isolated the third germylone species (**P,** Figure 3.1) which is also cyclic in nature.[16]

For the heavier elements of group-14 (Sn and Pb), the reduced tendency to form *sp*-hybrid orbitals limits their ability to create stable complexes. Thus, carbene adducts of Sn/Pb are often less stable and, therefore, more challenging to prepare and isolate compared to their lighter counterparts. Consequently, there have been fewer advancements in the realm of carbene-stabilized Sn/Pb complexes.[2] Nevertheless, a number of carbene supported Sn-complexes have been isolated and characterized which mainly includes the NHC stabilized Sn(II) complexes (**I2** and **Q,** Figure 3.1), the stannylene complex (**J2,** Figure 3.1) and the

stannylene Lewis acid adduct with W(CO)$_5$ (**K3,** Figure 3.1).[2,9,11,12b,17] Moreover, Jones and co-workers successfully isolated the diatomic Sn(0) NHC adduct (**M2,** Figure 3.1) and the corresponding Pb analogue is still not reported so far.[18] Inspired by these intriguing findings, we were eager to delve into the exploration of the recently synthesized bicyclic (alkyl)(amino) carbenes (*Me/iPr*BICAAC)[19] within the domain of group-14 chemistry, specifically focusing on germanium (Ge) and antimony (Sb). A thorough and comprehensive investigation of this exploration is provided in the forthcoming section.

3.2 Results and discussion

3.2.1 Synthesis and characterization of complexes L−GeCl$_2$ (L = *Me*BICAAC (1); L = *iPr*BICAAC (2):

The equimolar reaction of BICAAC (Me or *i*Pr) and GeCl$_2$·dioxane in toluene afforded yellow complexes **1** and **2** in 88 and 90 % yields, respectively (Scheme 3.1). The ^{1}H NMR spectrum of **1** showed two septets at δ = 2.74 and 2.55 ppm, corresponds to the Dipp group of
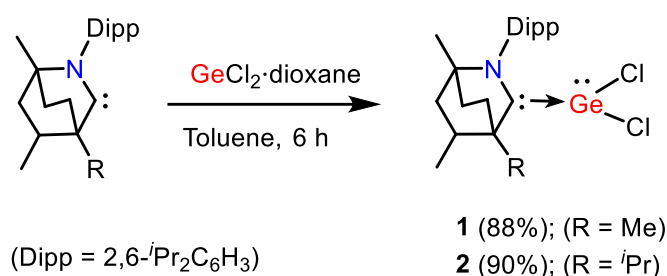
Scheme 3.1 Synthesis of *iPr*BICAAC−GeCl$_2$ (**1**).

the *Me*BICAAC backbone, while ^{13}C{^{1}H} NMR spectrum showed the signal at δ = 248 ppm for the carbenic carbon. Similarly, the ^{1}H NMR of **2** showed three septets centered at δ = 4.21, 2.81 and 2.46 ppm which corresponds to the three isopropyl groups of the *iPr*BICAAC backbone. In ^{13}C{^{1}H} NMR spectrum of **2** the signal for carbene carbon was found to resonate at δ = 257 ppm (δ = 336 ppm for free *iPr*BICAAC).[19] The HRMS spectrum of **1**

provides additional support for its formation, exhibiting a molecular ion peak at *m/z* = 420.1586 (calcd. 420.1513) corresponding to [M-Cl]$^+$.

Moreover, the spectroscopically derived composition of complexes **1** and **2** were corroborated by single-crystal X-ray diffraction analysis (Figure 3.2). In both the complexes the germanium center in tricoordinated and resides in the distorted trigonal pyramidal geometry. Both the complexes **1** and **2** crystallized in monoclinic crystal system and possesses Cc and *P2₁/c* space groups, respectively. The N1-C1 and C1-Ge1 bond distances were determined to be 1.309(3) and 2.148(2) Å, respectively, in **1**, and 1.313(5) and 2.189(4) Å, respectively, in **2**, which is in line with the previously reported literature data.[9]
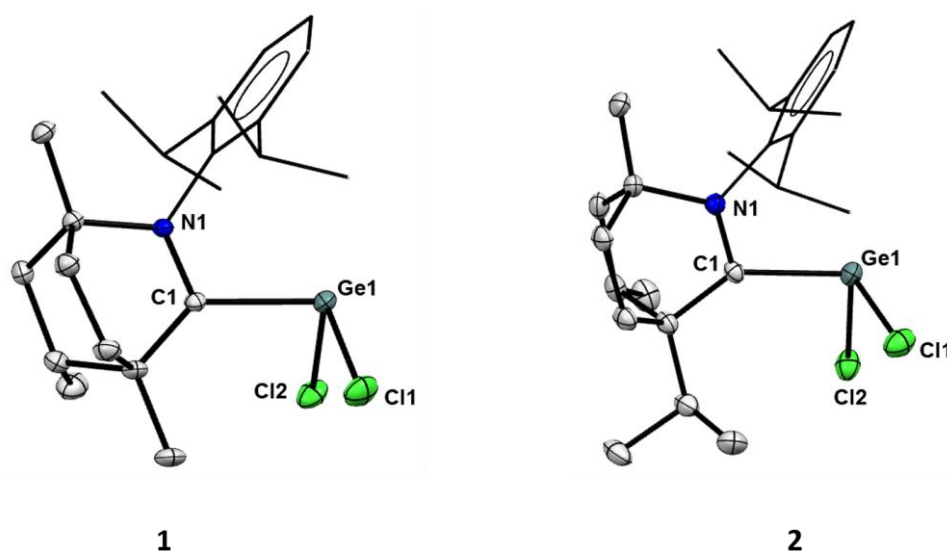
Figure 3.2 Single crystal X-ray structures of complexes **1** and **2**. Thermal ellipsoids are shown at 50% probability level. All the hydrogen atoms were omitted for clarity. Selected bond lengths (Å) and angles (°) for **1**: N1−C1 1.309(3), C1−Ge1 2.148(2), Ge1−Cl1 2.2979(9), Ge1−Cl2 2.2928(8); N1−C1−Ge1 113.93(17), C1−Ge1−Cl1 94.87(8), Cl1−Ge1−Cl2 99.25(3); for **2**: N1−C1 1.313(5), C1−Ge1 2.189(4), Ge1−Cl1 2.2909(12), Ge1−Cl2 2.2854(11); N1−C1−Ge1 109.0(2), C1−Ge1−Cl1 101.19(10), Cl1−Ge1−Cl2 98.02(4).

3.2.2 Synthesis and characterization of a germylone complex (*Me*BICAAC)₂Ge (3)

The *in-situ* two electron reduction of GeCl₂·dioxane in the presence of ^{Me}BICAAC and KC₈ in 1:2:2.2 molar ratio afforded the acyclic germylone complex **3** in 40 % yield as a green solid (Scheme 3.2).
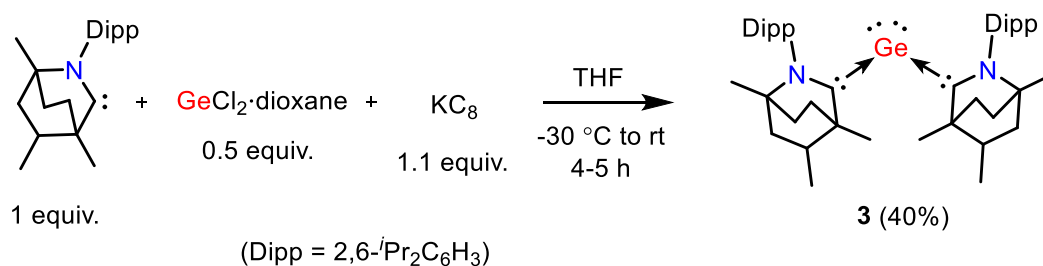
Scheme 3.2 Synthesis of a germylone complex (^{Me}BICAAC)₂Ge (**3**).

The HRMS spectrum of **3** showed the molecular ion peak at *m/z* = 697.4561 (calcd. 697.4526) as [M+H]⁺ also support its formation. Furthermore, the spectrometrically proposed composition was confirmed from single-crystal X-ray technique (Figure 3.3). Complex **3** was

3

Figure 3.3 Single crystal X-ray structure of the germylone **3**. Thermal ellipsoids are shown at 50% probability level. All the hydrogen atoms were omitted for clarity. Selected bond lengths (Å) and angles (°) for **3**: N1−C1 1.373(3), C1−Ge1 1.949(2); N1−C1−Ge1 113.90(17), C1−Ge1−C1' 117.30(15).

crystallized in the monoclinic crystal system having *C2/c* space group. In crystal structure the asymmetric unit of **3** contained half molecule of (*Me*BICAAC)₂Ge having BICAAC and Ge atom, the other *Me*BICAAC unit can be grown from a *C2*-symmetry. The solid-state structure revealed the presence of bent C−Ge−C core in **3**. The Ge−C$_{carbene}$ bond separation in **3** was found to be 1.949(2) Å which is in line with the previously reported germylones (*Me/Cy*CAAC)₂Ge (1.9386(16), 1.9417(15), 1.954(2), 1.9386(18) Å),[15b] and marginally shorter than those found in the reported cyclic germylone (1.965(3) and 1.961(3) Å),[15a,16] and slightly elongated when compared with the C−Si$_{carbene}$ bond distance of 1.840(4) Å in recently synthesized silylone (*Me*BICAAC)₂Si molecule.[7e] Furthermore, the C1−Ge1−C1' bons angle in **3** was found to be 117.30(15)° which is slightly wider than the corresponding CAAC analogues (*Me/Cy*CAAC)₂Ge (114.71(6), 115.27(6) and 117.24(8)°),[15b] and slightly shorter than the C1−Si1−C1' angle reported for (*Me*BICAAC)₂Si molecule (119.0(2)°).[7e]

3.2.3 Syntheses and characterization of complexes *Me*BICAAC−SnCl₂ (4), *Me*BICAAC−SnBr₂ (5), *iPr*BICAAC−SnCl₂ (6), *iPr*BICAAC−SnBr₂ (7)

The equimolar reaction of *Me/iPr*BICAAC with SnX₂ for 6 hours in toluene afforded the corresponding *Me/iPr*BICAAC−SnX₂ adducts (**4-7**) in good yields (Scheme 3.3). The ¹H NMR spectrum of complex **4** in CDCl₃ showed two septets centered at δ = 2.89 and 2.66 ppm for

4 (84%); (R = Me; X = Cl
5 (82%); (R = Me; X = Br
6 (86%); (R = *i*Pr; X = Cl
7 (81%); (R = *i*Pr; X = Br

(Dipp = 2,6-*i*Pr₂C₆H₃)

Scheme 3.3 Syntheses of *Me/iPr*BICAAC−SnX₂ adducts (**4-7**).

the Dipp group of BICAAC backbone and the $^{13}C\{^1H\}$ NMR spectrum of **4** showed the peak

for carbene carbon at δ = 262 ppm. The HRMS spectrum of **4** showed the molecular ion peak

at *m/z* = 500.0950 (calcd. 500.0925) as [M-H]⁺. Similarly, ^1H NMR spectrum of **5** showed the

positions of the septets for Dipp group at δ = 2.87 and 2.67 ppm, while, $^{13}C\{^1H\}$ NMR

spectrum exhibited peak for carbene carbon resonating at δ = 258 ppm. Moreover, the HRMS

spectrum of **5** showed the molecular ion peak at *m/z* = 510.0801 (calcd. 510.0811) as [M-

Br]⁺. Likewise, complexes **6** and **7** have also been characterized by spectroscopic techniques.

Both **4** and **5** crystallized in the monoclinic crystal system having *P2₁/n* and *P2₁/c*

space groups, respectively. In both the complexes the Sn atom adopts distorted trigonal

pyramidal geometry (Figure 3.4). The N1−C1 and C1−Sn1 bond distances in **4** were found

to be 1.310(6) and 2.346(5) Å respectively, and the same for **5** were found to be 1.312(4) and

2.331(3) Å, respectively. The C1−Sn1 bond length of 2.331(3) Å in complex **5** was found to

Figure 3.3 Single crystal X-ray structures of **4** and **5**. Thermal ellipsoids are shown at 50%
probability level. All hydrogen atoms were omitted for clarity. Selected bond lengths (Å) and
angles (°) for **4**: N1−C1 1.310(6), C1−Sn1 2.346(5), Sn1−Cl1 2.4707(14), Sn1−Cl2
2.4544(15); N1−C1−Sn1 113.8(3), C1−Sn1−Cl1 91.53(13), Cl1−Sn1−Cl2 98.13(6); for **5**:
N1−C1 1.312(4), C1−Sn1 2.331(3), Sn1−Br1 2.6372(5), Sn1−Br2 2.6191(4); N1−C1−Sn1
114.2(2), C1−Sn1−Br1 94.81(8), Br1−Sn1−Br2 99.979(14).

be marginally shorter than the corresponding CAAC analogue [^{Me}CAAC−SnBr$_2$] (2.352 Å).[17b] The N1−C1−Sn1 bond angles in **4** and **5** were found to be 113.8(3) and 114.2(2)°, respectively.

3.2.4 Syntheses and characterization of complexes ^{Me}BICAAC−SnCl$_2$−Fe(CO)$_4$ (8) and ^{Me}BICAAC−SnBr$_2$−Fe(CO)$_4$ (9)

Following the successful isolation of compounds **4** and **5**, we proceeded to examine their reactivity towards the Fe carbonyl, Fe$_2$(CO)$_9$, delving into their coordination chemistry. Treatment of complexes **4** or **5** with one equivalent of Fe$_2$(CO)$_9$ in C$_6$H$_6$ under gentle heating conditions resulted in the formation of donor-acceptor complexes **8** and **9** respectively, with good yields (Scheme 3.4).
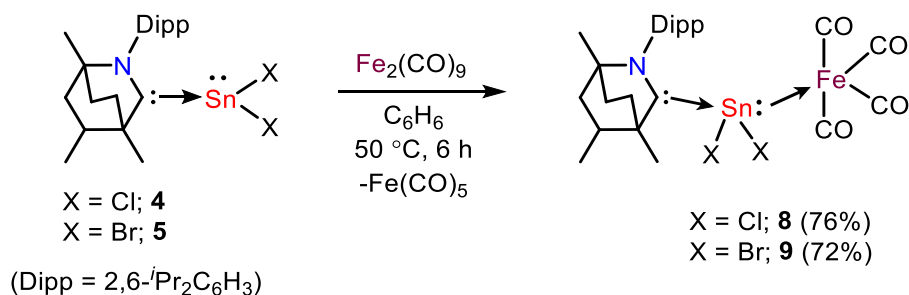
Scheme 3.4 Syntheses of ^{Me}BICAAC−SnX$_2$−Fe(CO)$_4$ adducts (**8** and **9**).

In the IR spectrum of **8** and **9,** three CO stretching bands were identified at ν = 1977, 1942 and 1914 cm^{-1} (for **8**), and ν = 1975, 1937, 1915 cm^{-1} (for **9**) as expected for M(CO)$_4$L (L = ligand other than CO) type systems.[20] Both **8** and **9** crystallized in the triclinic crystal system and possess $P\bar{1}$ space group. In **8** the C1−Sn1, Sn1−Cl1 and Sn1−Cl2 bond distances were calculated as 2.2667(15), 2.3955(4), and 2.3747(4) Å respectively (Figure 3.5), which are found to be shorter if compared to the similar bond distances in precursor **4** (2.346(5), 2.4707(14) and 2.4544(15) Å, respectively). The C1−Sn1 bond distance of 2.2667(15) Å in **8** is found to be similar to those found for the Sn−C^{NHC} bond distance in IPr−SnCl$_2$−Cr(CO)$_5$
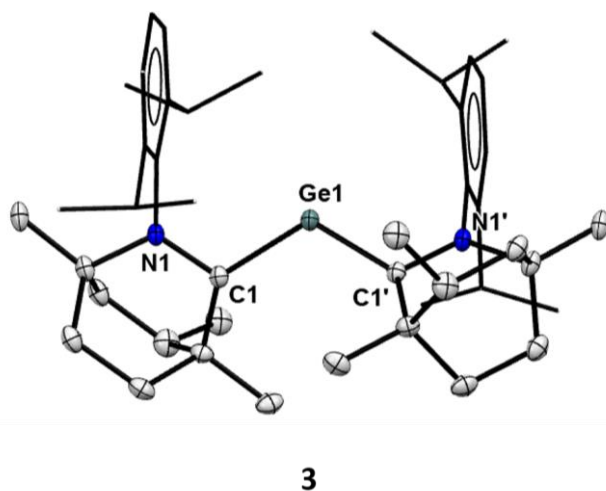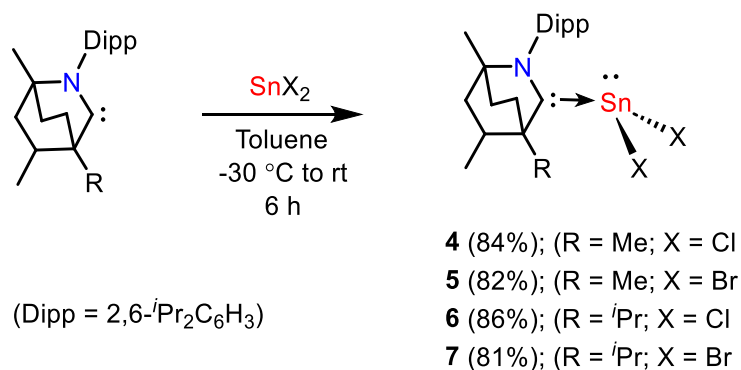
8   **9**
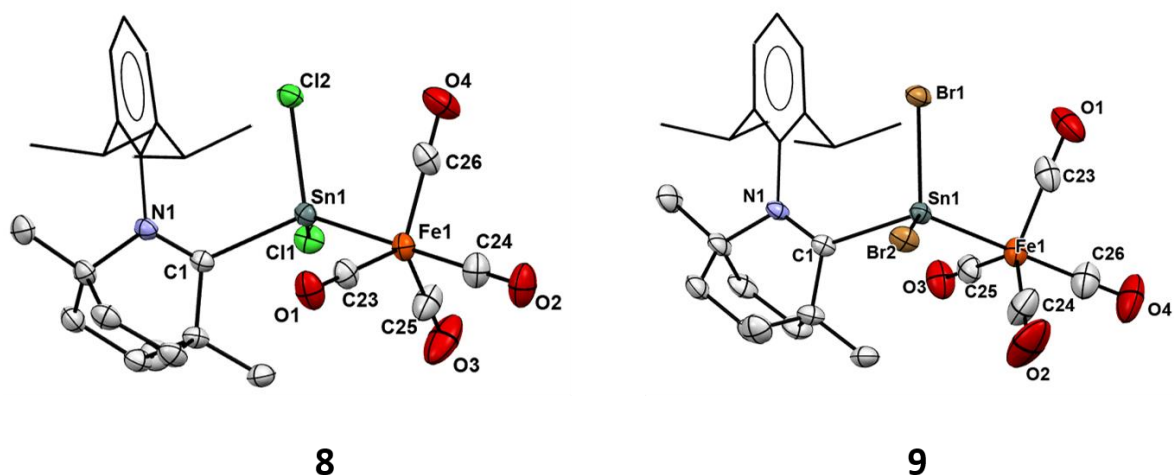
Figure 3.5 Single crystal X-ray structure of **8** and **9**. Thermal ellipsoids are shown at 50% probability level. All hydrogen atoms were omitted for clarity. Selected bond lengths (Å) and angles (°) for **8**: N1-C1 1.305(2), C1-Sn1 2.2667(15), Sn1-Cl1 2.3955(4), Sn1-Cl2 2.3747(4), Sn1-Fe1 2.4780(3); N1-C1-Sn1 126.86(11), C1-Sn1-Cl1 94.95(4), C1-Sn1-Fe1 121.10(4); for **9**: N1-C1 1.297(3), C1-Sn1 2.275(2), Sn1-Br1 2.5219(3), Sn1-Br2 2.5460(3), Sn1-Fe1 2.4796(4); N1-C1-Sn1 126.86(17), C1-Sn1-Br1 108.88(6), C1-Sn1-Fe1 121.12(6).

complex (2.256(4) and 2.270(4) Å) (Figure 3.5).[17c] Moreover, the Sn1−Fe1 bond distance in **8** was found to be 2.4780(3) Å which is significantly shorter than what is observed for [Cp$_2$Sn(Fe(CO)$_4$)]$_2$ (2.651 Å).[21] Similarly, in **9**, the C1−Sn1, Sn1−Br1 and Sn1−Br2 bond lengths were found to be 2.275(2), 2.5219(3) and 2.5460(3) Å respectively, which are also found to be shorter if compared to the similar bond distances in precursor **5** (2.331(3), 2.6372(5) and 2.6191(4) Å, respectively). Moreover, the C1−Sn1 bond separation of 2.275(2) Å in **9** was found to be slightly longer when compared to the [^{Me}CAAC−SnBr$_2$−Fe(CO)$_4$] complex (2.252 Å), while the Sn1−Fe1 separation in **9** was found to be 2.4796(4) Å, which is shorter than what is found in [^{Me}CAAC−SnBr$_2$−Fe(CO)$_4$] (2.483 Å).[17b]

3.2.5 Reactivity of 3 and 4 towards LiBH₄

In an effort to convert the BICAAC-SnX$_2$ complexes **4** and **5** into the corresponding Sn-dihydride complexes, we subjected **4/5** to react with two equivalents of LiBH$_4$ at -30 °C (Scheme 3.5). Unexpectedly, instead of obtaining the anticipated Sn-hydride, an uncontrolled
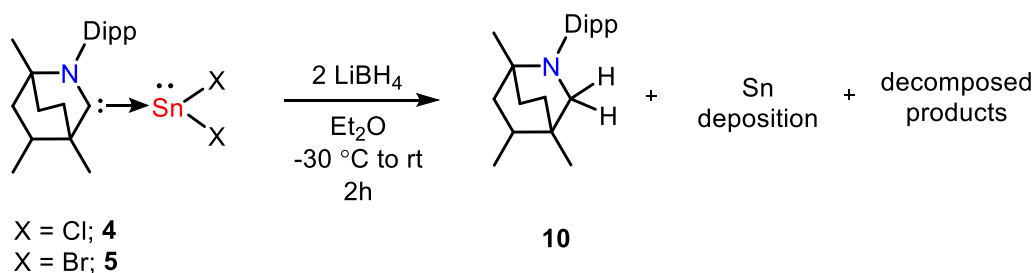
Scheme 3.5 Reactivity of **4** and **5** towards LiBH$_4$.

hydrogenation occurred, resulting in the addition of two hydrogens to the carbenic carbon of the BICAAC moiety.[17c] This led to the predominant formation of product **10**, along with some deposition of Sn-metal at the bottom of the flask. Unfortunately, the identification of other decomposed products remained elusive. Complex **10** was characterized by ¹H and ¹³C{¹H} NMR spectroscopic techniques. In the ¹H NMR spectrum of **10**, it was observed that the two protons attached to the carbene carbon resonates at different positions shown as two
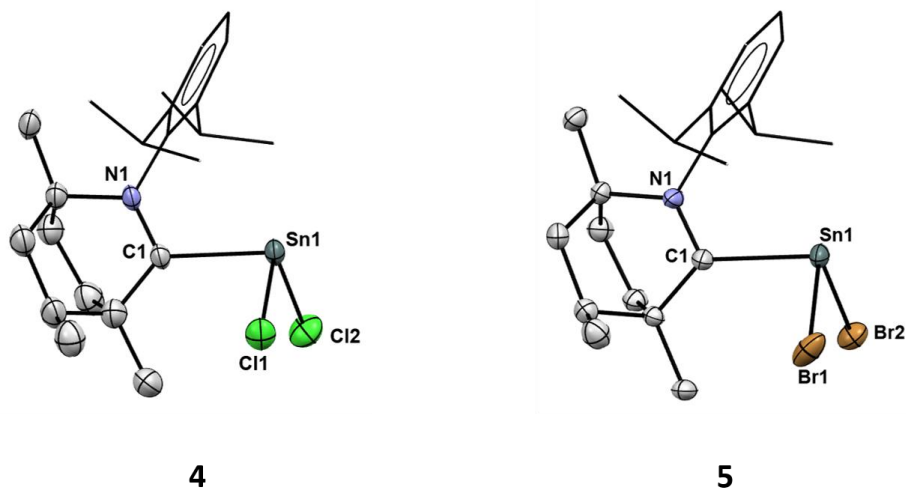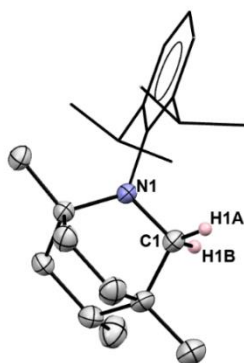

Figure 3.6 Single crystal X-ray structure of **10**. Thermal ellipsoids are shown at 50% probability level. All the hydrogen atoms were omitted for clarity except those attached with C1. Selected bond lengths (Å) and angles (°) for **10**: N1−C1 1.460(3), C1−H1A 0.990, C1−H1B 0.990; N1−C1−H1A 109.9.

doublets, indicative of their diastereomeric nature and the two septets for the Dipp groups was found to resonate at 3.61 and 3.47 ppm. Furthermore, the structure of **10** was confirmed from the single crystal X-ray technique (Figure 3.6). Complex **10** was crystallized in triclinic crystal system and possess $P\bar{1}$ space group.

3.3 Conclusion

In summary, we have successfully delved into the synthesis and characterization of Ge and Sn complexes supported by $^{Me/iPr}$BICAAC ligands. The ambiphilic behavior of BICAAC has been very crucial in forming the adducts with low-valent ions of Ge and Sn. Notable examples in this regard include ^{Me}BICAAC−GeCl$_2$ (**1**), ^{iPr}BICAAC−GeCl$_2$ (**2**) ^{Me}BICAAC−SnX$_2$ (X = Cl (**4**); X = Br (**5**)), and ^{iPr}BICAAC−SnX$_2$ (X = Cl (**6**); X = Br (**7**)). The *in-situ* reaction of ^{Me}BICAAC, GeCl$_2$·dioxane, and KC$_8$ yielded the germylone (^{Me}BICAAC)$_2$Ge (**3**). Additionally, the reaction of complexes **4** and **5** with Fe$_2$(CO)$_9$ resulted in the synthesis of ^{Me}BICAAC−SnX$_2$−Fe(CO)$_4$ adducts (X = Cl (**8**); X = Br (**9**)). However, attempts to convert Sn-halide adducts **4** and **5** into the corresponding hydrides, ^{Me}BICAAC−SnH$_2$, using slight excess of LiBH$_4$ led to over-hydrogenation, producing predominantly hydrogenated ^{Me}BICAAC (**10**) as the major identified products and deposition of metallic Sn.

3.4 Experimental section

3.4.1 General methods

All the manipulations were performed under an inert atmosphere of dry nitrogen or argon using a glove box or standard Schlenk techniques. All the glassware were dried at 150 °C in an oven for at least 12 h and assembled hot and cooled in vacuo prior to use. Solvents were

purified by MBRAUN solvent purification system MB SPS-800 and were used directly from the SPS system. Chemicals were purchased from Sigma-Aldrich, HIMEDIA, and Avra and were used without further purification. Bicyclic (alkyl)(amino) carbenes ($^{Me/iPr}$BICAACs) was synthesized using reported procedure.[19]

3.4.2 Physical measurements

The ^{1}H, and ^{13}C{^{1}H} NMR spectra were recorded using Bruker 400 MHz spectrometer with tetramethylsilane (TMS) (for ^{1}H and ^{13}C{^{1}H}) as external reference; chemical shift values are reported in ppm. IR spectra of complexes **8** and **9** were recorded (in the range 4000-400 cm^{-1}) with a Perkin-Elmer Lambda 35-spectrophotometer using Nujol mull. High resolution mass spectrometry (HRMS) was performed with Waters SYNAPT G2-S. Melting point of compounds were recorded in sealed capillary using Büchi B-540 melting point apparatus. Single crystal X-ray diffraction data of complexes **1-5**, **8-10** was collected using a Rigaku XtaLAB mini diffractometer equipped with Mercury375M CCD detector. The data was collected with MoKα radiation (λ = 0.71073 Å) using omega scans. During the data collection, the detector distance was 49.9 mm (constant) and the detector was placed at 2θ = 29.85° (fixed). The data were reduced using CrysAlisPro 1.171.38.46, and the space group determination was done using Olex2[22] with the SHELXT[23] structure solution program using Intrinsic Phasing and refined with the SHELXH-1997[24] refinement package using Least Squares minimization. All non-hydrogen atoms were refined anisotropically. Crystallographic data are summarized in Table 3.1, 3.2 and 3.3.

3.4.3 Syntheses and characterization of complexes 1-10

Synthesis and characterization of [^{Me}BICAAC−GeCl₂] (1): In a 100 mL Schlenk flask, ^{Me}BICAAC (0.31 g, 1.00 mmol) was dissolved in 10 mL of precooled toluene (-30 °C), subsequently, GeCl₂·dioxane (0.23 g, 1.00 mmol) was added into this mixture. The reaction

mixture immediately turned yellow and warmed to room temperature and further stirred for 6 hours to give yellow reaction mixture. The mixture was dried under reduced pressure and then washed twice with 20 mL of pentane which afforded complex **1** as a yellow solid. Crystals suitable for X-ray analysis were grown from a concentrated THF solution of **1** at room temperature conditions in 4 days. (Yield: 0.40 g, 88 %). **Mp** = 208-210 °C. **^{1}H NMR** (400 MHz, C_6D_5Br + C_6D_6) δ = 7.18-7.15 (m, 1H, Ar), 1.01-6.98 (m, 2H, Ar, merged with the solvent signal), 2.74 (sept, $^3J_{H-H}$ = 6.8 Hz, 1H, C*H*(CH$_3$)$_2$), 2.55 (sept, $^3J_{H-H}$ = 6.8 Hz, 1H, C*H*(CH$_3$)$_2$), 2.25 (s, 3H), 1.75-1.66 (m, 3H), 1.59-1.39 (m, 5H), 1.34 (d, J = 6.4 Hz, 3H), 1.25 (d, J = 6.4 Hz, 3H), 1.10-1.07 (m, 8H), 0.67 (s, 3H) ppm. **^{13}C{^{1}H} NMR** (100 MHz, C_6D_5Br + C_6D_6) δ = 248.2, 144.0, 143.7, 136.4, 125.2, 125.1, 66.0, 52.0, 43.2, 37.9, 34.4, 32.3, 28.6, 28.1, 25.6, 25.0, 24.8, 23.9, 22.5, 20.7, 20.6 ppm. **HRMS** (AP$^+$): *m/z* calculated for $C_{22}H_{33}NGeCl$: 420.1513; found: 420.1586 [M-Cl]$^+$.

Synthesis and characterization of [^{iPr}BICAAC−GeCl$_2$] (2): A similar synthetic procedure was followed as given for **1**. Reagent used: ^{iPr}BICAAC = 0.34 g (1.00 mmol) and GeCl$_2$·dioxane = 0.23 g, (1.00 mmol). Crystals suitable for X-ray analysis were grown from a concentrated toluene solution of **2** at -20 °C in 48 hours. (Yield: 0.44 g, 90 %). **Mp** = 144-145 °C. **^{1}H NMR** (400 MHz, C_6D_6): δ = 7.10-7.06 (m, 1H, Ar), 6.95-6.90 (m, 2H, Ar), 4.21 (sept, J = 6.8 Hz, 1H, -C*H*(CH$_3$)$_2$), 2.81 (sept, J = 6.8 Hz, 1H, -C*H*(CH$_3$)$_2$), 2.46 (sept, J = 6.8 Hz, 1H, -C*H*(CH$_3$)$_2$), 1.85-1.75 (m, 1H), 1.59 (d, J = 6.8 Hz, 3H), 1.45-1.41 (m, 6H), 1.39-1.33 (m, 2H), 1.19 (d, J = 7.2 Hz, 3H), 1.07 (d, J = 6.8 Hz, 3H), 0.97 (d, J = 6.8 Hz, 3H), 0.83 (d, J = 6.8 Hz, 3H), 0.55 (s, 3H), 0.30 (s, 3H) ppm. **^{13}C{^{1}H} NMR** (100 MHz, C_6D_6): δ = 256.8, 144.4, 144.1, 137.0, 130.7, 125.6, 125.3, 66.1, 58.3, 43.5, 33.8, 31.9, 29.2, 28.4, 27.0, 25.3, 25.2, 25.1, 24.6, 24.4, 22.8, 21.5, 21.3, 17.6 ppm.

Synthesis of germylone complex [(^{Me}BICAAC)$_2$Ge] (3): ^{Me}BICAAC (0.31 g, 1.00 mmol), GeCl$_2$·dioxane (0.11 g, 0.5 mmol) and KC$_8$ (0.15 g, 1.1 mmol) was added in a precooled (-30

°C) THF solution. The reaction mixture was then allowed to warm to room temperature and stirred for an additional six hours. Subsequently, the graphite was filtered off, giving rise to a green filtrate. The filtrate was subjected to vacuum drying for 10 hours, resulting in the isolation of complex **3** as a green solid. X-ray quality crystals were grown from a concentrated hexane solution of **3** at -30 °C in 4-5 days. (**Yield:** 0.14 g, 40 %). **Mp** = 184-185 °C. **HRMS** (AP$^+$): *m/z* calculated for $C_{44}H_{67}N_2Ge$: 697.4526; found: 697.4561 [M+H]$^+$.

Synthesis and characterization of [^{Me}BICAAC−SnCl$_2$] (4): In a 100 mL Schlenk flask, ^{Me}BICAAC (0.31 g, 1.00 mmol) was dissolved in 15 mL of precooled toluene (-30 °C), subsequently anhydrous SnCl$_2$ (0.19 g, 1.00 mmol) was added to this mixture. The reaction mixture was warmed to room temperature, at which point it started to appear green. The reaction mixture was further stirred for 6 hours at room temperature. The volatiles were evaporated under vacuum and washed with *n*-hexane which afforded complex **4** as a yellow-green solid. The crystals suitable for X-ray analysis were grown from concentration toluene/benzene solution at room temperature. (**Yield:** 0.42 g, 84 %). **Mp** = 131-132 °C. **^{1}H NMR** (400 MHz, CDCl$_3$): δ = 7.51-7.47 (m, 1H, Ar), 7.33-7.31 (m, 2H, Ar), 2.89 (sept, *J* = 6.4 Hz, 1H, -C*H*(CH$_3$)$_2$), 2.66 (sept, *J* = 6.4 Hz, 1H, -C*H*(CH$_3$)$_2$), 2.25-2.19 (m, 1H), 2.16 (s, 3H), 2.06-2.0 (m, 1H), 1.86-1.81 (m, 4H), 1.59-1.54 (m, 1H), 1.38-1.37 (d, *J* = 6.4 Hz, 3H), 1.33-1.29 (m, 9H), 1.17-1.15 (d, *J* = 7.2 Hz, 3H), 1.11 (s, 3H) ppm. **^{13}C{^{1}H} NMR** (100 MHz, CDCl$_3$): δ = 262.3, 144.7, 144.4, 138.2, 131.2, 125.9, 125.8, 66.6, 52.9, 43.9, 38.1, 33.4, 32.7, 28.9, 28.3, 25.7, 25.33, 25.30, 24.4, 23.0, 21.2, 21.1 ppm. **HRMS** (AP$^+$): *m/z* calculated for $C_{22}H_{32}NSnCl_2$: 500.0925; found: 500.0950 [M-H]$^+$.

Synthesis and characterization of [^{Me}BICAAC−SnBr$_2$] (5): A similar synthetic procedure was adopted for **5**, as given for **4**. Reagents quantity: ^{Me}BICAAC (0.31 g, 1.00 mmol), SnBr$_2$ (0.28 g, 1.00 mmol). (**Yield:** 0.48 g, 82 %). **Mp** = 218-220 °C (decomposition). **^{1}H NMR** (400 MHz, CDCl$_3$): δ = 7.49 (t, *J* = 8.0 Hz, 1H, Ar), 7.31 (d, *J* = 8.0 Hz, 2H, Ar), 2.87 (sept, *J*

= 6.8 Hz, 1H, -CH(CH$_3$)$_2$), 2.67 (sept, J = 6.8 Hz, 1H, -CH(CH$_3$)$_2$), 2.24-2.22 (m, 3H), 2.09-2.0 (m, 1H), 1.91-1.81 (m, 4H), 1.56-1.53 (m, 2H), 1.40-1.39 (m, 3H), 1.32-1.30 (m, 9H), 1.19-1.17 (m, 3H), 1.10 (s, 3H) ppm. **^{13}C{^{1}H} NMR** (100 MHz, CDCl$_3$): δ = 258.5, 144.7, 144.4, 138.0, 131.3, 126.0, 125.9, 66.6, 53.5, 43.7, 37.9, 33.7, 32.7, 28.8, 28.2, 26.4, 25.8, 25.4, 24.5, 23.0, 22.1, 21.3 ppm. **HRMS** (AP$^+$): m/z calculated for C$_{22}$H$_{33}$NSnBr: 510.0811; found: 510.0801 [M-Br]$^+$.

Synthesis and characterization of [^{iPr}BICAAC−SnCl$_2$] (6): A similar synthetic procedure was adopted for **6**, as given for **4**. Reagents quantity: ^{iPr}BICAAC (0.34 g, 1.00 mmol), SnCl$_2$ (0.19 g, 1.00 mmol). (Yield: 0.46 g, 86 %). **Mp** = 170-171 °C. **^{1}H NMR** (400 MHz, CDCl$_3$): δ = 7.56-7.52 (m, 1H, Ar), 7.35-7.32 (m, 2H, Ar), 2.91-2.85 (m, 1H), 2.81-2.74 (m, 1H), 2.72-2.65 (m, 2H), 2.56-2.48 (m, 1H), 2.37-2.24 (m, 2H), 1.93-1.83 (m, 1H), 1.71-1.63 (m, 2H), 1.36 (d, J_{H-H} = 6.8 Hz, 3H), 1.30-1.27 (m, 6H), 1.21 (d, J_{H-H} = 6.8 Hz, 6H), 1.17 (d, J_{H-H} = 6.8 Hz, 3H), 1.07-1.03 (m, 6H) ppm. **^{13}C{^{1}H} NMR** (100 MHz, CDCl$_3$): δ = 143.7, 143.4, 135.6, 132.2, 125.8, 125.7, 70.2, 52.1, 44.0, 36.2, 32.9, 30.1, 29.3, 27.3, 25.9, 25.3, 23.8, 22.9, 22.7, 21.9, 20.3, 19.8, 15.5 ppm.

Synthesis and characterization of [^{iPr}BICAAC−SnBr$_2$] (7): A similar synthetic procedure was adopted for **7**, as given for **4**. Reagents quantity: ^{iPr}BICAAC (0.34 g, 1.0 mmol), SnBr$_2$ (0.28 g, 1.0 mmol). (Yield: 0.50 g, 81 %). **Mp** = 189-190 °C (decomposition.). **^{1}H NMR** (400 MHz, CDCl$_3$): δ = 7.55-7.50 (m, 1H, Ar), 7.35-7.32 (m, 2H, Ar), 2.92-2.86 (m, 1H), 2.81-2.66 (m, 3H), 2.56-2.49 (m, 1H), 2.37-2.24 (m, 2H), 1.90-1.82 (m, 1H), 1.72-1.63 (m, 2H), 1.37 (d, J_{H-H} = 6.8 Hz, 3H), 1.30-1.27 (m, 6H), 1.22 (t, J_{H-H} = 6.8 Hz, 6H), 1.17 (d, J_{H-H} = 6.8 Hz, 3H), 1.07-1.03 (m, 6H) ppm. **^{13}C{^{1}H} NMR** (100 MHz, CDCl$_3$): δ = 143.7, 143.4, 135.6, 132.1, 125.8, 125.7, 70.1, 52.1, 44.0, 36.2, 33.0, 30.2, 29.3, 27.3, 26.0, 25.4, 23.8, 22.9, 22.8, 21.9, 20.4, 19.9, 15.6 ppm.

Synthesis and characterization of [^{Me}BICAAC−SnCl$_2$−Fe(CO)$_4$] (8): In a 100 mL Schlenk flask complex **4** (0.25 g, 0.5 mmol) was dissolved in 15 mL of C$_6$H$_6$ at room temperature under dark conditions, followed by the addition of Fe$_2$(CO)$_9$ (0.18 g, 0.5 mmol). The resulting mixture was sealed and stirred for about 6 hours at 50 °C to give the red solution having red precipitate. The reaction mixture was dried under vacuum for 10 hours to remove Fe(CO)$_5$. The resulting compound was washed with hexane to give complex **8** as a red solid. X-ray quality crystals of **8** were grown from a concentrated fluorobenzene solution at -10 °C in 5-6 days. (**Yield:** 0.25 g, 76 %). **Mp** = 160-162 °C. **IR** (cm^{-1})**:** 1914, 1942, 1977 (for CO).

Synthesis and characterization of [^{Me}BICAAC−SnBr$_2$−Fe(CO)$_4$] (9): Synthetic procedure adopted for **9** was similar to that of complex **8**. Reagents quantity: complex **5** (0.29 g, 0.5 mmol), Fe$_2$(CO)$_9$ (0.18 g, 0.5 mmol). X-ray quality crystals of **9** were grown from a concentrated benzene solution of **9** at room temperature in 5-6 days. (**Yield:** 0.27 g, 72 %). **Mp** = 156-158 °C (decomposition). **IR** (cm^{-1})**:** 1915, 1937, 1975 (for CO).

Synthesis and characterization of [^{Me}BICAAC−(H)$_2$] (10): In two 100 mL Schleck flasks, separate solutions were prepared by dissolving 0.25 g (0.5 mmol) of complex **4** or 0.29 g (0.5 mmol) of complex **5** in 15 mL of pre-cooled (-30 °C) diethyl ether. Subsequently, two equivalents of LiBH$_4$ (0.02 g, 1.0 mmol) were added to each flask. In both the reactions, addition of LiBH$_4$ induced rapid gas evolution. The reaction mixtures were then allowed to warm to room temperature and stirred for an additional two hours, resulting in a transparent liquid with a black precipitate. The reaction mixtures were filtered, and the obtained product was dried under vacuum. In both instances, the predominant result of the procedure was the identification of complex **10** as the major product. **^{1}H NMR** (400 MHz, CDCl$_3$) δ = 7.21-7.17 (m, 1H, *Ar*), 7.11-7.10 (m, 2H, *Ar*), 3.61 (sept, *J* = 6.8 Hz, 1H, -C*H*(CH$_3$)$_2$), 3.47 (sept, *J* = 6.8 Hz, 1H, -C*H*(CH$_3$)$_2$), 3.30 (dd, *J* = 8.4, 2.0 Hz, 1H), 2.725 (d, *J* = 8.0 Hz, 1H), 2.02-1.92

(m, 2H), 1.80-1.75 (m, 2H), 1.69-1.61 (m, 3H), 1.25-1.20 (m, 12H), 1.08 (d, J = 6.8 Hz, 3H), 0.80 (s, 3H), 0.66 (s, 3H) ppm. **^{13}C{^{1}H} NMR** (100 MHz, CDCl$_3$) δ = 151.9, 151.6, 142.9, 126.3, 124.0, 123.7, 57.5, 51.2, 47.4, 36.8, 36.4, 35.0, 33.2, 28.3, 27.9, 26.0, 25.7, 24.9, 24.7, 24.0, 23.6, 17.6 ppm.

3.5 Crystallographic data

Table 3.1 Crystallographic details of complexes **1-3.**

Compound[a]	1	2	3
Chemical formula	$C_{22}H_{33}Cl_2GeN$	$C_{55}H_{82}Cl_4Ge_2N_2$	$C_{44}H_{66}GeN_2$
Molar mass	454.98	1058.21	695.58
Crystal system	monoclinic	monoclinic	monoclinic
Space group	Cc	$P2_1/c$	$C2/c$
T [K]	150.0(1)	150.01(10)	100.0(2)
a [Å]	16.8685(10)	17.3937(6)	22.6787(13)
b [Å]	8.2153(3)	18.2095(5)	10.3990(5)
c [Å]	17.3632(8)	17.3753(5)	18.2689(10)
α [°]	90.00	90.00	90.00
β [°]	111.964(6)	98.513(3)	111.647(7)
γ [°]	90.00	90.00	90.00
V [Å^3]	2231.54(19)	5442.7(3)	4004.6(4)
Z	4	4	4
ρ(calcd.) [g·cm^{-3}]	1.354	1.291	1.154
μ [mm^{-1}]	1.618	1.337	0.796
F(000)	952.0		1504.0
Radiation Mo Kα (λ)	0.71073	0.71073	0.71073
Reflections collected	13019	39926	22814
Independent reflections	7251	9625	6948
Data/restraints/parameters	7251/2/242	9625/36/585	6948/0/208
$R1$, wR_2 [$I>2\sigma(I)$][a]	0.0434, 0.1023	0.0557, 0.1429	0.0651, 0.1741
R1, wR$_2$ (all data)[a]	0.0523, 0.1098	0.0738, 0.1611	0.1003, 0.2161
GOF	1.031	1.054	1.042

[a] $R1 = \Sigma||Fo| - |Fc||/\Sigma|Fo|$. $wR_2 = [\Sigma w(|Fo^2| - |Fc^2|)^2/\Sigma w|Fo^2|^2]^{1/2}$

Table 3.2 Crystallographic details of complexes **4**, **5** and **8**.

Compound[a]	4	5	8
Chemical formula	$C_{22}H_{33}NSnCl_2$	$C_{25}H_{36}Br_2NSn$	$C_{58}H_{71}Cl_4FFe_2N_2O_8Sn_2$
Molar mass	501.08	629.06	1434.05
Crystal system	monoclinic	monoclinic	triclinic
Space group	$P2_1/n$	$P2_1/c$	$P\overline{1}$
T [K]	150.0(1)	99.99(10)	150.01(10)
a [Å]	9.1681(3)	17.3817(5)	9.4695(2)
b [Å]	13.9810(4)	8.4133(2)	9.7128(2)
c [Å]	17.8027(6)	17.5554(4)	18.8787(3)
α [°]	90.00	90.00	83.409(2)
β [°]	92.665(3)	94.056(2)	77.955(2)
γ [°]	90.00	90.00	64.431(2)
V [Å^3]	2279.47(13)	2560.83(11)	1531.24(5)
Z	4	4	1
ρ(calcd.) [g·cm^{-3}]	1.460	1.632	1.555
μ [mm^{-1}]	1.362	4.130	1.500
F(000)	1024.0	1252.0	726.0
Radiation Mo Kα (λ)	0.71073	0.71073	0.71073
Reflections collected	16618	29422	34497
Independent reflections	4031	8966	10690
Data/restraints/parameters	4031/66/242	8966/156/327	10690/0/370
$R1$, wR_2 [$I>2\sigma(I)$][a]	0.0452, 0.1073	0.0456, 0.0873	0.0303, 0.0674
R1, wR$_2$ (all data)[a]	0.0573, 0.1147	0.0609, 0.0919	0.0345, 0.0707
GOF	**1.020**	1.216	1.129

[a] $R1 = \Sigma||Fo| - |Fc||/\Sigma|Fo|$. $wR_2 = [\Sigma w(|Fo^2| - |Fc^2|)^2/\Sigma w|Fo^2|^2]^{1/2}$

Table 3.3 Crystallographic details of complexes **9** and **10.**

Compound[a]	9	10
Chemical formula	$C_{29}H_{36}Br_2FeNO_4Sn$	$C_{22}H_{35}N$
Molar mass	796.95	313.51
Crystal system	triclinic	triclinic
Space group	$P\bar{1}$	$P\bar{1}$
T [K]	149.99(10)	100.01(10)
a [Å]	9.5169(4)	9.8273(5)
b [Å]	9.7660(3)	12.7150(5)
c [Å]	18.9472(7)	16.7709(9)
α [°]	82.754(3)	79.919(4)
β [°]	77.620(3)	85.608(4)
γ [°]	65.038(3)	70.461(4)
V [Å^3]	1558.11(10)	1944.06(16)
Z	2	4
ρ(calcd.) [g·cm^{-3}]	1.699	1.071
μ [mm^{-1}]	3.864	0.061
F(000)	790.0	696.0
Radiation [Å] Mo Kα (λ)	0.71073	0.71073
Reflections collected	21819	13988
Independent reflections	5519	6786
Data/restraints/parameters	5519/0/350	6786/120/511
$R1$, wR_2 [$I>2\sigma(I)$][a]	0.0228, 0.0567	0.0635, 0.1546
R1, wR$_2$ (all data)[a]	0.0261, 0.0585	0.0939, 0.1809
GOF	1.066	1.027

[a] R1 = Σ||Fo| − |Fc||/Σ|Fo|. wR$_2$ = [Σw(|Fo^2| − |Fc^2|)^2/Σw|Fo^2|^2]$^{1/2}$

3.6 References

1. (a) Wang, Y.; Robinson. G. H. *Inorg. Chem.* **2011**, *50*, 12326-12337; (b) Hopkinson, M. N.; Richter, C.; Schedler, M.; Glorius, F. *Nature* **2014**, *510*, 485-496; (c) Soleilhavoup, M.; Bertrand, G. *Acc. Chem. Res.* **2015**, *48*, 256-266; (d) Melaimi, M.; Jazzar, R.; Soleilhavoup, M.; Bertrand G. *Angew. Chem. Int. Ed.* **2017**, *56*, 10046-10068; (e) Kundu, S.; Sinhababu, S.; Chandrasekhar, V.; Roesky, H. W. *Chem. Sci.* **2019**, *10*, 4727-4741.

2. Nesterov, V.; Reiter, D.; Bag, P.; Frisch, P.; Holzner, R.; Porzelt, A.; Inoue, S. *Chem. Rev.* **2018**, *118*, 9678-9842.

3. Flanigan, D. M.; Romanov-Michailidis, F.; White, N. A.; Rovis, T. *Chem. Rev.* **2015**, *115*, 9307-9387.

4. Ramirez, F.; Desai, B.; Hansen, N. B.; McKelvie, N. *J. Am. Chem. Soc.* **1961**, *83*, 3539-3540.

5. (a) Tonner, R.; Öxler, F.; Neumüller, B.; Petz, W.; Frenking, G. *Angew. Chem. Int. Ed.* **2006**, *45*, 8038-8042; (b) Tonner, R.; Frenking, G. *Angew. Chem. Int. Ed.* **2007**, *46*, 8695-8698.

6. Dyker, C. A.; Lavallo, V.; Donnadieu, B.; Bertrand, G. *Angew. Chem. Int. Ed.* **2008**, *47*, 3206-3209.

7. (a) Eisenhut, C.; Szilvási, T.; Dübek, G.; Breit, N. C.; Inoue, S. *Inorg. Chem.* **2017**, *56*, 10061-10069; (b) Schneider, H.; Schmidt, D.; Radius, U. *Chem. Eur. J.* **2015**, *21*, 2793-2797; (c) Ghadwal, R. S.; Roesky, H. W.; Merkel, S.; Henn, J.; Stalke, D. *Angew. Chem. Int. Ed.* **2009**, *48*, 5683-5686; (d) Boesveld, W. M.; Gehrhus, B.; Hitchcock, P. B.; Lappert, M. F.; Schleyer, P. v. R. *Chem. Commun.* **1999**, 755-756; (e) Thakur, S. K.; De, S.; Adhikari, M.; Manar, K. K.; Koley, D.; Singh S. *ChemRxiv* 10.26434/chemrxiv-2023-36z0g.

8. (a) Wang, Y.; Xie, Y.; Wei, P.; King, R. B.; Schaefer, H. F., III; Schleyer, P. v. R.; Robinson, G. H. *Science* **2008**, *321*, 1069-1071; (b) Mondal, K. C.; Roy, S.; Dittrich, B.; Maity, B.; Dutta, S.; Koley, D.; Vasa, S. K.; Linser, R.; Dechert, S.; Roesky, H. W. *Chem. Sci*. **2015**, *6*, 5230-5234; (c) Mondal, K. C.; Samuel, P. P.; Tretiakov, M.; Singh, A. P.; Roesky, H. W.; Stückl, A. C.; Niepötter, B.; Carl, E.; Wolf, H.; Herbst-Irmer, R.; Stalke, D. *Inorg. Chem*. **2013**, *52*, 4736-4743; (d) Mondal, K. C.; Roesky, H. W.; Schwarzer, M. C.; Frenking, G.; Niepötter, B.; Wolf, H.; Herbst-Irmer, R.; Stalke, D. *Angew. Chem. Int. Ed*. **2013**, *52*, 2963-2967; (e) Li, Y.; Chan, Y.-C.; Li, Y.; Purushothaman, I.; De, S.; Parameswaran, P.; So, C.-W. *Inorg. Chem*. **2016**, *55*, 9091-9098.

9. Prabusankar, G.; Sathyanarayana, A.; Suresh, P.; Naga Babu, C.; Srinivas, K.; Metla, B. P. R. *Coord. Chem. Rev*. **2014**, *269*, 96-133.

10. Arduengo, A. J., III; Dias, H. V. R.; Calabrese, J. C.; Davidson, F. *Inorg. Chem*. **1993**, *32*, 1541-1542.

11. Gehrhus, B.; Hitchcock, P. B.; Lappert, M. F. *Dalton Trans*. **2000**, 3094-3099.

12. (a) Thimer, K. C.; Al-Rafia, S. M. I.; Ferguson, M. J.; McDonald, R.; Rivard, E. *Chem. Commun*. **2009**, 7119-7121; (b) Al-Rafia, S. M. I.; Malcolm, A. C.; Liew, S. K.; Ferguson, M. J.; Rivard, E. *J. Am. Chem. Soc*. **2011**, *133*, 777-779.

13. Yao, S.; Xiong, Y.; Driess, M. *Chem. Commun*. **2009**, 6466-6468.

14. Sidiropoulos, A.; Jones, C.; Stasch, A.; Klein, S.; Frenking, G. *Angew. Chem. Int. Ed*. **2009**, *48*, 9701-9704.

15. (a) Xiong, Y.; Yao, S.; Tan, G.; Inoue, S.; Driess, M. *J. Am. Chem. Soc*. **2013**, *135*, 5004-5007; (b) Li, Y.; Mondal, K. C.; Roesky, H. W.; Zhu, H.; Stollberg, P.; Herbst-Irmer, R.; Stalke, D.; Andrada, D. M. *J. Am. Chem. Soc*. **2013**, *135*, 12422-12428.

16. Su, B.; Ganguly, R.; Li, Y.; Kinjo, R. *Angew. Chem. Int. Ed.* **2014**, *53*, 13106-13109.

17. (a) Kuhn, N.; Kratz, T.; Bläser, D.; Boese, R. *Chem. Ber*. **1995**, *128*, 245-250; (b) Müller, C.; Andrada, D. M.; Bischoff, I.-A.; Zimmer, M.; Huch, V.; Steinbrück, N.; Schäfer, A. *Organometallics* **2019**, *38*, 1052-1061; (c) Al-Rafia, S. M. I.; Shynkaruk, O.; McDonald, S. M.; Liew, S. K.; Ferguson, M. J.; McDonald, R.; Herber, R. H.; Rivard, E. *Inorg. Chem*. **2013**, *52*, 5581-5589.

18. Jones, C.; Sidiropoulos, A.; Holzmann, N.; Frenking, G.; Stasch, A. *Chem. Commun*. **2012**, *48*, 9855-9857.

19. Mendivil, E. T.; Hansmann, M. M.; Weinstein, C. M.; Jazzar, R.; Melaimi, M.; Bertrand, G. *J. Am. Chem. Soc*. **2017**, *139*, 7753-7756.

20. Spessard G. O.; Miessler G. L. *Organometallic chemistry*, 2nd edition, Oxford university press, New York, **2010**.

21. Harrison, P. G.; King, T. J.; Richards, J. A. *Dalton Trans*. **1975**, *20*, 2097-2100.

22. Dolomanov, O. V.; Bourhis, L. J.; Gildea, R. J.; Howard, J. A. K.; Puschmann, H. *J. Appl. Cryst*. **2009**, *42*, 339-341.

23. Sheldrick, G. M. *Acta Cryst., Sect. A* **2015**, *71*, 3-8.

24. Sheldrick, G. M. *Acta Cryst., Sect. A* **2008**, *64*, 112-122.

Adducts of ECl₃ with bicyclic (alkyl)(amino) carbene (^Me^BICAAC) and their subsequent three-electron reduction for the preparation of BICAAC stabilized E-E bonded compounds (E = P, Sb)
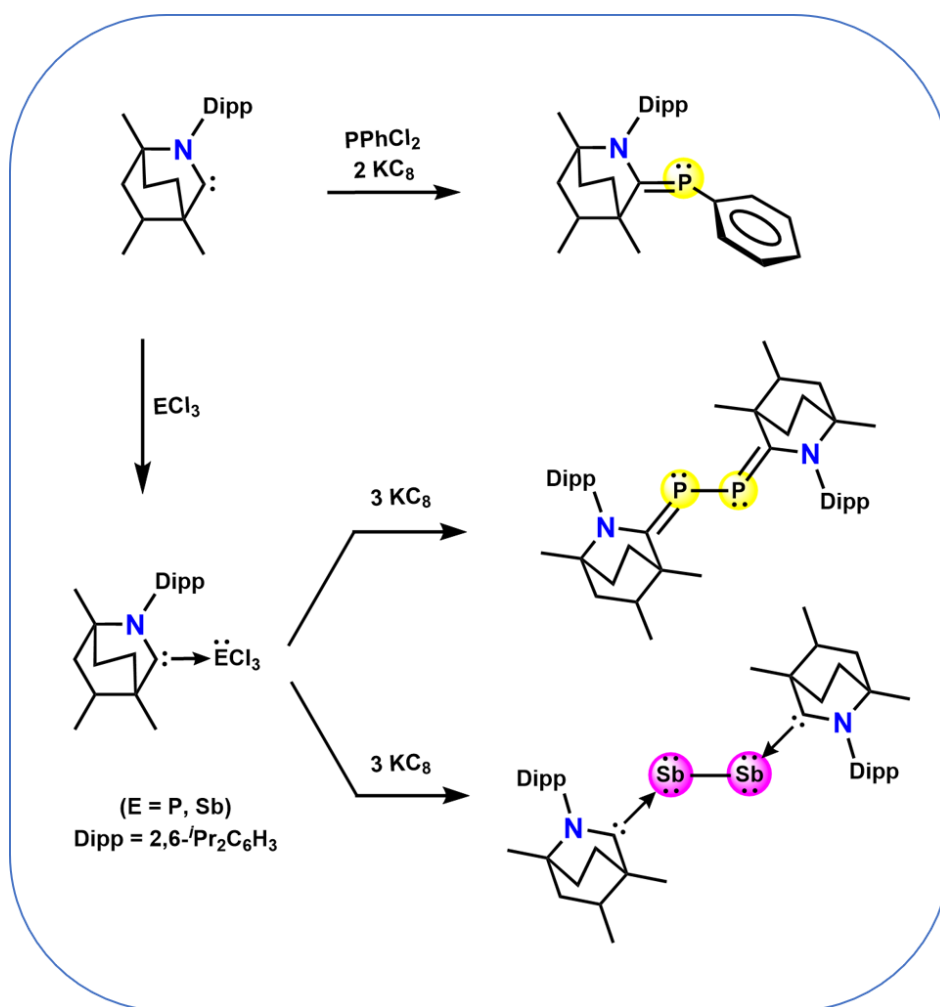
Adhikari, M.; Thakur, S. K.; Singh, S. Adducts of Bicyclic (Alkyl)(Amino)Carbene with ECl₃ and Three Electron Reduction Thereof: Syntheses of BICAAC Stabilized E-E Bonded Compounds (E = P, Sb). *Eur. J. Inorg. Chem.* **2023**, e202300379.

Abstract: The work described in this chapter explores the stoichiometric reactions of bicyclic (alkyl)(amino)carbene (BICAAC) with group 15 chlorides, ECl_3 (E = P, Sb), resulting in the formation of the Lewis adducts $BICAAC-ECl_3$ (E = P (**1**), and Sb (**2**)). BICAAC smoothly reacts with $PPhCl_2$ to produce the adduct, [$BICAAC-PPhCl_2$] followed by an *in-situ* two-electron reduction, using 2 equivalents of KC_8, that leads to the formation of the phosphinidene complex, $BICAAC=P-Ph$ (**3**). Additionally, the complete dechlorination of the $BICAAC-ECl_3$ adducts **1** and **2** with 3 equivalents of KC_8 leads to a three-electron reduction, giving rise to low-valent trans-bent *bis*(BICAAC)E_2 complexes (E = P (**4**) and Sb (**5**)), respectively. These complexes represent the initial instances of BICAAC adducts with pnictogens. All these compounds have been thoroughly characterized using various spectroscopic methods, and their solid-state structures have been elucidated through single-crystal X-ray diffraction. We found that the *bis*(BICAAC)P_2 complex predominantly exists in $BICAAC=P-P=BICAAC$ canonical form, while its Sb derivative favors $BICAAC:\rightarrow Sb-Sb\leftarrow :BICAAC$ canonical form.

4.1 Introduction

Ever since Arduengo and co-workers introduced the first stable N-heterocyclic carbene (NHC) in 1991,[1] there has been a significant surge of interest in carbenes. Subsequent developments have clearly illustrated the importance of carbenes in diverse domains, including their coordination with transition metals,[2] stabilization of main-group complexes,[3] contributions to homogeneous catalysis,[4] and roles in organocatalysis.[5] The tunability of electronic and steric properties within carbenes has opened-up avenues for the development of new categories of singlet carbenes.[6] At the forefront of these advancements were cyclic (alkyl)(amino) carbenes (CAACs), introduced by Bertrand and co-workers, which exhibits notably increased ambiphilicity when compared to NHCs.[7] Consequently, NHCs and their subsequent variations rapidly emerged as highly promising replacements for phosphine ligands. The use of NHCs and CAACs in the field of p-block chemistry enabled exploration into the realm of low-coordinate, low-valent main-group complexes, encompassing elements such as B,[8a-c] P,[8d-e] Si,[8f] Ge,[8g] Sn,[8h] Al,[8i] As[8j] and more.[8k] Moreover, CAACs have been widely used in the stabilization of transition metal complexes in their neutral (zero-valent) state and in several non-traditional oxidation states.[9, 10]

Over the past few years, there has been a noteworthy surge in research interest concerning the utilization of carbenes to stabilize low-valent derivatives of group 15 elements, predominantly focusing on phosphinidenes. Significant interest has been drawn to these compounds because of their potential as promising ligands, combining the characteristics of both carbenes and phosphines. In the year 2008, Robinson and co-workers accomplished the syntheses of NHC-stabilized *bis*(NHC)-P_2 molecules (**A**-**B**, Figure 4.1) by reducing the corresponding NHC$-$PCl$_3$ adducts (NHC = :C{N(2,6-Pr$^i_2$C$_6$H$_3$)CH}2 or :C{N(2,4,6-Me$_3$C$_6$H$_2$)CH}$_2$).[8d] Subsequently, in 2009, Bertrand and co-workers successfully
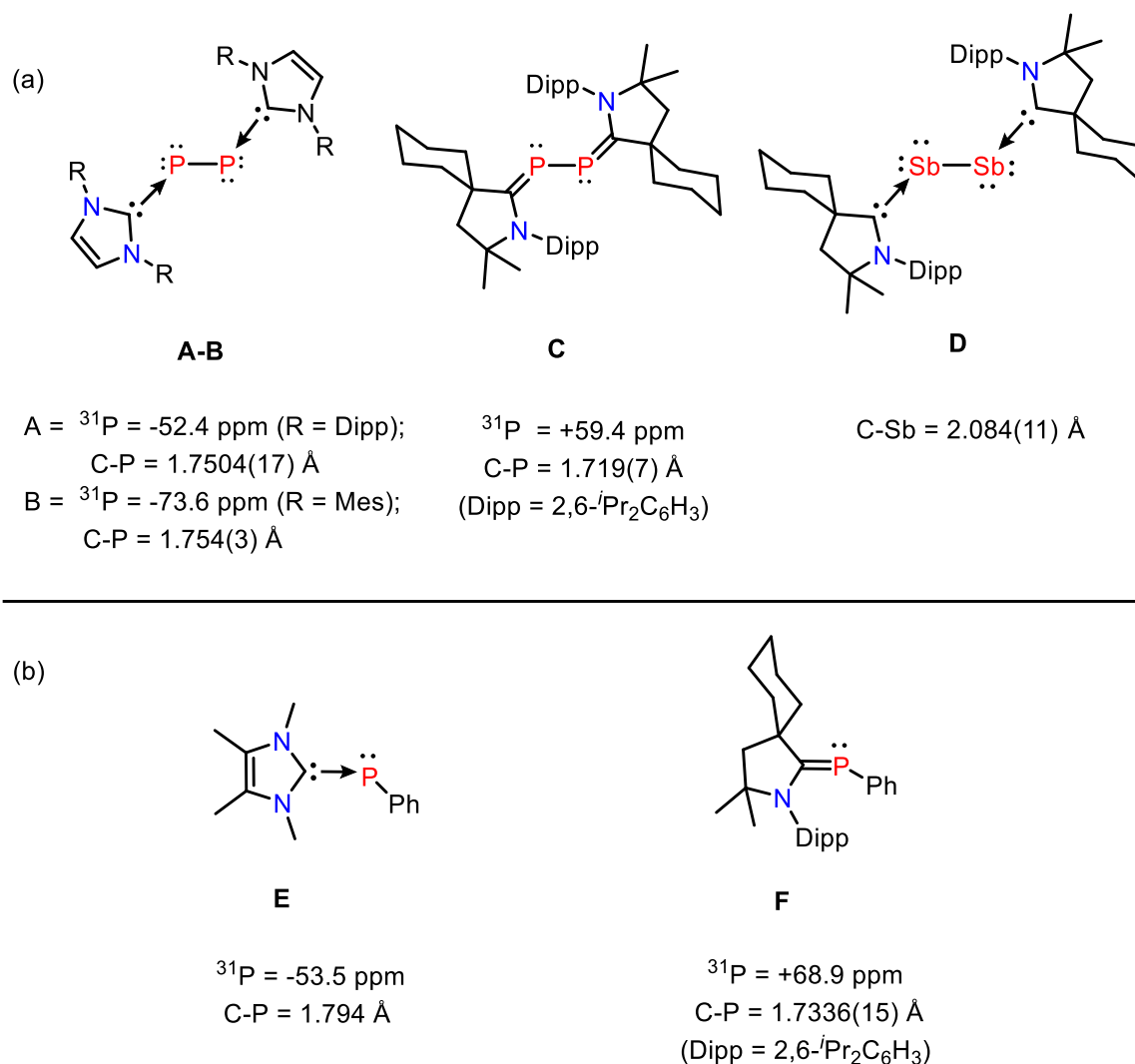
Figure 4.1 (a) Previous reports on *bis*-(carbene)P$_2$ compounds (**A** and **B**), *bis*phosphaalkene (**C**), and *bis*-(carbene)Sb$_2$ (**D**) with their key spectroscopic data; (b) comparison of the two canonical forms: carbene-phosphinidene adduct (**E**) and phosphaalkene (**F**).

isolated CAAC supported P$_2$ analogue, referred to as *bis*(CAAC)-P$_2$ (**C**, Figure 4.1).[11] Both experimental and computational studies have shown that *bis*(NHC)-P$_2$ molecules are best represented as *bis*-phosphinidene entities coordinated by two carbenes,[8d,12] while in the case of *bis*(CAAC)-P$_2$, the dominant bonding arrangement tilts toward the 2,3-diphospha-1,3-butadiene (*bis*-phosphaalkene) canonical form of *bis*-phosphinidene. This preference is a result of the increased electrophilic nature of CAAC carbenes in comparison to NHCs.[11] Notably, *bis*(CAAC)-P$_2$ was observed as a minor product when white phosphorus (P$_4$) was activated with CAAC.[11] Despite expectations of stability for the bulkier *bis*(NHC)-E$_2$

154

analogs (where E = Sb, Bi), endeavors to synthesize them resulted in unsuccessful outcomes.[13] The achievement of isolating the Sb_2 derivative, particularly *bis*(CAAC)-Sb_2 (**D**, Figure 4.1), was attributed to the better π-acceptor properties of CAACs when compared to NHCs.[14] To the best of our knowledge, compound **D** remains the only documented case of a low-valent Sb_2 core stabilized by carbenes.

The unique bonding arrangements of *bis*-phosphinidene and *bis*-phosphaalkenes, as previously explained for dinuclear compounds, are also evident in mononuclear phosphinidene complexes that are supported by carbenes. The carbene-phosphinidene adducts (**E**, Figure 4.1)[15] exhibits a noticeably extended P−C bond and a high-field chemical shift in the ^{31}P NMR, signifying that the phosphorus atom possesses an electron-rich nature. On the other hand, in phosphaalkenes (**F**, Figure 4.1),[16a] the P=C bond length is comparatively shorter and shows a high-field chemical shift in the ^{31}P NMR. The NMR spectroscopic data presented by Bertrand and co-workers,[16a] as well as summarized by Nelson and Nolan[16b] and Krachko and Slootweg[16c], unequivocally shows that a weaker π-acceptor carbene typically promotes the formation of carbene-phosphinidene adducts. In contrast, a strong π-acceptor carbene encourages the back donation of electrons from phosphorus to the carbene carbon, thus substantially contributing to the phosphaalkene form.[16a–f] Hudnall and co-workers reported similar results for phosphaalkenes stabilized by carbonyl-decorated carbenes (CDCs).[17] In 2017, Roesky and co-workers documented a series of CAAC-supported chlorophosphinidenes [(CAAC)P−Cl] which exist as two conformational isomers: phosphaalkenes (minor isomer) and phosphinidenes (major isomer) both in solution and solid state.[18]

In 2017, Bertrand and co-workers introduced a new class of carbenes known as bicyclic (alkyl)(amino) carbenes, abbreviated as BICAACs.[19a] Computational analysis revealed that the singlet-triplet energy gap for BICAAC (45.7 kcal/mol) is smaller compared

to CAAC (49.2 kcal/mol) and NHC (68 kcal/mol), indicating that BICAAC exhibits even more pronounced ambiphilic characteristics than NHC while slightly exceeding the capabilities of CAACs.[19b,c] In light of the qualities exhibited by BICAAC, we and a few other research groups recently ventured into a range of applications involving BICAAC.[20] As far as our understanding goes, there is no documented evidence of a stable CAAC−PCl_3 adduct, and only one report has provided information on the stabilization of the *bis*(carbene)-Sb_2 molecule supported by CAAC.[14] In this context, we offer the syntheses of BICAAC adducts with PCl_3 and $SbCl_3$, as well as BICAAC supported *bis*-phosphinidene and its corresponding Sb_2 analogue.

4.2 Results and discussion

4.2.1 Syntheses and characterization of complexes BICAAC−ECl_3 [E = P (1), Sb (2)]

BICAAC, known for its ambiphilic nature, readily reacted with PCl_3 in hexane and $SbCl_3$ in diethyl ether and afforded the hypervalent adducts, BICAAC−PCl_3 (1) and BICAAC−$SbCl_3$ (2) in substantial yields (Scheme 4.1). In the ^1H NMR analysis of complex 1 in C_6D_6, two distinct septets centered at δ = 3.27 and 3.34 ppm (compared to δ = 2.95 and 3.27 ppm for free BICAAC) were observed which belong to the Dipp group of the BICAAC ligand.[19a] The $^{31}P\{^1H\}$ NMR spectrum of compound 1 displayed a single peak at δ = 33.0 ppm, which

(Dipp = 2,6-$^iPr_2C_6H_3$)

1 (85%); E = P; [S] = hexane
2 (76%); E = Sb; [S] = Et_2O
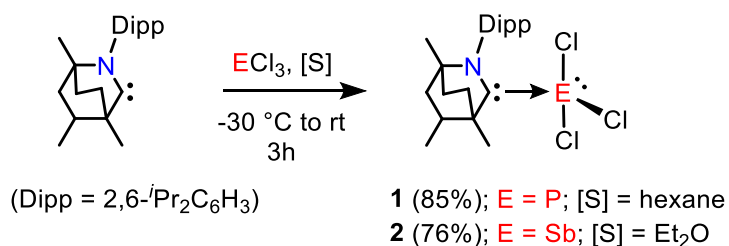
Scheme 4.1 Syntheses of BICAAC−ECl_3 adducts 1 and 2.

conclusively indicating the formation of adduct **1** (in comparison to ^{31}P signal for PCl$_3$ at δ = 219 ppm).[21] The ^{31}P NMR signal for complex **1** exhibits a relatively deshielded position compared to the previously reported PCl$_3$ adducts with NHC and 6-Dip carbene analogues (^{31}P δ = 16.9 ppm for NHC−PCl$_3$; 3.8 ppm for 6-Mes−PCl$_3$ and 10.9 ppm for 6-Dip−PCl$_3$ adduct),[8e,22] this could be attributed to better π-acidic nature of BICAAC. Similarly, the ^{1}H NMR spectrum of complex **2** showed two merged septets ranging from δ = 3.10-3.0 ppm and the ^{13}C{^{1}H} NMR spectrum exhibited the peak for the carbene carbon resonating at δ = 227.3 ppm (δ = 334 ppm for the free BICAAC[19a]). The formation of compounds **1** and **2** was additionally supported by their high-resolution mass spectrometry (HRMS) spectra, which displayed signals at *m/z* = 378.2097 (calcd. 378.2117) as [M-2Cl]$^+$ for **1** and *m/z* = 502.1048 (calcd. 502.1028) as [M-Cl]$^+$ for **2**, respectively.

The spectroscopically derived structures of **1** and **2** were further confirmed by the single crystal X-ray diffraction method. In the solid state, complexes **1** and **2** crystallized in the monoclinic (space group *P*2$_1$/c) and triclinic (space group *P*$\bar{1}$) crystal systems, respectively. Structural analysis in the solid state indicated that both the P and Sb centers in complexes **1** and **2**, respectively, exhibit a four-coordinated environment and adopt a seesaw geometry (Figure 4.2). In both the structures, two Cl atoms are located at the axial positions, while the equatorial sites are shared by BICAAC, one Cl atom, and a lone pair associated with P or Sb atom. The C1−P1 bond distance in **1** was found to be 1.902(4) Å, which is marginally longer than the bond distance of 1.871(11) Å, reported previously for NHC−PCl$_3$ adduct (NHC = :C{N(2,6-^{i}Pr$_2$C$_6$H$_3$)CH}$_2$).[8e] Similarly, the three P−Cl bond distances in complex **1** (P1−Cl1 2.0599(16), P1−Cl2 2.2156(18) and P1−Cl3A 2.4917(18) Å) are also in close agreement with those found for NHC−PCl$_3$ adduct (NHC = :C{N(2,6-^{i}Pr$_2$C$_6$H$_3$)CH}2).[8e] Furthermore, complex **2** possess the C1−Sb1 bond length of 2.2616(18) Å which is comparable with those reported previously for the CAAC−SbCl$_3$ (2.223(3) Å)[14]

Figure 4.2 Solid state structure of adducts **1** and **2**. Ellipsoids are shown at 50 % probability level. All hydrogen atoms have been omitted for clarity. Only one part of the disordered chlorides in **1** are shown for clarity. Selected bond lengths (Å) and bond angles (°) for **1**: N1−C1 1.303(5), C1−P1 1.902(4), P1−Cl1 2.0599(16), P1−Cl2 2.2156(18), P1−Cl3A 2.4917(18), N1−C1−P1 131.7(3), C1−P1−Cl1 105.39(14), C1−P1−Cl2 90.17(13), C1−P1−Cl3A 82.37(13); for **2**: N1−C1 1.304(2), C1−Sb1 2.2616(18), Sb1−Cl1 2.5746(5), Sb1−Cl2 2.5894(5), Sb1−Cl3 2.3588(6); N1−C1−Sb1 132.0(14), C1−Sb1−Cl1 80.50(5), C1−Sb1−Cl2 85.59(5), C1−Sb1−Cl3 100.46(5).

and 6-Dip−SbCl$_3$ (2.288(2) Å) adducts.[22] Moreover, the three Sb−Cl bond distances in **2** were found to be 2.5746(5), 2.5894(5) and 2.3588(6) Å respectively, for Sb1−Cl1, Sb1−Cl2 and Sb1−Cl3 that are also comparable with the previously reported CAAC−SbCl$_3$ and 6-Dip−SbCl$_3$ adducts.[14,22] The N1−C1−Sb1 bond angle in **2** was found to be 132.0(14)° which is significantly wider than the previously reported value for CAAC analogue (118.8(2)°).[14]

4.2.2 Synthesis and characterization of complex [(BICAAC)=P−Ph] (3)

Subsequently, we explored the versatility of the BICAAC ligand for synthesizing a carbene-phosphinidene adduct by employing dichlorophenylphosphine and KC$_8$ as the reducing agent. The subsequent carbene-phosphinidene adduct (BICAAC)=P−Ph was previously synthesized by Bertrand and co-workers employing BICAAC with

pentaphenylcyclopentaphosphane (PhP)$_5$.[19a] The reaction of BICAAC with PPhCl$_2$ and 2 equivalents of KC$_8$ afforded a yellow (BICAAC)=P—Ph adduct (**3**) in 66 % yield (Scheme 4.2). The ^{31}P{^{1}H} NMR spectrum of complex **3** showed a sharp signal at δ = 90 ppm, which is highly deshielded when compared with the previously reported phosphinidenes.[16a] This was primarily attributed to the electrophilic nature of the BICAAC ligand, which strongly favors the phosphaalkene canonical form over the phosphinidene. The HRMS spectrum of **3** exhibited the molecular ion peak at m/z = 420.2793 (calcd. 420.2820) as [M+H]$^+$.

(Dipp = 2,6-^{i}Pr$_2$C$_6$H$_3$)   **3** (66 %)

Scheme 4.2 Synthesis of complex **3**.

Single crystal X-ray diffraction study revealed that **3** crystallized in the monoclinic crystal system with space group *P*2$_1$/n. The N1—C1, C1—P1 and P1—C23 bond distances in **3** were found to be 1.377(3), 1.737(2) and 1.839(2) Å, respectively (Figure 4.3). The C1—P1

3

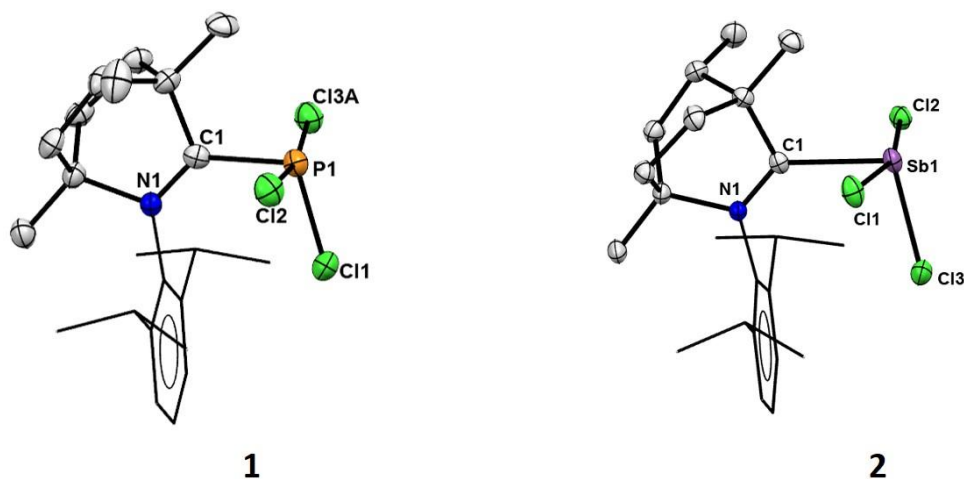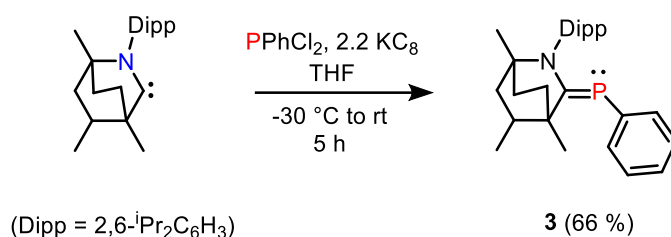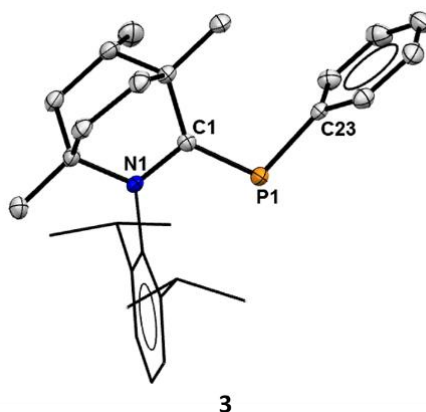**Figure 4.3** Solid state structure of **3**. Ellipsoids are shown at 50 % probability level. All hydrogen atoms have been omitted for clarity. Selected bond lengths (Å) and bond angles (°): N1-C1 1.377(3), C1-P1 1.737(2), P1-C23 1.839(2), N1-C1-P1 116.00(16), C1-P1-C23 108.25(10).

bond length of 1.737(2) Å in **3** is also consistent with the values found in the two previous instances of (CAAC)=P–Ph molecules for which the C–P bond lengths were found to be 1.743(8) and 1.7336(15) Å,[16a] while slightly shorter when compared with certain examples of (NHC):P–Ph in which the C–P bond lengths were found to be 1.794, 1.746, 1.763 Å.[15] The ^{31}P NMR chemical shift value and the shorter C1–P1 bond distance in compound **3** strongly support the presence of a C=P double bond character, thus favoring the phosphaalkene form over the phosphinidene.

4.2.3 Syntheses and characterization of complexes, *bis*(BICAAC)E$_2$ [E = P (4), Sb (5)]

Upon successful synthesis of the BICAAC adducts with PCl$_3$ and SbCl$_3$ and the synthesis of phosphaalkene **3,** the BICAAC-ECl$_3$ (E = P (**1**), Sb (**2**)) adducts were subjected to three electron reduction using KC$_8$ which afforded the BICAAC stabilized diphosphorus, *bis*(BICAAC)P$_2$ and diantimony, *bis*(BICAAC)Sb$_2$ complexes. The reduction of complex **1** with 3.3 equivalents of KC$_8$ resulted in the formation of *bis*(BICAAC)P$_2$ (**4**) in 58 % isolated yield as a yellow compound (Scheme 4.3), likewise, under similar conditions, adduct **2** was
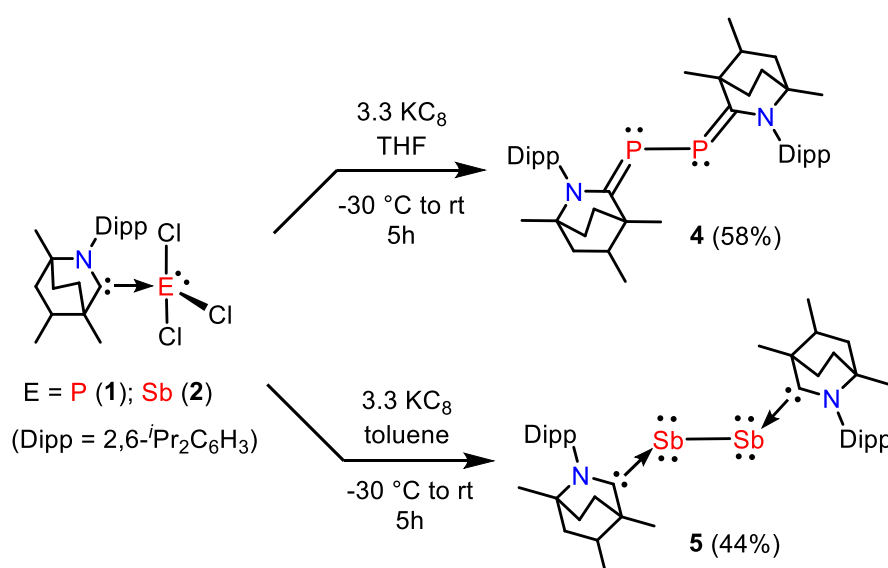
Scheme 4.3 Syntheses of *bis*(BICAAC)E$_2$ molecules (E = P (**4**); E = Sb (**5**)).

afforded the antimony counterpart, *bis*(BICAAC)Sb$_2$ (**5**), as a highly sensitive red-violet compound with an isolated yield of 44%. The formation of **4** was also supported by the HRMS spectrum which showed a peak at *m/z* = 684.4697 (calcd. 684.4701) as [M]$^+$. However, in the case of complex **5**, the HRMS measurements were primarily dominated by the signals of BICAAC alone.

In the ^{31}P{^{1}H} NMR spectrum of compound **4**, two closely spaced singlets of equal intensity were observed at δ = 65.5 and 65.3 ppm. We exclude the possibility of a solution equilibrium between *bis*(phosphinidine) and *bis*(phosphaalkene) forms and instead believe that the latter form is the dominant species. This conclusion is further supported by the presence of a deshielded ^{31}P{^{1}H} signal at ~65 ppm. Additionally, when compared to the similar (NHC-P)$_2$ counterparts, which exhibited ^{31}P{^{1}H} NMR chemical shift values in the upfield range {δ = -52.4 ppm, (NHC = :C{N(2,6-^{i}Pr$_2$C$_6$H$_3$)CH}$_2$); δ = -73.6 ppm, (NHC = :C{N(2,4,6-Me$_3$C$_6$H$_2$)CH}$_2$)},[8d] the deshielded chemical shift observed in complex **4** can be attributed to the increased electrophilicity of the BICAAC carbene. Moreover, to investigate the impact of temperature on the relative proportions of the ^{31}P{^{1}H} NMR signals, we carried out variable temperature (VT) ^{1}H and ^{31}P{^{1}H} NMR measurements in toluene-d$_8$, spanning a temperature range from -40 °C to +50 °C (Figure 4.4). No other changes were evident in VT ^{31}P{^{1}H} NMR spectra, apart from the temperature-dependent variation in the ^{31}P{^{1}H} signal (Figure 4.4). Likewise, the variable temperature (VT) ^{1}H NMR spectra displayed no discernible temperature related effects (Figure 4.5). These findings suggested that the observed signals do not arise from rotamers, which could result from the rotation around P-P or C−P bonds. Instead, we attribute these signals to the presence of two diastereomers of compound **4**, stemming from the combination of two enantiomers of BICAAC bridging the P−P bond. It is important to note that BICAAC itself is a racemic mixture of a single diastereomer.
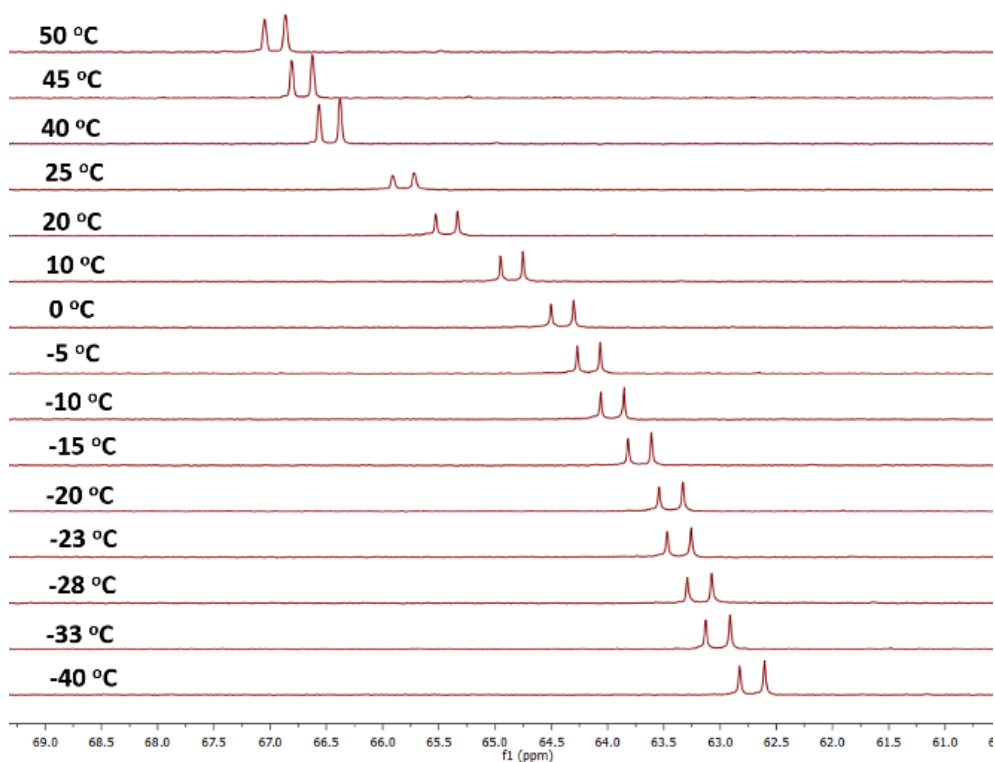
Figure 4.4 VT ^{31}P{^{1}H} NMR spectra of complex **4** in the range of (-40 to +50 °C).
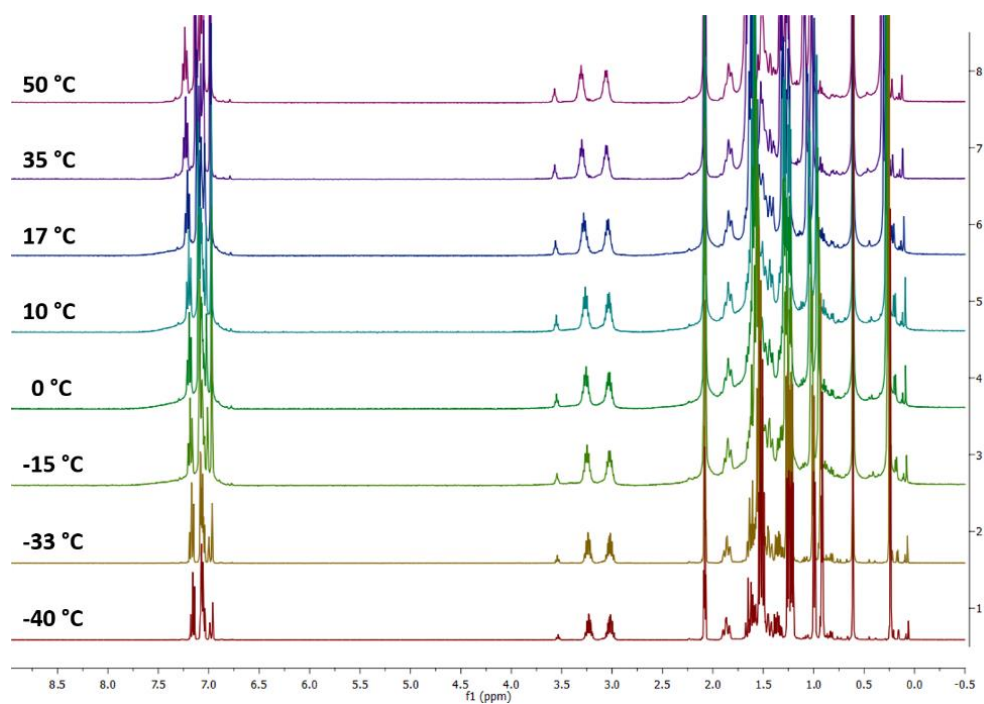
Figure 4.5 VT ^{1}H NMR spectra of complex **4** in the range of (-40 to +50 °C).

Single crystal X-ray diffraction analysis unveiled that compound **4** crystallizes in the orthorhombic crystal system with the *Fdd2* space group and exhibits a trans-bent configuration of BICAACs surrounding the P−P core (Figure 4.6). The C1−P1−P1'−C1' torsional angle in **4** was found to be 177.6(6)°. The C1−P1 bond distance in **4** was measured to be 1.734(14) Å, which is notably shorter in comparison to the C−P bond distance in previously known NHC:P−P:NHC molecules [1.7504(17) Å for (NHC = :C{N(2,6-Pr$^i_2$C$_6$H$_3$)CH}$_2$) and 1.754(3) Å for (NHC = :C{N(2,4,6-Me$_3$C$_6$H$_2$)CH}$_2$)][8d], and it is in line with the previously reported C−P bond length in CAAC:P−P:CAAC [1.719(7) Å].[11] The P−P' bond distance of 2.203(6) Å in **4** is in line with the P−P single bond distance found in the tetrahedral P$_4$ molecule (2.21 Å)[23] and also comparable with the previously reported NHC:P−P:NHC (2.2052(10) and 2.1897(11) Å)[8e] and CAAC:P−P:CAAC (2.184(3) Å)[11] molecules. The ^{31}P{^{1}H} NMR chemical shift value of +65 ppm and the relatively short C−P
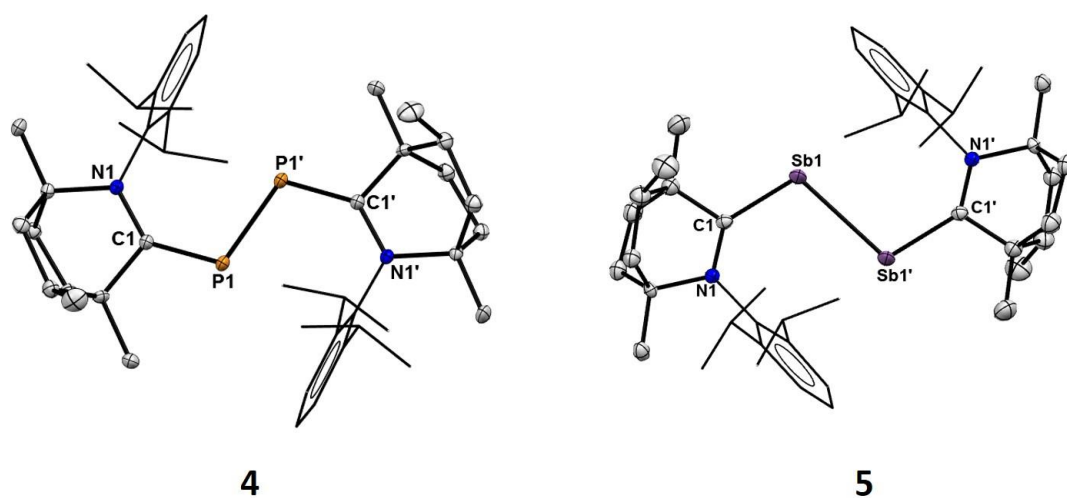
Figure 4.6 Solid state structure of complexes **4** and **5**. Ellipsoids are shown at 50% probability level. All hydrogen atoms have been omitted for clarity. Selected bond lengths (Å) and bond angles (°) for **4**: N1−C1 1.373(17), C1−P1 1.734(14), P1−P1' 2.203(6), N1−C1-P1 134.6(9), C1−P1−P1' 108.7(5); for **5**: N1−C1 1.34(2), C1−Sb1 2.085(15), Sb1−Sb1' 2.893(8), N1−C1−Sb1 134.6(13), C1−Sb1−Sb1' 105.5(4).

bond distance of 1.734(14) Å in **4** strongly indicate the prevalence of the 2,3-diphosphabutadiene structure over the *bis*(phosphinidene) form. Despite our multiple attempts to structurally characterize an alternative rotamer of **4**, all obtained data consistently demonstrated the same relative configuration of BICAACs around the P_2 core. Very recently, Kundu and co-workers disclosed findings on the synthesis of a range of halophosphinidine compounds stabilized by BICAAC, as well as a *bis*-phosphinidine compound similar to complex **4**, but obtained through a different method. Quantum chemical calculations revealed that all these complexes exhibit a preference for the phosphaalkene canonical form over the phosphinidine form, which aligns with the results obtained in our study.[24]

In the ^{1}H NMR spectrum of BICAAC:Sb−Sb:BICAAC (**5**), the aliphatic region displayed a complex pattern, characterized by septets and doublets originating from the 2,6-^{i}Pr$_2$ moiety of BICAAC backbone, making it difficult to systematically identify the signals. A similar difficulty was also seen in the ^{13}C{^{1}H} NMR spectrum of **5**. Complex **5** crystallized in the monoclinic crystal system with $P2_1/n$ space group and displayed a trans-bent arrangement of BICAACs around the Sb−Sb core, akin to **4** (Figure 4.6). The C1−Sb1−Sb1'−C1' torsional angle in **5** was found to be 180.0(6)° and can be compared to CAAC:Sb−Sb:CAAC complex which exhibits a anticlinal twisted-bent geometry with a C1−Sb1-Sb2-C2 torsion angle of 122.6(4)°).[14] The N1−C1 and C1−Sb1 bond distances in **5** were found to be 1.34(2) and 2.085(15) Å respectively, which are comparable to similar bond distances found in CAAC:Sb−Sb:CAAC complex (1.386(13) and 2.084(11) Å)[14] while the Sb1−Sb1' bond distance in **5** was found to be 2.893(8) Å which is slightly longer than those reported for the CAAC:Sb−Sb:CAAC complex (2.8125(10) Å).[14] Considering the observed C−Sb bond distances, we propose that complex **5** exists in a canonical form similar to that of the CAAC:Sb−Sb:CAAC complex.[14]

4.3 Conclusion

In summary, we have synthesized BICAAC−ECl₃ adducts (E = P, Sb) directly by reacting the free BICAAC and the corresponding trichlorides. These adducts exhibited a tetracoordinated arrangement with a see-saw geometry around the pnictogen center, where a stereochemically active lone pair of electrons occupied an equatorial position. Additionally, a phosphinidene, (BICAAC)=P−Ph, was isolated through *in-situ* reduction of the [BICAAC−PPhCl₂] adduct using KC₈. The phosphinidene displayed a short C−P bond distance, as expected owing to the C=P bond character. Leveraging the robust σ-donor properties of BICAAC, the stable BICAAC−ECl₃ (E = P, Sb) adducts have been utilized in the syntheses of *bis*(BICAAC)P₂ and the corresponding Sb analogue, wherein the pnictogen is maintained in a formal zero-valent state. The *bis*(phosphinidene) exhibited *bis*(phosphaalkene) characteristics, whereas the antimony analogue displayed the σ-donation properties of BICAAC to stabilize the Sb₂ core. This study is positioned to bring fresh momentum to the field of low oxidation state pnictogen chemistry, introducing innovative perspectives and opportunities.

4.4 Experimental section

4.4.1 General methods

All the manipulations were performed under an inert atmosphere of dry nitrogen or argon using a glove box or standard Schlenk techniques. All the glassware were dried at 150 °C in an oven for at least 12 h and assembled hot and cooled in vacuo prior to use. Solvents were purified by MBRAUN solvent purification system MB SPS-800 and were used directly from the SPS system. Chemicals were purchased from Sigma-Aldrich, HIMEDIA, and Avra and

were used without further purification. Bicyclic (alkyl)(amino) carbene (BICAAC) was prepared using reported procedure.[19a]

4.4.2 Physical measurements

FT-IR spectra were recorded on a Bruker Invinio R spectrophotometer. The NMR spectra were recorded using Bruker 400 MHz NMR spectrometer (^{1}H: 400 MHz, ^{13}C{^{1}H}: 100 MHz) at room temperature with tetramethylsilane (TMS) as an external standard and chemical shift values are reported in parts per million (ppm). High-resolution mass spectrometry (HRMS) measurement was recorded on a Waters SYNAPT G2-S. UV-vis spectroscopy measurements were recorded on Agilent Cary 5000 UV-vis-NIR Spectrophotometer. Energy dispersive X-Ray (EDX) analysis was performed with a JEOL JSM 7600F field emission electron microscope. Single crystal X-ray diffraction data of complexes **1**-**5** was collected using a Rigaku XtaLAB mini diffractometer equipped with Mercury375M CCD detector. The data was collected with MoKα radiation (λ = 0.71073 Å) using omega scans. During the data collection, the detector distance was 49.9 mm (constant) and the detector was placed at 2θ = 29.85° (fixed). The data were reduced using CrysAlisPro 1.171.38.46, and the space group determination was done using Olex2[25] with the SHELXT[26] structure solution program using Intrinsic Phasing and refined with the SHELXH-1997[27] refinement package using Least Squares minimization. All non-hydrogen atoms were refined anisotropically. Crystallographic data are summarized in Table 4.1 and 4.2.

4.4.3 Synthesis and characterization of complexes 1-5

Synthesis and characterization of [BICAAC−PCl₃] (1): In a 100 mL Schlenk flask, BICAAC (0.31 g, 1.0 mmol) was dissolved in 10 mL precooled hexane (-30 °C) under inert conditions. A solution of PCl₃ (88 μL, 1.0 mmol) (in 5 mL of cold hexane) was added to it in

a dropwise manner. A yellow precipitate was observed during the addition which increased with time. The reaction mixture was warmed to room temperature and allowed to stir for further 3 hours and then filtered off to collect the residue. The residue obtained was washed thrice with cold hexane (3×15 mL) to give analytically pure **1** as a yellow powder. Crystals suitable for X-ray analysis of the product were grown from a concentrated THF solution of complex **1** at -30 °C. (**Yiel**d: 0.38 g, 85%), **Mp**: 180-181 °C. **Anal** (%). calcd for $C_{22}H_{33}NPCl_3$: C, 58.87; H, 7.41; N, 3.12; found: C, 58.91; H, 7.38; N, 3.19. **^{1}H NMR** (400 MHz, C_6D_6) δ = 7.05-6.97 (m, 3H, Ar), 3.34 (sept, J = 6.8 Hz, ^{1}H, -CH(CH$_3$)$_2$), 3.27 (sept, J = 6.8 Hz, 1H, -CH(CH$_3$)$_2$), 2.81-2.74 (m, 1H), 1.895 (d, J = 11.6 Hz, 3H), 1.78-1.72 (m, 1H), 1.63 (d, J = 6.0 Hz, 3H), 1.55 (d, J = 6.4 Hz, 3H), 1.30-1.28 (m, 3H), 1.22-1.21 (m, 3H), 1.10-1.07 (m, 5H), 0.49 (s, 3H), 0.30 (s, 3H) ppm. **^{31}P{^{1}H} NMR** (162 MHz, C_6D_6) δ = 32.99 ppm. **^{13}C{^{1}H} NMR** (100 MHz, C_6D_6) δ = 145.8, 145.2, 134.9, 130.5, 126.1, 125.9, 71.6 (d, J_{C-P} = 5.0 Hz), 48.9 (d, J_{C-P} = 19 Hz), 43.0, 41.1, 39.4, 32.4, 29.5 (d, J_{C-P} = 4.0 Hz), 28.2, 27.6, 25.65 (d, J_{C-P} = 7.0 Hz), 22.9, 18.4, 18.1, 17.7 ppm. **HRMS** (AP$^+$): *m/z* calculated for $C_{22}H_{34}NPCl$: (378.2117) [M-2Cl]$^+$; found: (378.2097).

Synthesis and characterization of [BICAAC−SbCl$_3$] (2): In a 100 mL Schlenk flask, BICAAC (0.311 g, 1.0 mmol) was dissolved in 15 mL precooled (-30 °C) diethyl ether under inert conditions. A solution of SbCl$_3$ (0.228 g, 1.0 mmol) was added into it in a dropwise manner. After a few minutes the reaction mixture became dull grey in color. The reaction mixture was warmed to room temperature and stirred for further 3 hours and then filtered off to collect the residue. The grey residue obtained was washed thrice with diethyl ether (3 x 15 mL). Crystals suitable for X-ray analysis were grown from a concentrated dichloromethane solution of complex **2** at -30 °C. (**Yield:** 0.41 g, 76%), **Mp**: 191 °C. **Anal** (%). calcd for $C_{22}H_{33}NSbCl_3$: C, 48.97; H, 6.16; N, 2.60; found: C, 49.28; H, 6.19; N, 2.71. **^{1}H NMR** (400 MHz, CDCl$_3$) δ = 7.46-7.42 (m, 1H, Ar), 7.32-7.30 (m, 2H, Ar), 3.10-3.0 (two merged septet,

2H, -CH(CH$_3$)$_2$), 2.57-2.53 (m, 1H), 2.23-2.17 (m, 1H), 2.09 (s, 3H), 2.0-1.93 (m, 3H), 1.67-1.62 (m, 1H), 1.43-1.42 (m, 6H), 1.36-1.28 (m, 10H), 1.05 (s, 3H) ppm. **^{13}C{^{1}H} NMR** (100 MHz, CDCl$_3$) δ = 227.3, 145.2, 144.9, 135.3, 130.7, 126.0, 125.9, 72.1, 43.2, 38.7, 38.4, 32.4, 29.0, 28.8, 28.0, 27.4, 26.8, 26.0, 25.9, 22.9, 19.6 ppm. **HRMS** (ES$^+$): *m/z* calculated for C$_{22}$H$_{33}$NSbCl$_2$: (502.1028) [M-Cl]$^+$; found: (502.1048).

Synthesis and characterization of [BICAAC=P−Ph] (3): In a 100 mL Schlenk flask, BICAAC (0.311 g, 1.0 mmol), PPhCl$_2$ (136 μL, 1.0 mmol) and KC$_8$ (0.297 g, 2.2 mmol) were mixed in 10 mL of precooled (-30 °C) THF under inert conditions. The reaction mixture was warmed to room temperature and allowed to be stirred for 5 hours. Thereafter, the graphite and other insoluble material were filtered off to afford a yellow filtrate. The filtrate was concentrated to approximately 5 mL and kept at -10 °C for 5 days to give block-shaped yellow crystals of **3**. (**Yield:** 0.28 g, 66%), **Mp**: 243-245 °C. **Anal** (%). calcd for C$_{28}$H$_{38}$NP: C, 80.15; H, 9.13; N, 3.34; found: C, 79.82; H, 9.19; N, 3.45. **^{1}H NMR** (400 MHz, C$_6$D$_6$) δ = 7.70-7.67 (m, 2H, Ar), 7.24-7.20 (m, 1H, Ar), 7.14-7.13 (m, 2H, Ar), 7.07-7.02 (m, 3H, Ar), 3.27 (sept, *J* = 6.8 Hz, 1H, -CH(CH$_3$)$_2$), 3.07 (sept, *J* = 6.8 Hz, 1H, -CH(CH$_3$)$_2$), 1.91-1.82 (m, 2H), 1.635 (d, *J* = 6.4 Hz, 6H), 1.60-1.49 (m, 2H), 1.44-1.38 (m, 1H), 1.32-1.25 (m, 8H), 1.20-1.19 (m, 3H) ppm. **^{31}P{^{1}H} NMR** (162 MHz, C$_6$D$_6$) δ = 90.27 ppm. **^{13}C{^{1}H} NMR** (100 MHz, C$_6$D$_6$) δ = 201.6 (d, *J* = 71 Hz), 147.4 (d, J_{C-P} = 5 Hz), 147.2 (d, J_{C-P} = 6 Hz), 144.1 (d, J_{C-P} = 48 Hz), 138.5 (d, J_{C-P} = 6 Hz), 138.5 (d, J_{C-P} = 5 Hz), 136.6 (d, J_{C-P} = 13 Hz), 128.9, 127.4 (d, J_{C-P} = 3 Hz), 126.8, 125.3, 125.1, 57.6, 48.4 (d, J_{C-P} = 14 Hz), 45.1, 37.8 (d, J_{C-P} = 3 Hz), 37.4 (d, J_{C-P} = 2 Hz), 34.6, 29.1, 28.8, 27.1, 26.4 (t, *J* = 5 Hz), 25.1, 24.7 (d, J_{C-P} = 3 Hz), 24.5, 19.5 ppm. **HRMS** (ES$^+$): *m/z* calculated for C$_{28}$H$_{39}$NP: (420.2820) [M+H]$^+$; found: (420.2793).

Synthesis and characterization of [*bis*(BICAAC)P$_2$] (4): In a 100 mL Schlenk flask, the BICAAC-PCl$_3$ adduct **1** (0.45 g, 1.0 mmol) was dissolved in 10 mL of precooled THF (-30

°C) under inert conditions to give a yellow solution, then KC_8 (0.45 g, 3.3 mmol) was added to it. The reaction mixture was brought to room temperature and stirred for 5 hours. Thereafter, graphite and other insoluble material were filtered off to give a yellow filtrate. The filtrate was concentrated to approximately 5 mL and kept at 0 °C for 4 days to give block shaped yellow crystals of complex **4**. (**Yield:** 0.2 g, 58 %), **Mp**: 215 °C (decomposition). **Anal** (%). calcd for $C_{44}H_{66}N_2P_2$: C, 77.15; H, 9.71; N, 4.09; found: C, 77.47; H, 9.85; N, 3.98. **^{1}H NMR** (400 MHz, -40 °C, Tol-d_8) δ = 7.21-7.17 (m, 1H, Ar), 7.10-7.07 (m, 2H, Ar), 3.30-3.21 (sept, J = 8.0 Hz, 1H, -CH(CH$_3$)$_2$), 3.09-2.98 (sept, J = 8.0 Hz, 1H, -CH(CH$_3$)$_2$), 1.90-1.83 (m, 1H), 1.67-1.54 (m, 9H), 1.50-1.42 (m, 2H), 1.37-1.31 (m, 1H), 1.30-1.27 (m, 3H), 1.25-1.23 (m, 3H), 1.03 (d, J = 8.0 Hz, 3H), 0.96-0.95 (m, 3H) ppm. **^{31}P{^{1}H} NMR** (162 MHz, -40 °C, Tol-d_8) δ = 62.80, 62.60 ppm. **^{13}C{^{1}H} NMR** (100 MHz, Tol-d_8) δ = 186.4, 185.9, 185.3, 149.3, 148.9, 140.8, 124.6, 124.5, 58.1, 46.7, 45.2, 37.4, 37.3, 34.7, 28.7, 28.3, 26.5, 25.8, 25.3, 25.2, 25.1, 24.5, 18.7 ppm. **HRMS** (ES$^+$): m/z calculated for $C_{44}H_{66}N_2P_2$: (684.4701) [M]$^+$; found: (684.4697).

Synthesis and characterization of [*bis*(BICAAC)Sb$_2$] (5): In a 100 mL Schlenk flask, BICAAC-SbCl$_3$ adduct **2** (0.54 g, 1.0 mmol) was added in 10 mL of precooled toluene (-30 °C) under inert conditions, then KC_8 (0.45 g, 3.3 mmol) was added to it. The reaction mixture was brought to room temperature and stirred for 5 hours to give a dark red-violet reaction mixture. Thereafter, the graphite and other insoluble material were filtered off to give dark red-violet filtrate. All volatiles were removed under reduced pressure to give a red compound. The obtained residue was further dissolved in 4-5 mL of hexane and kept at 0 °C for 5 days to give block-shaped red crystals of complex **5**. (**Yield:** 0.19 g, 44 %), **Mp**: 160 °C (decomposition). **Anal** (%). calcd for $C_{44}H_{66}N_2Sb_2$: C, 60.99; H, 7.68; N, 3.23; found: C, 61.20; H, 7.71; N, 3.31. **^{1}H NMR** (400 MHz, C_6D_6) δ = 7.33-7.26 (m, 2H, Ar), 7.13-7.02 (m, 3H, Ar), 6.93-6.89 (m, 1H, Ar), 3.55-2.85 (m, 4H, overlapped signals), 1.88-1.49 (m, 28H,

overlapped signals), 1.32-1.14 (m, 22H, overlapped signals), 0.66 (3H, s), 0.58-0.57 (3H, overlapped signals) ppm.

4.5 Crystallographic data

Table 4.1 Crystallographic details of complexes **1**-**3.**

Compound[a]	1	2	3
Chemical formula	$C_{22}H_{33}Cl_3NP$	$C_{22}H_{33}Cl_3NSb$	$C_{28}H_{38}NP$
Molar mass	448.81	539.59	419.56
Crystal system	monoclinic	triclinic	monoclinic
Space group	$P2_1/c$	$P\bar{1}$	$P2_1/n$
T [K]	200.00(10)	100(2)	150.01(10)
a [Å]	10.1222(8)	9.0202(2)	10.1941(6)
b [Å]	14.6832(12)	9.4560(3)	19.7084(10)
c [Å]	15.4487(18)	15.1532(3)	12.2443(6)
α [°]	90.00	78.604(2)	90.00
β [°]	90.001(11)	87.357(2)	95.569(6)
γ [°]	90.00	66.531(2)	90.00
V [Å^3]	2296.1(4)	1161.44(5)	2448.4(2)
Z	4	2	4
ρ(calcd.) [g·cm^{-3}]	1.298	1.543	1.138
μ [mm^{-1}]	0.477	1.541	0.127
F(000)	952.0	548.0	912.0
Radiation [Å]	Mo Kα (λ = 0.71073)	Mo Kα (λ = 0.71073)	Mo Kα (λ = 0.71073)
Reflections collected	9307	26260	17597
Independent reflections	4061	8257	4325
Data/restraints/parameters	4061/0/251	8257/0/251	4325/36/278
$R1$, $wR_2[I>2\sigma(I)]$[a]	0.0676,	0.0338,	0.0492, 0.1203
R1, wR$_2$ (all data)[a]	0.1677	0.0774	0.0817, 0.1476
GOF	0.1039,	0.0405,	1.059
CCDC	**2268983**	**2268984**	**2268985**

[a] R1 = Σ||Fo| − |Fc||/Σ|Fo|. wR$_2$ = [Σw(|Fo^2| − |Fc^2|)^2/Σw|Fo^2|^2]$^{1/2}$

Table 4.2 Crystallographic details of complexes **4-5.**

Compound[a]	4	5
Chemical formula	$C_{44}H_{66}N_2P_2$	$C_{44}H_{66}N_2Sb_2$
Molar mass	684.92	866.49
Crystal system	orthorhombic	monoclinic
Space group	$Fdd2$	$P2_1/n$
T [K]	100.00(10)	150.00(10)
a [Å]	35.7414(13)	9.9506(5)
b [Å]	24.6909(8)	17.0969(5)
c [Å]	18.1915(11)	12.4543(5)
α [°]	90	90.00
β [°]	90	98.036(4)
γ [°]	90	90.00
V [Å^3]	16053.8(12)	2097.97(15)
Z	16	2
ρ(calcd.) [g·cm^{-3}]	1.134	1.372
μ [mm^{-1}]	0.140	1.318
F(000)	5984.0	892.0
Radiation [Å]	Mo Kα ($\lambda = 0.71073$)	Mo Kα ($\lambda = 0.71073$)
Reflections collected	37784	15049
Independent reflections	12287	3703
Data/restraints/parameters	12287/133/644	3703/288/448
$R1$, $wR_2[I>2\sigma(I)]$[a]	0.0630, 0.1481	0.0316, 0.0701
R1, wR$_2$ (all data)[a]	0.0825, 0.1632	0.0427, 0.0794
GOF	1.062	1.097
CCDC	**2268986**	**2268987**

[a] $R1 = \Sigma||Fo| - |Fc||/\Sigma|Fo|$. $wR_2 = [\Sigma w(|Fo^2| - |Fc^2|)^2/\Sigma w|Fo^2|^2]^{1/2}$

4.6 References

1. Arduengo, A. J.; III; Harlow, R. L.; Kline, M. *J. Am. Chem. Soc*. **1991**, *113*, 361-363.

2. (a) Hopkinson, M. N.; Richter, C.; Schedler, M.; Glorius, F. *Nature* **2014**, *510*, 485-496; b) Diez-Gonzalez, S.; Marion, N.; Nolan, S. P. *Chem. Rev*. **2009**, *109*, 3612-3676.

3. Wang, Y.; Robinson, G. H. *Inorg. Chem*. **2014**, *53*, 11815-11832.

4. Vougioukalakis, G. C.; Grubbs, R. H. *Chem. Rev*. **2010**, *110*, 1746-1787

5. Enders, D.; Niemeier, O.; Henseler, A. *Chem. Rev*. **2007**, *107*, 5606-5655

6. Frémont, P. D.; Marion, N.; Nolan, S. P. *Coord. Chem. Rev*. **2009**, *253*, 862-892

7. Lavallo, V.; Canac. Y.; Präsang, C.; Donnadieu, B.; Bertrand G. *Angew. Chem. Int. Ed*. **2005**, *44*, 5705-5709.

8. (a) Wang, Y.; Quillian, B.; Wei, P.; Wannere, C. S.; Xie, Y.; King, R. B.; Schaefer, H. F.; Schleyer, P. v. R.; Robinson, G. H. *J. Am. Chem. Soc*. **2007**, *129*, 12412-12413; (b) Wang, Y.; Quillian, B.; Wei, P.; Xie, Y.; Wannere, C. S.; King, R. B.; Schaefer, H. F.; Schleyer, P. v. R.; Robinson, G. H. *J. Am. Chem. Soc*. **2008**, *130*, 3298-3299; (c) Braunschweig, H.; Dewhurst, R. D.; Hammond, K.; Mies, J.; Radacki, K.; Vargas, A. *Science* **2012**, *336*, 1420-1422; (d) Wang, Y.; Xie, Y.; Wei, P.; King, R. B.; Schaefer, H. F., III; Schleyer, P. v. R.; Robinson, G. H. *J. Am. Chem. Soc*. **2008**, *130*, 45, 14970-14971; (e) Wang, Y.; Xie, Y.; Abraham, M. Y.; Gilliard, R. J.; Wei, P.; Schaefer, H. F.; Schleyer, P. v. R.; Robinson, G. H. *Organometallics* **2010**, *29*, 4778-4780; (f) Wang, Y.; Xie, Y.; Wei, P.; King, R. B.; Schaefer, H. F., III; Schleyer, P. v. R.; Robinson, G. H. *Science* **2008**, *321*, 1069-1071; (g) Sidiropoulos, A.; Jones, C.; Stasch, A.; Klein, S.; Frenking, G. *Angew. Chem. Int. Ed*. **2009**, *48*, 9701-9704; (h) Jones, C.; Sidiropoulos, A.; Holzmann, N.; Frenking, G.; Stasch, A. *Chem. Commun.* **2012**, *48*, 9855-9857; (i) Bag, P.; Porzelt, A.; Altmann, P. J.; Inoue, S. *J. Am. Chem.*

Soc. **2017**, *139*, 14384-14387; (j) Abraham, M. Y.; Wang, Y.; Xie, Y.; Wei, P.; Schaefer, H. F.; Schleyer, P. v. R.; Robinson, G. H. *Chem. Eur. J.* **2010**, *16*, 432-435; (k) Melaimi, M.; Jazzar, R.; Soleilhavoup, M.; Bertrand, G. *Angew. Chem. Int. Ed.* **2017**, *56*, 10046-10068.

9. Roy, S.; Mondal, K. C.; Roesky, H. W. *Acc. Chem. Res*. **2016**, *49*, 357-369.

10. Kundu, S.; Sinhababu, S.; Chandrasekhar, V.; Roesky, H. W. *Chem. Sci*. **2019**, *10*, 4727-4741.

11. Back, O.; Kuchenbeiser, G.; Donnadieu, B.; Bertrand, G. *Angew. Chem. Int. Ed.* **2009**, *48*, 5530-5533.

12. Wilson, D. J. D.; Couchman, S. A.; Dutton, J. L. *Inorg. Chem.* **2012**, *51*, 7657-7668.

13. (a) Wang, Y.; Robinson, G. H. *Dalton Trans*. **2012**, *41*, 337-345; (b) Aprile, A.; Corbo, R.; Vin Tan, K.; Wilson, D. J. D.; Dutton, J. L. *Dalton Trans*. **2014**, *43*, 764-768.

14. Kretschmer, R.; Ruiz, D. A.; Moore, C. E.; Rheingold, A. L.; Bertrand, G. *Angew. Chem. Int. Ed.* **2014**, *53*, 8176-8179.

15. (a) Arduengo, A. J.; Dias, H. V. R.; Calabrese, J. C. *Chem. Lett*. **1997**, *26*, 143-144; (b) Arduengo, A. J.; Calabrese, J. C.; Cowley, A. H.; Dias, H. V. R.; Goerlich, J. R.; Marshall, W. J.; Riegel, B. *Inorg. Chem*. **1997**, *36*, 2151-2158.

16. (a) Back, O.; Henry-Ellinger, M.; Martin, C. D.; Martin, D.; Bertrand, G. *Angew. Chem. Int. Ed.* **2013**, *52*, 2939-2943; (b) Nelson, D. J.; Nolan, S. P. *Chem. Soc. Rev*. **2013**, *42*, 6723-6753; (c) Krachko, T.; Slootweg, J. C. *Eur. J. Inorg. Chem.* **2018**, 2734-2754; (d) Li, Z.; Chen, X.; Li, Y.; Su, C.-Y.; Grützmacher, H. *Chem. Commun.* **2016**, *52*, 11343-11346; (e) Kundu, S.; Sinhababu, S.; Luebben, A. V.; Mondal, T.; Koley, D.; Dittrich, B.; Roesky, H. W. *J. Am. Chem. Soc*. **2018**, *140*, 151-154; (f)

Kundu, S.; Li, B.; Kretsch, J.; Herbst-Irmer, R.; Andrada, D. M.; Frenking, G.; Stalke, D.; Roesky, H. W. *Angew. Chem. Int. Ed.* **2017**, *56*, 4219-4223.

17. Rodrigues, R. R.; Dorsey, C. L.; Arceneaux, C. A.; Hudnall, T. W. *Chem. Commun.* **2014**, *50*, 162-164.

18. Roy, S.; Mondal, K. C.; Kundu, S.; Li, B.; Schürmann, C. J.; Dutta, S.; Koley, D.; Herbst-Irmer, R.; Stalke, D.; Roesky, H. W. *Chem. Eur. J.* **2017**, *23*, 12153-12157.

19. (a) Tomás-Mendivil, E.; Hansmann, M. M.; Weinstein, C. M.; Jazzar, R.; Melaimi, M.; Bertrand, G. *J. Am. Chem. Soc.* **2017**, *139*, 7753-7756; (b) Lavallo, V.; Canac, Y.; Donnadieu, B.; Schoeller, W. W.; Bertrand, G. *Angew. Chem. Int. Ed.* **2006**, *45*, 3488-3491; (c) Frey, G. D.; Lavallo, V.; Donnadieu, B.; Schoeller, W. W.; Bertrand, G. *Science* **2007**, *316*, 439-441.

20. (a) Manar, K. K.; Porwal, V. K.; Kamte, R. S.; Adhikari, M.; Thakur, S. K.; Bawari, D.; Choudhury, A. R.; Singh, S. *Dalton Trans.* **2019**, *48*, 17472-17478; (b) Manar, K. K.; Chakrabortty, S.; Porwal, V. K.; Prakash, D.; Thakur, S. K.; Choudhury, A. R.; Singh, S. *ChemistrySelect* **2020**, *5*, 9900-9907; (c) Yazdani, S.; Junor, G. P.; Peltier, J. L.; Gembicky, M.; Jazzar, R.; Grotjahn, D. B.; Bertrand, G. *ACS Catal.* **2020**, *10*, 5190-5201; (d) Chakrabortty, S.; Kaur, M.; Adhikari, M.; Manar, K. K.; Singh, S. *Inorg. Chem.* **2021**, *60*, 6209-6217; (e) Rajendran, N. M.; Gautam, N.; Sarkar. P.; Ahmed, J.; Das, A.; Das, S.; Pati, S. K; Mandal, S. K. *Chem. Commun.* **2021**, *57*, 5282-5285; (f) Nagyházi, M.; Almási, B.; Lukács, Á.; Bényei, A.; Nagy, T.; Kéki, S.; Tuba, R. *J. Mol. Str.*, **2022**, *1256*, 132483; (g) Gautam, N.; Logdi, R.; Sreejyothi, P.; Rajendran, N. M.; Tiwari, A. K.; Mandal, S. K. *Chem. Commun.* **2022**, *58*, 3047-3050; (h) Thakur, S. K.; Kaur, M.; Manar, K. K.; Adhikari, M.; Choudhury, A. R.; Singh S. *Chem. Eur. J.* **2022**, *28*, e202202237; (i) Dutta, S.; Maity, B.; Thirumalai, D.; Koley, D. *Inorg. Chem.* **2018**, *57*, 3993-4008.

21. Morrow, B. A.; Lang, S. J.; Gay, I. D. *Langmuir* **1994**, *10*, 756-760.

22. Sidiropoulos, A.; Osborne, B.; Simonov, A. N.; Dange, D.; Bond, A. M.; Stasch, A.; Jones, C. *Dalton Trans*. **2014**, *43*, 14858-14864.

23. Cotton, F. A.; Wilkinson, G.; Murillo, C.; Bochmann, M. *Advanced Inorganic Chemistry*, 6th ed.; Wiley: New York, **1999**.

24. Yadav, R.; Das, B.; Singh, A.; Anmol; Sharma, A.; Majumder, C.; Kundu, S. *Dalton Trans.* **2023***, 52,* 16680-16687.

25. Dolomanov, O. V.; Bourhis, L. J.; Gildea, R. J.; Howard, J. A. K.; Puschmann, H. *J. Appl. Cryst*. **2009**, *42*, 339-341.

26. Sheldrick, G. M. *Acta Cryst., Sect. A* **2015**, *71*, 3-8.

27. Sheldrick, G. M. *Acta Cryst., Sect. A* **2008**, *64*, 112-122.

Neutral and cationic Ir(I)-complexes supported by BICAAC: Application of Ir(^{Me}BICAAC)Cl(COD) complex as a catalyst for transfer hydrogenation of carbonyls and imines

Abstract: The present chapter deals with the syntheses and detailed characterization of ^{Me}BICAAC and ^{iPr}BICAAC (BICAAC = bicyclic (alkyl)(amino)carbene) supported stable neutral and cationic Ir(I) complexes, [Ir(^{Me}BICAAC)Cl(COD) (**1**), [Ir(^{iPr}BICAAC)Cl(COD) (**2**), [Ir(^{Me}BICAAC)(COD)][SbF$_6$] (**3**), and [Ir(^{Me}BICAAC)(CH$_3$CN)(COD)][SbF$_6$] (**4**). Complexes **1**-**4** showed good catalytic activity in the transfer hydrogenation (TH) of the model substrate 4-chlorobenzaldehyde, employing ^{i}PrOH as the hydrogen donor agent with the TOF value ranging between 6269-8093 h^{-1}. Given its relatively straightforward preparation, complex **1**, was selected for further investigation as an active catalyst in the transfer hydrogenation of a diverse range of aldehydes, ketones, and imines. A library of carbonyl and imine substrates featuring electron-withdrawing and -donating substituents have been surveyed and afforded their reduced products in moderate to good yields. A heating experiment was performed to check the thermal stability of complex Ir(^{Me}BICAAC)Cl(COD)that showed no detachment of the ^{Me}BICAAC or COD units from the metal center upon prolonged heating in toluene-D_8 or isopropanol-D_8 solvents which evidenced good thermal stability of the complex that is essential for the catalytic reactions. The outcomes of the Hg drop test and hot filtration test support the assertion that the transfer hydrogenation (TH) reaction catalyzed by complex **1** operates in a homogeneous mode. The results of deuterium labelling experiments support the monohydride mechanistic pathway operated in the TH. Further, other control experiments support the formation of Ir-O^{i}Pr species as a key intermediate in the proposed catalytic cycle of transfer hydrogenation.

5.1 Introduction

The reduction of carbonyl (aldehyde and ketone) and imine functionalities is one of the most vital topic in molecular transformations,[1-3] because their corresponding saturated products (alcohols and amines) exhibit wide range of applications in pharmaceutical, polymer, dye, agrochemical and pesticide industry.[4-6] To fulfil the demand of these essential molecules, the typically practiced method includes the use of an stoichiometric amount of reducing agents (LiAlH$_4$, NaBH$_4$, NaBH$_3$CN etc.) and the use of molecular hydrogen (H$_2$).[2,7-8] In addition to the aforementioned strategies, transfer hydrogenation (TH) and hydroelementation reactions are emerging as promising alternative methodologies.[9-10] TH reaction involves the addition of hydrogen to a molecule using a hydrogen source other than H$_2$, stands out as a convenient and potent method for accessing a diverse range of hydrogenated compounds. In general, TH process can be defined in two steps: (1) metal-assisted abstraction of hydride from hydrogen donor solvent (oxidation step); (2) insertion of this hydride into the unsaturated acceptor substrates (reduction step).[11] Isopropanol (^{i}PrOH) is the most common solvent used for this purpose due to its low cost, easy availability and non-toxic nature.[12] In the last two decades, the transfer hydrogenation process has been intensely investigated , which eventually led to the development of a number of transition metal (Ru, Rh, Ir, Pd, Os, Ni, Co, Au etc.) based catalysts for reduction of C=O, C=N and C=C bonds using different hydrogen donor (MeOH, EtOH, glycerol, H$_2$O, ^{i}PrOH etc) (**A**-**H**, Figure 5.1A).[13-20] Among the reported catalysts, some of them showed catalytic activity in base free conditions but required external additives or an inert atmosphere to attain the best catalytic protocol.[15d,21-24]

Ir catalysts supported by different ligand backbones and their catalytic properties are majorly studied in this context.[25] In homogeneous catalysis, stability of the applied catalyst is considered as the first prerequisite to spike up its catalytic performance. Due to the strong
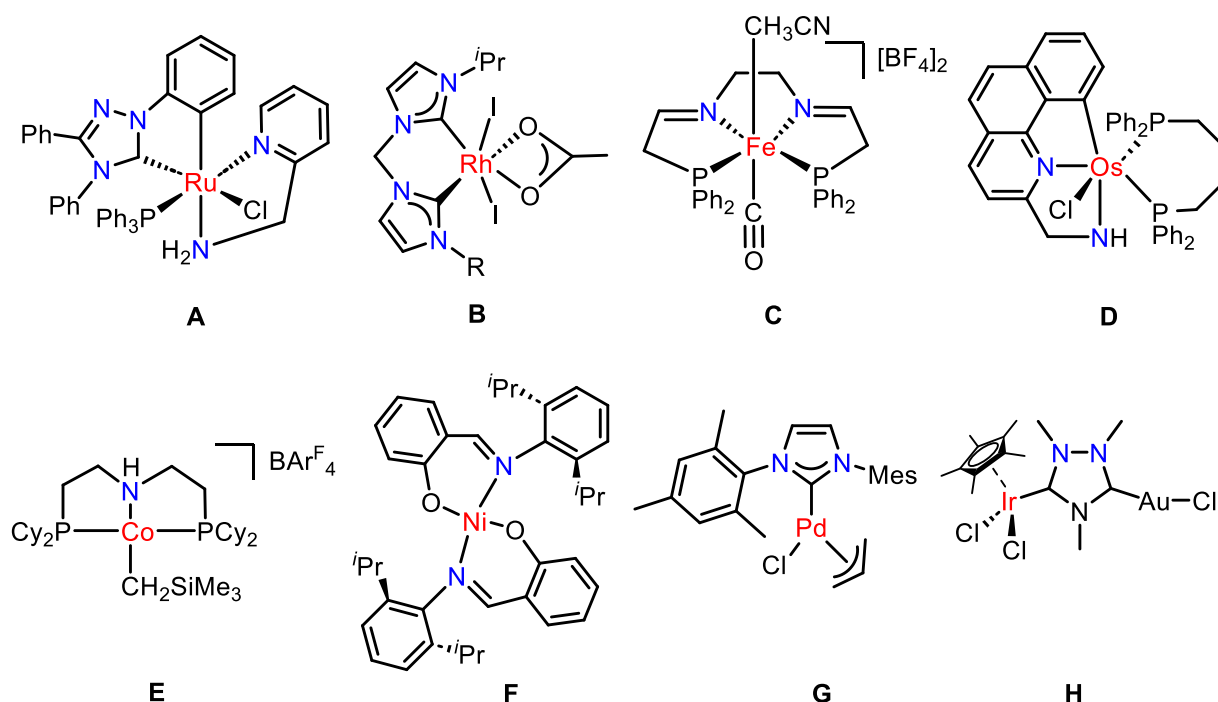
Figure 5.1A Selected examples of transition metal-based catalysts used for transfer hydrogenation of diverse unsaturated groups.

coordinating ability (σ-donor ability) and tunable steric and electronic properties, carbene ligands provide remarkable robustness to the catalyst. In this context, Ir complexes of carbene have shown promising results in TH catalysis.[26-27]

Nolan and co-workers in 2001 demonstrated the use of NHC transition metal complexes particularly [Ir(cod)(py)(NHC)]PF$_6$ (**A**-**C**, Figure 5.1B) in catalytic transfer hydrogenation reaction of substrates including ketones, olefins, and nitroarenes with isopropanol as hydrogen delivery agent.[28] Some selected examples of Ir(I)-complexes with different types of carbenes (classical imidazoles, triazolium and Fischer carbene) (**D**-**I**, Figure 5.1B) that are especially employed to reduce carbonyl and imine functionalities using *i*PrOH.[29] Contrary to the classical methods, development of efficient catalysts for greener and safer TH reactions is still an active area of research. Considering the capability of Ir(I) complexes comprised of different carbene scaffolds for TH reactions, we became interested in synthesizing Ir-based
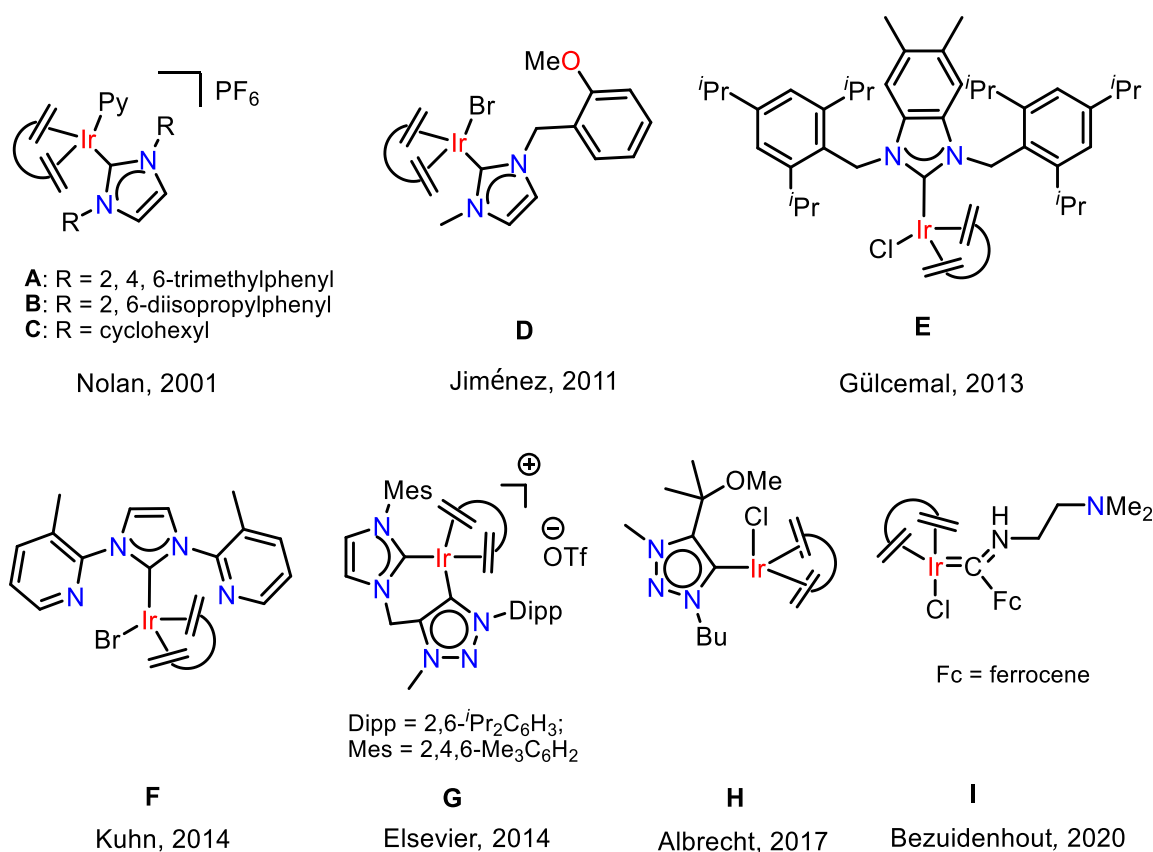
Figure 5.1B A set of Ir(I)-carbene catalysts used for the transfer hydrogenation reaction.

complexes supported by recently discovered bicyclic (alkyl)(amino)carbene (BICAAC) ligand. Recent experimental and computational studies showed the better σ-donor and π-acceptor properties of the BICAAC ligand compared to standard NHCs.[30] These engrossing electronic properties can offer robustness to catalysts. However, only few reports on BICAAC supported metal complexes (Au, Pd, and Zn) have been published so far for different organic transformations such as hydroamination, hydrohydrazination, cross-coupling, and alkyne protoboration.[31-34]

Consequently herein, we have synthesized a series of new Ir(I) complexes outfitted with BICAAC ligand Ir(^{Me}BICAAC)Cl(COD) (**1**), Ir(^{iPr}BICAAC)Cl(COD) (**2**), [Ir(^{Me}BICAAC)(COD)][SbF$_6$] (**3**) and [Ir(^{Me}BICAAC)(CH$_3$CN)(COD)][SbF$_6$] (**4**). The catalytic efficacy of these complexes was investigated in the transfer hydrogenation of aldehydes, ketones, and imines, employing ^{i}PrOH as the hydrogen donor. The remarkable σ-

donor characteristics of BICAAC conferred stability to the catalysts even at elevated temperatures. Stoichiometric experiments and deuterium labeling studies substantiate the iridium-monohydride mechanistic picture where ^{i}PrOH served as a source of hydrogen. The initial documented syntheses of complexes, Ir(^{Me}BICAAC)Cl(COD) (**1**) and [Ir(^{Me}BICAAC)(COD)][SbF$_6$] (**3**) were documented by Prakash[35] and Yogesh[36], respectively that were subsequently optimized and the composition of the complexes were fully established in the present work. Consequently, the systematically optimized experimental process reported herein affords a high yield synthesis of these complexes and presents a through characterization as well.

5.2 Results and discussion

5.2.1 Syntheses and characterization of complexes Ir(^{Me}BICAAC)Cl(COD) (1) and Ir(^{iPr}BICAAC)Cl(COD) (2)

The reaction of $^{Me/iPr}$BICAAC with 0.5 equivalent of [IrCl(COD)]$_2$ in a precooled tetrahydrofuran (THF) for 4-5 h exclusively afforded the bench stable complexes Ir(^{Me}BICAAC)Cl(COD) (**1**), Ir(^{iPr}BICAAC)Cl(COD) (**2**) as an yellow-orange solid in 85 and 82 % yields, respectively (Scheme 5.1). The formation and high purity of **1** and **2** were recognized from NMR and HRMS data.

Dipp = 2,6-^{i}Pr$_2$C$_6$H$_3$

1, R = Me, (85%)
2, R = ^{i}Pr, (82%)
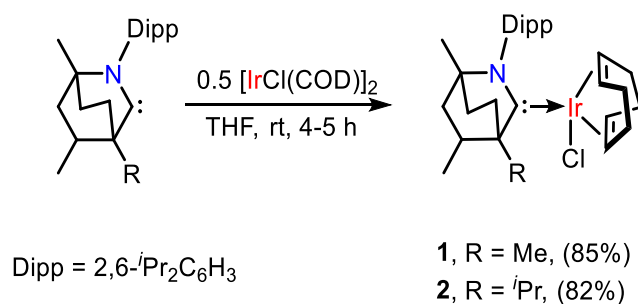
Scheme 5.1 Syntheses of complexes Ir($^{Me/iPr}$BICAAC)Cl(COD) (**1** and **2**).

The ^{1}H NMR spectrum of resulting complex **1** in CDCl$_3$ showed two distinct septets centered at δ = 3.52 and 2.90 ppm, which corresponds to the Dipp group of the BICAAC ligand along with four multiplets located at δ = 4.54-4.49, 4.30-4.25, 3.19-3.15 and 2.68-2.64 ppm corresponds to the COD olefinic protons. The signal at δ = 262 ppm in the ^{13}C{^{1}H} NMR spectrum of **1** corresponds to the metal-bounded carbene carbon, which is significantly up-field shifted when compared to the free ^{Me}BICAAC (δ = 334.4 ppm) and can be attributed to the electrophilic nature of the BICAAC unit. Additionally, HRMS spectrum of complex **1** showed the molecular ion signal [M]$^+$ at *m/z* = 647.2838 (calcd. 647.2863). Similarly, the ^{1}H and ^{13}C{^{1}H} NMR spectra of **2** are also consistent with the anticipated structure of the complex.

The spectroscopically derived structures of complexes **1** and **2** were further confirmed by single crystal X-ray diffraction technique. Yellow-orange crystals of **1** and **2**, suitable for X-ray diffraction, were successfully obtained through the slow evaporation method from a mixture of dichloromethane and hexane. Both the complexes **1** and **2** were found to crystallize in the orthorhombic crystal system, with complex **1** possessing the *P2$_1$2$_1$2$_1$* space group and complex **2** exhibiting the *Pbca* space group. The structure divulged that the iridium centre resides in a distorted square planar coordination environment with an unsaturated 16 electron electronic configuration (Figure 5.2). In both the structures the iridium centre is connected to carbene carbon (C1) and one chloride (Cl1); the remaining sites are engaged by one COD unit connected in (η^2:η^2) mode. The N1−C1, C1−Ir1 and Ir1−Cl1 bond distances in **1** were found to be 1.328(7), 2.030(6) and 2.3667(15) Å respectively, while the N1−C1−Ir1 and C1−Ir1−Cl1 bond angles were found to be 127.0(4) and 89.25(17) ° respectively. Similarly, the N1−C1, C1−Ir1 and Ir1−Cl1 bond separations in **2** were found to be 1.329(5), 2.054(4), 2.3814(9) Å respectively, whereas the N1−C1−Ir1 and C1−Ir1−Cl1 bond angles were found to be 125.8(3) and 87.72(10) ° respectively.
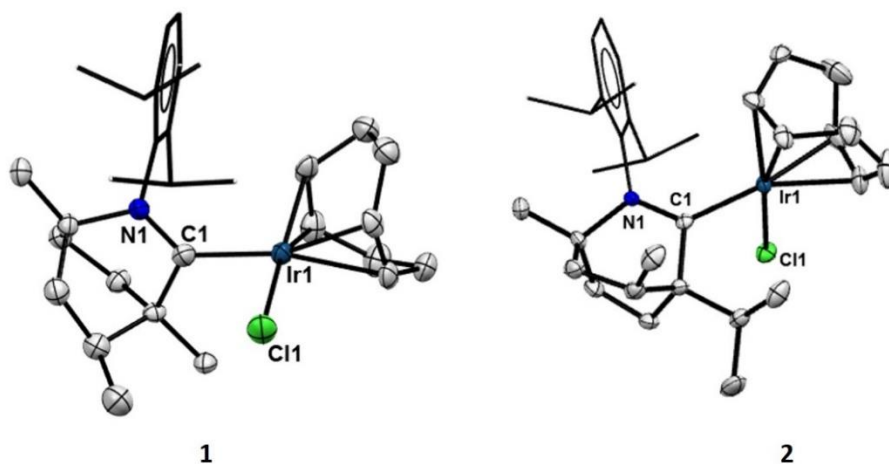
Figure 5.2 Single-crystal X-ray structure of complexes Ir($^{Me/iPr}$BICAAC)Cl(COD) (**1** and **2**). Ellipsoids are shown at 50 % probability level. All hydrogen atoms are omitted for clarity. Selected bond lengths (Å) and bond angles (°) for **1**: Ir1−C1 2.030(6), Ir1−Cl1 2.3667(15), N1−C1 1.328(7), N1−C1−Ir1 127.0(4), C1−Ir1−Cl1 89.25(17); for **2**: Ir1−C1 2.054(4), Ir1−Cl1 2.3814(9), N1−C1 1.329(5), N1−C1−Ir1 125.8(3), C1−Ir1−Cl1 87.72(10).

The UV-vis spectrum of the orange complex **1** was recorded in dichloromethane at room temperature. It exhibits three low-energy absorption bands (Figure 5.3) corresponding to d-d transitions found at λ_{max} = 360, 431 and 487 nm (molar extinction coefficient: 1679, 1375 and 358 Lmol^{-1}cm^{-1}, respectively) and two high energy bands due to intra-ligand charge
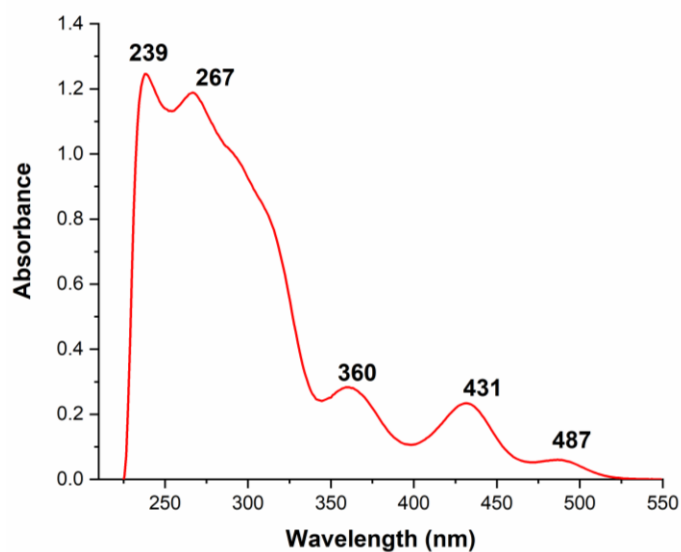

Figure 5.3 UV-vis spectrum of complex **1** at room temperature in dichloromethane at 1.66 × 10^{-4} molar concentration.

transfer (ILCT) at λ_{max} = 267 and 239 nm (molar extinction coefficient: 5168 and 3822 Lmol^{-1}cm^{-1}, respectively). Additionally, energy dispersive X-ray (EDX) of **1** verified the composition of Ir and Cl atoms as 1:1 (Figure 5.4).
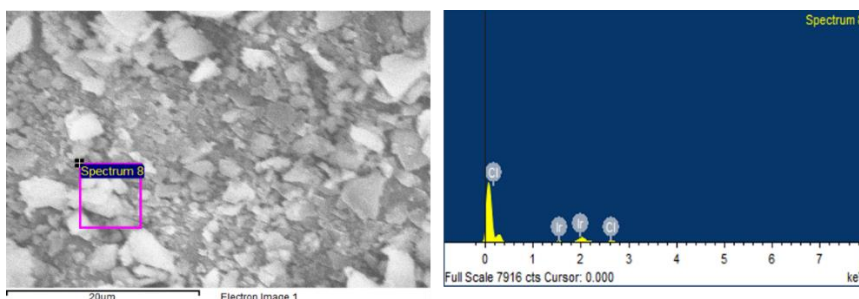

Figure 5.4 Energy dispersive X-ray (EDX) spectrum of complex **1**.

In further examination, the thermal stability test of complex **1** was performed. For this purpose, a series of heating experiments were conducted at various temperatures in solution. Utilizing toluene-D$_8$ and isopropanol-D$_8$ in separate NMR tubes, complex **1** was heated within the temperature range of 100-120 °C (Figures 5.5 and 5.6), and ^{1}H NMR spectra were recorded at different time intervals. The stacked ^{1}H NMR spectra strongly affirmed the absence of any decomposition of units (^{Me}BICAAC or COD) from the iridium center, emphasizing the notable thermal stability of complex **1**. Similarly, when complex **1** was dissolved in ^{i}PrOH and subjected to heating at 120 °C for 24 hours, no decomposition of **1** was observed (Figure 5.7).
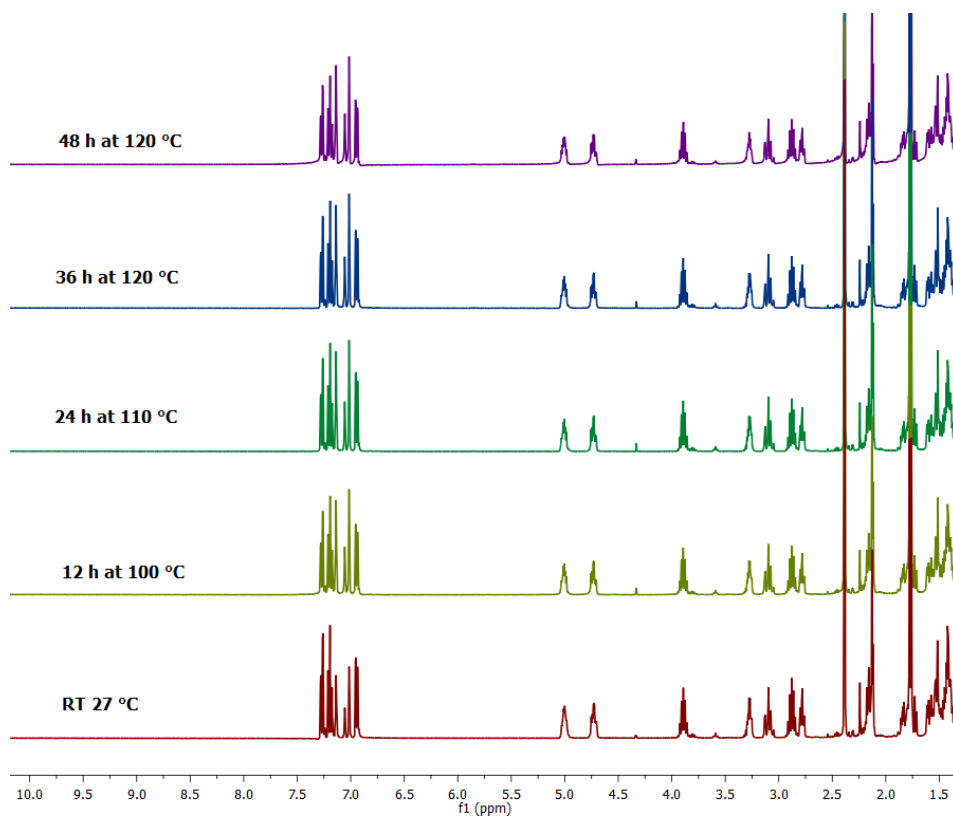
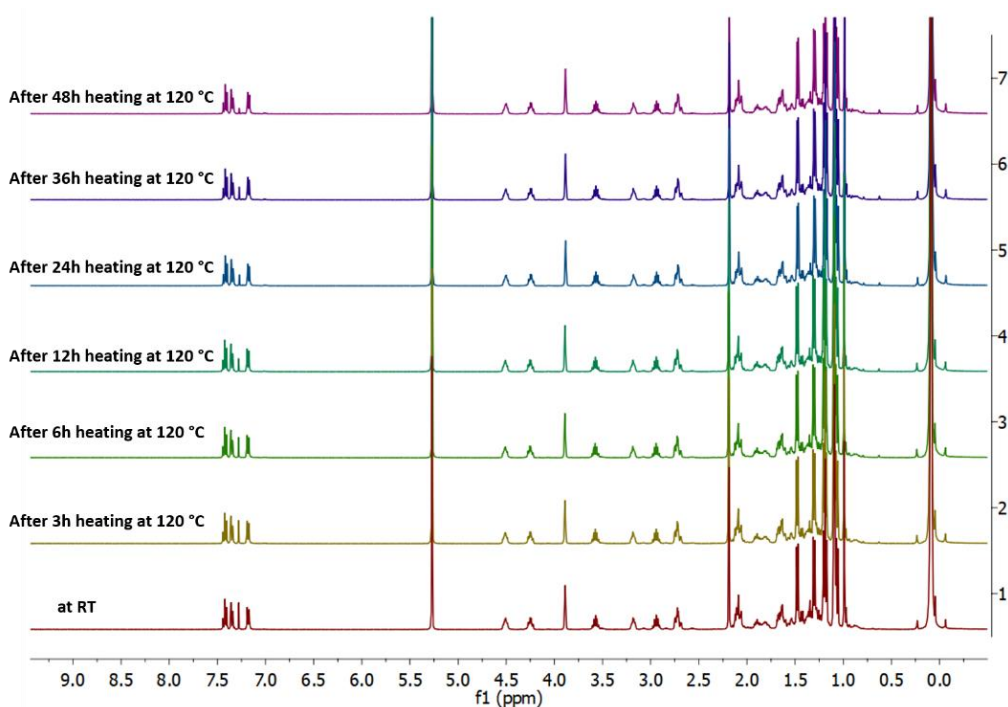**Figure 5.5** Thermal stability test of complex **1** in toluene-D_8 solution at various temperature and time intervals.

Figure 5.6 Thermal stability test of complex **1** in isopropanol-D_8 at various temperatures and time intervals.
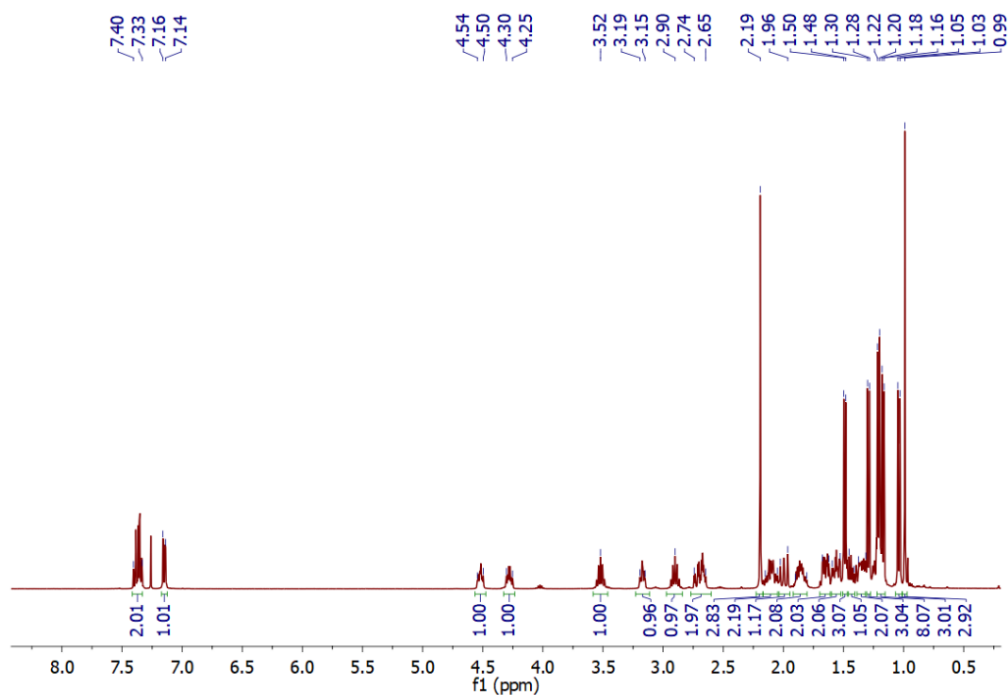
Figure 5.7 Thermal stability test of complex **1** after heating its solution in isopropanol at 120 °C for 24 hours. The ^{1}H NMR spectrum of the recovered material in CDCl$_3$ confirmed no thermal decomposition of **1**.

5.2.2 Syntheses and characterization of [Ir(^{Me}BICAAC)(COD)][SbF$_6$] (3) and [Ir(^{Me}BICAAC)(CH$_3$CN)(COD)][SbF$_6$] (4) complexes

Next, we aimed for the synthesis of a cationic iridium complex and further examined its reactivity towards Lewis bases for example acetonitrile. An equimolar reaction of **1** and AgSbF$_6$ in toluene for one hour under dark conditions afforded the red cationic complex [Ir(^{Me}BICAAC)(COD)]$^+$[SbF$_6$]$^-$ (**3**) in 96% yield (Scheme 5.2).
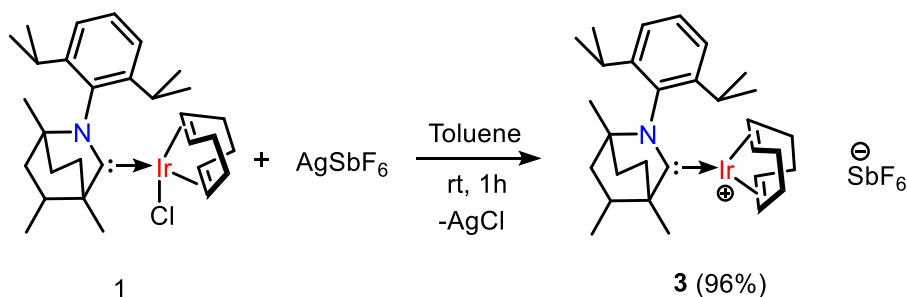
Scheme 5.2 Synthesis of complex [Ir(^{Me}BICAAC)(COD)][SbF$_6$] (**3**).

The ^{1}H NMR spectrum of **3** showed modest shift in the characteristic signals of olefinic COD protons observed as multiplets at δ = 4.56-4.53, 4.24-4.21, 3.64-3.60, and 3.16-3.12 ppm with respect to the **1** (δ = 4.54-4.49, 4.30-4.25, 3.19-3.15, 2.68-2.64 ppm). Similarly, the septets corresponding to the Dipp group were found to resonate in the upfield region at δ = 3.01 and 2.55 ppm with respect to the **1** (δ = 3.52 and 2.90 ppm). A ^{1}H NMR spectral comparison of complexes **1** and **3** showing the shift in the septets is given in Figure 5.8. The ^{13}C{^{1}H} NMR spectrum showed the metal bound carbene carbon was resonating at δ = 214.4 ppm, which was 47.5 ppm up-field shifted in comparison to the **1** (δ = 261.9 ppm). The formation of **3** was further supported by its HRMS spectrum which showed signals in positive ion mode at m/z = 612.3185 (calcd. 612.3182) as [M]$^+$ for [Ir(^{Me}BICAAC)(COD)] and a signal at m/z = 234.8788 (calcd. 234.8942) for anion part [SbF$_6$].
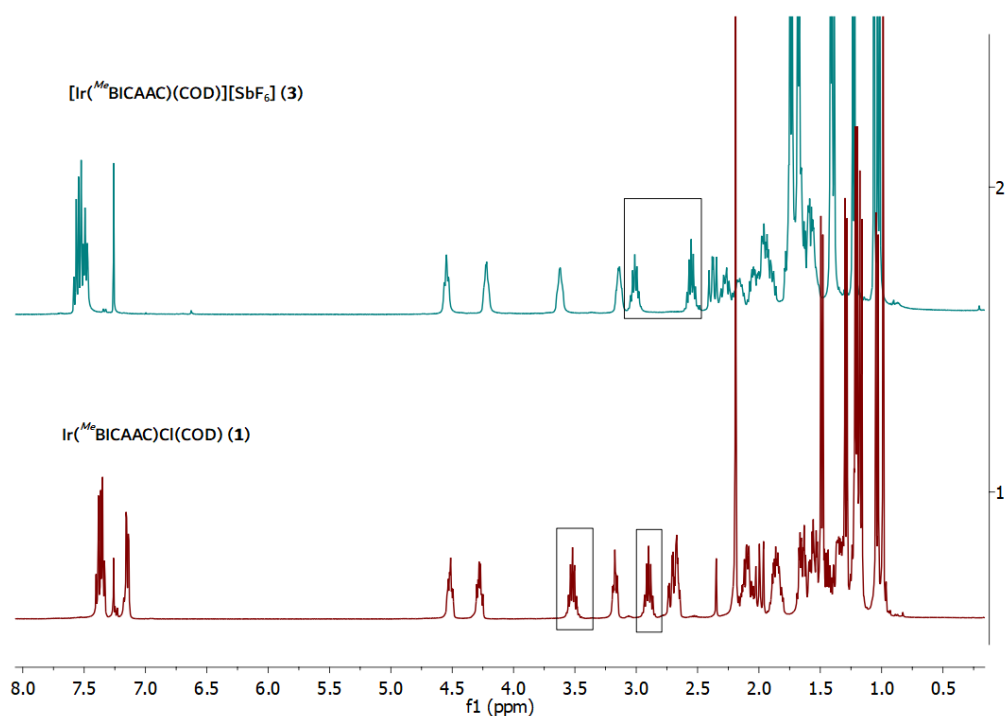

Figure 5.8 ^{1}H NMR (400 MHz, CDCl$_3$) spectral comparison of complex **1** (red) and **3** (blue).

Furthermore, the reaction of **3** with one equivalent of acetonitrile in chloroform for 1 h afforded the adduct [Ir(^{Me}BICAAC)(CH$_3$CN)(COD)]$^+$[SbF$_6$]$^-$ (**4**) as yellow solid in 92% yield (scheme 5.3). The ^{1}H NMR spectrum of complex **4** showed two merged septets

resonating at δ = 2.81-2.88 ppm for the dipp groups while $^{13}C\{^1H\}$ NMR spectrum revealed signal at δ = 257.5 ppm for the metal bound carbene carbon. The ^1H NMR spectrum of **4** exhibit signal for the coordinated acetonitrile moiety at δ = 2.62 ppm (for C*H*$_3$) while the $^{13}C\{^1H\}$ NMR spectrum revealed the signal for the same at δ = 3.6 ppm (for CH$_3$). The HRMS spectrum of **4** showed a signal at *m/z* = 653.3463 (calcd. 653.3447) in the positive ion mode corresponding to the cationic portion, [Ir(^{Me}BICAAC)(CH$_3$CN)(COD)]$^+$.
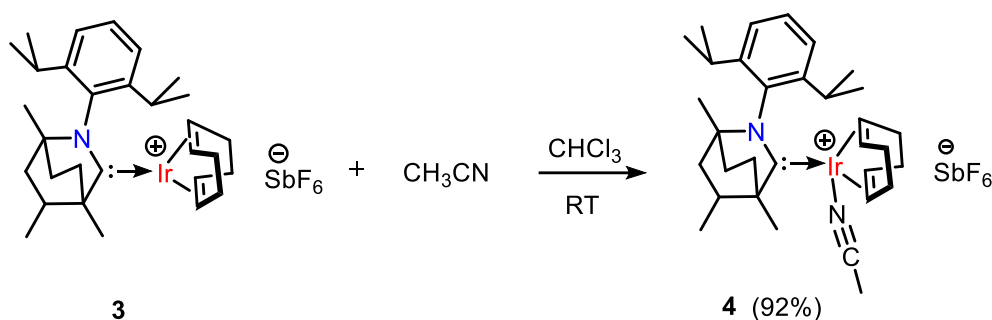
Scheme 5.3 Synthesis of complex **4**.

The solid-state structures of complexes **3-4** were confirmed from the single crystal X-ray diffraction studies. Complex **3** crystallized in monoclinic crystal system with *I*2/m space group. The Ir1−C1 bond length in **3** was found to be 2.043(8) Å which is comparable to its precursor **1** (2.030(6) Å), and the N1−C1−Ir1 bond angle was calculated as 102.8(5)° (Figure 5.9). The removal of chloride ion from **1** creates a vacant site at the iridium center in **3**, as a result, the iridium center in **3** showed a weak interaction with the ipso carbon of the Dipp group (C9 atom), with the Ir1−C9 bond separation of 2.358(8) Å and the N1−C1−Ir1 bond angle of 102.8(5)° (Figure 5.9). Complex **4** crystallized in monoclinic crystal system and possess *P21/c* space group. The Ir1−C1 bond separation of 2.038(4) Å in **4** is comparable to its precursor complex **3** (2.043(8) Å) (Figure 5.9). Upon attaching the acetonitrile molecule to the iridium center in **3**, the interaction originating from the ipso carbon C9 atom was no longer observed in **4**. The Ir1−N2 bond length in **4** was found to be

2.065(4) Å and the N1−C1−Ir1 and C1−Ir1−N2 bond angles were found to be 129.7(3) and 90.16(14)° respectively.
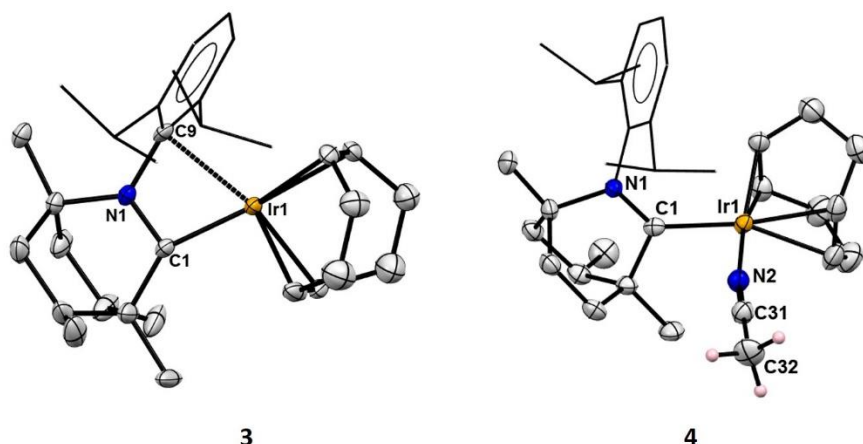

Figure 5.9 Single-crystal X-ray structures of complex **3** and **4**. Ellipsoids are shown at 50 % probability levels. All hydrogen atoms are omitted for clarity except for those attached with C32 in **4**. The anion $[SbF_6]^-$ is not shown in both the structures for clarity. Selected bond lengths (Å) and bond angles (°) for **3**: N1−C1 1.305(10), C1−Ir1 2.043(8), Ir1−C9 2.358(8), N1−C1−Ir1 102.8(5), C1−Ir1−C9 61.8(3); **4**: N1−C1 1.325(5), C1−Ir1 2.038(4), Ir1−N2 2.065(4), N1−C1−Ir1 129.7(3), C1−Ir1−N2 90.16(14).

The extent of steric hindrance posed by phosphine and carbene ligands within their complexes can be assessed through the calculation of percent buried volume (%V_{bur}) and the analysis of steric maps. %V_{bur} is defined as the fraction of the space surrounding the metal center, within a 3.5 Å radius, occupied by a specific ligand.[37a] The calculated %V_{bur} for $^{Me/iPr}$BICAAC-Ir(I) complexes were found to be 36.1 (for **1**), 39.0 (for **2**), 50.8 (for **3**) and 36.7 (for **4**) (Figure 5.10). The %V_{bur} for neutral complexes **1** and **2** (36.1 and 39.0, respectively) were found to be slightly higher than those reported for NHC based Ir(I)-complexes, (26.1 for (IDM)IrI(COD); 27.3 for (ICy)IrCl(COD); 35.7 for (I^{t}Bu)IrCl(COD); 33.5 for (IMes)IrCl(COD) and 34.9 for (IPr)IrCl(COD)[37b] (where IDM = 1,3-bismethylimidazol-2-ylidene; Icy = 1,3-biscyclohexylimidazol-2-ylidene; I^{t}Bu = 1,3-bistert-butylimidazol-2-ylidene; IMes = 1,3- dimesitylimidazol-2-ylidene; SIMes = 1,3-dimesityl-

4,5-dihydroimidazol-2-ylidene; and IPr =1,3-bis(2,6-di-iso-propylphenyl)imidazol-2-ylidene) and comparable with some CAAC-metal complexes.[37c] The slightly higher values of %V_{bur} for complexes **1**-**4** are attributed to higher steric demand of $^{Me/iPr}$BICAAC ligands.
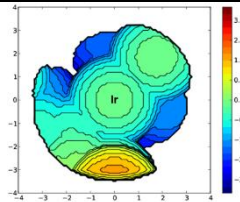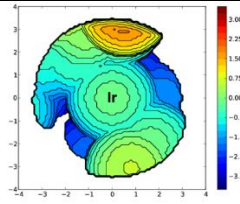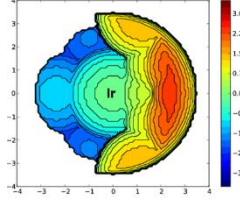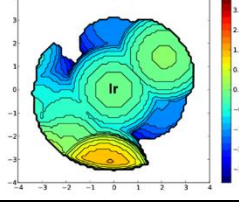
	%V_{bur} for M-carbene length at 2.00 Å	%V_{bur} in each quadrant	Steric maps
1	36.1	SW = 47.2 NW = 22.5 NE = 40.1 SE = 34.5	
2	39.0	SW = 27.4 NW = 44.7 NE = 39.1 SE =44.9	
3	50.8	SW = 27.5 NW = 27.5 NE = 74.1 SE = 74.4	
4	36.7	SW = 49.2 NW = 23.0 NE = 41.8 SE =32.8	

Figure 5.10 Calculated %buried volume and the corresponding steric maps for complexes **1**-**4**.

5.2.3 Catalytic activity of complexes 1-4 for transfer hydrogenation reaction

Transfer hydrogenation of carbonyls: Following the successful synthesis of complexes **1**-**4** we proceeded to explore their application in transfer hydrogenation reactions. Our investigation commenced with the use of 4-chlorobenzaldehyde as the model substrate and

*i*PrOH as the hydrogen delivery agent. The reaction was carried out in the presence of 0.5 mol% of **1** and 10 mol% of KOH at 100 °C and provided the product, (4-chlorophenyl)methanol **5d** in 95% of isolated yield after 3 h (Table 5.1, entry 1). Under the same set of reaction conditions, we explored various bases, among them, Cs$_2$CO$_3$ and NaH proved to be effective in producing the desired product in good yield, while the utilization of

Table 5.1. Optimization of reaction conditions for transfer hydrogenation of benzaldehyde with complexes **1-4**[a]
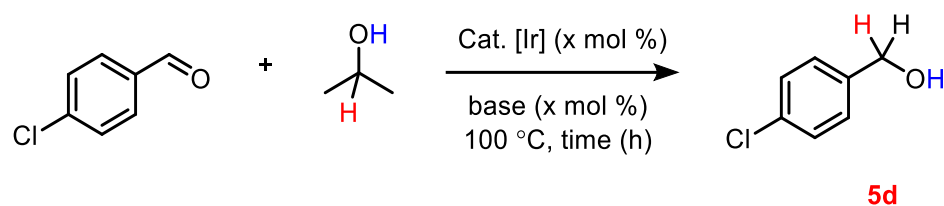
Entry	Catalyst (mol%)	Base (10 mol%)	Time (h)[b]	Yield (%)[c]
1	**1** (0.5)	KOH	3	95
2	**1** (0.5)	Cs$_2$CO$_3$	3	95
3	**1** (0.5)	NEt$_3$	3	5
4	**1** (0.5)	NaOAc	3	65
5	**1** (0.5)	NaH	3	90
6	**1** (0.5)	*t*BuOK	3	10
7	***1* (0.1)**	**KOH**	**30 min**	**95**
8	**2** (0.1)	KOH	30 min	96
9	**3** (0.1)	KOH	30 min	95
10	**4** (0.1)	KOH	30 min	93
11	-	KOH	3	Nd[d]

[a]Reaction Conditions: 4-chlorobenzaldehyde (2 mmol), isopropanol 3 mL, catalyst, base loading and time as specified in the table at 100 ˚C; [b]time in hours except for entries 7-10, [c]yield of isolated products are mentioned; [d]not detectable.

other bases had a detrimental impact on the product yield (Table 5.1, entries 2-6). Thereafter, we reduced the catalyst load to 0.1 mol% and reaction time to 30 minutes in combination with KOH (10 mol%) and we found no destructive impact on the yield of product **5d** (Table 5.1, entry 7). Subsequently, we assessed the catalytic performance of complexes **2**, **3**, and **4** under the aforementioned optimized conditions (catalyst loading 0.1 mol% and KOH 10 mol% in 30 minutes), all the complexes furnished good yield of the product in 30 minutes (Table 5.1, entries 8-10). Altogether, a combination of 0.1 mol% catalyst and 10 mol% KOH at 100 °C in ^{i}PrOH proved to be an efficient optimal protocol for 4-chlorobenzaldehyde in 30 minutes (Table 5.1, entry 7). As expected, the absence of catalysts led to a failure in product formation, clearly indicating the indispensable role of the catalyst in facilitating the hydride transfer step (Table 5.1, entry 11).

The reaction profiles for complexes **1**-**4** were monitored by ^{1}H NMR measurements for 4-chlorobenzaldehyde as the substrate under the conditions: catalyst loading 0.1 mol%, KOH 10 mol%, 100 °C in ^{i}PrOH. Catalyst **1** showed 98% conversion in 25 minutes with a TOF value of 2400 h^{-1} [TOF (turnover frequency): [{(mol of product)/(mol of catalyst)}/time(h)], TOF was determined once a minimum conversion of 98% had been attained (Figure 5.11). Similarly, complex **2** exhibited 99% conversion in 20 minutes (TOF of 3000 h^{-1}), and complexes **3** and **4** both showed 98% conversions in 25 minutes (TOFs of 2400 h^{-1}) (Figure 5.11).

The outcomes prompted us to investigate the broader applicability of the catalyst by assessing a range of electronically rich and poor aldehydes using the established procedure. Although all complexes **1**-**4** demonstrated similar catalytic performance, we opted complex **1** to delve further into the investigation, primarily due to its straightforward synthesis. The findings listed in Table 5.2 demonstrate that benzaldehyde and its derivatives containing electron-withdrawing groups such as -Cl, -Br, -CN smoothly underwent the TH reaction to
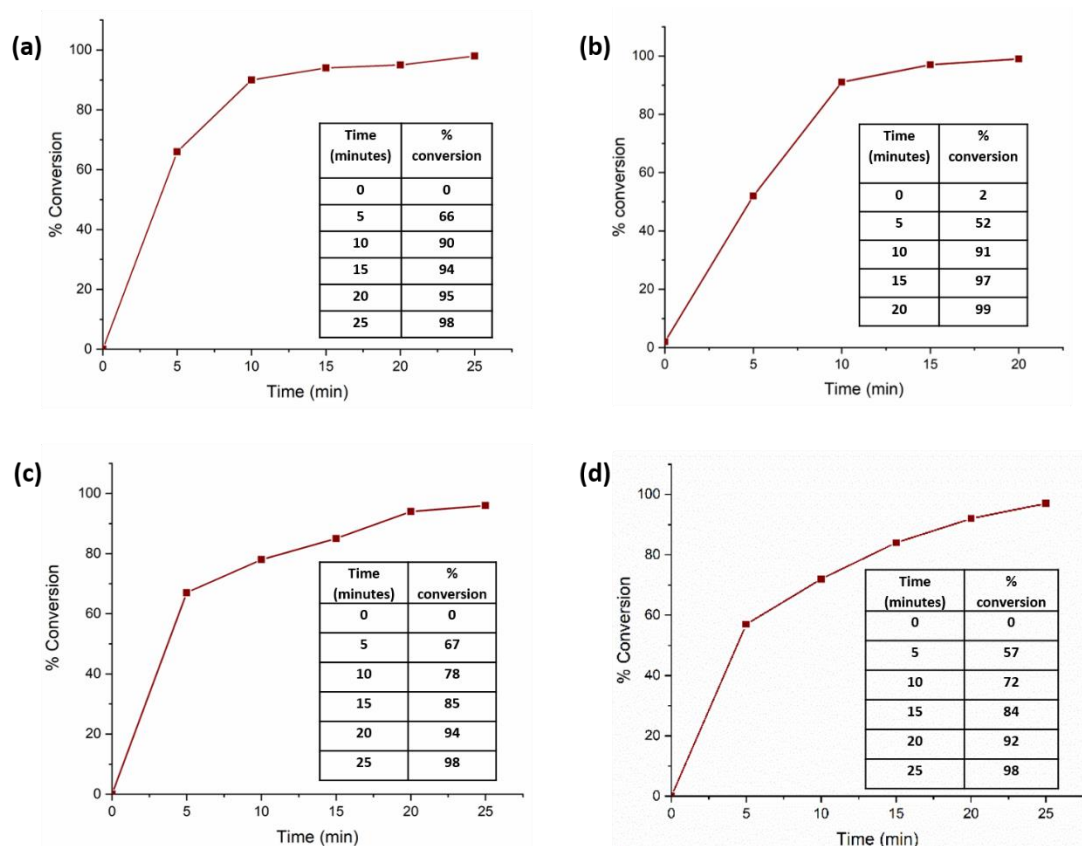
Figure 5.11 Time profile curves for transfer hydrogenation of 4-chlorobenzaldehyde using catalysts **1** (plot **a**), **2** (plot **b**), **3** (plot **c**) and **4** (plot **d**). The % conversion was calculated from ^{1}H NMR measurements.

give the reduced products in good yields (82-97%) in30 minutes (Table 5.2, **5a-5f**). The potentially reducible -CN and -NO$_2$ groups remained unaffected, emphasizing the catalyst's selectivity only towards the carbonyl moiety. The 4-cyanobenzaldehyde yields 82% reduced product in 30 minutes, while the 4-nitrobenzaldehyde yields only 42% of **5g** in 30 minutes, however extending the reaction for 3 h yields 90% of **5g** (Table 5.2). The benzaldehyde derivatives containing electron-donating groups were observed to undergo reduction at a slower rate compared to substrates with halogen groups. Benzaldehyde derivatives having -Me, -OMe and -^{i}Pr groups supplied the corresponding alcohols in good yields (88-96%) in 1-3 hours (Table 5.2, **5h-5k**). Moreover, the sterically hindered 1-naphthaldehyde and 1-anthracenealdehyde were also found acceptable for TH reaction, yielding the corresponding

Table 5.2 Screening of substrates for transfer hydrogenation of aldehydes and ketones catalyzed by Ir(^{Me}BICAAC)Cl(COD)^{a,b,c}
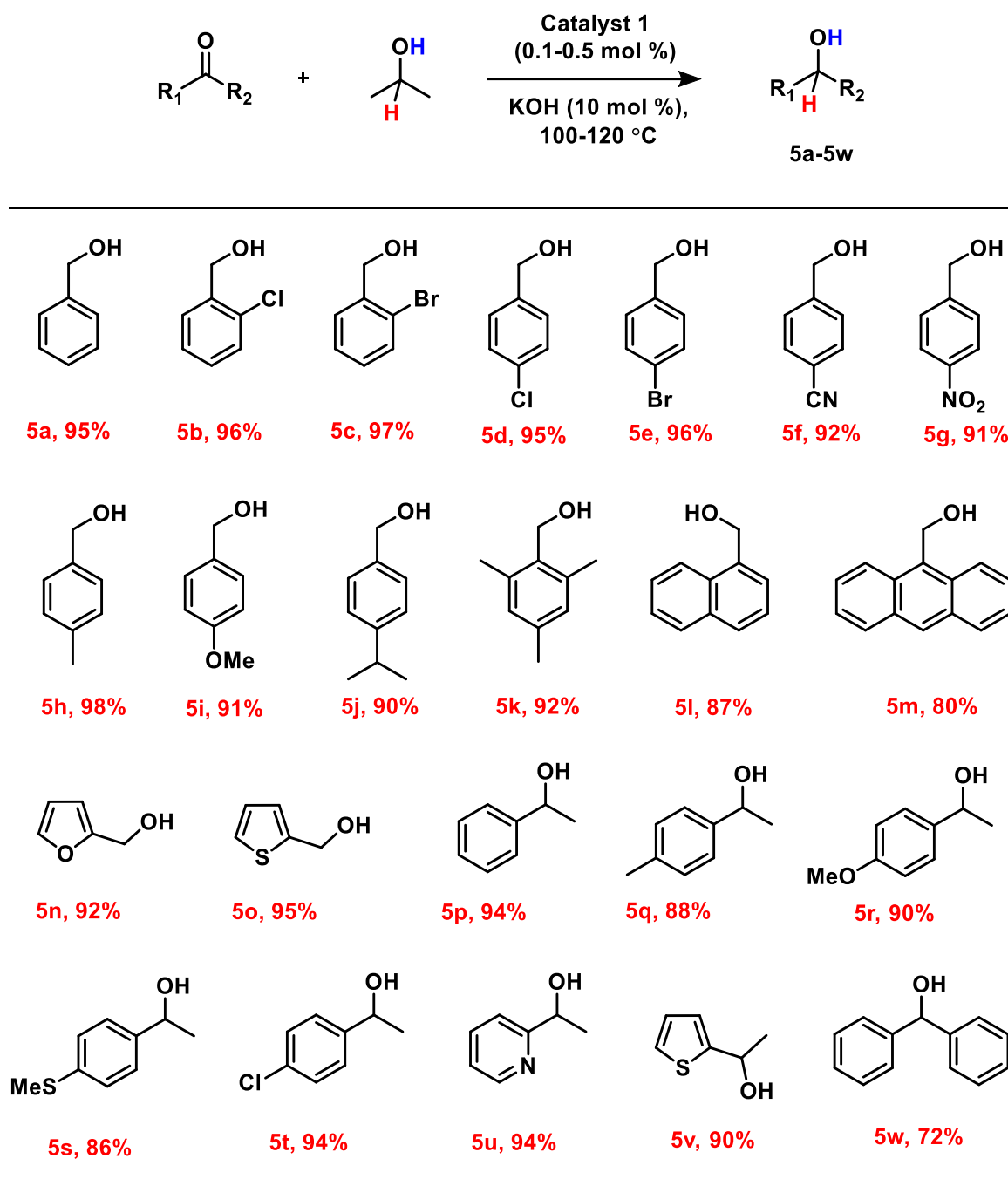
^{a}Reaction conditions: For aldehydes (2 mmol), catalyst **1** (0.1 mol%), KOH (10 mol%) in isopropanol (3 mL) stirred at 100 ˚C for specified time in the Table; ^{b}For ketones (1 mmol), catalyst **1** (0.5 mol%), KOH (10 mol%) in isopropanol (3 mL) stirred at 120 ˚C for 24 h; ^{c}Isolated yields.

reduced products in 85 and 79% yields, respectively, within 30 minutes (Table 5.2, entries **5l-5m**). Furthermore, the heteroaromatic aldehydes such as furan-2-carbaldehyde and thiophene-2-carbaldehyde were well tolerated, yielding the reduced products in 84% and 88% yield, respectively in 30 minutes (Table 5.2, 5n-5o).

Having accomplished the successful transformation of various aldehydes into alcohols, we focused towards the TH of more challenging ketone moieties. This endeavor commenced with acetophenone serving as the model ketone substrate, and the reduction was performed under the previously optimized conditions (0.1 mol% catalyst and 10 mol% KOH). This catalytic protocol afforded the reduced product, 1-phenylethanol **5p** in slightly lower yield of 55% even after 24 h. In an effort to enhance the product yield, we introduced some modifications to the previously mentioned reaction conditions. By increasing the catalyst loading to 0.5 mol% and raising the temperature to 120 °C, we achieved the formation of **5p** with a notable increase in yield, reaching 94% in 24 hours (Table 5.2) (TOF = 7.84 h^{-1}). Nevertheless, the most favorable turnover frequency (TOF) value, amounting to 50,000 h^{-1} for the transfer hydrogenation of benzophenone, was documented by Crabtree and co-workers utilizing an iridium bis-carbene complex.[38a] Following that, we evaluated the compatibility of catalyst **1** with a range of electronically diverse ketone derivatives as part of the substrate scope assessment under the modified protocol. The TH of acetophenone, incorporating electron-rich (-Me, -OMe, and -SMe) as well as electron-deficient (-Cl) substituents, proceeded efficiently and the anticipated reduced products were obtained in good to high yields (86-94%) (Table 5.2, entries **5q-5t**). Additionally, the catalytic activity of **1** was examined for more challenging heteroaromatic substrates, 2-acetylpyridine and 2-acetylthiophene. Their tendency to coordinate to the metal center often poses a challenge to the catalyst's efficiency.[38b] Despite this, the successful generation of their respective products **5u** and **5v** in good yields (90-94%) highlighted the efficacy of the catalyst (Table

5.2). When sterically hindered benzophenone was subjected to transfer hydrogenation, a yield of 72% for the desired product **5w** was achieved (Table 5.2).

Transfer hydrogenation of imines: Subsequently, we explored the efficacy of the catalyst **1** for the TH of imine functionalities, which are known to be more resistant to reduction compared to ketones.[28,29d,g] We commenced the investigation by evaluating (E)-N,1-diphenylmethanimine as the benchmark substrate using the protocol established for ketones: 0.5 mol% catalyst loading, 10 mol% KOH, at 120 °C for 24 hours, afforded the amine product **6a** in 75% of isolated yield. Pleasingly, when the catalyst loading was increased to 1

Table 5.3 Screening of imine substrates for transfer hydrogenation catalyzed by Ir(*Me*BICAAC)Cl(COD)[a,b]

6a, 92%   6b, 92%   6c, 90%   6d, 94%

6e, 85%   6f, 87%   6g, 95%   6h, 90%

6i, 55%
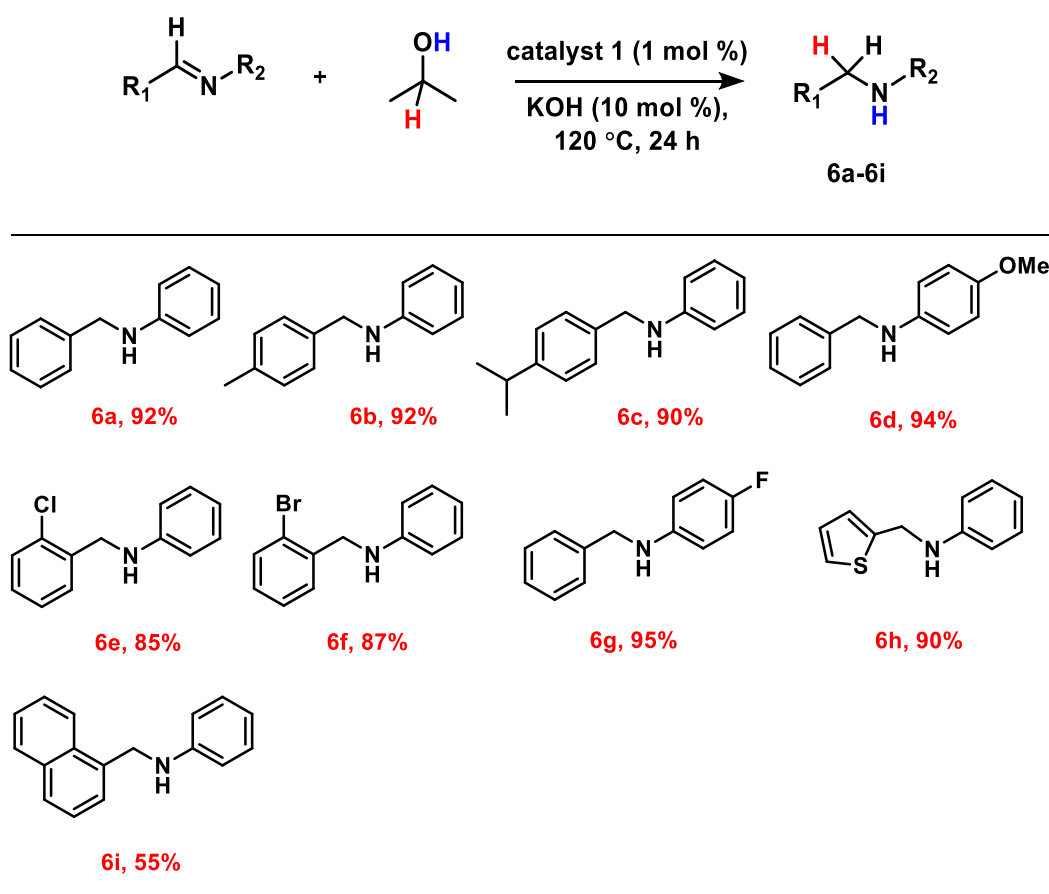
[a]Reaction conditions: Imines (1 mmol), catalyst 1 (1 mol%), KOH (10 mol%) in isopropanol (3 mL) stirred at 120 ˚C for 24 h; [b]Isolated yields

mol%, the corresponding amine product **6a** was isolated with a yield of 92% (TOF = 3.8 h^{-1}) (Table 5.3). Nevertheless, even in this case, an extended reaction time of 24 hours was necessary. This could be attributed to the favorable coordination of the imine nitrogen to the Ir-center. Following that, we investigated the potency of catalyst **1** for a different set of imines. The imines containing electron-donating groups such as -Me, -^{i}Pr, and -OMe were converted into their respective amines **6b**, **6c**, and **6d** in good yields (90-94%) (Table 5.3). The imines containing halogens (-Cl, -Br, and -F) exhibited no significant influence of their electronic factors on the yield of the final products **6e**, **6f** and **6g**, with yields ranging from 85-95% (Table 5.3). Moreover, the heterocyclic imine, (E)-N-phenyl-1-(thiophen-2-yl)methanimine, was successfully converted into the corresponding amine **6h** with a yield of 90% (Table 5.3). Regrettably, subjecting the reaction to a bulky imine under optimal catalytic conditions resulted in a lower yield of the amine product 6i (55%) (Table 5.3). Next, we sought to assess the feasibility of TH using methanol as a more challenging hydrogen source. Unfortunately, a test reaction with benzaldehyde in methanol under the optimized protocol resulted in a mixture of products. Our catalyst did not demonstrate compatibility with methanol for the TH strategy.

Furthermore, to investigate the operational mode of catalyst **1** (whether it acts as a homogeneous or heterogeneous catalyst), we conducted the mercury drop test and the hot filtration test for both model reactions (transfer hydrogenation and hydrosilylation). In both cases, we obtained good yields of the respective products. The results of both experiments support that catalyst **1** operates as a homogeneous catalyst, as its catalytic activity was not affected by the presence of Hg, and no nanoparticle formation was observed during the hot filtration test. To verify the possibility of nanoparticle formation during the transfer hydrogenation (TH) reaction conditions, we conducted a catalytic TH reaction with an increased amount of catalyst **1** (20 mol%). After heating the reaction mixture for 3 and then 6

hours, no decomposition of the catalyst was observed in terms of detachment of carbene and COD unit, as evidenced by the absence of signals for cyclooctane and hydrogenated BICAAC in the ^{1}H NMR spectrum of the recovered catalyst.

5.2.4 Mechanistic insights

Deuterium labelling experiment: To gain insight into the mechanistic pathway, we have performed a deuterium labeling experiment. The reaction of benzophenone with isopropanol-D_8 under the optimized reaction protocol, as used for ketones, was carried out. The isolated product **5w'** demonstrated up to 95% deuterium incorporation at the carbonyl carbon (Scheme 5.4). The absence of deuterium incorporation at the oxygen can be attributed to the acidic nature of the OH proton, causing rapid H/D exchange during the reaction and work-up processes. The deuterium labelling experiment confirmed that isopropanol-D_8 was the sole source of hydrogen available in
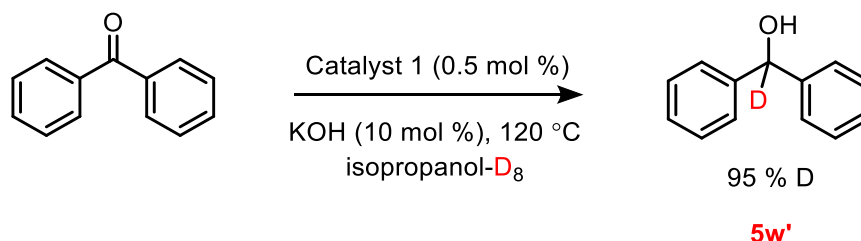
Scheme 5.4 Transfer hydrogenation of benzophenone in isopropanol-D$_8$.

the reaction. A similar experiment was carried out using isopropanol-D_7 (CD$_3$)$_2$C(D)OH, which afforded approximately 95% deuterium incorporation at the carbonyl carbon. This observation provides support for the likelihood of a monohydride pathway for transfer hydrogenation.[38a, 39]

Cross experiments: To gain insights into the key operating steps involved in the present case, we conducted a stoichiometric reaction of ^{i}PrOK with Ir(^{Me}BICAAC)Cl(COD) in an NMR tube in C$_6$D$_6$ (Scheme 5.5). After 4 hours at room temperature, the ^{1}H NMR spectrum

displayed the persistence of the septet (δ = 4.16 ppm) and the doublet (δ = 1.28 ppm) corresponding to ^{i}PrOK which indicates no reaction has occurred at room temperature (Figure 5.12). However, upon heating the NMR tube at 80 °C for 12 h, a notable up-field shift in the previously mentioned characteristic signals to δ = 3.77 and 1.05 ppm, respectively, was observed which suggested the binding of the -O^{i}Pr unit to the iridium center (Figure 5.13). Additionally, the appearance of a signal at δ = 1.56 ppm has been attributed to the concurrent formation of acetone, supporting the occurrence of a facile β-hydride elimination from the Ir-isopropoxide moiety (Figure 5.14).
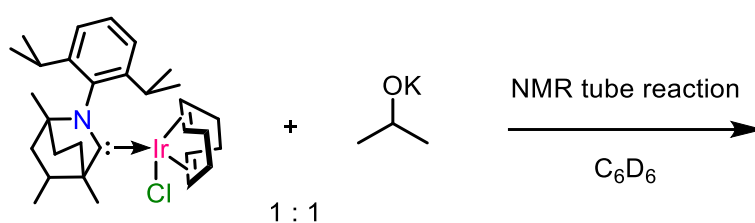
Scheme 5.5 Stoichiometric NMR tube reaction of **1** and ^{i}PrOK in C$_6$D$_6$.
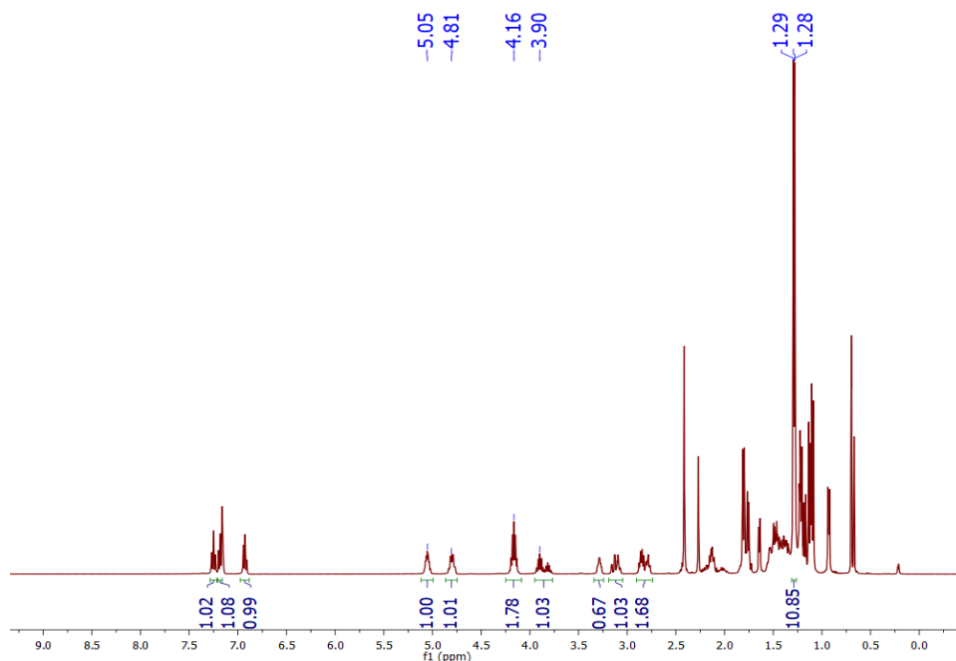
Figure 5.12 ^{1}H NMR (400 MHz, C$_6$D$_6$) spectrum of room temperature stoichiometric reaction of Ir(^{Me}BICAAC)Cl(COD) with ^{i}PrOK. The septet (δ = 4.16 ppm) and doublet (δ = 1.28 ppm) that correspond to ^{i}PrOK, and signals for Ir(^{Me}BICAAC)Cl(COD) indicate no reaction.

200
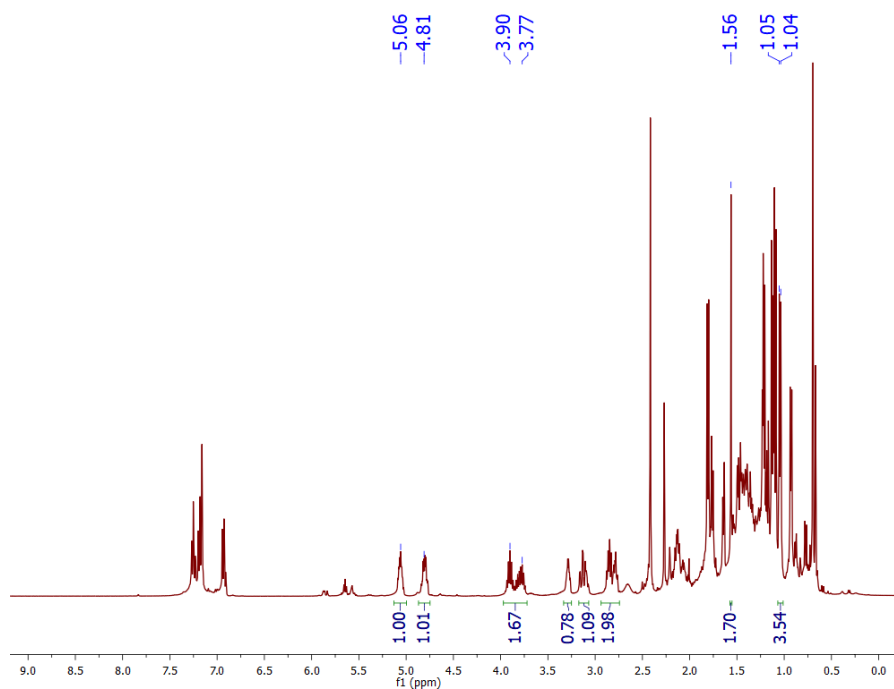
Figure 5.13 ^{1}H NMR (400 MHz, C$_6$D$_6$) spectrum of the above reaction mixture after heating the NMR tube at 80 °C for 12 h; showing the disappearance of the septet and doublet (at δ = 4.16 and 1.28 ppm, respectively) and appearance of a new septet and a doublet (at δ = 3.77 and 1.05 ppm, respectively).
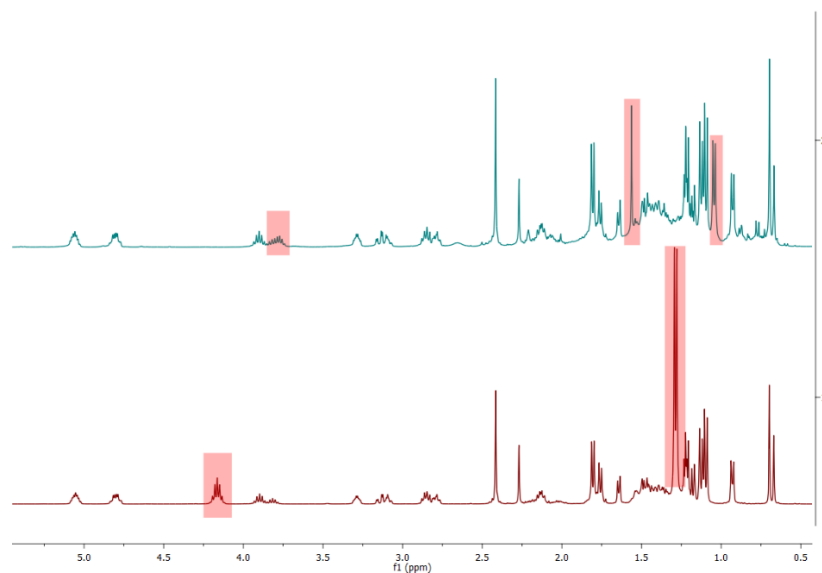
Figure 5.14 ^{1}H NMR (400 MHz, C$_6$D$_6$) spectral comparison of stoichiometric reaction of Ir(^{Me}BICAAC)Cl(COD) with ^{i}PrOK; (1) ^{1}H NMR spectrum without heating of the reaction mixture (below), (2) ^{1}H NMR spectrum after heating of the reaction mixture (above); showing shift in the positions of the septet and the doublet along with the emergence of acetone signal.

Subsequently, one equivalent of benzaldehyde (PhCHO) was added to the NMR tube and the reaction progress was monitored at different intervals of time. The ^{1}H NMR spectrum after 2 h at room temperature displayed the slight up-field shift of septet (δ = 3.72 ppm) and doublet (δ = 0.99 ppm) of Ir-bonded -O^{i}Pr (Figure 5.15). The appearance of a new singlet at δ = 4.41 ppm (PhCH_2O-Ir) suggests the transfer of hydride to the carbonyl carbon of the benzaldehyde (Figure 5.15). To expedite the reaction, the sample was subjected to heating at 45 °C and then at 80 °C, the acceleration in the rate of reaction was noticed (Figure 5.16). With time, the intensity of the signals corresponding to the benzaldehyde at δ = 9.64 ppm and iridium- bound -O^{i}Pr (δ = 3.72 and 0.99 ppm) were diminished and the signal at δ = 4.41 ppm intensified (Figures 5.16-5.18). The complete consumption of benzaldehyde occurred after 16 h at 80 °C. The signal for acetone formed (δ = 1.56 ppm) remained present throughout the experiment.
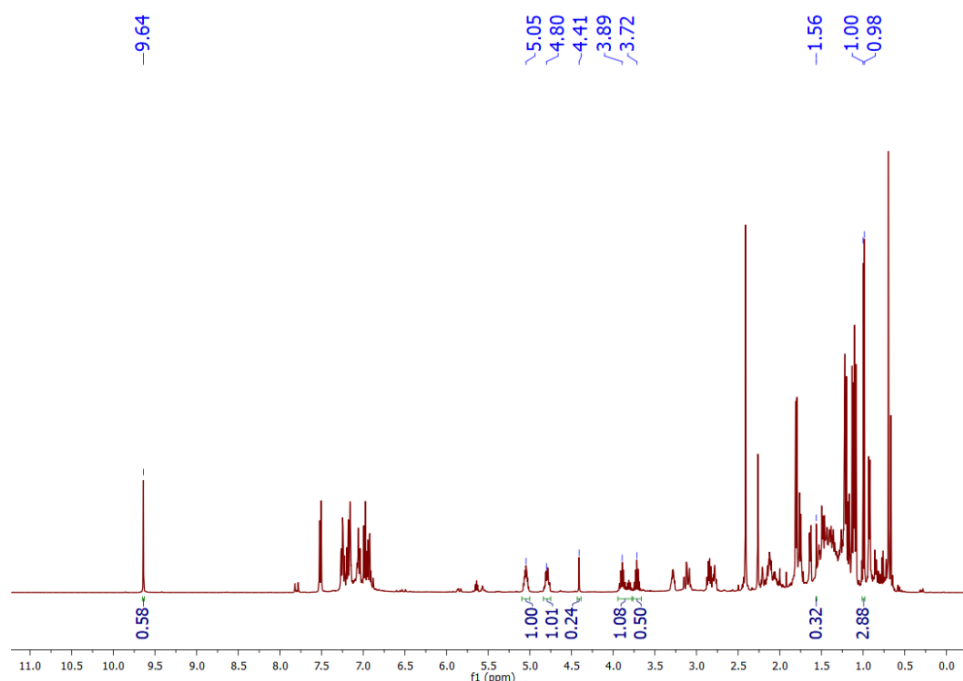
Figure 5.15 ^{1}H NMR (400 MHz, C$_6$D$_6$) spectrum after the addition of stoichiometric amount of PhCHO in the previous reaction mixture. The emergence of new signal at δ = 4.41 ppm indicating the transfer of hydride from iridium center to the carbonyl carbon of benzaldehyde.
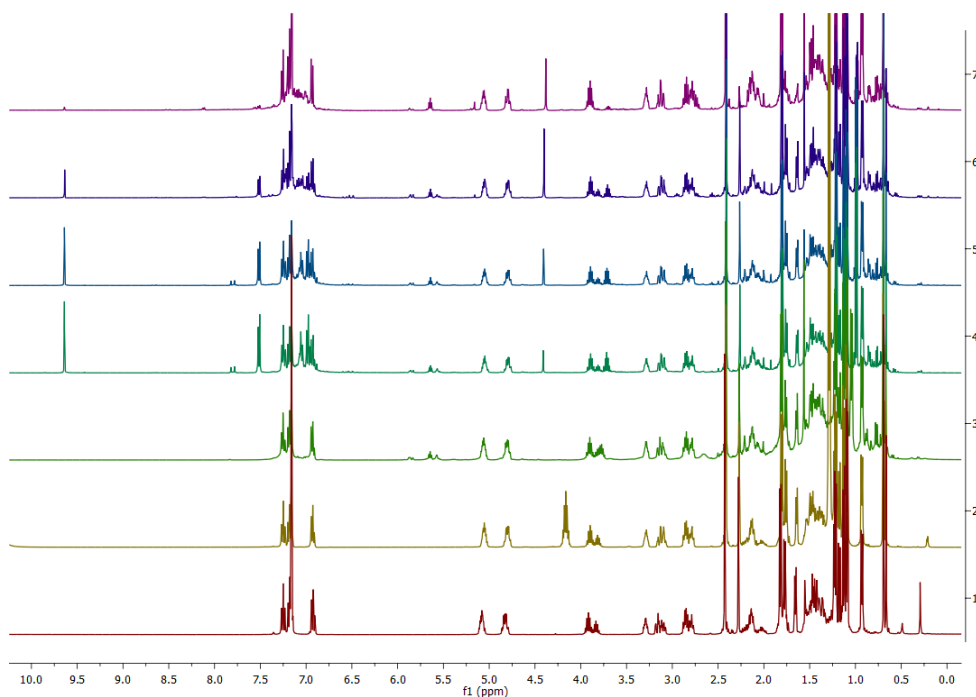
Figure 5.16 ^{1}H NMR (400 MHz, C$_6$D$_6$) spectral comparison (bottom to top): (1) rt ^{1}H NMR of Ir(^{Me}BICAAC)Cl(COD) (2) stoichiometric reaction of Ir(^{Me}BICAAC)Cl(COD) with ^{i}PrOK performed at rt; (3) after 12 h heating; (4) addition of stoichiometric amount of PhCHO in the reaction mixture at rt, sample recorded after 2 h; (5) 20 min heating at 45 °C; (6) 5 h heating at 80 °C; (7) 16 h heating at 80 °C.

Figure 5.17. Expansion of the selected spectral region of ^{1}H NMR (400 MHz, C$_6$D$_6$) spectra and comparison of the spectra presented above in Figure 5.16.

203

We made attempts to crystallize Ir(^{Me}BICAAC)(O^{i}Pr)(COD) complex by performing reaction of ^{i}PrOK and Ir(^{Me}BICAAC)Cl(COD) as discussed above. The efforts to obtain crystals suitable for X-ray diffraction were not successful, however, the HRMS measurements on the product showed the signal at m/z = 669.3453 (calcd. 669.3524) that was attributed to the molecular ion peak for [Ir(^{Me}BICAAC)(COD)(Me$_2$CO)]$^+$ as [M]$^+$ and another signal at m/z = 612.3195 (calcd. 612.3182) corresponds to [M-O^{i}Pr]$^+$ moiety (Figures 5.19-5.20). Additionally, we have made several attempts to isolate the Ir-hydride complex by reacting Ir(^{Me}BICAAC)Cl(COD) with different hydride sources like KH and NaBH$_4$, but these attempts remained unsuccessful.
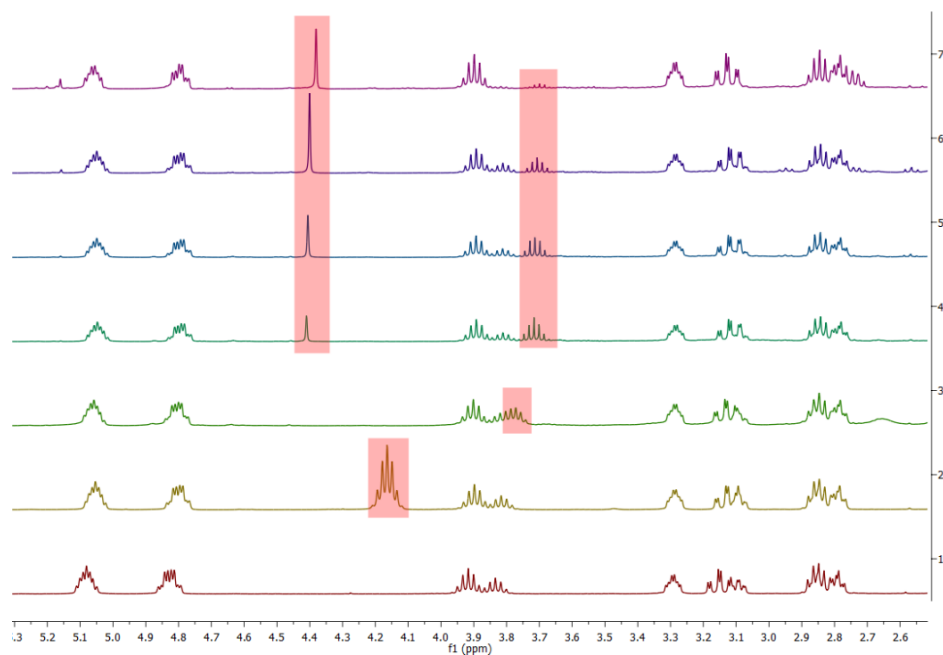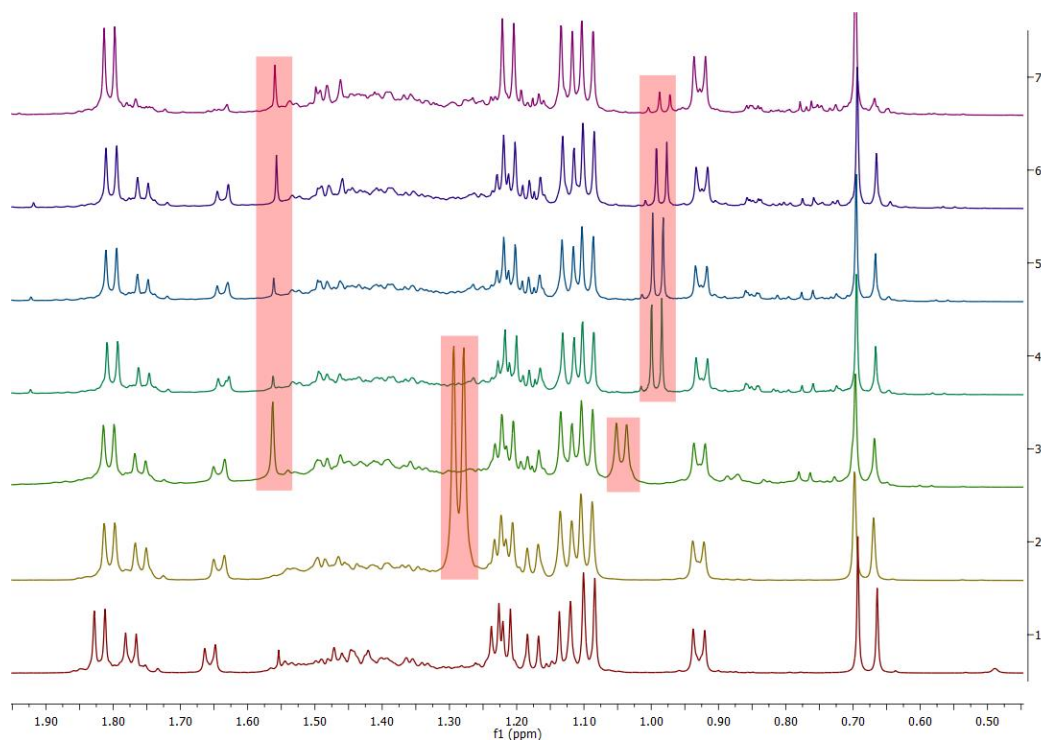

Figure 5.18 Expansion of the selected spectral region of ^{1}H NMR (400 MHz, C$_6$D$_6$) spectra and comparison (bottom to top) of the spectra presented above in Figure 5.16.
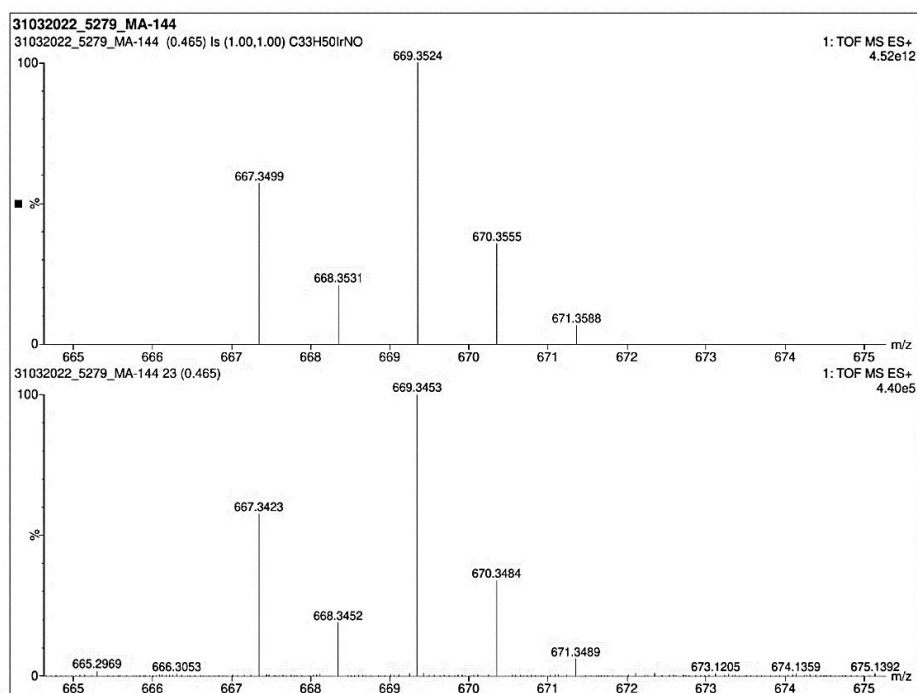
Figure 5.19 HRMS (ESI$^+$) spectrum of [M'-Me$_2$CO]$^+$.
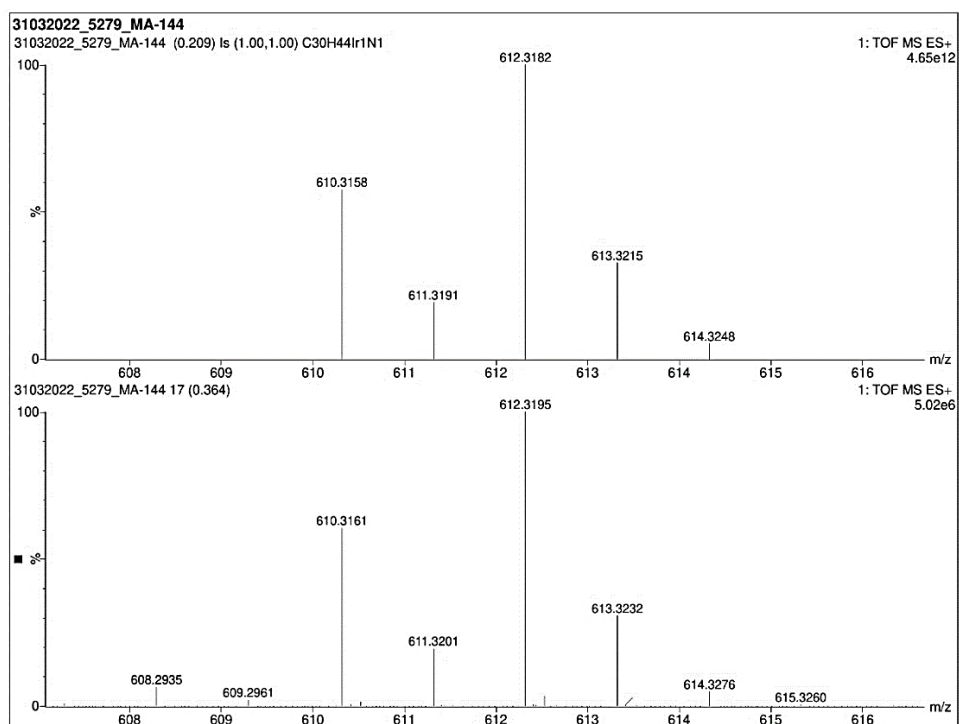
Figure 5.20 HRMS (ESI$^+$) spectrum of [M-O^{i}Pr]$^+$.

The widely accepted mechanism for TH reactions typically involves three main steps: a) the formation of the metal-alkoxide complex; b) followed by the generation of the metal-hydride; and c) subsequent delivery of the hydride to the unsaturated substrates. Based upon

205

the results obtained from the deuterium labelling test and control experiments, we have postulated a plausible mechanism presented in Scheme **5.6**. The initial step involves the extrusion of KCl in the presence of KOH to create a vacant site for -O^{i}Pr to interact with the iridium center and led to the formation of Ir-alkoxide species **A**. As per the literature reports, the unsaturated coordination sphere around the iridium center in **A** favors the β-hydride elimination and generates the acetone coordinated Ir-H complex **B** which undergo the removal of acetone molecule to afford the Ir−H complex **C**. It is to be noted that the Ir−H species **C** could not be characterized by spectroscopic means and its formation is proposed based on the formation of acetone in the reaction mixture. Subsequently, in the next step, the hydride from the Ir-centre is transferred to the carbonyl carbon of the substrate as shown in **D**
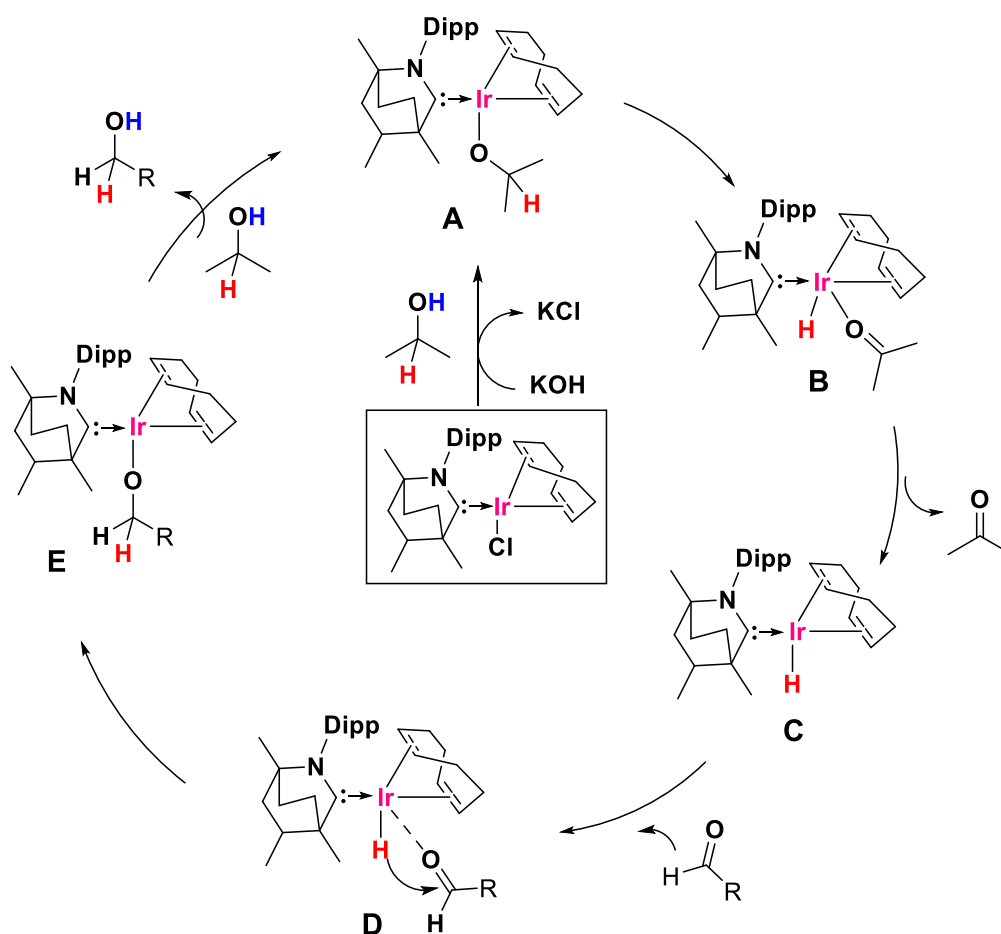
Scheme 5.6 Proposed catalytic cycle for transfer hydrogenation reaction with Ir(^{Me}BICAAC)Cl(COD) complex.

which results in the formation of the Ir-alkoxide complex **E**. Finally, proton transfer from isopropanol to **E** delivered the desired reduced product with the regeneration of the active catalyst **A** for the next cycle. We believe that a similar reaction pathway is also followed for ketones as well as imines.

5.3 Conclusions

In this chapter we have discussed the syntheses and characterization of bicyclic (alkyl)(amino)carbene ($^{Me/iPr}$BICAAC) supported covalent and cationic Ir complexes, Ir(^{Me}BICAAC)Cl(COD) (**1**), Ir(^{iPr}BICAAC)Cl(COD) (**2**), [Ir(^{Me}BICAAC)(COD)][SbF$_6$] (**3**) and [Ir(^{Me}BICAAC)(CH$_3$CN)(COD)][SbF$_6$] (**4**). All complexes exhibited comparable activity for the transfer hydrogenation of 4-chlorobenzaldehyde. However, owing to its ease of synthesis, complex **1** was selected as the catalyst for the transfer hydrogenation of various functionalities, including aldehydes, ketones, and imines, using isopropanol as the hydrogen source. A diverse range of substrates functionalized with both electron-withdrawing and donating substituents were systematically investigated, yielding the corresponding reduced products in moderate to good yields. Deuterium labeling studies provided confirmation of the role of isopropanol as the hydrogen delivery agent. Additionally, a series of control experiments were conducted, revealing the participation of Ir−O^{i}Pr species as a reaction intermediate.

5.4 Experimental section

5.4.1 General methods

All the manipulations were performed under an inert atmosphere of dry nitrogen or argon using a glove box or standard Schlenk techniques. All the glassware were dried at 150 °C in

an oven for at least 12 h and assembled hot and cooled in vacuo prior to use. Solvents were purified by MBRAUN solvent purification system MB SPS-800 and were used directly from the SPS system. Chemicals were purchased from Sigma-Aldrich, HIMEDIA, and Avra and were used without further purification. Bicyclic (alkyl)(amino) carbene ($^{Me/iPr}$BICAAC) was prepared using reported procedure.[30]

5.4.2 Physical measurements

FT-IR spectra were recorded on a Bruker Invinio R spectrophotometer. The NMR spectra were recorded using Bruker 400 MHz NMR spectrometer (^{1}H: 400 MHz, ^{13}C{^{1}H}: 100 MHz) at room temperature with tetramethylsilane (TMS) as an external standard and chemical shift values are reported in parts per million (ppm). High-resolution mass spectrometry (HRMS) measurement was recorded on a Waters SYNAPT G2-S. UV-vis spectroscopy measurements were recorded on Agilent Cary 5000 UV-vis-NIR Spectrophotometer. Energy dispersive X-Ray (EDX) analysis was performed with a JEOL JSM 7600F field emission electron microscope. SambVca tool as a web application for the calculation of the %buried volume was used.[40]

Single crystal X-ray diffraction data of complexes **1-3** was collected using a Rigaku XtaLAB mini diffractometer equipped with Mercury375M CCD detector. The data was collected with MoKα radiation (λ = 0.71073 Å) using omega scans. During the data collection, the detector distance was 49.9 mm (constant) and the detector was placed at 2θ = 29.85° (fixed). The data were reduced using CrysAlisPro 1.171.38.46, and the space group determination was done using Olex2[41] with the SHELXT[42] structure solution program using Intrinsic Phasing and refined with the SHELXH-1997[43] refinement package using Least Squares minimization. All non-hydrogen atoms were refined anisotropically. Crystallographic data are summarized in Table 5.4.

5.4.3 Syntheses and characterization of complexes 1-4

Synthesis and characterization of Ir(*Me*BICAAC)Cl(COD) (1): In a 50 mL Schlenk flask, *Me*BICAAC (0.31 g, 1.0 mmol) was dissolved in 10 mL precooled THF under inert conditions. Subsequently, half an equivalent of [Ir(COD)Cl]$_2$ (0.34 g, 0.5 mmol) was added to it. The reaction mixture was stirred for 4-5 hours at room temperature. All the volatiles were removed under reduced pressure which afforded a fluffy yellow solid. The compound was further dissolved in approximately 1-2 mL of dichloromethane, and then 10 mL of hexane was added into it to precipitate the impurities. The resultant mixture was filtered and the filtrate was kept at room temperature. After 4-5 days, slow evaporation of solvents afforded block shaped orange-colored air stable crystals of Ir(*Me*BICAAC)Cl(COD) (1) (**yield:** 0.55 g, 85%). **Mp**: 243 °C (decomposition). **FT-IR** (cm^{-1}) ν: 2956, 2930, 2878, 2831, 1474, 1453, 1411, 1385, 1266, 1172, 1058, 996, 803, 740. **^{1}H NMR** (400 MHz, CDCl$_3$) δ = 7.40-7.34 (m, 2H, m-Ar), 7.16-7.14 (m, 1H, p-Ar), 4.54-4.49 (m, 1H, alkene), 4.30-4.25 (m, 1H, alkene), 3.52 (sept, J = 8.0 Hz, 1H, C*H*(CH$_3$)$_2$), 3.19-3.15 (m, 1H, alkene), 2.90 (sept, J = 8.0 Hz, 1H, C*H*(CH$_3$)$_2$), 2.74-2.64 (m, 2H, alkene signal merged with aliphatic signal), 2.19 (s, 3H), 2.12-1.96 (m, 3H), 1.89-1.82 (m, 2H), 1.69-1.62 (m, 2H), 1.59-1.53 (m, 2H), 1.49 (d, J = 8.0 Hz, 3H), 1.45-1.41 (m, 1H), 1.37-1.33 (m, 2H), 1.29 (d, J = 8.0 Hz, 3H), 1.21-1.16 (m, 8H), 1.02 (d, J = 8.0 Hz, 3H), 0.99 (s, 3H). **^{13}C{^{1}H} NMR** (100 MHz, CDCl$_3$) δ = 261.9, 148.0, 144.4, 141.4, 128.8, 126.0, 123.8, 86.3, 84.3, 65.5, 55.3, 52.5, 48.2, 41.7, 40.2, 36.0, 33.8, 33.0, 30.9, 28.84, 28.81, 28.3, 27.8, 27.5, 26.0, 25.6, 24.3, 24.1, 21.0 ppm. **HRMS** (AP$^+$): *m/z* calculated for C$_{30}$H$_{45}$NIrCl: (647.2863) [M]$^+$; found: (647.2838).

Synthesis and characterization of [Ir(*iPr*BICAAC)(COD)][SbF$_6$] (2): Synthesis of complex **2** was carried out in a manner similar to that for **1**. Quantity of the reagents used were: *iPr*BICAAC (0.33 g, 1.0 mmol), [Ir(COD)Cl]$_2$ (0.34 g, 0.5 mmol). (**yield:** 0.55 g, 82%). **Mp**: 209-210 °C. **^{1}H NMR** (400 MHz, CDCl$_3$) δ = 7.41-7.39 (m, 2H, m-Ar), 7.15-7.11 (m,

1H, p-Ar), 4.78-4.74 (m, 1H, alkene), 4.23-4.18 (m, 1H, alkene), 3.69-3.58 (two merged sept, 2H, CH(CH$_3$)$_2$), 2.97-2.87 (m, 2H), 2.70-2.66 (m, 1H, alkene), 2.44-2.34 (m, 2H), 2.32-2.24 (m, 1H), 2.10-2.03 (m, 4H), 2.01-1.94 (m, 1H), 1.90-1.75 (m, 2H), 1.67-1.45 (m, 8H), 1.28 (d, J = 6.4 Hz, 4H), 1.22 (d, J = 6.8 Hz, 4H), 1.231.21 (m, 10H), 0.94 (s, 3H). ^{13}C{^{1}H} NMR (100 MHz, CDCl$_3$) δ = 262.1, 147.7, 144.6, 142.6, 128.8, 126.3, 123.5, 87.1, 82.9, 65.3, 62.9, 56.2, 48.6, 43.9, 35.9, 35.7, 34.4, 32.5, 31.2, 30.0, 29.1, 28.9, 27.9, 27.4, 26.1, 25.9, 25.8, 25.4, 24.6, 24.5, 24.3, 19.7 ppm.

Synthesis and characterization of [Ir(^{Me}BICAAC)(COD)][SbF$_6$] (3): In a 50 mL Schlenk flask, **1** (0.32 g, 0.5 mmol) was dissolved in 10 mL toluene at room temperature to give a yellow solution, subsequently, AgSbF$_6$ (0.17 g, 0.5 mmol) was added in the reaction mixture under dark conditions. Immediate red precipitation was observed upon the addition of AgSbF$_6$ and the reaction mixture was stirred for 1 hour. The volatiles were removed under vacuum then the desired product was extracted in 10 mL of DCM. X-ray quality crystals were grown from a concentrated solution of **3** in chloroform at room temperature to give block-shaped air-stable crystals (**Yield:** 0.41 g, 96 %;). **Mp**: 216-217 °C (decomposition). ^{1}**H NMR** (400 MHz, CDCl$_3$) δ = 7.58-7.47 (m, 3H, Ar), 4.56-4.53 (m, 1H, alkene), 4.24-4.21 (m, 1H, alkene), 3.64-3.60 (m, 1H, alkene), 3.16-3.12 (m, 1H, alkene), 3.01 (sept, J = 8.0 Hz, 1H, CH(CH$_3$)$_2$), 2.55 (sept, J = 8.0 Hz, 1H, CH(CH$_3$)$_2$), 2.41-2.35 (m, 1H), 2.31-2.24 (m, 1H), 2.20-2.12 (m, 1H), 2.07-1.86 (m, 4H), 1.76-1.65 (m, 11H), 1.60-1.55 (m, 3H), 1.42-1.39 (m, 6H), 1.24-1.22 (d, J = 8.0 Hz, 3H), 1.06 (s, 3H), 1.025 (d, J = 4.0 Hz, 3H) ppm. ^{13}C{^{1}H} NMR (100 MHz, CDCl$_3$) δ = 214.4, 149.1, 144.6, 133.1, 129.0, 128.4, 109.8, 98.8, 98.4, 66.2, 57.2, 56.3, 51.1, 43.3, 38.6, 35.6, 34.5, 32.8, 32.3, 31.4, 30.6, 28.3, 25.8, 25.7, 25.7, 25.3, 23.1, 21.0, 20.3, 19.3 ppm. **HRMS** (ES$^+$): m/z calculated for C$_{30}$H$_{45}$NIr: (612.3128) [M-SbF$_6$]$^+$; found: (612.3185). **HRMS** (ES$^-$): m/z calculated for SbF$_6$: (234.8942), found: (234.8788).

Synthesis and characterization of [Ir(^{Me}BICAAC)(CH₃CN)(COD)][SbF₆] (4): In a 50 mL Schlenk flask **3** (0.13 g, 0.15 mmol) was dissolved in 5 mL of chloroform at room temperature to give red colored solution then acetonitrile (7.8 μL, 0.15 mmol) was added into it. The color of reaction mixture immediately turned yellow and this mixture was then further stirred for 1 hour. The volatiles were removed under reduced pressure to give yellow complex **4**. Crystals suitable for X-ray analysis were grown from a concentrated solution of **4** in CHCl₃ at room temperature. (**Yield:** 0.12 g, 92%). **Mp**: 218-219 °C (decomposition). **¹H NMR** (400 MHz, CDCl₃) δ = 7.47-7.43 (m, 1H, Ar), 7.38-7.36 (m, 1H, Ar), 7.22-7.20 (m, 1H, Ar), 4.32-4.28 (m, 1H, alkene), 4.03-3.98 (m, 1H, alkene), 3.73-3.70 (m, 1H, alkene), 3.16-3.12 (m, 1H, alkene), 2.88-2.75 (two merged septet, 2H, CH(CH₃)₂), 2.62 (s, 3H, CH₃CN), 2.17-2.13 (m, 2H), 2.09 (s, 3H), 2.01-1.95 (m, 1H), 1.80-1.62 (m, 8H), 1.515 (d, J = 6.4 Hz, 3H), 1.35-1.25 (m, 10H), 1.15 (d, J = 8.0 Hz, 3H), 1.07 (s, 3H), 1.03 (d, J = 8.0 Hz, 3H) ppm. **¹³C{¹H} NMR** (100 MHz, CDCl₃) δ = 257.5, 146.6, 144.4, 140.5, 129.7, 125.9, 124.9, 124.6, 84.9, 82.6, 66.8, 66.0, 60.9, 55.3, 41.6, 39.2, 35.2, 32.9, 32.5, 31.2, 29.8, 29.2, 28.7, 28.6, 28.2, 26.2, 26.0, 25.9, 24.3, 23.6, 21.1, 3.6 ppm. **HRMS** (ES⁺): *m/z* calculated for C₃₂H₄₈N₂Ir: (653.3447) [M]⁺; found: (653.3463).

5.4.4 General procedure for transfer hydrogenation reactions

Procedure for transfer hydrogenation of aldehydes: A 10 mL pressure tube was charged with 2.0 mmol of aldehyde, 0.1 mol% (1.3 mg) of catalyst **1** and 10 mol% (11.2 mg) of KOH then approximately 3 mL of isopropanol was added. The resultant mixture was allowed to stir at 100 °C. The time required for completion of the reaction varies for different substrates as mentioned in the manuscript. The final products were purified by column chromatography using silica (hexane/EtOAc). The isolated products were analyzed by ¹H and ¹³C{¹H} NMR spectroscopy.

Procedure for transfer hydrogenation of ketones: A 10 mL pressure tube was charged with 1.0 mmol of ketone, 0.5 mol% (3.2 mg) of catalyst **1** and 10 mol% (5.6 mg) of KOH then approximately 3 mL of isopropanol was added. The resulting solution was stirred at 120 °C for 24 hrs. The final products were purified by column chromatography using silica (hexane/EtOAc). The isolated products were analyzed by ^{1}H and ^{13}C{^{1}H} NMR spectroscopy.

Procedure for transfer hydrogenation of imines: A 10 mL pressure tube was charged with 1.0 mmol of imine, 1.0 mol% (6.4 mg) of catalyst **1** and 10 mol% (5.6 mg) of KOH then approximately 3 mL of isopropanol was added. The resulting solution was stirred at 120 °C for 24 hrs. Then the mixture was cooled, dried under vacuum, and then extracted with 15 mL of hexane. The final products were purified by column chromatography using silica (hexane/EtOAc). The isolated products were analyzed by ^{1}H and ^{13}C{^{1}H} NMR spectroscopy.

5.5 Crystallographic data

Table 5.4 Crystallographic details of complexes **1-4.**

Compound[a]	1	2	3	4
Formula	$C_{30}H_{45}NIrCl$	$C_{32}H_{49}ClIrN$	$C_{30}H_{44}F_6IrNSb$	$C_{33}H_{49}Cl_3F_6IrN_2Sb$
Molar mass	647.32	675.37	846.61	1008.04
Crystal system	orthorhombic	orthorhombic	monoclinic	monoclinic
Space group	$P2_12_12_1$	$Pbca$	$I2/m$	$P2_1/c$
T [K]	150.01(10)	150.00(10)	100.02(10)	290.0(10)
a [Å]	10.8373(4)	14.7044(5)	9.9595(3)	10.7032(3)
b [Å]	15.1809(5)	15.2047(6)	16.9733(5)	11.0429(3)
c [Å]	16.4108(8)	26.8784(11)	18.1630(5)	32.1828(8)
α [°]	90.00	90.00	90.00	90.00
β [°]	90.00	90.00	99.104(3)	94.682(2)
γ [°]	90.00	90.00	90.00	90.00
V [Å³]	2699.90(19)	6009.4(4)	3031.70(15)	3791.14(18)
Z	4	8	4	4
ρ(calcd.) [g·cm⁻³]	1.593	1.493	1.855	1.766
μ [mm⁻¹]	5.063	4.552	5.333	4.485
F(000)	1304.0	2736.0	1652.0	1976.0
Radiation [Å] MoKα (λ)	0.71073	0.71073	0.71073	0.71073
Reflections collected	13560	42511	11510	27789
Independent reflections	4758	5320	2787	6714
Data/restraints/ parameters	4758/102/305	5320/0/324	2787/78/237	6714/168/523
$R1$, $wR_2[I>2\sigma(I)]$[a]	0.0277, 0.0633	0.0278, 0.0651	0.0350, 0.0847	0.0276, 0.0678
R1, wR₂ (all data)[a]	0.0287, 0.0645	0.0318, 0.0686	0.0359, 0.0854	0.0300, 0.0698
GOF	1.079	1.105	1.044	1.089

[a] $R1 = \Sigma||Fo| - |Fc||/\Sigma|Fo|$. $wR_2 = [\Sigma w(|Fo^2| - |Fc^2|)^2/\Sigma w|Fo^2|^2]^{1/2}$

5.6 References

1. Nishimura, S. *Heterogeneous Catalytic Hydrogenation for Organic Synthesis*; John Wiley & Sons: New York, **2001**.

2. Vries, J. G. de and Elsevier, C. J. *The Handbook of Homogeneous Hydrogenation*; Wiley−VCH: Weinheim, **2007**.

3. Magano, J.; Dunetz, J. R. *Org. Process Res. Dev*. **2012**, *16*, 1156-1184.

4. McDonnell, G.; Russell, A. D. *Clin. Microbiol. Rev*. **1999**, *12*, 147-179.

5. Bhat, S. V.; Nagasampagi, B. A.; Sivakumar, M. *Chemistry of Natural Products*; Springer: Berlin, **2005**.

6. Schreiber, S. L.; Kapoor, T.; Wess, G. *Chemical Biology: From Small Molecules to Systems Biology and Drug Design*; Eds.; Wiley-VCH: Weinheim, Germany, **2007**; Vols. 1-3.

7. Yoon, N. M. *Pure Appl. Chem*. **1996**, *68*, 843-848.

8. Seyden-Penne, J. *Reductions by the Allumino- and Borohydride in Organic Synthesis*, 2nd ed.; Wiley-VCH: New York, **1997**.

9. Zassinovich, G.; Mestroni, G.; Gladiali, S. *Chem. Rev*. **1992**, *92*, 1051-1069.

10. Wang, D.; Astruc, D. *Chem. Rev*. **2015**, 115, 6621-6686.

11. Samec, J. S. M.; Bäckvall, J.-E.; Andersson, P. G.; Brandt, P. *Chem. Soc. Rev*. **2006**, *35*, 237-248.

12. Wang, C.; Wu, X.; Xiao, J. *Chem. Asian. J*. **2008**, *3*, 1750-1770.

13. (a) Ikariya, T.; Blacker, A. J. *Acc. Chem. Res*. **2007**, *40*, 1300-1308; (b) DePaasquale, J.; Kumar, M.; Zeller, M.; Papish, E. T. *Organometallics* **2013**, *32*, 966-979; (c) Dubey, A.; Khaskin, E. *ACS Catal*. **2016**, *6*, 3998-4002; (d) Figliolia, R.; Cavigli, P.; Comuzzi, C.; Del Zotto, A.; Lovison, D.; Strazzolini, P.; Susmel, S.; Zuccaccia, D.; Ballico, M.; Baratta, W. *Dalton Trans*. **2020**, *49*, 453-465; (e) Blanco, C. O.; Llovera,

L.; Herrera, A.; Dorta, R.; Agrifoglio, G.; Venuti, D.; Landaeta, V. R.; Pastrán, J. *Inorg. Chim. Acta*, **2021**, *524*, 120429; (f) Ghosh, R.; Jana, N. C.; Panda, S.; Bagh, B. *ACS Sustain. Chem. Eng.* **2021**, *9*, 4903-4914.

14. (a) Koto, Y.; Shibahara, F.; Murai, T. *Chem. Lett*. **2016**, *45*, 1327-1329; (b) Zhang, X.; Chen, J.; Khan, R.; Shen, G.; He, Z.; Zhou, Y.; Fan, B. *Org. Biomol. Chem*. **2019**, *17*, 10142-10147; (c) Wang, F.; Zheng, L.-S.; Lang, Q.-W.; Yin, C.; Wu, T.; Phansavath, P.; Chen, G.-Q.; Ratovelomanana-Vidal, V.; Zhang, X. *Chem. Commun*. **2020**, *56*, 3119-3122; (d) Gu, Y.; Norton, J. R.; Salahi, F.; Lisnyak, V. G.; Zhou, Z.; Snyder, S. A. *J. Am. Chem. Soc*. **2021**, *143*, 9657-9663.

15. (a) Wang, Y.; Huang, Z.; Leng, X.; Zhu, H.; Liu, G.; Huang, Z. *J. Am. Chem. Soc*. **2018**, *140*, 4417-4429; (b) Chen, S.-J.; Lu, G.-P.; Cai, C. *RSC Adv*. **2015**, *5*, 13208-13211; (c) Ruff, A.; Kirby, C.; Chan, B. C.; O'Connor, A. R. *Organometallics* **2016**, *35*, 327-335; (d) Wang, R.; Tang, Y.; Xu, M.; Meng, C.; Li, F. *J. Org. Chem*. **2018**, *83*, 2274-2281; (e) Wang, R.; Han, X.; Xu, J.; Liu, P.; Li, F. *J. Org. Chem*. **2020**, *85*, 2242-2249; (f) Pandey, P.; Daw, P.; Din Reshi, N. U.; Ehmann, K. R.; Hölscher, M.; Leitner, W.; Bera, J. K. *Organometallics* **2020**, *39*, 3849-3863.

16. (a) Cummings, S. P.; Le, T.-N.; Fernandez, G. E.; Quiambao, L. G.; Stokes, B. J. *J. Am. Chem. Soc*. **2016**, *138*, 6107-6110; (b) Xuan, Q.; Song, Q. *Org. Lett*. **2016**, *18*, 4250-4253; (c) Cao, B.; Wei, Y.; Shi, M. *Chem. Commun*. **2018**, *54*, 14085-14088.

17. (a) Vega, E.; Lastra, E.; Gamasa, M. P. *Inorg. Chem*. **2013**, *52*, 6193-6198; (b) Park, B. Y.; Luong, T.; Sato, H.; Krische, M. J. *J. Org. Chem*. **2016**, *81*, 8585-8594; (c) Gichumbi, J. M.; Omondi, B.; Friedrich, H. B. *Eur. J. Inorg. Chem*. **2017**, 915-924.

18. (a) Xu, H.; Yang, P.; Chuanprasit, P.; Hirao, H.; Zhou, J. *Angew. Chem. Int. Ed*. **2015**, *54*, 5112-5116; (b) Garduno, J. A.; Garcia, J. J. *ACS Omega* **2017**, *2*, 2337-2343; (c)

Hu, X.; Wang, G.; Qin, C.; Xie, X.; Zhang, C.; Xu, W.; Liu, Y. *Org. Chem. Front.* **2019**, *6*, 2619-2623.

19. (a) Zhang, G.; Yin, Z.; Tan, J. *RSC Adv*. **2016**, *6*, 22419-22423; (b) Chen, F.; Sahoo, B.; Kreyenschulte, C.; Lund, H.; Zeng, M.; He, L.; Junge, K.; Beller, M. *Chem. Sci.* **2017**, *8*, 6239-6246; (c) Ai, W.; Zhong, R.; Liu, X.; Liu, Q. *Chem. Rev*. **2019**, *119*, 2876-2953.

20. (a) Lu, Z.; Cherepakhin, V.; Demianets, I.; Lauridsen, P.; Williams, T. *Chem. Commun*. **2018**, *54*, 7711-7724; (b) Iglesias, M.; Oro, L. A. *Chem. Soc. Rev*. **2018**, *47*, 2772-2808.

21. Corberán, R.; Peris, E. *Organometallics* **2008**, *27*, 1954-1958.

22. Sepúlveda, F.; Carrión, M. C.; Phillips, A. D.; Jalón, F. A.; Dyson, P. J.; Manzano, B. R. *Eur. J. Inorg. Chem*. **2017**, 630-638.

23. Cesari, C.; Cingolani, A.; Parise, C.; Zacchini, S.; Zanotti, V.; Cassani, M. C.; Mazzoni, R. *RSC Adv*. **2015**, *5*, 94707-94718.

24. Yang, Z.; Cheng, W.; Li, Z. *Catalysis Communications*, **2018**, *117*, 38-42.

25. Malacea, R.; Poli, R.; Manoury, E. *Coord. Chem. Rev*. **2010**, *254*, 729-752.

26. (a) Crabtree, R. H. *Coord. Chem. Rev*. **2013**, *257*, 755-766; (b) Hopkinson, M. N.; Richter, C.; Schedler, M.; Glorius, F. *Nature* **2014**, *510*, 485-496; (c) Peris, E. *Chem. Rev*. **2018**, *118*, 9988-10031; (d) Vivancos, Á.; Segarra, C.; Albrecht, M. *Chem. Rev*. **2018**, *118*, 9493-9586; (e) Reshi, N. U. D.; Bera, J. K. *Coord. Chem. Rev*. **2020**, *422*, 213334.

27. Tiwari, C. S.; Illam, P. M.; Donthireddy, S. N. R.; Rit, A. *Chem. Eur. J*. **2021**, *27*, 16581-16600.

28. Hillier, A. C.; Lee, H. M.; Stevens, E. D.; Nolan, S. P. *Organometallics* **2001**, *20*, 4246-4252.

29. (a) Gnanamgari, D.; Moores, A.; Rajaseelan, E.; Crabtree, R. H. *Organometallics* **2007**, *26*, 1226-1230; (b) Türkmen, H.; Pape, T.; Hahn, F. E.; Çetinkaya, B. *Eur. J. Inorg. Chem.* **2008**, 5418-5423; (c) Jiménez, M. V.; Fernández-Tornos, J.; Pérez-Torrente, J. J.; Modrego, F. J.; Winterle, S.; Cunchillos, C.; Lahoz, F. J.; Oro, L. A. *Organometallics* **2011**, *30*, 5493-5508; (d) Gülcemal, S.; Gökçe, A. G.; Çetinkaya, B. *Inorg. Chem.* **2013**, *52*, 10601-10609; (e) Riener, K.; Bitzer, M. J.; Pöthig, A.; Raba, A.; Cokoja, M.; Herrmann, W. A.; Kühn, F. E. *Inorg. Chem.* **2014**, *53*, 12767-12777; (f) Sluijter, S. N.; Elsevier, C. J. *Organometallics* **2014**, *33*, 6389-6397; (g) Mazloomi, Z.; Pretorius, R.; Pàmies, O.; Albrecht, M.; Diéguez, M. *Inorg. Chem.* **2017**, *56*, 11282-11298; (h) Ramollo, G. K.; Strydom, I.; Fernandes, M. A.; Lemmerer, A.; Ojwach, S. O.; van Wyk, J. L.; Bezuidenhout, D. I. *Inorg. Chem.* **2020**, *59*, 4810-4815.

30. Tomás-Mendivil, E.; Hansmann, M. M.; Weinstein, C. M.; Jazzar, R.; Melaimi, M.; Bertrand, G. *J. Am. Chem. Soc.* **2017**, *139*, 7753-7756.

31. Yazdani, S.; Junor, G. P.; Peltier, J. L.; Gembicky, M.; Jazzar, R.; Grotjahn, D. B.; Bertrand, G. *ACS Catal.* **2020**, *10*, 5190-5201.

32. Chakrabortty, S.; Kaur, M.; Adhikari, M.; Manar, K. K.; Singh, S. *Inorg. Chem.* **2021**, *60*, 6209-6217.

33. Nagyházi, M.; Almási, B.; Lukács, Á.; Bényei, A.; Nagy, T.; Kéki, S.; Tuba, R. *Journal of Molecular Structure*, **2022**, *1256*, 132483.

34. Rajendran, N. M.; Gautam, N.; Sarkar, P.; Ahmed, J.; Das, A.; Das, S.; Pati, S. K.; Mandal, S. K. *Chem. Commun.* **2021**, *57*, 5282-5285.

35. Prakash, D. MS thesis dissertation, *Synthesis of Bicyclic (alkyl)(amino)carbene Complexes of Mn(II), Mn(0), Au(I), Ir(I) and Zn(II)*, IISER Mohali, **2019**.

36. Yogesh, Y. MS thesis dissertation, *Bicyclic (Alkyl)(Amino) carbene (BICAAC) supported iridium complex, [(BICAAC)Ir(COD)Cl] for hydrosilylation reactions*, IISER Mohali, **2022**.

37. (a) Gómez-Suárez, A.; Nelson, D. J.; Nolan, S. P. *Chem. Commun.* **2017**, *53*, 2650-2660; (b) Clavier, H.; Nolan, S. P. *Chem. Commun.* **2010**, *46*, 841-861; (c) Termühlen, S.; Dutschke, P. D.; Hepp, A.; Hahn, F. E. *Eur. J. Inorg. Chem.* **2022**, e202101065.

38. (a) Albrecht, M.; Miecznikowski, J. R.; Samuel, A.; Faller, J. W.; Crabtree, R. H. *Organometallics* **2002**, *21*, 3596-3604; (b) Melle, P.; Manoharan, M.; Albrecht, M. *Inorg. Chem.* **2018**, *57*, 11761-11774.

39. (a) Victoria Jiménez, M.; Fernandez-Tornos, J.; Javier Modrego, F.; Perez-Torrente, J. J.; Oro, L. A. *Chem. Eur. J.* **2015**, *21*, 17877-17889; (b) Pàmies, O.; Bäckvall, J.-E. *Chem. Eur. J.* **2001**, *7*, 5052-5058.

40. (a) Poater, A.; Cosenza, B.; Correa, A.; Giudice, S.; Ragone, F.; Scarano, V.; Cavallo, L. *Eur. J. Inorg. Chem.* **2009**, 1759-1766; (b) Falivene, L.; Cao, Z.; Petta, A.; Serra, L.; Poater, A.; Oliva, R.; Scarano, V.; Cavallo, L. *Nat. Chem.* **2019**, *11*, 872-879.

41. Dolomanov, O. V., Bourhis, L. J., Gildea, R. J., Howard, J. A. K. and Puschmann, H. *J. Appl. Cryst.* **2009**, *42*, 339-341.

42. Sheldrick, G. M. *Acta Cryst., Sect. A* **2015**, *71*, 3-8.

43. Sheldrick, G. M. *Acta Cryst., Sect. A* **2008**, *64*, 112-122.

Summary and future scope

(BICAAC)
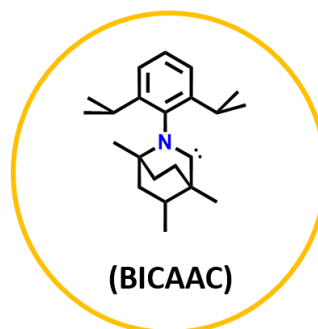
Summary:

The research presented in this thesis is organized into five main chapters. Chapter 1 provides a comprehensive introduction to the history and development of carbenes, offering a detailed overview of their evolution over time. This chapter thoroughly explores various applications of carbenes, highlighting their versatility and significance in different fields. It delves into the pivotal role that carbenes have played in advancing chemical research and their diverse use in synthetic chemistry, catalysis, and materials science. The historical context and progression of carbenes are discussed to set the foundation for the subsequent chapters.

Chapter 2 mainly focused on the application of BICAAC-boron trihalides and hydroborane adducts for the synthesis of low-valent multiply bonded complexes (Chapter 2A) and cationic boron complexes (Chapter 2B), respectively. In summary, Chapter 2A disclosed the syntheses and detailed characterization of stable diborane and diborene compounds supported by BICAAC ligands. The reactivity of the diborene complex was further explored in reactions with various coinage metal salts, specifically CuCl, AgBr, and CuI. Structural and computational studies revealed significant lengthening of both the $>B=B<$ double bond and the B-C$_{BICAAC}$ bonds upon metalation of the diborene. Energy Decomposition Analysis (EDA) calculations indicated that the interaction between the $>B=B<$ unit and the Cu or Ag metal centers is predominantly electrostatic. Additionally, TDDFT calculations were conducted, and the results showed a strong correlation with the experimentally observed absorption spectra of these complexes.

Chapter 2B details the synthesis and characterization of a series of BICAAC-supported borenium ion equivalent complexes. Quantitative assessment of the Lewis acidity of these complexes revealed acceptance numbers (AN) in the range of 93.5-93.9, underscoring their significant Lewis acidic nature. Furthermore, these complexes exhibited

remarkable catalytic activity in the hydrosilylation of a wide variety of carbonyl compounds. Notably, under a catalyst loading of 1 mol% and a reaction time of just 5 minutes, [BICAAC→BH$_2$−H−BH$_2$←BICAAC][H-B(C$_6$F$_5$)$_3$] complex proved to be an efficient catalyst for the hydrosilylation of numerous aldehydes and ketones, achieving a turnover frequency (TOF) as high as 1200 h^{-1} with benzaldehyde. In addition, this complex also showed catalytic activity in the hydrosilylation of *para*-quinone methides.

Chapter 3 focuses on the syntheses and comprehensive characterization of a series of BICAAC-supported Ge and Sn complexes. Additionally, we have successfully synthesized and characterized a BICAAC-stabilized germylone species, [BICAAC→Ge←BICAAC]. Moreover, the reactivity of BICAAC−SnX$_2$ adducts was further explored with the iron carbonyl complex [Fe$_2$(CO)$_9$]. Efforts to convert the BICAAC tin halides to hydrides complexes using LiBH$_4$ were undertaken, which ultimately led to over-reduction and resulted in the synthesis of a di-hydrogenated BICAAC complex, (BICAAC-H$_2$).

Chapter 4 details the syntheses of BICAAC-ECl$_3$ adducts (E = P, Sb), accomplished through direct reactions between free BICAAC and the corresponding trichlorides. Additionally, we successfully isolated and characterized a phosphinidene, (BICAAC)=P−Ph, by *in-situ* reduction of the [BICAAC−PPhCl$_2$] adduct using KC$_8$. The phosphinidene is characterized by a short C−P bond distance, indicative of the C=P bond character. Leveraging the strong σ-donor properties of BICAAC, the stable BICAAC−ECl$_3$ (E = P, Sb) adducts were further utilized in the synthesis of *bis*(BICAAC)P$_2$ and its corresponding Sb analogue, maintaining the pnictogen in a formal zero-valent state. The *bis*(phosphinidene) compound dominates the *bis*(phosphaalkenes) canonical structure, whereas the antimony analogue demonstrates the ability of BICAAC to stabilize the Sb$_2$ core through σ-donation.

Chapter 5 focuses on the synthesis and detailed characterization of a series of stable neutral and cationic Ir(I) complexes supported by $^{Me/iPr}$BICAAC ligands. These complexes, demonstrated excellent catalytic activity in the transfer hydrogenation of 4-chlorobenzaldehyde, with TOF values between 6269-8093 h^{-1}. [Ir(^{Me}BICAAC)Cl(COD)] complex was further investigated for its catalytic performance across a variety of aldehydes, ketones, and imines, achieving moderate to good yields. Thermal stability tests confirmed that this complex retains its structure upon prolonged heating, essential for catalytic applications. Homogeneity of the catalytic process was supported by Hg drop and hot filtration tests, while deuterium labeling and other control experiments indicated a monohydride mechanistic pathway and the formation of an Ir−OiPr intermediate in the catalytic cycle.
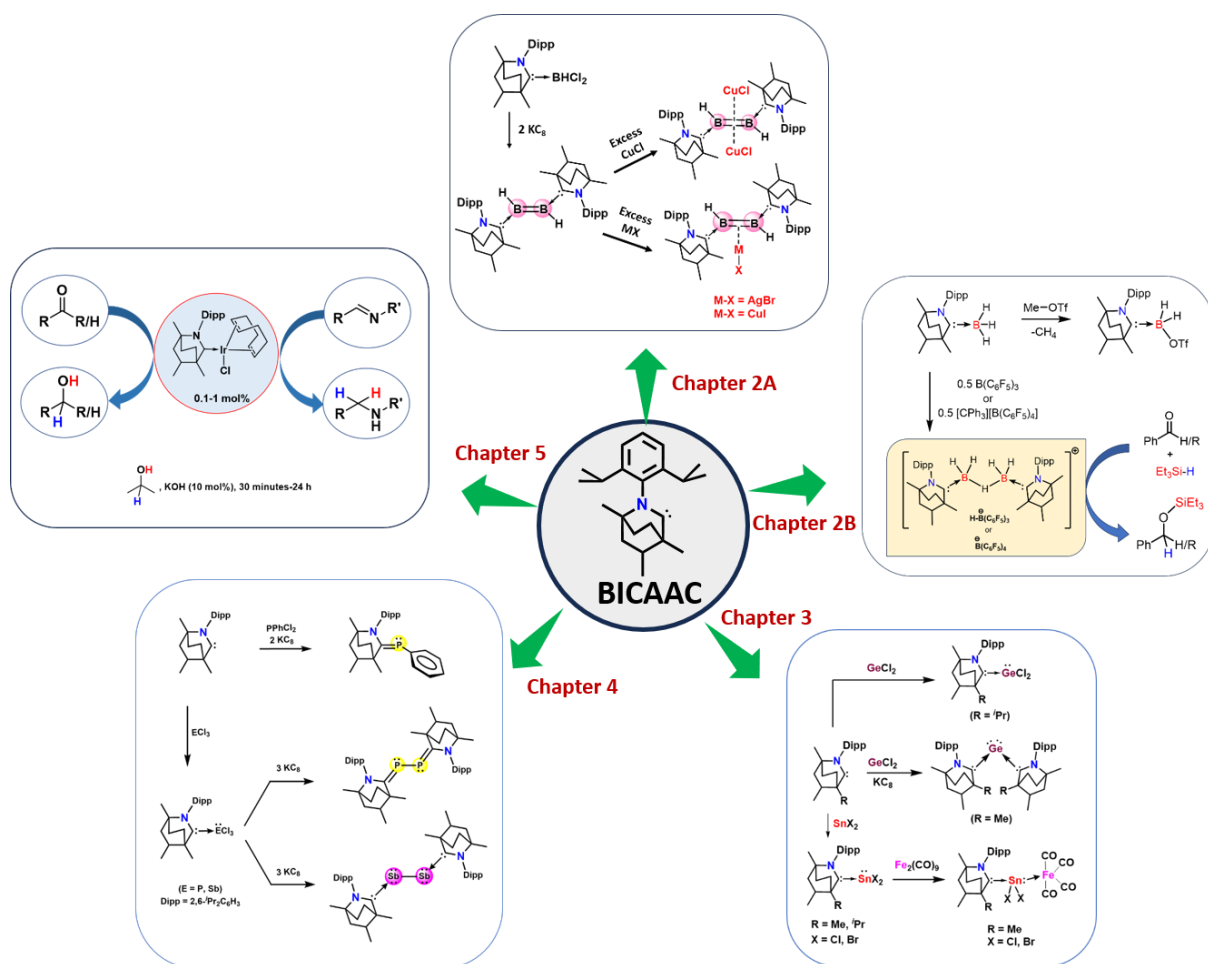
Future scope:

In continuation to the research presented in the thesis, the following avenues for future exploration are proposed:

1. The recently synthesized BICAAC-stabilized diborene and its coinage metal π-complexes present an excellent opportunity to study their photophysical properties, offering significant potential for future research.
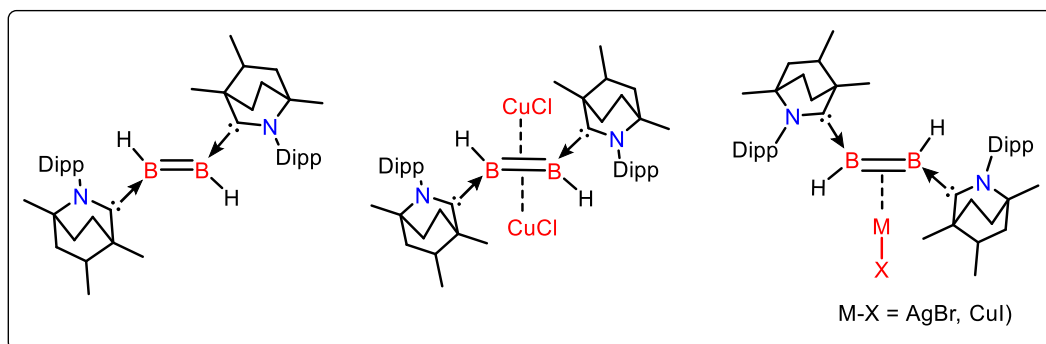

2. Similarly, the ambiphilic properties of BICAAC can be leveraged to synthesize a tricoordinate organoboron species, which will be isoelectronic with amines. This complex can subsequently be used to generate a dicoordinate boron cation.
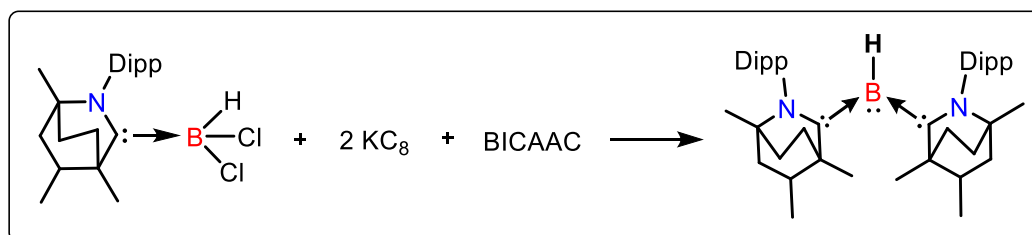

3. The catalytic potential of [Ir(BICAAC)Cl(COD)] complex, as well as borenium ion equivalent complexes, [BICAAC→BH$_2$−H−BH$_2$←BICAAC][H−B(C$_6$F$_5$)$_3$] and [BICAAC→BH$_2$−H−BH$_2$←BICAAC][B(C$_6$F$_5$)$_4$], can be explored in future research for various organic transformations, with a detailed emphasis on mechanistic aspects.

4. We reported the isolation of a germylone complex, [(BICAAC)$_2$Ge]. Similarly, the excellent donor properties of BICAAC can be utilized to isolate a digermanium(0) complex, [BICAAC→Ge=Ge←BICAAC].
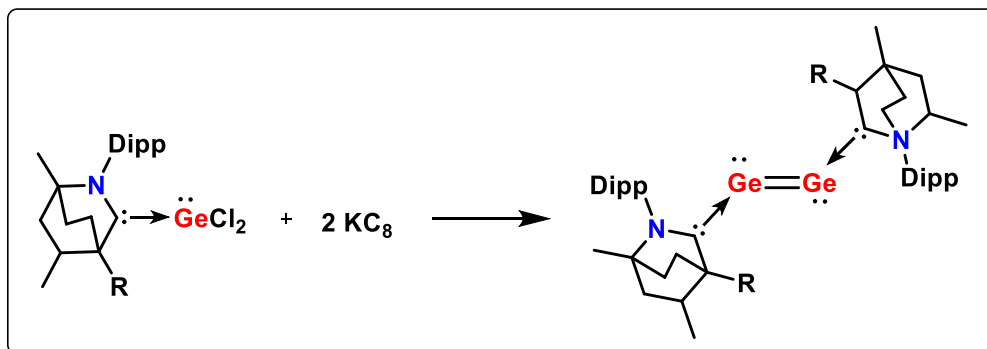
5. We also reported the *bis*-antimony complex [BICAAC→Sb−Sb←BICAAC]. To date, the antimony analogue of germylone has not been reported, and BICAAC can be utilized to synthesize this complex, [(BICAAC)$_2$Sb].
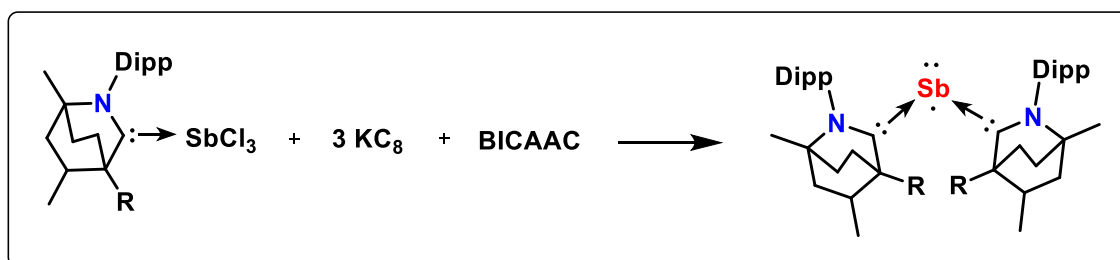
List of publications

1. Adhikari, M.[1]; Kaur, M.[1]; Manar, K. K.; Yogesh, Y.; Prakash, D.; Singh, S. BICAAC-Derived Covalent and Cationic Ir(I) Complexes: Application of Ir(BICAAC)Cl(COD) Complexes as Catalysts for Transfer Hydrogenation and Hydrosilylation Reactions. *Inorg. Chem.* **2024**, *63*, 1513-1523. ([1]equal contributions)

2. Adhikari, M.; Thakur, S. K.; Singh, S. Adducts of Bicyclic (Alkyl)(Amino) Carbene with ECl_3 and Three Electron Reduction Thereof: Syntheses of BICAAC Stabilized E-E Bonded Compounds (E = P, Sb). *Eur. J. Inorg. Chem.* **2023**, e202300379.

3. Adhikari, M.; De, S.; Manar, K. K.; Thakur, S. K.; Kamte, R. S.; Koley, D.; Singh S. Diborane, Diborene and M(I)-η^2-Diborene Complexes Stabilized by Bicyclic (Alkyl)(Amino)Carbene (M = Cu and Ag) *Eur. J. Inorg. Chem.* **2024**, e202400129.

4. Bansal, S.; Biswas, A.; Kundu, A.; Adhikari, M.; Singh, S.; Adhikari, D. Ambiphilic Alcohol Dehydrogenation by BICAAC Mimicking Metal-Ligand Cooperativity. *ACS Catal.* **2024**, *14*, 8087–8095.

5. Thakur, S. K.; De, S.; Adhikari, M.; Manar, K. K.; Koley, D.; Singh S. Low-Valent Si Complexes Supported by Bicyclic (Alkyl)(Amino)Carbene (MeBICAAC): Syntheses, Characterization, and Reactivity Studies. *ChemRxiv 10.26434/chemrxiv-2023-36z0g*.

6. Thakur, S. K.; Kaur, M.; Manar, K. K.; Adhikari, M.; Choudhury, A. R.; Singh S. Well-Defined Ni(0) and Ni(II) Complexes of Bicyclic (Alkyl)(Amino)Carbene (*Me*BICAAC): Catalytic Activity and Mechanistic Insights in Negishi Cross-Coupling Reaction. *Chem. Eur. J.* **2022**, *28*, e202202237.

7. Chakrabortty, S.; Kaur, M.; Adhikari, M.; Manar, K. K.; Singh, S. A Bis (BICAAC) Palladium(II) Complex: Synthesis and Implementation as Catalyst in Heck-Mizoroki and Suzuki-Miyaura Cross Coupling Reactions. *Inorg. Chem.* **2021**, *60*, 6209-6217.

8. Manar, K. K.; Porwal, V. K.; Kamte, R.; Adhikari, M.; Thakur, S. K.; Bawari, D.; Choudhury, A. R.; Singh, S. Reactions of BICAAC with hydroboranes: propensity for Lewis adduct formation and carbene insertion into B-H bond. *Dalton Trans*. **2019**, *48*, 17472-17478.

9. Adhikari, M.; Thakur, S. K.; Singh S. BICAAC stabilized borenium cation equivalents: Syntheses, characterization and application in hydrosilylation of carbonyls. *Manuscript under preparation.*

10. Adhikari, M.; Thakur, S. K.; Singh S. Syntheses, structure and reactivity of BICAAC stabilized Ge(II)/Sn(II) dihalide complexes. *Manuscript under preparation.*